THE
PHYSICAL REVIEW
A Journal of Experimental and Theoretical Physics Established by E. L. Nichols in 1893
VOL. 59, No. 1 JANUARY 1, 1941 SECOND SERIES

Electric Fields Produced by Cosmic Rays

FOSTER EVANS
Ryerson Physical Laboratory, The University of Chicago, Chicago, Illinois
(Received August 23, 1940)

With recognition of the existence in interstellar space of a finite density of matter, the following four assumptions are made regarding the conditions under which electric currents flow in interstellar space: (1) The current is related to the electric field producing it by Ohm's law; (2) the interchange of electric charge between a star and its surroundings has reached a steady state; (3) the conditions around a star are spherically symmetric, which implies that the star has no magnetic moment; (4) the forces due to gravity, radiation pressure, and diffusion can be neglected simultaneously. The validity of these assumptions is discussed. The electric field E in the neighborhood of a single star is given by the equation, $A=-\sigma r^2 E$, where A is proportional to the rate at which the star intercepts, or emits, cosmic-ray particles all of the same charge, σ is the electrical conductivity in interstellar space, and r is the distance of the point under consideration from the center of the star. It is found that both charge density and current density vanish in interstellar space. Numerical calculations indicate that the star will acquire a very small potential when it only intercepts cosmic rays. For a typical star this is of the order of 10^{-12} volt. In the case of emission an upper limit to the potential is found to be approximately one volt. The limitations of the applicability of the present analysis for the case of emission are discussed. It is concluded that the existence in interstellar space of cosmic rays as charged particles predominantly of one sign will result in the production of negligible electric fields. Calculations are made to determine the dimensions of the ion sheath that will be produced around a star by the ions in interstellar space.

INTRODUCTION AND STATEMENT OF ASSUMPTIONS

IN theoretical investigations concerning the source of primary cosmic-ray particles and their subsequent transmission through interstellar space, the problem of the possible electric fields produced is an important one. Experimental evidence indicates that both positively and negatively charged primaries enter the earth's atmosphere, but whether there is an appreciable excess of particles of one sign in space is not known. It is true that the latitude effect indicates that positive primaries produce more effect at the earth's surface than do negative primaries. This might indicate an excess of positives in space, or merely a difference in penetrating power. It has been the purpose of this investigation to consider the electrical fields that would result from a net charge carried by the primary rays. Some years ago Swann[1] showed that if cosmic rays were present in empty space as charged particles predominantly of one sign, the resultant space charge would produce enormous potential differences between relatively near points in space. His calculations indicated further that: "Any attempt to picture particles of one sign as emanating from the stars or other heavenly bodies would result in a condition in which the particles would become bound to their respective stars as a sort of space charge unless both signs of charged particles were emitted." Strictly, however, it is not correct to consider

[1] W. F. G. Swann, Phys. Rev. **44**, 124 (1933).

interstellar space as being empty. Astronomical observations show evidence for the existence of a finite density of electrons and ions. Swann pointed out that the presence of such interstellar charges would neutralize the space charge caused by cosmic rays. Working upon this hypothesis Alfvén[2] has made some calculations from which he concluded that the magnetic field produced by the electric current caused by cosmic rays would have a limiting effect upon the amount of such current.

In order to consider the hypothesis of space charge neutralization in more detail the following assumptions—the validity of which will be discussed later—are made. (1) Ohm's law is valid for electric currents flowing in the very rare gas which fills interstellar space. (2) The interchange of electric charge between a star and its surroundings has reached a steady state. (3) The conditions around the star are spherically symmetric. As implied in this assumption, the effect of stellar magnetic moments has been neglected. (4) The forces due to gravity, radiation pressure, and diffusion can be neglected simultaneously for small electric fields.

Derivation of Equations

Consider a single star immersed in the gas which fills interstellar space, and let the constant $4\pi A$ be the total amount of electric charge intercepted, or emitted, by the star per second in the form of cosmic rays. There will also be a current flow to the star resulting primarily from the motion of interstellar electrons. Throughout this discussion the expression "interstellar electrons" will refer to the slow electrons that occupy interstellar space and are not to be confused with high energy electrons which may make up a part of the cosmic radiation. The current due to the interstellar electrons is given, according to the first assumption, by the expression

$$i_{\text{elect}}=4\pi r^2\sigma E, \tag{1}$$

where σ is the electrical conductivity of the interstellar gas and E is the electric field in which the electrons are moving at a distance r from the center of the star. This current plus that caused by the cosmic rays, given by

$$i_{\text{c.r.}}=4\pi A, \tag{2}$$

represents the total amount of current flowing across the boundary of a sphere of radius r drawn with its center at the center of the star. Both currents are independent of r, according to the second assumption. Furthermore, the algebraic sum of these two currents is zero since electricity is not created or destroyed in the star. Therefore, by adding the right-hand sides of Eqs. (1) and (2) and equating to zero, we obtain, after solving for the electric field E,

$$E=-A/\sigma r^2. \tag{3}$$

If ρ, ρ_+ and $\rho_{\text{c.r.}}$ are, respectively, the charge densities caused by electrons, positive ions, and cosmic rays, it is possible to write

$$\text{div } E=4\pi(\rho+\rho_+ +\rho_{\text{c.r.}})$$

and from Eq. (3) it is seen that

$$\rho+\rho_+ +\rho_{\text{c.r.}}=0, \tag{4}$$

which is in agreement with the hypothesis of space charge neutralization. In other words, E is caused entirely by a charge $Q=A/\sigma$ on the star. Further, since a condition of spherical symmetry surrounds the star it follows that the current density is equal to zero at all points and there is no magnetic field caused by cosmic rays.

Alfvén[3] states that a process similar to that just described, that is an isotropic emission of equal numbers of positive and negative particles from the surface of a sphere, is unstable if the medium around the sphere is conducting. This statement, however, seems untenable in view of the fact that spherical electrodes immersed in the positive column of a discharge tube have been observed to be surrounded by stable, spherical ion sheaths through the surfaces of which passed equal numbers of positive and negative particles.

The conductivity σ may be written as the product of the charge density ρ caused by the interstellar electrons, and the mobility κ. From kinetic theory the mobility is given by

$$\kappa=e\lambda/mu,$$

[2] A. Alfvén, Phys. Rev. **55**, 425 (1939).

[3] Reference 2, p. 427.

where e is the charge, λ the mean free path, m the mass and u the average velocity of the electron. Again from kinetic theory

$$u=(3kT/m)^{\frac{1}{2}}, \quad \text{and} \quad \lambda=1/\pi s^2 n,$$

where k is Boltzmann's constant, T is the translation temperature of interstellar electrons, s is the sum of the radius of the electron and the average radius of the particles in interstellar space and n is the total density of such particles. Substitute these formulae for u and λ into the formula for κ and there results

$$\kappa=[e/\pi s^2(3mkT)^{\frac{1}{2}}](1/n).$$

Now let β be the fraction of the total density of the interstellar gas that consists of electrons, and the charge density of electrons becomes $\rho=e\beta n$. Then, since $\sigma=\rho\kappa$ it is found upon substitution into Eq. (3) that

$$E=-\pi s^2(3mkT)^{\frac{1}{2}}A/e^2\beta r^2, \qquad (5)$$

which indicates that the electric field E is independent of the density n. Upon integration of Eq. (5) it is seen that the potential produced on a star of radius a as a result of interception or emission of cosmic rays is given by

$$V=-\pi s^2(3mkT)^{\frac{1}{2}}A/e^2\beta a. \qquad (6)$$

Interstellar Electrons

At this point it seems advisable to digress slightly in order to give a brief outline of the present ideas concerning electrons in interstellar space. In a recent publication by Dunham[4] it is calculated that in interstellar space between the earth and χ^2 Orionis the density of electrons is approximately equal to $10/\text{cm}^3$. He suggests, however, that it is probable that this value should be reduced by a factor of ten or more. Dunham determines a value for the density of hydrogen which is approximately equal to that of electrons, while the total density of sodium, potassium, calcium and titanium is less than 1.4×10^{-4}. This indicates that the fraction β used in the above formulae is approximately equal to $\frac{1}{2}$. The translation temperature of interstellar gas which is usually adopted in astrophysical calculations is of the order of[5,6] 10,000°K.

[4] T. Dunham, Jr., Proc. Am. Phil. Soc. **81**, 277 (1939).
[5] A. Corlin, Zeits. f. Astrophysik **18**, 1, 11 (1939).
[6] O. Struve, Proc. Nat. Acad. Sci. **25**, 37 (1939).

Discussion of Assumptions

A necessary condition for the application of Ohm's law is that the velocity gained by an interstellar electron over the mean free path shall be small compared with the average velocity of temperature agitation. The limit within which this requirement is fulfilled is discussed below. Also, in order that Ohm's law be obeyed for the conduction of electric currents through the interstellar gas, it is necessary that an electron make enough collisions with atomic particles in interstellar space to reach a terminal velocity before it collides with a star. In other words, the interstellar electrons must make many more collisions with atomic particles than they do with stars. In order to determine whether or not this is so, the approximate mean free paths L_1, for electrons colliding with atomic particles, and L_2 for electrons colliding with stars were calculated from the formula for mean free path given above. In order to obtain L_1, let the density N_1 of interstellar particles be equal to twice the density of electrons. In view of the discussion in the previous section this latter density will be taken as one electron per cubic centimeter. Let s_1, the sum of the radii of the electron and the particles of atomic size which consist principally of hydrogen atoms and ions, be one angstrom, then

$$L_1=1/\pi s_1^2 N_1=1.68\times10^{-3} \text{ light yr.}$$

Let the density N_2 of the stars in our galaxy be 0.1 per cubic parsec,[7] and let the average stellar radius (see below) be the radius of the sun, i.e., $s_2=6.95\times10^{10}$ cm, then

$$L_2=1/\pi s_2^2 N_2=2.05\times10^{16} \text{ light yr.}$$

By comparing L_1 and L_2 it is seen that the probability of an electron colliding with a star is much smaller than that of its colliding with an interstellar particle of atomic size. Suppose that instead of there being one or more electrons per cubic centimeter in interstellar space, the average electron density is as low as 10^{-3} per cm^3. Then L_1 would be of the order of magnitude of the average distance between stars in the galaxy. Although in these circumstances an electron might travel such a distance before making a

[7] J. H. Jeans, *Astronomy and Cosmogony*, second edition (Cambridge, 1929), p. 15.

collision, there still would be very little likelihood of its colliding with a star because of the small cross sections of the stars as compared with the total cross section of all the atoms of the interstellar gas.

The conditions within the interstellar gas might then be roughly compared to those in the positive column of a discharge tube with the stars behaving like floating electrodes. It seems justifiable, therefore, to use Ohm's law for weak fields.

The second assumption as to the existence of a steady state seems to be entirely reasonable.

The third assumption concerning the symmetry conditions is not unreasonable for the present purpose in view of the very small order of magnitude of the numerical results that are obtained. Of course, near a star, the stellar magnetic field is of importance and the electrons will not move in such a way as to allow the currents to be spherically symmetric. The magnetic field probably increases the density of electrons and ions near the star as well as the effective diameter of the star. For these reasons it is doubtful whether the effects of magnetic fields can be neglected without further consideration. However, it is not desirable at present to introduce the complications that would result from considering such effects. The magnetic field drops off rapidly with the distance away from the star, so by choosing r properly in the above equations the flow of current to the star can without excessive error be considered spherically symmetric.

To justify the fourth assumption for the present case, the following considerations must be made. The force acting on an electron in the neighborhood of a charged star is not caused exclusively by the presence of an electric field, but, rather, it is the resultant of the effects of gravity and radiation pressure in addition to a possible electric field. As soon as one introduces gravitational forces, however, it becomes necessary to consider diffusion. In the atmosphere surrounding a neutral star there is a balance between the rate at which particles are drawn toward the surface of the star by gravity, and the rate at which particles diffuse away from the surface because of the density gradient in the atmosphere. Included in this balance is the effect of radiation pressure. Now, if an electric charge is placed on the star, there will be an additional accelerating force applied to the charged particles surrounding the star, in particular to the electrons. This will alter the previous balance. The assumption made here is that the additional current produced by the electric field is related to the field in the manner described by Ohm's law. That this assumption represents only an approximation to the actual facts is evident, but it appears to be a closer approximation than would be obtained by introducing the effect of one of the above-mentioned factors, say gravity, without also considering the others.

Numerical Calculations

By substituting the following numerical values into Eq. (6)

$$e=4.8\times10^{-10}\text{ e.s.u.};\quad s=10^{-8}\text{ cm};\quad m=9\times10^{-28}\text{ g}$$

$$k=1.37\times10^{-16}\text{ erg/deg.};\quad T=10{,}000^{\circ}\text{K}$$

there results

$$V=-[1/(1.2\times10^{16}\beta)](A/a). \qquad (7)$$

To determine the value of A for the case of a star which only intercepts cosmic rays we shall assume that the particles move with a constant velocity c, the velocity of light, in random directions. Then the charge intercepted by the star per cm^2 per second, if all the cosmic-ray particles carry a charge of the same magnitude and sign is given by $Nce/4$, where N is the density of cosmic-ray particles and e is the magnitude of the charge on each. The total charge intercepted per second by a star of radius a is then given by

$$4\pi A=4\pi a^2Nce/4, \quad \text{and} \quad A=\tfrac{1}{4}Ncea^2.$$

If[2] $N=10^{-10}$ per cm^3, $c=3\times10^{10}$ cm per second and $e=4.8\times10^{-10}$ e.s.u., this becomes

$$A=3.6\times10^{-10}a^2\text{ e.s.u. sec.}^{-1}.$$

With this value of A and with $\beta=\frac{1}{2}$, it is found from Eq. (7) that a star of radius equal to that of the sun which is intercepting cosmic rays all of one sign will acquire an approximate potential of

$$V=1.3\times10^{-12}\text{ volt.}$$

Although the potential produced on each star as just calculated is very small it might be that

the galaxy would acquire a large potential as a result of the accumulative effect of such a charge on each star in the galaxy. The potential V on a spherical star of radius a is equivalent to a charge Va. So, if the galaxy is taken to be a sphere of radius R, and G is the total number of stars in the galaxy, the resultant potential of the galaxy, with respect to infinity, caused by an average charge Va on the stars is

$$V_G = GVa/R.$$

Then giving to V and a the same magnitudes as above and to G and R the values[7]

$$G = 1.45\times10^{9}; \quad R = 1.56\times10^{22} \text{ cm},$$

the potential produced on the galaxy as a result of stellar interception of cosmic rays is approximately

$$V_G = 8.4\times10^{-15} \text{ volt}.$$

To estimate A in the case of a star emitting cosmic rays, take as an upper limit to the energy so radiated the total energy of spectral radiation. Let the latter be represented by $4\pi S$ ergs per second. Then if each cosmic-ray particle represents energy of the amount W electron volts and carries a charge e e.s.u., the total amount of charge radiated per second is given by

$$4\pi A = 4\pi Se/(1.59\times10^{-12})W,$$

where 1.59×10^{-12} is the number of ergs in one ev. Then, if $e = 4.8\times10^{-10}$ e.s.u. and $W = 10^{10}$ ev,

$$A = 3.02\times10^{-8}S.$$

An average of several stars gives[8] $S = 5\times10^{34}$ ergs per second, so

$$A = 1.51\times10^{27} \text{ e.s.u. sec.}^{-1}.$$

By substituting into Eq. (7) it is seen that a star of radius equal to that of the sun emitting cosmic rays as charged particles all of one sign at the rate indicated will acquire a potential less than

$$V = 1086 \text{ volts}.$$

It is to be noted that in using Ohm's law for the conduction of electric currents through a gas the condition is imposed that the energy which an ion, or in this case an electron, acquires in traveling a distance equal to the length of a mean free path in the electric field must be small compared to the average energy of agitation of the atoms in the gas. The translation temperature of electrons in interstellar space corresponds to an energy of approximately one electron volt. This indicates that the energy acquired by an electron in traveling through a mean free path one terminus of which is at the surface of a star at a potential of 1000 volts will, if the electron's path is in the direction of a radius vector, be greater than the average energy of agitation of electrons by a factor of approximately 10^3. The case of a star that emits cosmic-ray energy of the amount indicated here as an upper limit cannot, therefore, be treated under the assumption of Ohm's law. This type of analysis will apply only to stars emitting cosmic rays at such a rate that the constant A has a value less than 10^{24} e.s.u. per second, resulting in a potential less than one volt. It should be remembered that it is not likely that a star will emit as much energy in the form of cosmic rays as it does in the form of heat.

Stellar Ion Sheaths

The analogy between a star immersed in the interstellar gas and a floating electrode in the positive column of a discharge tube can be used to determine what sort of ion sheath will be produced around a star as a result of its interception of the electrons and positive ions which make up a large part of the interstellar gas. This analogy was used in order to determine whether or not stellar ion sheaths would be of such dimensions as to influence the calculations already made.

Consider a single star and suppose it to be spherical in shape. It is placed in a gas made up of electrons and positive ions in equal number that move in random directions with a Maxwellian distribution of velocities the average of which corresponds to a translation temperature $T = 10{,}000°\text{K}$. Because of the higher mobility of the electrons the star will intercept in unit time more electrons than positive ions and hence become negatively charged. Positive ions will then be attracted to the star and a positive ion sheath will be formed in such a way that the

[8] Physics staff, University of Pittsburgh, *Atomic Physics* (Wiley, 1933), p. 291.

negative charge on the star will be just neutralized by the positive charge caused by all the ions in the sheath. In the final state the number of high energy electrons which are able to reach the star in unit time will be equal to the rate at which positive ions fall into the star as a result of its negative charge. To calculate the dimensions of the ion sheath use was made of the "orbital" and "space charge" equations developed by Langmuir and his co-workers in their theoretical study of spherical probes. These equations relate the total current flow of electrons and positive ions to the potential of the probe and the radius of its ion sheath.

If i_+ and i_- represent the total currents flowing to the star caused by positive ions and electrons, respectively, and I_+ and I_- are the current densities of these particles as intercepted by the star, the orbital equations are written[9]

$$i_+=4\pi r^2 I_+[1-(1-b^2)\exp[-b^2 f/(1-b^2)]], \quad (8)$$

$$i_-=-4\pi r^2 I_- b^2 e^{-f}, \quad (9)$$

where, for the present case, a is the radius of the star, r is the radius of the ion sheath, b is the ratio a/r and $f=eV/kT$ which becomes $1.16V$, or approximately, $f=V$. The space charge equation is written[10]

$$i_+'=(4/9)(2e/M)^{\frac{1}{2}}\nu/\alpha^2, \quad (10)$$

where

$$\nu=V^{\frac{1}{2}}[1-0.0247(T/V)]\backsimeq V^{\frac{1}{2}},$$
$$\alpha=(\log b)-0.38(\log b)^2+\cdots,$$

and M is the positive ion mass which in this case is taken to be the mass of the hydrogen atom. Since the star corresponds to a floating electrode the net current flow to it is zero. On substituting Eqs. (8) and (9) into

$$i_++i_-=0,$$

there results

$$1/b^2-[(1-b^2)/b^2]\exp[-b^2V/(1-b^2)]=40e^{-V}, \quad (11)$$

where the ratio I_-/I_+, which is equal to the square root of the ratio of the masses of the hydrogen atom and the electron, is replaced by its approximate value 40.

[9] H. M. Mott-Smith and I. Langmuir, Phys. Rev. **28**, 727 (1926).

[10] I. Langmuir and K. B. Blodgett, Phys. Rev. **24**, 49 (1924).

Now substitute Eqs. (9) and (10) into

$$i_+'+i_-=0$$

and obtain after solving for α and substituting numerical values

$$\alpha=5.63\times10^{-7}V^{3/4}e^{V/2}. \quad (12)$$

It is found that Eqs. (11) and (12) will be solved simultaneously only for a value of b greater than 0.999. This indicates that if an ion sheath exists as a result of the interstellar gas, it is a very thin sheath.

Summary and Conclusions

The purpose of the investigation is to consider from a theoretical standpoint what electric fields would be set up if cosmic rays originated on stars and (or) traversed interstellar space as charged particles predominantly of one sign. Four assumptions are made regarding the conditions under which electric currents traverse interstellar space. In these assumptions account is taken of the astrophysical evidence for the existence of a finite density of matter in the space between the stars. The justification for these assumptions is discussed in some detail.

An equation is derived in which the electric field produced at a point in the neighborhood of a single star that intercepts, or emits, cosmic rays as charged particles all of one sign, is related to the rate at which the rays are intercepted, or emitted, by the star, the distance of the point from the center of the star, and the conductivity in interstellar space. It is shown that charge density and current density in interstellar space vanish.

Numerical calculations are made to determine what electric potential will result on a typical star as it intercepts, or emits, cosmic rays as charged particles under the conditions defined by the original assumptions. For the case of interception, the potential is found to be extremely small—of the order of 10^{-12} volt. The potential that would result on the galaxy from the combined average effect of all the stars in the galaxy is even smaller. In the case of emission, an upper limit to the rate at which energy might be emitted in the form of cosmic rays is taken to be the rate of spectral radiation. It turns out

that the assumptions made will not be valid for a star which emits cosmic-ray particles, all carrying the same charge, at this rate. The range of applicability is limited, in the case of a typical star, to rates of emission which are less than this indicated upper limit by a factor of at least 10^{-3}. This still might reasonably be termed an upper limit, and will result in producing a potential on the star of the order of one volt.

The calculations indicate, then, that the cosmic-ray particles will produce very small potentials on the stars. Since these potentials represent the only electric fields set up by the rays, one is led to the general conclusion that, as far as regards the electric fields that would be produced, theoretically it is possible for cosmic rays to originate, and to exist in interstellar space, as charged particles predominantly of one sign.

ACKNOWLEDGMENTS

It is with pleasure that the author acknowledges the continual assistance of Professor Carl Eckart under whose supervision this research was carried out. Appreciation also is expressed to Professor A. H. Compton who suggested the problem, and to Professors Otto Struve and S. Chandrasekhar of the Yerkes Observatory and Doctor W. F. G. Swann of the Franklin Institute for helpful suggestions.

JANUARY 1, 1941 PHYSICAL REVIEW VOLUME 59

The East-West Asymmetry of the Cosmic Radiation at High Latitudes

F. G. P. SEIDL*
Rensselaer Polytechnic Institute, Troy, New York
(Received October 30, 1940)

The sea-level east-west asymmetry of unabsorbed cosmic radiation and of that radiation penetrating two thicknesses of lead, 20° from the vertical, has been measured at geomagnetic latitude 54°N, well above the knee of the latitude effect. Two methods were used to calculate the asymmetry from the data. The results are given in Table I.

THE Stoermer-Lemaître-Vallarta theory of the trajectories of primary cosmic rays in the earth's magnetic field explains the east-west asymmetry near the equator, but this effect should vanish above the knee of the latitude effect where field sensitive rays are not able to penetrate to sea level. Nevertheless, a small sea-level asymmetry has been found[1] at geomagnetic latitudes up to 51°N, approximately 10° higher than the recognized position of the knee. Moreover, experiments 6288 ft. above sea level by Johnson[2] indicated that an asymmetry exists as far north as geomagnetic latitude 56°. While these latter experiments lacked precision, some slight influence of the primary asymmetry might still have been present in the former; therefore, it seemed important to investigate the asymmetry again as accurately as possible at higher latitudes in order to make sure of the existence of such an asymmetry and to ascertain if any variation of this high latitude asymmetry with latitude is detectable. The measurements to be described were made in Troy, New York, geomagnetic latitude 54°N. In order to obtain the greatest precision in a limited time, all the measurements were made at one zenith angle, 20°. However, various thicknesses of lead absorber were used to remove the softer radiation.

A double-coincidence cosmic-ray counter was used to measure the asymmetry. This apparatus was placed in a wooden structure of uniform wall

* Now at the Randal Morgan Laboratory of Physics, University of Pennsylvania, Philadelphia, Pennsylvania.

[1] T. H. Johnson, Phys. Rev. **48**, 287 (1935); T. H. Johnson and E. C. Stevenson, *ibid.* **44**, 125 (1933); E. C. Stevenson, *ibid.* **44**, 855 (1933); J. C. Stearns and R. D. Bennett, *ibid.* **43**, 1038 (1933); A. Ehmert, Physik. Zeits. **35**, 20 (1934); J. C. Stearns and D. K. Froman, Phys. Rev. **46**, 535 (1934).

[2] T. H. Johnson, Phys. Rev. **43**, 381A (1933) and J. Frank. Inst. **214**, 665 (1932).

thickness located upon a hill, from which there were no obstructions in the paths of the rays to be measured. Figure 1 shows the arrangement of the coincidence units and lead absorber. The two trays of G-M tubes and the lead were supported by a sturdy wooden frame free to rotate around a vertical axis. The frame could be tilted at any angle away from the vertical. The sensitive solid angle determined by the apparatus extended almost 20° in either direction beyond the zenith-angle setting—as is evident from Fig. 1—and 37° in either direction of the azimuthal setting.

Two spirit levels mounted on the frame, one perpendicular, the other parallel to the axes of

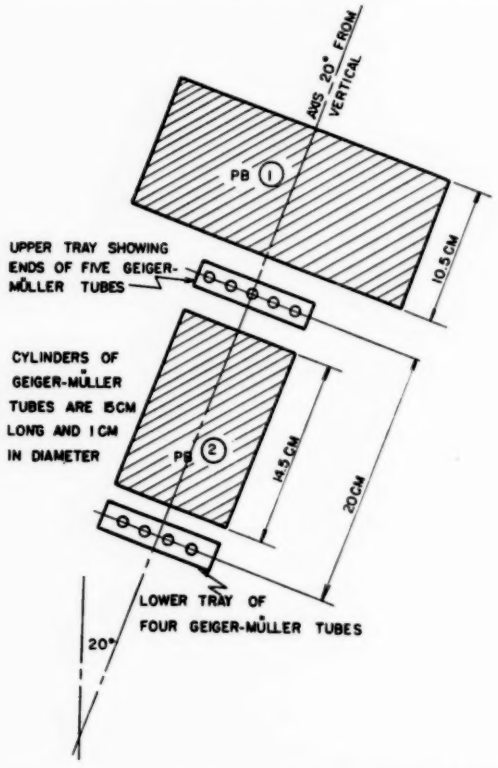
AXIS 20° FROM VERTICAL
PB (1)
10.5 CM
UPPER TRAY SHOWING ENDS OF FIVE GEIGER-MÜLLER TUBES
CYLINDERS OF GEIGER-MÜLLER TUBES ARE 15CM LONG AND 1CM IN DIAMETER
PB (2)
14.5 CM
20 CM
LOWER TRAY OF FOUR GEIGER-MÜLLER TUBES
20°

FIG. 1. Arrangement of counter tubes and of lead for measurement of the asymmetry at 20°.

the G-M tubes, enabled the zenith angle to be reproduced after each reversal of azimuth to better than ±0.1°. Azimuthal settings were made perpendicular to a magnetic meridian which was determined by sighting away from Polaris at an angle equal to the magnetic declination.

Figure 2 shows a circuit diagram of the apparatus. Each unit of the double-coincidence counter was a tray of G-M tubes connected in parallel; the upper tray contained five tubes side by side in a plane, the lower tray contained four tubes. All these tubes were the same, having cathode cylinders of seamless copper tubing, 15.1 cm long, 1.0 cm inside diameter, and tungsten wire anodes 3 mils in diameter. They were operated in an atmosphere of 94 percent argon and 6 percent oxygen at 8 cm of Hg pressure with −760 volts on their cathodes. This high voltage was obtained from a Street-Johnson[3] regulated high voltage circuit. *B* and *C* voltages were taken from a regulated voltage supply having a circuit very similar to that of an RCA TMV-118-B regulated power unit. Finally, in order to avoid spurious counting, the whole apparatus including G-M tubes, recording circuit, power supplies, and cables were shielded electrostatically.

Frequent tests showed that the only counts recorded originated from G-M counter discharges. With the two coincidence units separated horizontally by 85 cm, the number of accidental coincidences was found to be 3.80±0.22 counts per hour; but, since the asymmetry is a relative measurement, any correction for accidentals, showers, or inefficiency is unimportant, because these effects are constant with azimuth.

The mechanical recorder, operated by the plate current of a type 89 tube, consisted of a small electromagnet working the escapement wheel of an Ingersoll watch. During part of the investigation, two of these recorders were connected in series and found to give the same number of counts. The counting periods were timed to about one part in ten thousand by two electric clocks.

The apparatus was run on a 24-hour schedule almost continuously from December 1, 1939 until August 2, 1940. During this time, runs were made with 25 cm of lead absorber (blocks No. 1 and No. 2 of Fig. 1 in place), with 14.5 cm of lead (block No. 2 in place), and with no absorber (blocks No. 1 and No. 2 removed). According to the Bethe-Bloch theory of ionization,[4] 25 cm of lead is the range of a mesotron of 3.5×10^8 ev and

[3] J. Street and T. H. Johnson, J. Frank. Inst. **214**, 155 (1932).

[4] See S. H. Neddermeyer and C. D. Anderson, Rev. Mod. Phys. **11**, 191 (1939).

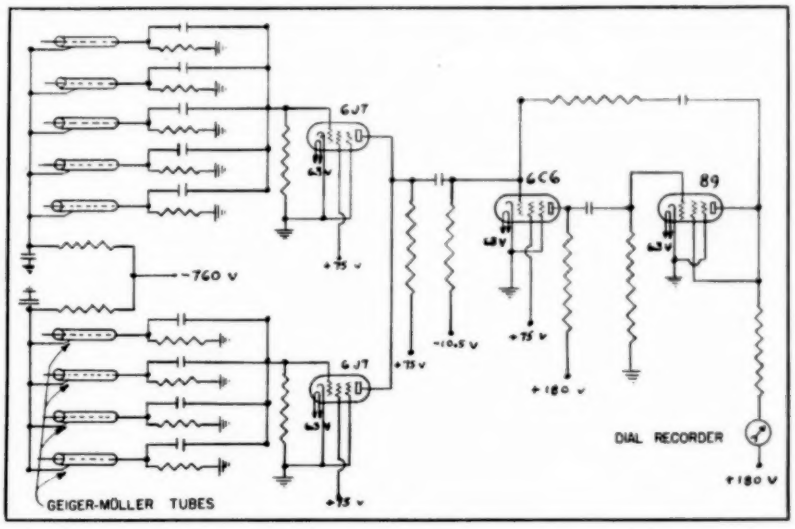

FIG. 2. Double-coincidence counter circuit.

14.5 cm of lead is the range of a 2.2×10^8-ev mesotron.

Data collected during most of April, 1940, exhibit a barometer effect of the expected magnitude. These data were taken by turning the apparatus towards the west for 12 hours, towards the east for 12 hours, then back to the west again, etc. Upon comparing the number of times a barometer correction would increase the value of the asymmetry to the number of times such a correction would decrease the asymmetry, it was found that a barometer correction of this particular data would not have appreciably influenced the average value of the asymmetry. This justifies neglecting the correction to the data for barometric fluctuations, especially, since about $\frac{2}{3}$ of the data for the no-lead value and $\frac{2}{3}$ for the 14.5-cm-of-lead value have been obtained from a series of six-hour runs made in the order of east-west-west-east-east-west, etc.

In order to remove any possible influence of diurnal cosmic-ray intensity variations, the times of day during which intensities from the east and west were recorded were interchanged once a week.

Two methods were used to obtain the asymmetry from the data. The result of the first method is denoted by $\alpha_{20°}$ and was obtained by the relation

$$\alpha_{20°}=2(\bar{j}_w-\bar{j}_e)/(\bar{j}_w+\bar{j}_e), \qquad (1)$$

where $\bar{j}_w$ and $\bar{j}_e$ are, respectively, the average cosmic-ray intensities from west and east with the apparatus tilted 20° from the vertical. The probable error of $\alpha_{20°}$ was obtained from the probable errors of $\bar{j}_w$ and $\bar{j}_e$; and the probable errors of the latter were taken as $\pm0.6745(\bar{j}/\sqrt{N})$, where N is the total number of counts used to determine $\bar{j}$. In the second method the intensities $\bar{j}_w$ and $\bar{j}_e$ used in Eq. (1) were replaced by j_w and j_e to obtain an asymmetry for each pair of east-west runs. The arithmetic mean of these asymmetries was calculated by weighting each asymmetry according to the length of time used in the determination of its j_w and j_e, and this mean is denoted by $\bar{\alpha}_{20°}$. The probable error of $\bar{\alpha}_{20°}$ is taken to be

$$\pm0.6745[(n-1)\sum_n f_i]^{-\frac{1}{2}}[\sum_n f_i d_i^2]^{\frac{1}{2}},$$

where f_i is the weight of the asymmetry for the ith pair of runs and d_i is its deviation from the mean.

Table I shows the values of the asymmetry for various thicknesses of lead absorber together with their probable errors. It may be noticed that the values for $\alpha_{20°}$, $\bar{\alpha}_{20°}$, and their probable errors are practically identical except for 25.0 cm of lead. In this case the discrepancies can be accounted for by an uncertainty in the operation of the recorder, leading to larger fluctuations but, presumably, to no systematic errors.

The value for the asymmetry of the total unabsorbed radiation is in agreement with asymmetry observations made 20° from the

TABLE I. *Data on asymmetry. E_{min} is the minimum energy required to penetrate the lead shielding.*

E_{MIN} (EV)	CM Pb	ASYMMETRY $\alpha_{20°}$	ASYMMETRY $\bar{\alpha}_{20°}$	INTENSITY AT 20° FROM VERTICAL (COUNTS/HOUR) 20°W	20°E	AVE.
—	0.0	+0.0009	+0.0010	249.03	248.81	248.92
		±0.0022	±0.0022	±0.40	±0.40	±0.28
2.2×10^8	14.5	+0.0075	+0.0073	174.02	172.72	173.37
		±0.0026	±0.0027	±0.32	±0.31	±0.22
3.5×10^8	25.0	+0.0062	+0.0056	164.40	163.38	163.89
		±0.0032	±0.0048	±0.37	±0.37	±0.26

vertical by Johnson[5] at geomagnetic latitude 51°N, although he obtained values at neighboring angles more nearly in accord with those found in the present work with the lead shields. Comparison of these results indicates no marked difference in the asymmetries in latitudes 51°N and 54°N.

The theory of the asymmetry resulting from deflections of charged particles in the atmosphere has been developed by Johnson,[6] and in the light of his theory it is interesting to compare the effect of lead absorbers upon the asymmetry with a corresponding effect of lead shields upon the excess in the number of positive over negative mesotrons found in cloud-chamber photographs at sea level. Although Hughes[7] and Jones[8] have found no significant difference in the ratio of positives to negatives when a 10-cm lead plate was inserted between their controlling counters, Leprince-Ringuet and Crussard[9] found the positive excess was considerably amplified when 14 cm of lead were used. Their results may thus have some relation to the difference found in the present work between the asymmetries with and without shields. For example both results would be explained if the lead absorbs negative rays selectively and allows a larger fraction of positives in the low energy range to pass through. In attempting to explain the apparent effect of lead shields upon the asymmetry it must be noted that the present results contain rather large probable errors and there is a distinct possibility that the effect may be the result of statistical fluctuations.

The author is greatly indebted to Dr. T. H. Johnson for suggesting this problem and for his generous, helpful advice and to Dr. R. A. Patterson and other members of the Department of Physics, Rensselaer Polytechnic Institute, who made this investigation possible.

[5] T. H. Johnson, Phys. Rev. **48**, 287 (1935).
[6] T. H. Johnson, Phys. Rev. **59**, 11 (1941), following paper.
[7] D. Hughes, Phys. Rev. **57**, 592 (1940).
[8] H. Jones, Rev. Mod. Phys. **11**, 235 (1939).
[9] L. Leprince-Ringuet and J. Crussard, J. de phys. et rad. **8**, 207 (1937).

The East-West Asymmetry of the Cosmic Radiation in High Latitudes and the Excess of Positive Mesotrons

THOMAS H. JOHNSON
Bartol Research Foundation of the Franklin Institute, Swarthmore, Pennsylvania
(Received October 30, 1940)

The slight east-west asymmetry of the cosmic radiation in high latitudes, now confirmed by Seidl, is interpreted to be the result of the deflection by the earth's magnetic field of the mesotron component while the rays are losing energy by ionization in the atmosphere. Since this component contains about twenty percent more positive than negative rays these deflections result in an asymmetry. Orbits of rays, including those in the range of energy where rest mass cannot be neglected, have been investigated and the deflections determined. It is assumed that deflections without energy loss, namely, those of the primary rays described by the theory of Lemaître and Vallarta, result in a symmetrical distribution for the energy ranges concerned. The asymmetry is traced to the *difference* between the actual deflection and that of a ray which loses no energy. The "difference" deflection δ shifts the angular distribution so that rays which, in the absence of a field, would have produced an intensity proportional to $\cos^2\zeta$ at zenith angle ζ actually produce this intensity at an angle $\zeta+\delta$. Asymmetries calculated in this way agree with the observed values, and give the correct variation of asymmetry with zenith angle and elevation. Although the data are meager, the theory seems to be in accord with the existing evidence regarding the effect of absorbing material upon the asymmetry.

INTRODUCTION

IT is now recognized that the east-west asymmetry of the cosmic radiation occurring in the equatorial zone is produced by the deflection of primary cosmic rays before their entry into the earth's atmosphere, and that it arises from an excess of positive particles in that part of the primary radiation responsible for the intensity in the lower part of the atmosphere. These primary deflections, however, do not explain the slight asymmetry observed in high latitudes nor the comparatively large asymmetries noted at zenith angles near the horizon within the equatorial belt. Since the slight increase of cosmic-ray intensity with latitude at latitudes above the so-called knee of the latitude effect has now been explained as a temperature effect,[1] it is probable that no rays in the field sensitive range of energy at these high latitudes make their effects felt at sea level. It has been shown by Lemaître and Vallarta that rays of energy greater than the field sensitive range, the only rays whose effects are felt at sea level in high latitudes, are incident uniformly from all directions, and the high latitude asymmetry cannot be traced to the deflections of the primary rays themselves. But as rays lose energy in the atmosphere, they are deflected by the magnetic field from their primary orbits. Since the observations of Hughes and others[2] have shown the presence in the atmosphere of about twenty percent more positive than negative mesotrons, these deflections produce an asymmetry in the angular distribution.

Deflections of this type have been discussed by Bowen[3] and by Rossi[4] who have shown that no appreciable part of the equatorial asymmetry can be explained in this way, but it appears from the present treatment that this effect can account for the high latitude asymmetry and for the asymmetries at large zenith angles in the equatorial belt. Since we now have a considerably greater knowledge of the behavior and the composition of the cosmic radiation than was available at the time of the former discussions of this effect, the present treatment is somewhat different from those of the above authors.

The first evidence of an east-west effect was observed by Johnson and Street[5] on the summit of Mount Washington, New Hampshire, geomagnetic latitude 56°, considerably above the knee of the latitude effect which recent investigations have placed at about the latitude of 40°.

[1] A. H. Compton and R. N. Turner, Phys. Rev. **52**, 799 (1937); P. M. S. Blackett, *ibid.* **54**, 973 (1938).

[2] D. J. Hughes, Phys. Rev. **57**, 592 (1940); P. M. S. Blackett, Proc. Roy. Soc. **A159**, 1 (1937); L. Leprince-Ringuet and J. Crussard, J. de phys. et rad. **8**, 207 (1937).

[3] I. S. Bowen, Phys. Rev. **45**, 349 (1934).

[4] B. Rossi, Rendi Lincei **15**, 62 (1932).

[5] T. H. Johnson, J. Frank. Inst. **214**, 665 (1932); T. H. Johnson and J. C. Street, Phys. Rev. **43**, 381 (1933).

Later and more accurate measurements in Pennsylvania and in Colorado by Johnson and Stevenson[6] and by Stearns and Froman[7] have confirmed the existence of a high latitude asymmetry and have shown that it amounts to about one percent at 30° from the zenith, probably increasing to about five percent at 60°. The effect is almost independent of elevation up to the summit of Mount Evans, 14,000 feet above sea level. In a recent extended series of observations carried out at Troy, New York, 54° N geomagnetic latitude, Seidl[8] has measured the asymmetry at an average zenith angle of 20° and has shown that it is not much affected by lead absorbing screens up to 25 cm thick, but probably diminishes slightly with increase of lead thickness. In the equatorial belt the writer[6] has noted an indication of an abnormally high asymmetry close to the horizon where the normal asymmetry should disappear because of atmospheric absorption.

In order to account for these effects, we assume that the rays reaching sea level are symmetrically distributed upon their arrival at the top of the atmosphere or at the point where they are produced as secondaries of such symmetrically distributed primary radiation, but as the rays are slowed down by atmospheric ionization their paths become more and more curved and when they have reached the observer they have experienced a slight deflection from their original direction or the direction they would have had in the absence of energy losses. Any unbalance in the numbers of positives and negatives results in an asymmetry, for if the average deflection is δ, the intensity at zenith angle $\zeta+\delta$ corresponds to that occurring at angle ζ in the symmetrical distribution. The deflection is toward the west for positive rays and towards the east for negatives. When treated in this way it becomes unnecessary to consider the details of atmospheric absorption or of the instability of the mesotron, for the influence of these phenomena upon the probability that a ray will arrive at sea level from the direction concerned is already taken into account in determining the normal symmetric distribution.

Theory of the Deflections

Since we are concerned with an explanation of the east-west asymmetry, we will consider rays whose orbits lie in the east-west vertical plane. In calculating the deflection suffered by a cosmic ray during its trip through the atmosphere, the approximation will be used that the rate of loss of energy by ionization is independent of the energy and is equal to αm_0c^2 per cm of air at a pressure of one atmosphere. This approximation is accurate within a few percent for mesotron energies greater than about ten million volts and is expressed by

$$d\epsilon/ds=\alpha p, \tag{1}$$

where p is the pressure in atmospheres, s is the orbital distance measured backwards along the orbit from the position of the observer, and ϵm_0c^2 is the energy of the ray, i.e., $\epsilon=(1-\beta^2)^{-\frac{1}{2}}-1$. The radius of curvature of the ray in the earth's field, whose horizontal component is H, is given by

$$\rho=R(\epsilon^2+2\epsilon)^{\frac{1}{2}}, \tag{2}$$

where R stands for the quantity m_0c^2/eH.

The variation of ρ with orbital distance is then given by

$$d\rho/ds=(d\rho/d\epsilon)(d\epsilon/ds)=\alpha Rp(\epsilon+1)(\epsilon^2+2\epsilon)^{-\frac{1}{2}} \tag{3}$$

or by making use of Eq. (2)

$$d\rho/ds=\alpha Rp(1+R^2/\rho^2)^{\frac{1}{2}}. \tag{4}$$

[6] T. H. Johnson, Phys. Rev. **48**, 287 (1935); T. H. Johnson and E. C. Stevenson, *ibid.* **44**, 125 (1933).
[7] D. K. Froman and J. C. Stearns, Phys. Rev. **46**, 535 (1934).
[8] F. G. P. Seidl, Phys. Rev. **59**, 7 (1941), preceding paper.

TABLE I. *The atmospheric deflection δ, expressed in radians, for mesotrons of various energies as a function of the zenith angle of the orbits and the elevation of the observer.*

FINAL ENERGY EV $\times 10^{-9}$	0	1	2	4	8	15	30	60
Sea level								
$\zeta = 0°$	0.077	0.049	0.039	0.028	0.017	0.010	0.0041	0.0015
20°	0.079	0.050	0.040	0.030	0.018	0.0105	0.0047	0.0017
40°	0.083	0.054	0.045	0.033	0.022	0.014	0.0060	0.0024
60°	0.093	0.063	0.054	0.042	0.030	0.0195	0.010	0.0044
Alt. 4300 m								
$\zeta = 20°$	0.11	0.064	0.049	0.032	0.019	0.0095	0.0036	0.0012
40°	0.12	0.073	0.057	0.040	0.023	0.012	0.0049	0.0017
60°	0.13	0.080	0.069	0.052	0.033	0.019	0.0086	0.0034

If h_0 is the extent of the homogeneous atmosphere, the pressure at any height x above sea level is given approximately by $p = \exp(-x/h_0)$. Since, as the calculation will show, the maximum deflection does not exceed a few degrees, x may be replaced by $x_0 + s\cos\zeta$ where ζ is the zenith angle of the ray when it reaches the observer, and x_0 is the height above sea level of the observer. Then Eq. (4) may be written

$$d\rho/ds = \alpha R(1+R^2/\rho^2)^{\frac{1}{2}} \exp[(-x_0 - s\cos\zeta)/h_0]. \tag{5}$$

The integral of (5) is

$$\rho = [(a - be^{-\gamma s})^2 - R^2]^{\frac{1}{2}}, \tag{6}$$

where $a = [\rho_0^2 + R^2]^{\frac{1}{2}}$, ρ_0 is the initial radius of curvature of the ray upon its entry into the atmosphere at a height considered to be great compared with h_0 but small compared with the radius of the earth, b is R times the energy, expressed in units of m_0c^2, of a ray just able to penetrate from the top of the atmosphere to the observer, i.e.,

$$b = \alpha R h_0 \sec\zeta \exp(-x_0/h_0) \quad \text{and} \quad \gamma = (\cos\zeta)/h_0.$$

Writing $z = be^{-\gamma s}/a$ and $k = R/a$, the deflection of a ray during its passage through the atmosphere is

$$\theta = \int_{s=0}^{s_1} ds/\rho = -(1/\gamma a)\int_{z=b/a}^{(b/a)\exp(-\gamma s_1)} [z^{-1}(z^2 - 2z + 1 - k^2)^{-\frac{1}{2}}]dz, \tag{7}$$

where s_1 is some distance, large compared with $h_0 \sec\zeta$ but small compared with the radius of the earth. On integrating Eq. (7) and putting in the limits, the total deflection is

$$\theta = (1/\gamma a)(1-k^2)^{-\frac{1}{2}}\{\log[\{[1-(b/a)e^{-\gamma s_1}]^2 - k^2\}^{\frac{1}{2}} + (1-k^2)^{\frac{1}{2}} - (b/a)e^{-\gamma s_1}(1-k^2)^{-\frac{1}{2}}]$$
$$- \log[\{[1-(b/a)]^2 - k^2\}^{\frac{1}{2}} + (1-k^2)^{\frac{1}{2}} - (b/a)(1-k^2)^{-\frac{1}{2}}]\} + (s_1/a)(1-k^2)^{-\frac{1}{2}}. \tag{8}$$

The last term of Eq. (8) is the deflection

$$\theta_0 = \int_{s=0}^{s_1} \frac{ds}{\rho_0},$$

which the ray would have experienced over the same path if no energy had been lost by atmospheric ionization, a deflection which we assume would have resulted in a symmetric distribution at sea level. The increased deflection resulting from atmospheric energy losses is then $(\theta - \theta_0)$ and in the limit $(s_1 = \infty)$ this converges to

$$\delta = \lim_{s_1=\infty}(\theta - \theta_0) = \frac{1}{\gamma a(1-k^2)^{\frac{1}{2}}} \log \frac{2}{1 - \dfrac{b}{a(1-k^2)} + \left[\dfrac{(1-b/a)^2 - k^2}{1-k^2}\right]^{\frac{1}{2}}}. \tag{9}$$

The deflections calculated from Eq. (9) for mesotrons reaching the observer from various zenith angles at sea level and at 4300 m elevation are shown as a function of the final energy in Table I. In making these calculations the following values of the constants have been used: $\alpha=2.5\times10^{-5}$, corresponding to a mass energy of the mesotron of 10^8 electron volts, and an ionization loss of 2500 volts per cm at normal atmospheric pressure; $H=0.18$ c.g.s. unit, the value of the horizontal component of the earth's field at Troy; $h_0=8.0\times10^5$ cm; $R=18.5\times10^5$ cm.

It is an interesting feature of this form of the theory that a ray is completely stopped before it has been deflected through a very large angle. For example, a ray with initial radius of curvature $\rho_0=(b^2+2bR)^{\frac{1}{2}}$, having just enough energy to reach sea level along the orbit inclined at angle ζ from the zenith, is deviated by only 4° 21′ at $\zeta=0°$.

Calculation of the Asymmetry

Since the deflection is a function of the final energy of the ray, the average deflection depends upon the energy distribution of the radiation at sea level. Studies of the magnetic bending of cosmic rays in the cloud chamber[9] have shown this distribution to be of the form

$$N(E)dE=(A/E^n)dE, \quad \text{with } n \text{ about } 3.$$

The average deflection is then

$$\bar{\delta}=(n-1)E_1^{n-1}\int_{E_1}^{\infty}[\delta(E)/E^n]dE, \qquad (10)$$

where the limit E_1 of the integral corresponds to the stopping power of the instrument, or, if no absorber is used in the instrument, this limit is about 2×10^8 electron volts below which it has been found[9] that very few mesotrons are present in the atmosphere. In Seidl's apparatus two thicknesses of lead shields have been used, one 14.5 cm thick and the other 25 cm thick, whereas in the experiments of the writer and in one of Seidl's experiments no lead was used. Corresponding to these thicknesses the low energy limits are 2.2×10^8 electron volts and 3.5×10^8 electron volts, respectively. The values of $\bar{\delta}$ calculated from Eq. (10) are shown in Table II.

If the positive or the negative rays are considered alone, the first-order effect of these deflections is to shift the angular distribution through the angle $\bar{\delta}$. The intensity which in the absence of this phenomenon would have appeared at any zenith angle ζ will actually be found at the angle $\zeta+\bar{\delta}$. Since the length of the path through the atmosphere is not greatly altered by these deflections, it is not necessary to bring into consideration phenomena which affect the probability that a ray will reach sea level along a given orbit, for these phenomena are operative in determining the normal angular distribution of the radiation. To a close approximation this distribution is given by

$$j(\zeta)=j_0\cos^2\zeta. \qquad (11)$$

Hence, the difference of the intensities on the two sides of the zenith at angle ζ is

$$j(\zeta+\bar{\delta})-j(\zeta-\bar{\delta})=2\bar{\delta}(dj/d\zeta)=4\bar{\delta}j(\zeta)\tan\zeta.$$

The asymmetry, then, of the purely positive or of the purely negative component is

$$\alpha=2(j_w-j_e)/(j_w+j_e)=4\bar{\delta}\tan\zeta.$$

If, on the other hand, a fraction f of the total radiation consists of positives unbalanced by negatives, the asymmetry will have the value

$$\alpha=4f\bar{\delta}\tan\zeta.$$

The observations of Hughes indicate that $f=0.20$, there being more positives than negatives. With this value of f the calculated values of the asym-

Table II. *Values of the average deflection $\bar{\delta}$ in radians.*

Low Energy Limit	Sea Level			4300 Meters		
	$\zeta=20°$	40°	60°	20°	40°	60°
$E_1=2.2\times10^8$ ev	0.031	0.033	0.045	0.034	0.043	0.054
$E_1=3.5\times10^8$ ev	0.023	0.024	0.030	0.023	0.029	0.042

Table III. *Calculated values of the asymmetry at various zenith angles and altitudes for two lead thicknesses.*

Low Energy Limit	Sea Level			4300 Meters		
	$\zeta=20°$	40°	60°	20°	40°	60°
$E_1=2.2\times10^8$ ev	0.0089	0.022	0.061	0.010	0.029	0.075
$E_1=3.5\times10^8$ ev	0.0065	0.015	0.043	0.007	0.020	0.058

[9] P. M. S. Blackett. Proc. Roy. Soc. **A159**, 1 (1937).

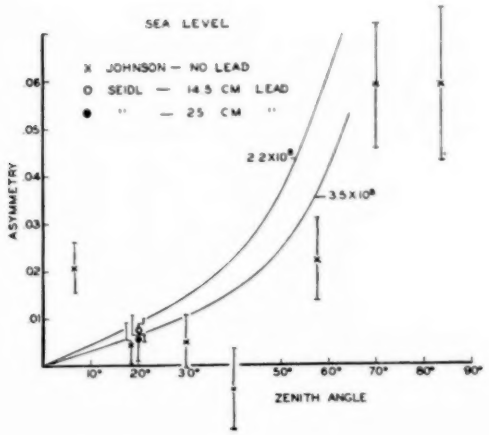

FIG. 1. The high latitude asymmetry at sea level, plotted against zenith angle. The curves show the theoretical values based upon an energy distribution proportional to E^{-3}, with lower limits at 2.2×10^8 electron volts and at 3.5×10^8 electron volts, corresponding respectively to lead absorber thicknesses of 14.5 cm and 25 cm. The points represent the experimental values obtained by Seidl and Johnson.

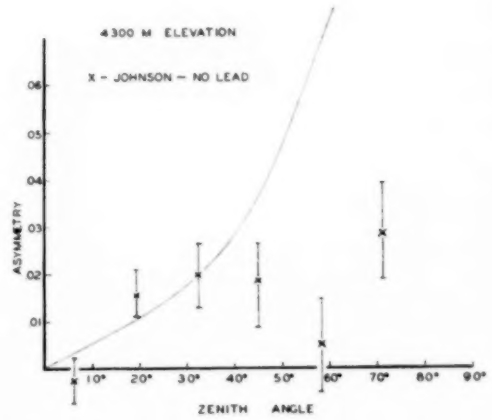

FIG. 2. The high latitude asymmetry at an elevation of 4300 meters above sea level (0.6 atmosphere). The curve shows the theoretical values based upon an E^{-3} distribution with a lower energy limit at 2.2×10^8 electron volts.

metry for the two lead thicknesses are given in Table III. Figures 1 and 2 show the variations of the asymmetry with zenith angle at the two elevations. The curves represent the calculated values, while the points indicate the values found by Seidl and the writer. In every case the probable errors are large, but there seems to be some justification for the belief that the theory gives an adequate representation of the data, both as regards the magnitude of the asymmetry and its variations with zenith angle and thickness of lead absorber. The theory gives a somewhat larger asymmetry than is observed near the horizon, especially at the higher elevation. This may indicate that the predominance of the positive component is not as pronounced at the higher elevations as that corresponding to the value $f=0.20$. This could be explained by the presence at the higher elevations of a larger fraction of soft component rays consisting of equal numbers of positive and negative electrons.

It may also be noted that Blackett[10] in a more recent paper points out that the spectrum is nearly constant for energies less than 10^9 volts and at higher energies it falls off as E^{-2} or a little faster. An energy distribution of this type would give a higher average energy than that of the E^{-3} distribution upon which the calculations have been based, and a consequent lower asymmetry. Thus it seems possible to bring the theory into better accord with the asymmetry at zenith angles close to the horizon without disturbing its agreement with the data at higher angles at sea level. At the higher elevation, however, it would be necessary to invoke some asymmetry of the primary rays to explain the apparent peak at 30°. Such an assumption would not necessarily be out of harmony with other facts for the knee of the latitude effect may well lie above 51° at that elevation.

In conclusion, the writer takes pleasure in acknowledging several stimulating discussions of this problem with Mr. F. G. P. Seidl who has contributed essential elements in its final formulation.

[10] P. M. S. Blackett, Proc. Roy. Soc. **A165**, 11 (1938).

The Scattering of Alpha-Particles in Helium*

JOHN ARCHIBALD WHEELER
Princeton University, Princeton, New Jersey

(Received November 8, 1940)

Deviations from the scattering to be expected on the basis of an inverse square law of force between alpha-particles receive a satisfactory interpretation in terms of the influence on particles of zero, two and four units of angular momentum of a specific nuclear interaction having a range less than 9×10^{-13} cm. The semistable state of the compound nucleus Be^8 formed in certain disintegration experiments is found from the scattering analysis to have an energy of about 3 Mev, a mean life of 0.8×10^{-21} sec., and *zero* angular momentum. There is also some evidence for a semistable state of still shorter life with two units of angular momentum and an energy of 4 to 5 Mev.

(1) INTRODUCTION

THE observations on the scattering of alpha-particles in helium accumulated from 1927 to the present[1–6] have led so far on the theoretical side to relatively little of positive value either for the understanding of nuclear structure in general or even for the description of the interaction between two alpha-particles.

The first serious attempt to analyze the anomalous scattering of alpha-particles on the basis of the wave description of matter was made by Taylor.[7,8] He assumed that exclusively those particles which collide with zero mutual angular momentum come close enough to experience departures from the inverse square law of force. In the hands of Breit and his collaborators this assumption has since proved a safe starting point for interpreting the proton-proton scattering,[9] where the classical distance of closest approach, λ, of particles with even one unit of angular momentum is already large compared to the extension of the forces ($\lambda = h/\text{velocity}\cdot\text{reduced mass} = \text{wave-length}/2\pi = 9\times10^{-13}$ cm for 1-Mev protons). For 7-Mev alpha-particles scattered in helium, however, this distance is sufficiently small in comparison with nuclear dimensions that particles of three or four units of angular momentum must be influenced by the departures from the inverse square law ($\lambda = 1.7\times10^{-13}$ cm as against an estimated alpha-particle diameter of 5 or 6×10^{-13} cm). We therefore have to expect that the scattered alpha-particle wave is a complicated superposition of partial waves including the zero-order wave as well as waves corresponding to two and four units of angular momentum (waves of odd order not appearing because the alpha-particles obey the symmetric statistics). In fact, while Taylor found that an anomalous zero-order partial wave of suitable magnitude superposed on the normal (inverse square law) scattered wave gave a fair fit to the intensity of scattering at 45° and 37°, he encountered[8] a disagreement with subsequent observations[4] at 10° quite outside the experimental error. Moreover, the assumed interaction potential predicted not only a very stable Be^8 nucleus, in contradiction to all available evidence, but also, as is readily shown, anomalous partial waves of higher orders with amplitudes so great as to prove the analysis internally inconsistent.

An attempt was soon made to follow up Taylor's most suggestive beginning, to allow for the influence of higher order waves, and to

* The present work was initiated in the winter of 1933–34 when the author was a National Research Fellow at New York University. He wishes to express his appreciation to Professor G. Breit for many suggestive discussions on this and other subjects at that time. Completion of the analysis of the alpha-particle scattering has only been made possible, as pointed out in the text, through the recent measurements of Mohr and Pringle and of Devons. The author is indebted to Dr. Mohr and Dr. Pringle for much helpful correspondence in connection with this work.

[1] E. Rutherford and J. Chadwick, Phil. Mag. **4**, 605 (1927).
[2] J. Chadwick, Proc. Roy. Soc. **A128**, 120 (1930).
[3] P. M. S. Blackett and F. C. Champion, Proc. Roy. Soc. **A130**, 380 (1931).
[4] P. Wright, Proc. Roy. Soc. **A137**, 677 (1932).
[5] C. B. O. Mohr and G. B. Pringle, Proc. Roy. Soc. **A160**, 193 (1937).
[6] S. Devons, Proc. Roy. Soc. **A172**, 564 (1939).
[7] H. M. Taylor, Proc. Roy. Soc. **A134**, 103 (1931).
[8] H. M. Taylor, Proc. Roy. Soc. **A136**, 605 (1932).
[9] See G. Breit, H. M. Thaxton and L. Eisenbud, Phys. Rev. **55**, 1018 (1939) and earlier work there cited.

determine their amplitudes.[10] The angular distribution of scattered particles was not known in sufficient detail, however, to lead to a unique or acceptable analysis of the data. Only now, with the additional and indispensable observations of Mohr and Pringle[5] and of Devons[6] available, does it become possible to narrow down the possible alternative interpretations of the scattering to one. This analysis, given below, is in reasonable accord not only with the observations but also with indirect information about the interaction between two alpha-particles provided by certain disintegration experiments in which the compound nucleus Be^8 is formed in an excited unstable state.

The information obtained from anomalous scattering in the present paper is combined in the following article[11] with other observational evidence (a) to determine as completely as possible the properties of the compound nucleus Be^8 and (b) particularly to test, and on the whole confirm, the predictions for this nucleus of a suitably formulated alpha-particle model of light nuclei based on symmetry arguments rather than on any assumed law of force between alpha-particles. The difficulties which in fact lie in the way of any attempt to give a *detailed* account of the interaction between two alpha-particles are especially emphasized by Professor H. Margenau[12] in an accompanying paper. There he shows that hopes of calculating the interaction between two alpha-particles, along the general lines he and others have followed so successfully in dealing with the van der Waals interaction between atoms, must in the last analysis be renounced because the range of the interactions between the constituent neutrons and protons is short in comparison with nuclear dimensions.

The following theoretical analysis of the scattering experiments takes a simple form through the employment of vectors in the complex number plane to represent the amplitudes of the various partial waves, the corresponding "phase shifts" being simply related to the direction of these vectors (Section 2). Geometrical arguments lead, in Section 3, to a simple procedure to determine the phase shifts or, equivalently, the strengths of the partial waves of orders zero, two, and four. Between the three alternative sets of values so found for the three phase shifts, a decision is not possible on the basis of the scattering observations alone. Additional experimental and theoretical information however, clearly singles out as correct a particular set of phase shifts from the behavior of which it follows that the semistable state of Be^8 obtained in certain disintegration experiments has an angular momentum, not of two units as previously generally believed, but of zero (Section 4). The strength of the fourth-order wave gives an approximate estimate of the range of the interaction between alpha-particles (Section 5). Section 6 gives a theoretical treatment of the variation of phase shift with energy near a resonance level, taking account in a semiclassical approximation the influence of the long range forces, and the results allow a determination of some of the properties of the semistable state of Be^8 (Section 7).

(2) Representation of the Scattered Amplitude as a Superposition of Partial Waves

The quantum formula for the ratio, R, of actual number of particles observed at an angle φ compared to the number given by Rutherford's law is[7, 8]

$$R(\varphi)=|A'(\varphi)+A''(\varphi)+\sum_{L=0}^{\infty}A_L(\varphi)(1-\exp 2iK_L)|^2. \tag{1}$$

Here the terms

$$A'(\varphi)=\cos^2\varphi(\sin^4\varphi+\cos^4\varphi)^{-\frac{1}{2}}\exp i\cdot(4e^2/\hbar v)\ln(1/\sin^2\varphi) \tag{2}$$

and

$$A''(\varphi)=A'(\tfrac{1}{2}\pi-\varphi)=\sin^2\varphi(\sin^4\varphi+\cos^4\varphi)^{-\frac{1}{2}}\exp i\cdot(4e^2/\hbar v)\ln(1/\cos^2\varphi) \tag{3}$$

[10] J. A. Wheeler, Phys. Rev. **45**, 746 (1934), and independently by E. Feenberg, according to a private communication of his results in April, 1934, for which the author wishes here to make appreciative acknowledgment.
[11] J. A. Wheeler, Phys. Rev. **59**, 27 (1941), following paper.
[12] H. Margenau, Phys. Rev. **59**, 37 (1941), this issue.

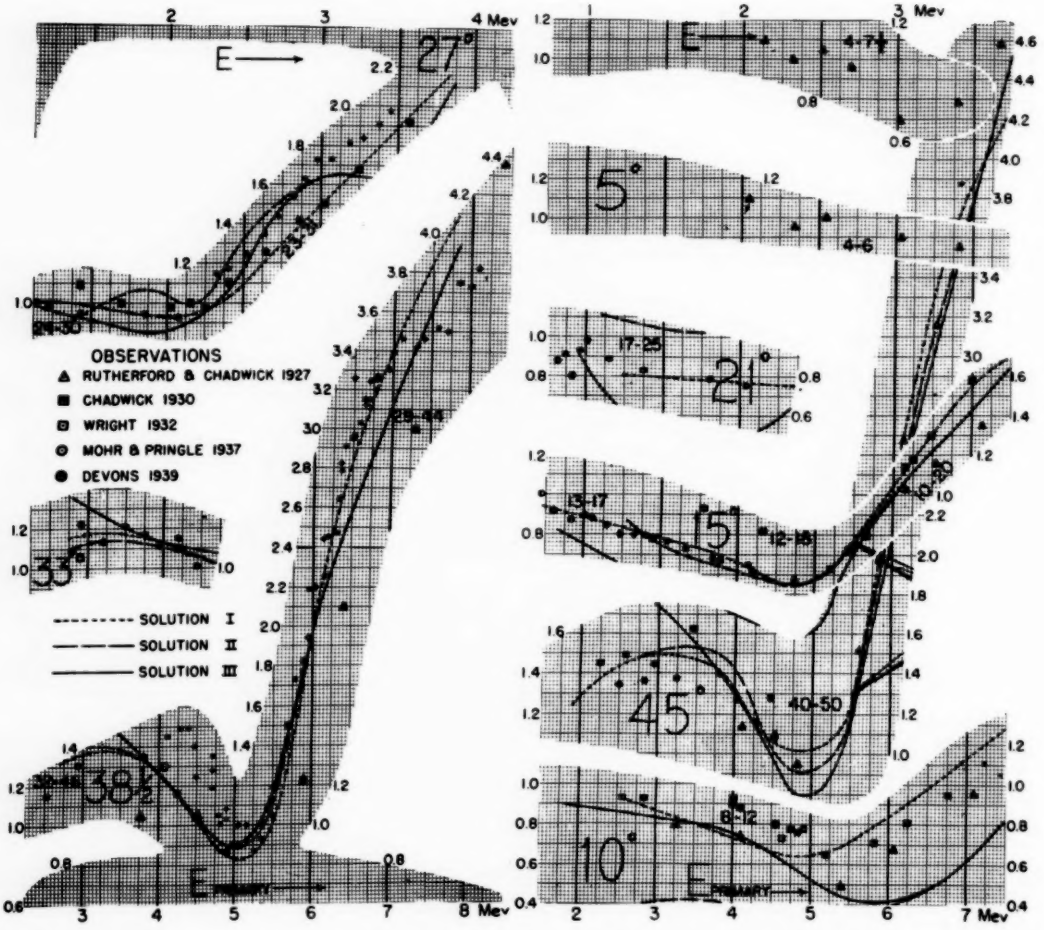

FIG. 1 (left). The square root of the ratio between the actual scattering and that predicted by the Rutherford law is plotted vertically as a function of the energy, E_{primary}, of the incident alpha-particle or of the excitation energy, E available for formation of a temporary compound nucleus Be^8. Included in the figure are all observations except early ones (reference 3) performed with a cloud chamber and without special attempt to reduce the statistical errors to a point where a measurement of anomalous scattering would result. Angular aperture of the diaphragms which defined the scattering volume is indicated for each angle by a notation near the corresponding set of experimental values. The curves are calculated from Eq. (1) and the three alternative sets of phase shifts shown in Figs. 4 and 5. Only solution III is in accord with additional experimental and theoretical evidence cited in the text.

FIG. 2 (right). Continuation of Fig. 1. The measurements at 15° indicated by the compass points are used in Fig. 3(A).

represent in relative magnitude and phase the amplitudes of the waves which would be scattered and knocked on, respectively, at an angle φ, and for a velocity v, if the inverse square law of force applied. The absolute values of the amplitudes are so defined that addition of the corresponding *intensities* gives unity: $|A'|^2+|A''|^2=1$. The addition of amplitudes rather than intensities in Eq. (1) brings about a quantum-mechanical interference effect and consequent deviation from classical scattering which was first noted by Mott.[13] Moreover, the specific nuclear interaction itself alters the scattering amplitude. Equation (1) expresses this alteration as the sum of terms of the type $A_L(\varphi)(1-\exp 2iK_L)$. Each term represents the modification of a partial wave of a particular order, L (L is an even integer). The first factor in the term does not depend on the nature of the forces and is given by the expression

$$A_L(\varphi)=-2i(hv/4e^2)(1/\sin^4\varphi+1/\cos^4\varphi)^{-\frac{1}{2}}(2L+1)P_L(\cos 2\varphi)$$
$$\times\exp 2i\{\arctan(4e^2/hv)+\arctan(1/2)(4e^2/hv)+\cdots+\arctan(1/L)(4e^2/hv)\}. \quad (4)$$

[13] H. M. Mott, Proc. Roy. Soc. **A126**, 259 (1929).

The second factor, $1-\exp 2iK_L$, is determined by the constant difference, K_L, which exists at large distances between (a) the phase of the actual radial wave function associated with the motion of two alpha-particles of mutual angular momentum L and (b) the phase calculated on the basis of inverse square forces (in which case the wave function varies asymptotically as $\sin\{(r/\lambda)-(4e^2/hv)\ln(2r/\lambda)-L(\pi/2)+\text{the phase of the gamma-function of the quantity } L+1+i\cdot 4e^2/hv\}$). An argument given elsewhere[14] shows that the interchange of neutrons and protons in close collisions between two alpha-particles does not impair the validity of Eq. (1). It is only required that no inelastic scattering occur, a condition which is certainly fulfilled at the energies available from natural alpha-ray sources.

Amplitudes are of more direct theoretical significance than are intensities, as we see from the form of Eq. (1). Therefore we designate as relative scattering amplitude the square root, $R^{\frac{1}{2}}$, of the ratio of observed to classical scattering. Figures 1 and 2 give the relative scattering amplitude as function of energy for all angles at which observations have been made.

Interpretation of complex numbers as vectors in a plane is the basis of a simple geometrical means to calculate the relative scattering amplitude (see Fig. 3A) when the phase shifts are known. The inverse of this procedure—determination by ruler and compass of one phase shift from a knowledge of the scattering amplitude and all other phase shifts—materially simplified the following phase shift analysis.

(3) Procedure for Determining the Strength of the Partial Waves

From the observations at a given energy we have to find the phase shifts K_0, K_2, $\cdots$. The arguments in the introduction indicate that the specific nuclear interaction does not appreciably distort partial waves of order higher than four. Our unknowns, therefore, number only three, K_0, K_2, and K_4. To determine them requires at the least a knowledge of the scattering at three angles. When φ is 15.27° or 35.07°, the scattering does not depend upon the fourth-order phase shift because at those angles the coefficient $A_4(\varphi)$ in Eq. (1) vanishes. Thus the observations at 15° and 35° suffice, in principle, to determine the phase shifts K_0 and K_2. The scattering at a third angle then fixes K_4. In particular, let this third angle be 27.37°; then the number of deflected particles depends only on K_0 and K_4. The former quantity being known, the latter is readily found.

Figure 3B illustrates the above outlined procedure to determine the three unknown phase shifts, and shows how due allowance is made for experimental error in measurement of the intensity of scattering. It is seen that there are several regions in the diagram which give reasonable accord with the observations at 15°, 27°, and 35°. The measurements at a fourth angle (45°) give enough additional information (a) to reduce somewhat the number of possible alternative solutions of the phase shift problem, and particularly (b) to determine more precisely for each solution the values of the phases which give the best attainable agreement with the observations at all four angles.

The analysis illustrated in Fig. 3 has been carried out for ten values of the energy and leads, in the end, to three alternative solutions (solutions I, II and III) of the phase shift problem[15] (see Figs. 4 and 5). We should like to decide between them by using all the observational material. With this aim in mind we use Eq. (1) to calculate as a function of energy the scattering to be expected for each choice of the phase shifts, with the results shown by the curves in Figs. 1 and 2.

Before comparing the calculated curves with the experimental points, we have to show that no important error comes into the observations due either to multiply scattered particles or to the finite opening of the apertures defining the angle of scattering. The mean angle of deviation due to multiple small angle deflections will be equal in order of magnitude to the square root of the average number of helium atoms contained in a cylindrical tube whose extension agrees with the length of path of the alpha-particle in the

[14] J. A. Wheeler, Phys. Rev. **52**, 1111 (1937).

[15] Additional solutions appear for a few values of the energy but are excluded because they fail to join continuously on to any solution acceptable at the remaining values of the energy.

apparatus and whose radius is the distance of closest approach calculated classically for the inverse square law of force.[16] The latter distance is 2.9×10^{-13} cm for alpha-particles of 4 Mev energy. For a reasonable representation of the path lengths used in the experiments we adopt a figure of 1 cm at a pressure of one atmosphere. The angle characterizing the multiple scattering will be $\{\pi\times(3\times10^{-13})^2\times3\times10^{19}\}^{\frac{1}{2}}=3\times10^{-3}$ radian or $(\frac{1}{6})$ degree, in order of magnitude. The effect of multiple scattering is, therefore, too small to be appreciable.

Lack of definition of the angle of scattering results less from the finite size of source and counter in the usual experimental arrangement than from the finite aperture of the diaphragms which define the scattering volume. Assuming that all the spread in angle is due to the latter cause, we can easily calculate a factor $W(\varphi)$ which tells with what weight each angle in a given interval contributes to the observed value, R_{obs}, of the ratio of actual to Rutherford scattering:

$$R_{obs}(\varphi_1, \varphi_2)=\int_{\varphi 1}^{\varphi 2} R(\varphi)W(\varphi)d\varphi \Big/ \int_{\varphi 1}^{\varphi 2} W(\varphi)d\varphi.$$

From the curves for $W(\varphi)$ in Fig. 6 and from the observed rate of variation of $R(\varphi)$ with angle we

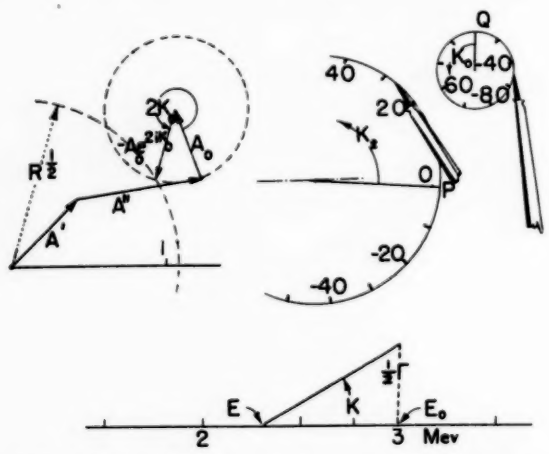

FIG. 3A. The distance, in the diagram at the left, from the origin to the end of the vector A'' represents the relative scattering amplitude, $R^{1/2}$, at a given angle of observation and a given energy, provided that the interaction between the two alpha-particles follows the inverse square law. Anomalous scattering signifies a different value for $R^{1/2}$, shown in the diagram. If it is known that the actual field of force modifies only the zero-order wave, the intersection of two circles of radii $R^{1/2}$ and A_0 determines the two possible values of the phase shift K_0, corresponding to the two points a and b. The left-hand diagram is purely schematic while the one at the right shows the construction, to the same scale, when two phase shifts K_0 and K_2 determine the scattering, as is the case when the angle of observation is 15°. The values of the vectors A are correct for a primary energy of 5.5 Mev ($E=2.8$ Mev) but the general geometrical relationships change only slowly with energy. The separation of the compass points corresponds to the value of $R^{1/2}$ shown in Fig. 2 and the distance from P to Q is determined by the vector sum of A' and A''. The lower diagram illustrates the variation of phase shift with energy, E, near a resonance level of energy E_0 and natural width Γ, provided the de Broglie wave-length is large compared to nuclear dimensions. The actual variation is more complicated.

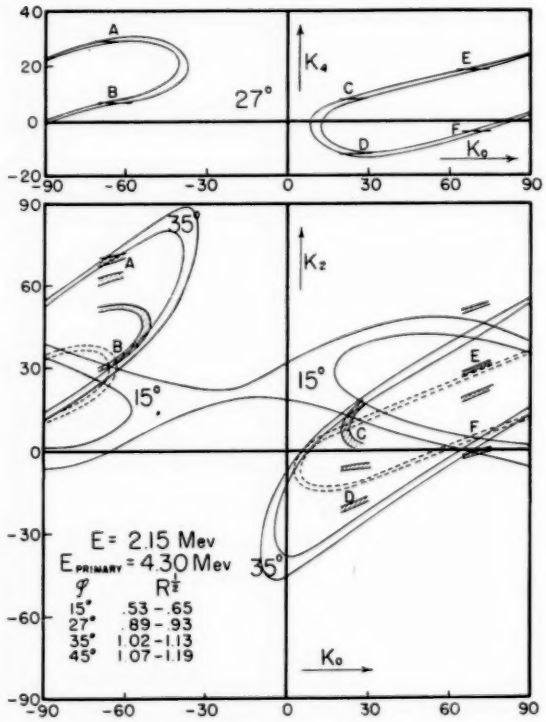

FIG. 3B. For a given energy the anomalous scattering at 15° determines by the construction of Fig. 3A a curve in the K_0, K_2 plane, every point on which is consistent with the observed value of $R^{1/2}$. The experimental uncertainties broaden out the line into a band. The intersection of this band with a similar band for 35° gives four sets of values for K_0 and K_2. For each of the four values of K_0 we can find in a similar way from the scattering at 27° two values of K_4, corresponding to the lettered regions in the upper diagram. K_4 being so determined, the scattering at 45°, which depends on all three phase shifts, gives a relation between K_0 and K_2 shown by the broken curves in the lower diagram. The solutions I, II and III of the phase shift problem mentioned in the text correspond, respectively, to regions C, B and F in the lower diagram. The dashed curve is obtained from the measurements at 45° on the assumption $K_4=0$°. The phases are measured in degrees and the diagrams repeat periodically every 180°.

[16] For a derivation of this result and a more detailed treatment of multiple scattering in general see E. J. Williams, Proc. Roy. Soc. **A169**, 531 (1939) or J. A. Wheeler, Phys. Rev. (to be published).

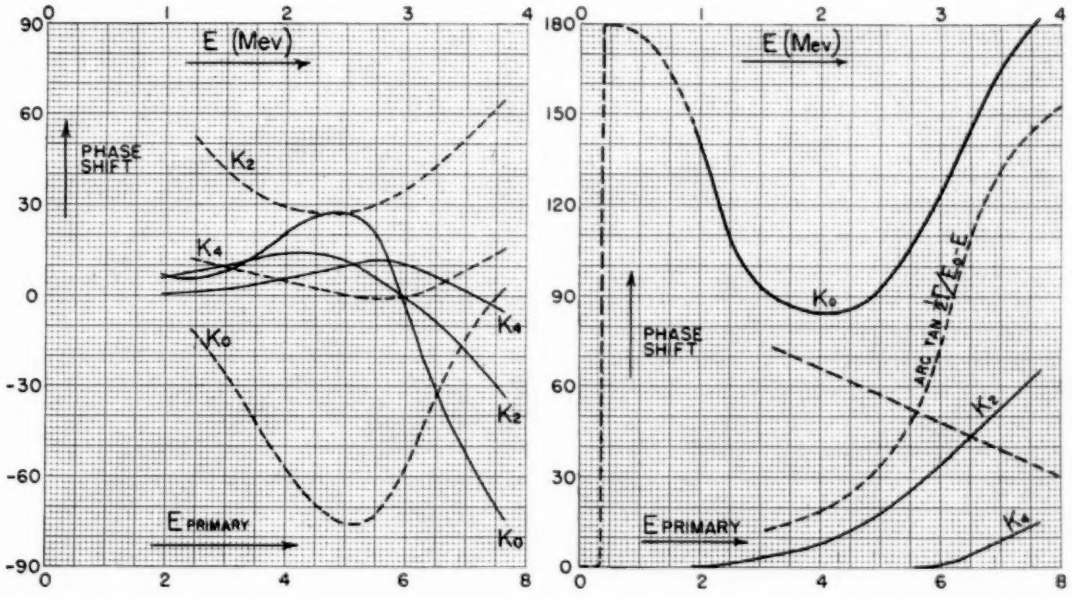

FIG. 4 (left). The problem of representing the observed scattering at seven angles in terms of three parameters, the phase shifts K_0, K_2 and K_4, leads, on account of the uncertainty in the measurements, to three alternative sets of values. Plotted here, in degrees, are solution I (smooth curves) and solution II (dashed curves), both of which are, however, excluded by additional experimental and theoretical evidence.

FIG. 5 (right). The only set of values for the phase shifts in acceptable accord at the same time with the scattering observations and other information about the interaction between two alpha-particles. Within the errors associated with the uncertainties in the measured scattering, the phase shift K_0 is representable as the sum of a contribution varying regularly with energy and a resonance term of the form arctan $(\frac{1}{2}\Gamma/E_0-E)$, with $E_0=3.1$ Mev and $\Gamma=0.8$ Mev. This decomposition of K_0 is shown by the two dashed curves in the region above $E=1.5$ Mev. The observations do not extend to the range of energies below $E_{\text{primary}}=2$ Mev. There the dashed curve represents only the probable course of the zero-order phase shift.

conclude that the corrections for angular spread are relatively unimportant except in the two cases when the angular spread is from 10° to 20° and from 29° to 44°. We dispense with the observations in these two cases because the recent measurements of Mohr and Pringle and of Devons give the desired information and were made with considerably narrower apertures.

Now that we can safely compare the calculated scattering curves in Figs. 1 and 2 with the experimental points, we come to the following conclusions: (a) Solution I of the phase shift problem leads to as good agreement as can be expected with the observations at the seven angles 10°, 15°, 21°, 27°, 33°, 38½° and 45°. (b) Solution II gives fairly good agreement except at 21°, where calculated and observed values are appreciably out of accord, and at 10°, where the discrepancy seems too great to be attributed to experimental error. (c) Solution III predicts scattering curves which agree reasonably well with the observations at 27°, 33°, 38½° and 45°. At 10° the calculated scattering amplitude agrees with the measurements except at the higher energies where the counts are few and the statistical errors greatest (Rutherford and Chadwick used the scintillation method). At 15° the predicted values are appreciably lower than those observed in the interval from 2 Mev to 5 Mev, but above 5 Mev there is good agreement. At 21° we find accord at the highest and lowest energies employed in the experiments, but the measurements are again higher than the calculated values near 3 Mev.

(4) Additional Evidence Leads to a Unique Solution

If the determination of the phase shifts for the various partial waves were a purely mathematical problem, based entirely on measurements of scattering, we should undoubtedly conclude that solution I is in the best agreement with experiment. However, there is good observational

evidence[17] that two alpha-particles can form a semistable compound nucleus Be^8 of about 2.8 Mev excitation energy. The existence of a temporary state of this nature implies that one of the partial waves representing scattered alpha-particles of a particular angular momentum must show an anomalous behavior when the energy of the impinging particles is in the neighborhood of 5.6 Mev, and, indeed, the corresponding phase shift must increase through the resonance region by approximately 180°, according to the dispersion theory of nuclear reactions.[18] Solution I definitely fails to satisfy this requirement, and must be ruled out. Solutions II and III, on the other hand, show at the higher energies a rapid rise in the phase shift of the wave of zero angular momentum. This behavior is consistent with the existence of a semistable state of the nucleus Be^8 and, in fact, not only independently indicates the existence of such a state with just the properties required by disintegration experiments (as we shall see below) but also reveals the angular momentum of this state.

Extent of agreement with the scattering experiments is sufficiently comparable for solutions II and III as not to decide between them. These solutions are, however, distinguished by the behavior of the phase shifts of orders two and four. K_2 and K_4 decrease monotonically with diminishing energy for solution III while for solution II they decrease initially at the higher energies but then rise at lower energies. The latter behavior is contrary to every reasonable expectation based on the fact that the wavelength of the colliding particles becomes greater than the range of interaction in inverse proportion to the velocity. In particular, we have to expect for every phase shift a certain energy below which that phase falls off continuously; and in general this energy will lie not far below the first semistable level of the compound system, the angular momentum of which corresponds to the order of the given phase shift. Both the behavior of the phases K_2 and K_4 themselves and other experimental and theoretical considerations[17] supply arguments against

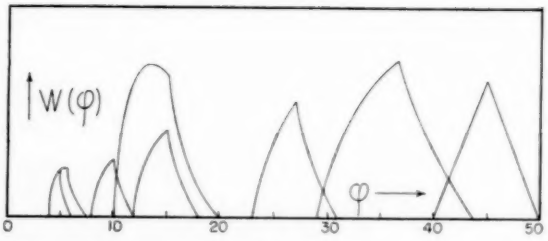

FIG. 6. Observations on the scattering from the region lying within a given angular aperture depend with the weight $W(\varphi)$ on the ratio, $R(\varphi)$, of actual to Rutherford scattering at all intermediate angles.

the existence of any semistable levels of Be^8 with angular momentum of two or four units lying sufficiently low to account for such a behavior of the second- and fourth-order phases as is shown by solution II. For solution III, on the other hand, the phases K_2 and K_4 vary with energy in accordance with the just-mentioned expectations. We therefore conclude that *solution III is the only solution of the phase shift problem* in acceptable accord at the same time with the scattering experiments, with experimental evidence for a semistable state of the nucleus Be^8, and with requirements as to the variation with energy of higher order phase shifts. Moreover, the magnitude of the fourth-order phase shift is sufficiently small to indicate that sixth and higher order phases are negligible and thus to justify the internal consistency of the above analysis.

Previous to the present scattering analysis, the level of the nucleus Be^8 at 2.8 Mev indicated by disintegration experiments has been generally believed to possess two units of angular momentum. A simple demonstration that this cannot be so is, therefore, of interest. The relative scattering amplitudes at 15° depends on the phase angles K_0 and K_2 in the manner illustrated by Fig. 3A, and is independent of K_4. Increase of $2K_2$ near resonance by approximately 360°, implied by the supposed existence of a level of two units of angular momentum, would (as is seen in the figure) cause the scattering to rise to a value much larger than permitted by the observations, whatever might be the assumed simultaneous variation with energy of K_0.

(5) RANGE OF THE INTERACTION

Principal direct conclusions from the above-determined phase shifts concern the range of the

[17] Summarized briefly in the following paper, J. A. Wheeler, Phys. Rev. **59**, 27 (1941).

[18] See in this connection G. Breit and F. L. Yost, Phys. Rev. **48**, 207 (1935) and R. Peierls and P. L. Kapur, Proc. Roy. Soc. **A166**, 277 (1938).

interaction between two alpha-particles and the properties of the semistable state of the compound nucleus Be^8. The behavior of the phase shift K_4 shows that particles with four units of mutual angular momentum first have appreciable nonelectrostatic interaction when the energy of the primary particle is above 6 Mev. At an energy of 6 Mev, the previously mentioned distance λ (wave-length/2π), which characterizes the minimum dimensions of a wave packet, is sufficiently small (1.86×10^{-13} cm) to justify an approximate estimate of the distance between centers of the two alpha-particles on the basis of the classical formula:

$$\text{Distance of closest approach} = (\text{product of charges/primary energy}) + \{(\text{charge product/energy})^2 + (\text{angular momentum})^2/(\text{half-energy} \times \text{mass of alpha-particle})\}^{\frac{1}{2}}$$
$$= 0.96\times10^{-13} + \{(0.96\times10^{-13})^2 + 20\lambda^2\}^{\frac{1}{2}} = 9\times10^{-13} \text{ cm}. \quad (5)$$

This estimate undoubtedly represents an upper limit for the range of the interaction because we have inserted in the formula the lowest possible value for the energy at which there may be said to be appreciable forces of specific nuclear character between two alpha-particles of the given angular momentum. There does not appear to exist at present any method to obtain a well-defined value for the range of the interaction.

(6) Variation of Phase Shift Near Resonance

Existence of a semistable compound state has what consequences for the variation with energy of the corresponding phase shift? Conversely, a knowledge of the energy dependence of the phase leads to what information on the properties of the semistable state? Without a detailed knowledge of the interaction, only certain general conclusions can be drawn. Those already given by the dispersion theory[18] we wish to supplement here by taking into account in a semiclassical approximation the influence of electrostatic and centrifugal forces.

At a certain initial moment, $t=0$, there will be complete certainty that the two alpha-particles are in the given compound state. This state of affairs will be represented by a probability amplitude $\psi_c(r_1\sigma_1, r_2\sigma_2, \cdots, r_8\sigma_8)$, a function of the coordinates and spins of the eight constituent particles which has negligible magnitude outside of nuclear dimensions. The probability amplitude function at any later instant will have appreciable magnitude both in the region of nuclear dimensions, where it will have fallen off exponentially with time, and at greater distances, where it will represent a wave train moving outward with a group velocity equal to the natural velocity of separation of the alpha-particles. This wave train must be mathematically equivalent to a superposition of the proper functions which describe the probability amplitude for well-defined values of the energy. But as each such proper function is characterized by its phase at large distances, the just mentioned mathematical equivalence will imply certain conditions as to the variation of phase with energy.

The mean life of the radioactive state defines a certain energy, Γ (the natural width of the level), through the relation

$$\text{reciprocal of mean life} = \text{radioactive decay constant} = \Gamma/\hbar.$$

In a series of experiments with the same initial conditions, the energy of the emitted particles will scatter around a certain average energy, E_0, with a spread of the order of magnitude of Γ. The corresponding uncertainty in the velocity of separation will cause a smearing out of the general structure of the outgoing wave train after it has traveled for a time of the order of magnitude of (E_0/Γ) times the mean life of the radioactive state, or for a distance of the order of velocity times $(E_0/\Gamma)(\hbar/\Gamma)$, as may easily be shown. We shall concern ourselves in the following, however, with separations sufficiently small that we can neglect this spreading effect. Then the amplitude of the outgoing wave at a distance r and an instant t will be proportional to the probability amplitude of the compound state at a preceding moment $t-t_{ar}$. Here t_{ar} is the time required according to classical mechanics to bring about the given separation of the two alpha-particles starting with them at a distance a equal in order of magnitude to the range of the specific

nuclear interaction:

$$t_{ar}=\int_a^r dr/v_r=\int_a^r dr$$

times the derivative of the relative momentum of the particles at a given point with respect to their energy, equals

$$\int_a^r (dp/dE)dr. \tag{6}$$

The probability that the compound nucleus shall disintegrate during a time interval dt at the instant $t-t_{ar}$ will be $(\Gamma dt/\hbar)\exp(-\Gamma(t-t_{ar})/\hbar)$. If it so disintegrates, the alpha-particles will have a separation between r and $r+v_r dt$ at the moment t, and, therefore, the absolute magnitude of the probability amplitude at that distance and time must be $(\Gamma/\hbar v_r)^{\frac{1}{2}}\exp\Gamma(t_{ar}-t)/2\hbar$. According to the semiclassical approximation treatment of Wentzel, Kramers and Brillouin, the phase of the probability amplitude will increase with distance at a rate given by the momentum p_0 at the point in question divided by $\hbar$, and will decrease with time at the rate $E_0/\hbar$. Thus, to the accuracy in which we are interested, the complete expression for the outgoing wave train will be[19]

$$(\Gamma/\hbar v_r)^{\frac{1}{2}}\exp\left(i\cdot\text{constant}+i\int_a^r p_0 dr/\hbar+\Gamma(t_{ar}-t)/2\hbar-iE_0 t/\hbar\right). \tag{7}$$

It is supposed here that the difference $t-t_{ar}$ is positive. A negative value of this difference will signify, according to classical mechanics, that sufficient time has not elapsed for the alpha-particles to attain the given separation and, therefore, the probability amplitude will then be zero in the approximation in question.

The dependence upon time of the probability amplitude is not that of a proper state of a given circular frequency $E/\hbar$, but rather corresponds to a superposition of such states, of the form

$$\int dE\psi_E(r)\exp(-iEt/\hbar). \tag{8}$$

From a knowledge of the outgoing wave in its dependence upon position and time we are interested in obtaining a knowledge of how the individual proper states $\psi_E(r)$ depend upon r. Following the standard inversion procedure of Fourier analysis, we multiply the probability amplitude at r by the expression $(dt/2\pi\hbar)\exp(iEt/\hbar)$, integrate over all values of the time which contribute (extending from $t=t_{ar}$ to $t=\infty$ for a point r outside nuclear dimensions), and thereby find $\psi_E(r)$:[20]

$$\psi_E^{(1)}(r)=(\Gamma/\hbar v_r)^{\frac{1}{2}}\{1/2\pi i(E-E_0+\tfrac{1}{2}i\Gamma)\}\exp\left\{i\cdot\text{constant}+i\int_a^r p_0 dr/\hbar+i(E-E_0)t_{ar}/\hbar\right\}. \tag{9}$$

By use of Eq. (6) and trigonometry we rewrite this result in the form

$$-\pi\{(E-E_0)^2+(\tfrac{1}{2}\Gamma)^2\}^{\frac{1}{2}}\psi_E^{(1)}(r)$$
$$=(\Gamma/\hbar v_r)^{\frac{1}{2}}(1/2i)\exp\left\{i\cdot\text{constant}+i\int_a^r p_E dr/\hbar+i\arctan(\tfrac{1}{2}\Gamma/E_0-E)\right\}. \tag{10}$$

We do not however, obtain the complete expression for the proper function in question by taking into account only the existence of a diverging wave train. A wave train converging upon the region of

[19] Actually expression (7) has to be multiplied by the internal wave functions for the two alpha-particles, and to the product have to be added, with the proper signs, similar products in which the coordinates of neutrons and protons have been suitably interchanged. This complication introduces, however, no essential new features in the treatment in the text, except to exclude altogether radial waves of odd angular momentum.

[20] No acquaintance with the mathematics of Fourier analysis is necessary to recognize that the above procedure is analogous to the determination for an electromagnetic wave train of the amplitude of a given monochromatic constituent. The retardation in time of the disturbances coming from different points of a grating corresponds to the multiplying factor $\exp(iEt/\hbar)$ and the summation by a lens of the amplitudes from all parts of the grating is, in principle, the same as the above integration with respect to time.

specific nuclear interaction will exist at times preceding the initial instant $t=0$, according to the principle of reversibility of time. In its wave-mechanical formulation, this principle states that if the probability amplitude is represented by a real function at the time $t=0$ (as may be achieved in our case by a suitable choice of the phase of ψ_c), then the mathematical expression for the incoming wave will be obtained by reversing simultaneously the sign of t and the sign of i in (7). Therefore, we obtain $\psi_E(r)$ by adding to the outgoing wave $\psi_E^{(1)}(r)$ of Eq. (10) an incoming wave $\psi_E^{(2)}(r)$ which differs from it only through the change in sign of i. We conclude that the proper function corresponding to an energy E varies with distance as

$$(\Gamma/\hbar v_r)^{\frac{1}{2}} \sin\left\{\text{constant}+\int_a^r p_E dr/\hbar+\arctan\,(\tfrac{1}{2}\Gamma/E_0-E)\right\}. \tag{11}$$

This result will be valid to the same extent as any semiclassical representation of a wave function (provided that the value of the energy in question differs from E_0 by an amount not so great in comparison with the natural width Γ that the proper function fails to play an appreciable role in the representation of the disintegration process).

We are interested in the difference K between the actual phase of the proper function and the phase calculated on the basis of inverse square law forces. The latter phase will be $\pi/4$ plus the integral $\int p_E dr/\hbar$ extended from the classical distance r_E of closest approach to the point r in question,[21] according to the same semiclassical approximation upon which the above calculations are based. Comparison with expression (11) gives for the phase shift the approximate equation

$$K(E)=\text{constant}+\int_a^{r_1} p_E dr/\hbar-\int_{r_E}^{r_1} p_E dr/\hbar+\arctan\,(\tfrac{1}{2}\Gamma/E_0-E). \tag{12}$$

Here the momentum p_E is to be calculated classically (a) for the actual field of force in the first integral and (b) in the second integral for the inverse square law of interaction. The two fields of force are the same beyond a certain distance r_1, which appears as the upper limit in the integrals.

In applying Eq. (12) to problems of nuclear scattering we have to expect that the range of the specific nuclear forces will be of the same order of magnitude as a. By neglecting altogether the difference between r_1 and a we will, therefore, obtain a first approximation to the actual state of affairs: The variation with energy of the phase shift near resonance will be ascribed to two effects, of which one, represented by the term arctan $(\frac{1}{2}\Gamma/E_0-E)$, is determined by the position and sharpness of the resonance level, while the second will depend upon the size of the compound nucleus, and be described by the integral

$$-\int_{r_E}^{a} p_E dr/\hbar.\,^{22}$$

The latter integral (according to a simple numerical evaluation for the case of two alpha-particles of zero angular momentum) is practically a linear function of energy above 1.5 Mev (that is, when the primary energy exceeds 3 Mev) provided that the distance a is 3×10^{-13} cm or greater. Thus, in the problem in question we have, to a first approximation, the result:

$$K(E)=\text{a smoothly varying function of energy nearly linear in the neighborhood of resonance}+\arctan\,(\tfrac{1}{2}\Gamma/E_0-E). \tag{13}$$

In the next approximation, the unknown departure from the inverse square law outside a will make it

[21] Numerical evaluation shows that this semiclassical calculation gives for the phase at large distances of the zero-order Coulomb wave functions a value in error by at most 12° in the energy range of interest for the alpha-particle scattering.

[22] When the conditions are satisfied for applying the above semiclassical treatment to neutrons, the integral in question gives just the variation of phase with energy which follows from the treatment of H. A. Bethe and G. Placzek (Phys. Rev. **51**, 450 (1937)) without, however, requiring the introduction of a fictitious repulsive nuclear potential of range equal to a.

TABLE I. *The radial wave functions F_L^* oscillate at large distances as sine functions with unit amplitude and with the phase $\{(r/\lambda\!\!\!^{-})-(4e^2/\hbar v)\ln(2r/\lambda\!\!\!^{-})-L(\pi/2)+$phase of gamma-function of $(L+1+i\cdot 4e^2/\hbar v)+$the phase K_L of Fig. 5$\}$ and are calculated here for the point $r=9\times10^{-13}$ cm on the assumption that inverse square forces hold down to that distance. Energies are given in Mev.*

E_{PRIMARY}	E	$\hbar v/4e^2$	K_0	F_0^*	rdF_0^*/F_0^*dr	K_2	F_2^*	rdF_2^*/F_2^*dr
2.48	1.24	1.25	118	0.39	6.22	2	0.62	4.47
3.57	1.79	1.50	92	0.65	4.13	6	1.02	1.28
4.86	2.43	1.75	89	1.03	1.00	16	1.20	−0.27
6.35	3.17	2.00	139	0.27	−16.7	40	0.69	−5.29
8.04	4.02	2.25	(185)	−0.99	1.63	(72)	−0.52	8.44

impossible to calculate the actual behavior of the first term in (13) but every reasonable law of force will still lead to a smoothly varying function of energy.

(7) Properties of the Semistable State of Be^8

The zero-order phase shift shown in Fig. 5 is resolved satisfactorily into two parts in accordance with Eq. (13) when we insert for E_0 and Γ, respectively, the values 3.1 Mev and 0.8 Mev, figures for which, however, the variation of the phase shift will be unable to give very accurate values until the scattering has been measured for primary energies in the range 7 Mev to 10 Mev. The just stated values for the disintegration energy and natural breadth of the semistable level are in reasonable accord with the figures 2.8 Mev and 0.8 Mev obtained[23] from disintegration experiments in which the nucleus Be^8 is formed in a radioactive state. This agreement helps to confirm the phase shift analysis given above. The actual value of the natural width corresponds to a mean life, h/Γ, amounting to 0.8×10^{-21} sec.

If departure from the inverse square law were negligible outside the distance a referred to above, we should obtain for this quantity a value of about 3×10^{-13} cm from the slope in the neighborhood of resonance of the first term in (13). The steepened slope at lower energies of this nonresonance component of the phase shift curve (see Fig. 5) indicates, however, that the specific nuclear interaction must extend to distances considerably greater than 3×10^{-13} cm.

Existence of a semistable state of mean life still shorter than 10^{-21} sec. and an angular momentum of two units is suggested by the nature of the rise of the phase shift K_2 at the higher energies in Fig. 5. The observations do not extend to energies sufficiently great to allow much more than a rough estimate that such a state, if it exists, has an energy of the order of 4 or 5 Mev.

Values of the wave functions near the nucleus furnish what is, in some ways, a more significant representation of the observations than that provided by the phase shifts. The knowledge of the asymptotic behavior of the wave functions implied by the phase shifts in Fig. 5; the negligible effect of the specific nuclear forces down to a distance of $r=9\times10^{-13}$ cm; and formulae and tables of wave functions in an inverse square field of force[24] allow us to calculate the values of the wave functions and their derivatives listed in Table I. From the values in the table it does not seem possible to deduce in a simple way any straightforward conclusions about the interaction between two alpha-particles over and above what has already been revealed by the behavior of the phase shifts.

(8) Summary

Anomalies in the scattering of alpha-particles in helium receive a satisfactory interpretation in terms of the distortion by a specific nuclear interaction of the partial waves of zero, two and four units of angular momentum. The actual magnitude of the distortion of the fourth-order wave sets an upper limit of about 9×10^{-13} cm for the range of the interaction. The behavior of the zero-order wave gives information about a semistable state of the nucleus Be^8 formed in certain disintegration experiments. The variation with energy of the second-order wave suggests the existence of another state of energy 4 to 5 Mev and still shorter lifetime.

[23] P. I. Dee and C. W. Gilbert, Proc. Roy. Soc. **A154**, 279 (1936); H. A. Bethe, Rev. Mod. Phys. **9**, 218 (1937).

[24] J. A. Wheeler, Phys. Rev. **52**, 1123 (1937).

The Alpha-Particle Model and the Properties of the Nucleus Be^8

JOHN ARCHIBALD WHEELER
Palmer Physical Laboratory, Princeton, New Jersey
(Received November 8, 1940)

Reasons are given for renouncing any attempt to interpret the scattering of alpha-particles in helium in terms of a hypothetical law of force between alpha-particles. The analysis of scattering observations in the preceding paper is employed in conjunction with other information from theory and experiment to draw conclusions about the normal state and the first two excited levels of the compound nucleus Be^8:

ENERGY	WIDTH	LIFE	J
125 kev	1 to 100 ev	10^{-15} to 10^{-17} sec.	0
2.8 Mev	0.8 Mev	10^{-21} sec.	0
—	Very great	—	2

Difficulties remain in the interpretation of the reaction of B^{11} with protons to yield Be^8.

1. THE ALPHA-PARTICLE MODEL CONTRASTED WITH THE PICTURE OF ALPHA-PARTICLES AS PERMANENT UNITS IN NUCLEAR STRUCTURE

ALPHA-PARTICLES lost all claim to consideration as permanent units in nuclear structure when a general theory of nuclear constitution was developed.[1] Existence of such units, it was recognized, would be inconsistent with the large kinetic energy of zero-point motion of the elementary particles composing the nucleus and with the extremely close coupling between neutrons and protons. The nature of the elementary interactions, however, with their saturation character and apparent symmetry with respect to spin and charge, first clearly recognized by Breit, Feenberg and Wigner,[2] emphasized just as strongly the special stability of nuclei composed of even and equal numbers of neutrons and protons. The subsequent study of various simple laws of force having such properties, aided by instructive methods of group theory, led to a number of more detailed conclusions as to the energy and symmetry properties of low levels of light nuclei, including Be^8.

An alternative account of some of the symmetry properties of light nuclei is obtained, as the writer stressed,[3] by recognizing the existence within the nucleus of temporary alpha-particle groupings obeying the Bose-Einstein statistics. Indeed, for the symmetry of an alpha-particle structure to be able to manifest itself in the exclusion of certain states of oscillation and rotation otherwise to be expected, it is sufficient that the period of the motion in question be short in comparison with the time of rearrangement of the groupings. This condition was shown to be approximately satisfied in a number of cases. Thus low energy levels could be predicted in the even-even nuclei Be^8, C^{12}, O^{16},[3] and Ne^{20}.[4] This type of alpha-particle model was extended by Hafstad and Teller[5] to nuclei containing one extra elementary particle. For both kinds of nuclei the predictions of the simple model accorded to a striking extent with the results of the more abstract and apparently quite different calculations of Wigner, Feenberg, Phillips and Hund.[6,7] In combination with well-known selection rules these predictions have since proved of value in correlating a number of features of transformations observed in light nuclei.

The above-mentioned formulation of the alpha-particle model has to be sharply distinguished from the early conception of alpha-particles as permanent units in nuclear structure. That picture assumed not only that the interaction

[1] N. Bohr, Nature **137**, 344 (1936); N. Bohr and F. Kalckar, Kgl. Danske Vid. Sels. Math.-fys. Medd. **14**, No. 10 (1937).
[2] G. Breit and E. Feenberg, Phys. Rev. **50**, 850 (1936); E. Wigner, *ibid.* **51**, 106 (1937).
[3] J. Wheeler, Phys. Rev. **52**, 1083 (1937).
[4] E. Teller and J. A. Wheeler, Phys. Rev. **53**, 778 (1938).
[5] L. R. Hafstad and E. Teller, Phys. Rev. **54**, 681 (1938).
[6] E. Feenberg and E. Wigner, Phys. Rev. **51**, 95 (1937).
[7] E. Feenberg and M. Phillips, Phys. Rev. **51**, 597 (1937); F. Hund, Zeits. f. Physik **105**, 202 (1937).

between two alpha-particles could be described by a potential function, but also that forces were additive when several alpha-particles were present. For neither of these assumptions do present views of nuclear constitution give any well founded justification.[8] Any attempt to give a detailed account of the coupling between even two alpha-particles in terms of a potential function leads to unavoidable difficulties of principle, as is emphasized particularly in the accompanying paper of Margenau.[9] The alpha-particle model thus properly concerns itself, not with any special picture of the forces between the temporary alpha-particle groupings, but with the rotational and symmetry properties of the nucleus and a relatively small group of related questions.[10]

To attempt to determine a law of interaction of universal applicability from the scattering of alpha-particles in helium would be, from the above point of view, a mistaken endeavor. On the other hand, we shall be entirely justified in using the scattering analysis of the preceding paper[11] (a) to draw such conclusions as are there given about the range of the specific nuclear interaction, (b) to test the predictions of the alpha-particle model for the compound nucleus Be^8 and (c) in conjunction with this model to correlate the related experimental evidence and obtain as complete a picture as possible of the properties of this nucleus.

The nucleus Be^8, according to the alpha-particle model, may be compared to a symmetric diatomic molecule. In addition to a ground state of zero angular momentum ($^1S_0$), the properties of which are discussed in Section 2 below, it will on this view possess excited rotational states with even-valued angular momentum ($^1D_2$, $^1G_4$, $\cdots$). Energies of the order of 3 Mev and 9 Mev for the first two excited states were calculated[3] from an early estimate of the moment of inertia. A smaller inertial moment and a correspondingly increased energy of 5 or 6 Mev for the first stage of rotational excitation are suggested by Dennison[12] since he finds in the case of O^{16} that a similar alteration correlates the predictions of the model with observation. Besides the just mentioned rotational levels the beryllium nucleus will have other states some of the lowest of which according to the model, will be to a certain extent comparable with the first few vibrational levels of a diatomic molecule.

Dee and Gilbert[13] proposed that the nucleus Be^8 is formed, as an intermediate product in the reaction $B^{11}+H^1 \rightarrow 3He^4$, in a short-lived state with about 2.8 Mev of excitation. On this basis they found a satisfactory explanation for the distribution in energy of the alpha-particles observed by Oliphant, Kempton and Rutherford.[14] As a check Fink performed several interesting experiments[15] with counters in coincidence from the results of which it seemed necessary to doubt the interpretation in question. A closer study of the coincidence experiments, however, confirms the hypothesis of Dee and Gilbert (Section 3 below).

The level at 2.8 Mev had already, previous to Fink's experiments, been identified as[16] the $^1D_2$ state predicted both by the alpha-particle model[3] and by a more elaborate calculation[6] based on a Hartree model. Nevertheless, the observed level is actually one of zero angular momentum, according to the scattering analysis in the preceding paper.[11] Whether this particular state should now be correlated with the lowest excited vibrational state of the alpha-particle model is not certain. That the predicted $^1D_2$ level is much broader than the 2.8-Mev state is, however, clear from the analysis of the scattering of alpha-particles in helium. Evidence supporting this conclusion and indirectly confirming that the 2.8-Mev level has zero angular momentum is found by studying the distribution in energy of alpha-particles which result from the beta-ray decay of Li^8 (Section 4). The existence of a very broad $^1D_2$ level is one of the few checks on the alpha-particle model at present available in the case of Be^8.

[8] Arguments against additivity of forces are given by B. O. Grönblom and R. E. Marshak, Phys. Rev. **55**, 229 (1939).

[9] H. Margenau, Phys. Rev. **59**, 37 (1941).

[10] It has been applied for example to the treatment of nuclear spins and magnetic moments: H. A. Bethe, Phys. Rev. **53**, 842 (1938) and R. G. Sachs, *ibid.* **55**, 825 (1939).

[11] J. A. Wheeler, Phys. Rev. **59**, 16 (1941).

[12] D. M. Dennison, Phys. Rev. **57**, 454 (1940).

[13] P. I. Dee and C. W. Gilbert, Proc. Roy. Soc. **A154**, 291 (1936).

[14] M. L. E. Oliphant, A. E. Kempton and E. Rutherford, Proc. Roy. Soc. **A150**, 251 (1935).

[15] K. Fink, Ann. d. Physik **34**, 717 (1939).

[16] G. Breit and E. Wigner, Phys. Rev. **50**, 1191 (1936); **51**, 593 (1937).

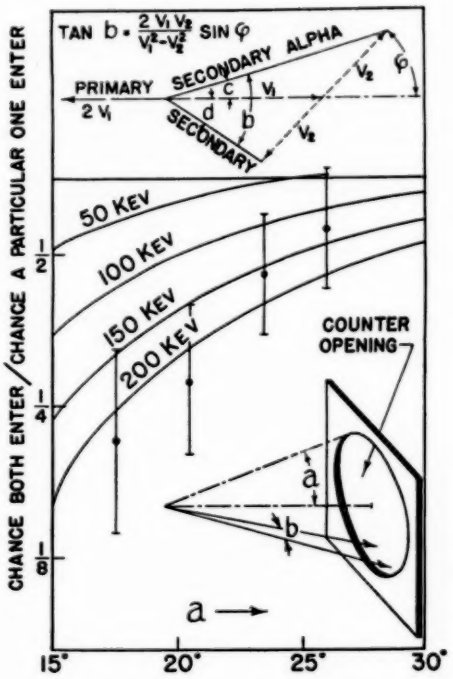

FIG. 1. The energy released in the disintegration of Be^8 determines the maximum angle of divergence between the secondary alpha-particles from the reaction of B^{11} with protons. The chance both secondaries shall enter a counter of aperture a is calculated for various assumed values of the energy of disintegration of normal Be^8, and compared with the observations of Laaff.

The application of standard selection rules gives a satisfactory account of most nuclear transformations which lead to the three states of Be^8 whose properties are investigated in Sections 2, 3 and 4. However, phenomena observed in the disintegration of B^{11} by protons lead to a number of unsolved questions (Section 5).

2. THE NORMAL STATE OF Be^8

The isotope Be^8 certainly is not present in natural beryllium to a relative abundance greater than 10^{-4}, according to Bleakney and his collaborators.[17] Nevertheless the question of the instability of this nucleus is left in doubt by even the most precise determination of its mass by the indirect method of energy balances; Allison, Skaggs and Smith[18] conclude Be^8 is stable by 65 ± 140 kilovolts.

That a normal Be^8 nucleus set in motion disintegrates into two alpha-particles before ionization losses have robbed it of appreciable energy was first shown by Kirchner, Laaff and Neuert[18a] and later confirmed by observations of Laaff[19] and of Fink.[15] From their ingenious experiments they could say that the energy of disintegration probably lies in the range 100 to 200 kev, but with no single value in this range could they obtain an account of their observations at all satisfactory. To propose an energy release indeterminate by a matter of almost 100 kilovolts or a probability of disintegration of Be^8 varying with direction would be equally unacceptable explanations of this difficulty. Theoretical estimates[20] give 10^{-16} to 10^{-19} second as the order of magnitude of the lifetime of a Be^8 nucleus unstable by 100 to 200 kev. This nucleus separates from the primary alpha-particle in the reaction

$$B^{11}+H^1\rightarrow C^{12}\rightarrow Be^8(\text{normal})+He^4\rightarrow 3He^4 \quad (1)$$

with a speed of 2.5×10^9 cm/sec. Its disintegration will therefore occur at a distance between 10^{-10} and 10^{-7} cm, too far away to be influenced in either direction or energy by the alpha-particle. Furthermore, the principle of uncertainty correlates with the lifetime an indeterminacy in energy or natural width of 0.01 kev to 10 kev, far too small to be significant in these experiments. However, a closer study reveals a much simpler source of the difficulties of interpretation encountered by Fink and Laaff.

The arrangement of Laaff consists of a counter which can distinguish between the entry of a single alpha-particle and a pair, and count the number of events of each kind. The proportion of pairs increases as the angular aperture a of the counter is enlarged (see Fig. 1). The chance a given alpha-particle shall enter the counter may be taken to be

$$S=\pi a^2/4\pi=a^2/4, \quad (2)$$

if we neglect the difference between an angle and its sine and assume random direction of emission. An accompanying alpha-particle which diverges from the first by an angle b may also enter, with a probability given by the fraction of a ring of angular radius b included within the

[17] W. Bleakney, J. P. Blewett, R. Sherr and R. Smoluchowski, Phys. Rev. **50**, 545 (1936).
[18] S. K. Allison, L. S. Skaggs and N. M. Smith, Jr., Phys. Rev. **57**, 550 (1940).
[18a] F. Kirchner, O. Laaff and H. Neuert, Naturwiss. **39**, 794 (1937).
[19] O. Laaff, Ann. d. Physik **32**, 760 (1938).
[20] H. A. Bethe, Rev. Mod. Phys. **9**, 167 (1937).

counter opening. Averaging this fraction over the possible points of entry of the first alpha-particle we obtain for the chance, C, of a double count the result

$$C=(a^2/2\pi)\{\arccos(b/2a)-(b/2a)(1-b^2/4a^2)^{\frac{1}{2}}\}. \quad (3)$$

For a given value of the energy of radioactive decay, the angle of divergence b will vary, as illustrated in the upper portion of Fig. 1, according to the angle φ between the velocity v_1 of the disintegrating nucleus and the velocity v_2 with which either secondary alpha-particle is ejected. With sufficient approximation we may write

$$b/2a=(1/2a)\arctan 2v_1v_2\sin\varphi/v_1^2-v_2^2 = v_1v_2\sin\varphi/a(v_1^2-v_2^2). \quad (4)$$

An isotropic distribution of disintegrations gives $\sin\varphi d\varphi$ as the probability that φ lie in any range $d\varphi$ between 0 and $\pi/2$ (Laaff assumed all values of φ are equally probable, thus underweighting the larger values of b). Averaging expression (3) over φ, we find as chance of a double count the result

$$D=(a^2/4)\{1+(4/3\pi)(c^{-1}-c)K(c)-(4/3\pi)(c^{-1}+c)E(c)\}, \quad (5)$$

when $c=v_1v_2/a(v_1^2-v_2^2)$

is less than 1. When c is greater than 1 we have to replace the complete elliptic integrals $K(c)$ and $E(c)$ in (5) by $-cK(c^{-1})$ and $cE(c^{-1})$, respectively. Noting that an alpha-particle of velocity v_1 has an energy of 1.4 Mev[19] we can evaluate (5) for various assumed values of the energy of disintegration. The ratio, D/S, of the chance of a double count to the chance for a single chosen alpha-particle to enter the counter is plotted in Fig. 1 for comparison with Laaff's results. There is seen to be a range of values of the disintegration energy, any one of which now gives a satisfactory representation of the observations.

In interpreting the observations of Fink[15] it is necessary to take account of the isotropic distribution of the disintegration of normal Be^8 nuclei just as in the experiments of Laaff. Fink's arrangement allows a somewhat more accurate determination of the energy of disintegration. A counter (II), biased to respond only to long range primary alpha-particles, stands on one side of his thin boron target. On the other

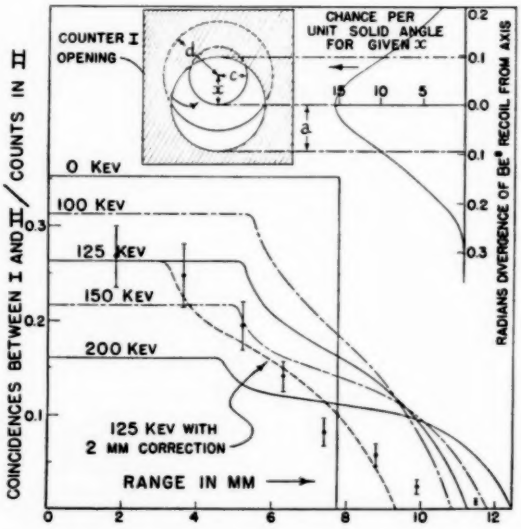

FIG. 2. Coincidences between two diametrically opposed counters, one of which responds only to fast primary alpha-particles, as increasingly thick foils are placed over the other counter (I). The observations of Fink come into satisfactory accord with curve calculated for 125 kev energy of disintegration if it be assumed that energy equivalent to 2 mm range is partly lost in the boron target, partly required to operate the counter.

side is a counter (I) into which should fly 35 percent of the recoiling Be^8 nuclei, if they were stable. The number of coincidences to be expected on this assumption between counts in I and counts in II is so small because counter I has an appreciable aperture, the target has a finite size, and the forward momentum of the compound nucleus C^{12} makes the direction of the recoiling Be^8 not quite opposite that of the primary alpha-particle. The distribution in direction of the recoils shown in the upper right-hand portion of Fig. 2 allows for all three effects and has, for simplicity, been averaged over azimuth. (The interpretation of the experiments would have been much simplified if counter I had had a considerably larger opening.) As stopping material is introduced before I there should come a moment, if normal Be^8 is stable, when all recoils are suddenly excluded, as shown by the curve marked 0 kev in Fig. 2. Fink's observations, also given in the figure, contradict this prediction. In fact, we know from Laaff's experiment that Be^8 disintegrates with an energy of the order of 150 kev. This value corresponds to a lifetime so short that already within the target the two secondary alpha-particles will have been pro-

duced and will be diverging from the original direction of the Be^8 by angles c and d, respectively, as indicated in Fig. 1. When a Be^8 nucleus starts off at an angle x with respect to the axis of counter I, a count will no longer be certain when x is smaller than the angular semiaperture a of the instrument, except in the case that $c+d$ is less than $2a$ and simultaneously x is less than $(a^2-cd)^{\frac{1}{2}}$. In every other case the probability of a pulse will be obtained by adding the fractions of the arcs of circles of radii c and d included within the opening. This probability then has to be averaged with respect to x in accordance with the curve in the upper right-hand portion of Fig. 2. We thus obtain the probability of a count in I simultaneous with one in II provided (a) that the line of disintegration of Be^8 is inclined at a definite angle x to the line of recoil and (b) that the normal velocities $v_1+v_2\cos\varphi$ and $v_1-v_2\cos\varphi$ of both secondary alpha-particles are sufficient to penetrate any foils over the counter. If only one secondary can enter to produce a pulse the chance of a count will be determined solely by the average fraction of arc of circle c included within the opening of the instrument. The chance of a count has finally to be averaged with respect to φ with the weight factor $\sin\varphi d\varphi$. The results of the rather long numerical calculations are plotted in Fig. 2 for comparison with Fink's results. No theoretical curve agrees entirely with his findings as they stand. If it be assumed, however, that energy corresponding to 2 mm of range is partly lost in the boron target and partly required to operate the counter, as does not seem unreasonable, then we obtain a satisfactory representation of the observations with an energy of disintegration of 125 kev, and a possible uncertainty in either direction of the order of 25 kev.

Combining all available evidence about the normal state of the nucleus Be^8, we conclude from the experiments of Laaff and Fink that the ground level is unstable by about 125 kev; from the alpha-particle model and also from the universal rule for even-even nuclei that it has zero angular momentum and even parity; and from the theory of radioactive decay[20] that it has a mean life of the order of 10^{-17} to 10^{-15} sec., corresponding to a natural width of the order of 1 to 100 ev.

3. The Hypothesis of Dee and Gilbert

Formation of Be^8 in the above-discussed normal state occurs in only a small percentage of the disintegrations of B^{11} by protons. Moreover, it leads to a quite characteristic distribution in energy of alpha-particles: primaries of 5.6 Mev, secondaries in the range $[\frac{1}{2}(5.6\text{ Mev})^{\frac{1}{2}} \pm \frac{1}{2}(0.125\text{ Mev})^{\frac{1}{2}}]^2$ or 1.02 to 1.86 Mev. Just below the primary group begins a very much more intense continuous spectrum of alpha-particles, extending down to the lowest energies at which observations have been made ($\sim$1.5 Mev) and effectively masking the just mentioned group of secondary alpha-particles. Dee and Gilbert[13] interpreted the strong spectrum as composed of two parts, one caused by primary alpha-particles recoiling from the Be^8 nuclei excited to a level at 2.8 Mev, the other caused by secondaries from the isotropic disintegration of such unstable nuclei. Working out this interpretation in more detail, Bethe obtained a satisfactory representation[20] of the observations of Oliphant, Kempton and Rutherford by assuming that the fraction of Be^8 nuclei, thus excited, with energy between E and $E+dE$, is given by

$$N(E)dE=\pi^{-1}\tfrac{1}{2}\Gamma dE/[(\tfrac{1}{2}\Gamma)^2+(E-E_0)^2], \quad (6)$$

with $E_0=2.8$ Mev, $\Gamma=0.8$ Mev.

To test Dee and Gilbert's hypothesis about an excited state of Be^8, Fink used the same arrangement of counters which he had employed in the experiments on normal Be^8, only increasing the thickness of covering foils to exclude the slow secondaries resulting from the decay of the latter nucleus. He varied the bias of the two counters with respect to energy and measured the ratio of coincidences to single counts. The ratios observed were less by an order of magnitude than those his calculations had led him to expect if an unstable Be^8 nucleus with about 2.8 Mev excitation were formed as an immediate step in the reaction of B^{11} with protons. Is there any escape from this difficulty?

Whether or not the hypothesis of a temporary Be^8 be true, the laws of conservation of momentum and energy can always be described by saying that a "primary" alpha-particle is ejected from an excited C^{12} nucleus; the remainder of the system recoils with equal and opposite total momentum, carrying within it any surplus

energy not used as kinetic energy; this surplus goes into energy of separation of two "secondary" alpha-particles. If the second division occurs before the first alpha-particle has really left, the distinction between the two stages of the disintegration process is of course purely formal, the disintegration being really a three-body process. Nevertheless from measurements on the energy and momentum of the three alpha-particles from an individual transmutation, performed with whatever elaborate conceivable arrangement of counters in coincidence, it is in principle not possible to say whether or not the given reaction took place in one or two stages. Therefore one cannot, without further assumptions conclude that the peak in the energy distribution of Oliphant, Kempton and Rutherford indicates a two-step process. Nor even if one does assume that the process has this character can he deduce from their observations the probability distribution of energy of excitation of the intermediate Be^8 nuclei without information as to the correlation in direction between the two division processes. But any mechanism of three-body disintegration which could give the observed well-defined peak would be so specialized and improbable as to argue for the formation of a rather defined intermediate Be^8 nucleus; and in proportion as this nucleus is well separated from the primary alpha-particle, all directions for its dissociation into secondaries are to be expected as equally probable. Not only is the existence of such excited nuclei and their isotropic disintegration thus very probable, but also these assumptions lead, as already noted, to a consistent interpretation of the observations of the Cambridge group. In the light of Fink's verdict against the hypothesis of Dee and Gilbert we must, however, inquire whether they and Bethe have adopted for the distribution in energy of intermediate Be^8 nuclei the *only* law giving an acceptable representation of the observations.

Let $f(E)dE$ denote the fraction of Be^8 nuclei excited in the interval E to $E+dE$. Disintegration of such nuclei in every direction being assumed equally probable, and the total energy release in the boron reaction being $Q=8.8$ Mev, the secondaries from the given nuclei will be distributed uniformly in energy between the limits

$$Q/6+E/3\pm(E/3)^{\frac{1}{2}}(Q-E)^{\frac{1}{2}}. \tag{7}$$

Primaries and secondaries counted together, the total number of alpha-particles per disintegration in the energy interval A to $A+dA$ will be

$$g(A)dA=f(Q-3E/2)3dA/2 + \int_{E_{\min}}^{E_{\max}}[2dA/2(E/3)^{\frac{1}{2}}(Q-E)^{\frac{1}{2}}]f(E)dE, \tag{8}$$

where

$$E_{\max},\ E_{\min}=Q/4+3E/4 \pm E^{\frac{1}{2}}(9Q/8-27E/16)^{\frac{1}{2}}. \tag{9}$$

To obtain the excitation law $f(E)$ from a knowledge of the distribution function $g(A)$, introduce new variables θ, φ and t:

$$E=(Q/2)(1-\cos\theta)$$
$$A=(Q/2)(1-\cos\varphi).$$
$$g=3t/2.$$

Also extend the domain of definition of t and φ by writing

$$-t(-\varphi)=t(\varphi)=-t(2\pi-\varphi)$$
$$-f(-\varphi)=f(\varphi)=-f(2\pi-\varphi).$$

Equation (8) then reduces to

$$t(\varphi)=f(\varphi)+(2/3^{\frac{1}{2}})\int_{2\pi/3-\varphi}^{2\pi/3+\varphi}f(\varphi)d\varphi. \tag{10}$$

Analysis of this equation in terms of its characteristic functions $\sin n\varphi (n=1, 2, 3, \cdots)$ shows that it possesses a solution if and only if the distribution in energy of emergent alpha-particles satisfies the condition of energy conservation,

$$\int_0^{\pi}\cos\varphi t(\varphi)\sin\varphi d\varphi=0. \tag{11}$$

This solution is unique only up to an arbitrary additive multiple of $\sin 2\theta$:

$$f(\theta)=t(\theta)+\cos 2\theta\left\{\int_0^{\theta}(4/3) + \int_{2\pi/3-\theta}^{2\pi/3+\theta}(4/3)\right\}\sin 2\varphi t(\varphi)d\varphi$$
$$-\sin 2\theta\left\{\int_0^{\theta}4+\int_{\theta}^{2\pi/3-\theta}(8/3) + \int_{2\pi/3-\theta}^{2\pi/3+\theta}(4/3)\right\}\cos 2\varphi t(\varphi)d\varphi$$
$$+\text{const}\cdot\sin 2\theta. \tag{12}$$

An entirely general distribution function $t(\varphi)$ being given, the excitation function $f(\varphi)$ will generally be found to be negative somewhere in the interval $\varphi=0$ to $\varphi=\pi$, and therefore unacceptable from a physical point of view, *whatever* be the choice of the arbitrary constant. Consequently it is of interest that when the observed distribution[21] is put into the right side of Eq. (12) and $f(\theta)$ is calculated, one and *only* one value for the arbitrary constant leads to an acceptable excitation function. This unique law of distribution of excitation energy for immediate Be^8 nuclei must therefore be essentially identical with that of Bethe and, except that outside the resonance region proper $f(\theta)$ falls off somewhat more rapidly than would be expected from Eq. (6), the similarity is very close indeed.

Dee and Gilbert's hypothesis being thus satisfactory in every other respect, does it actually lead to discrepancy with the coincidence experiments of Fink? Denote the angular semiaperture of the two opposed counters by a_1 and a_2, respectively. They respond only to alpha-particles whose energy is greater than B_1 and B_2. In the course of a given observation let $Nf(E)dE$ disintegrations of B^{11} occur with ejection in equal probability in all directions of Be^8 nuclei excited between E and $E+dE$. Of the recoiling primary alpha-particles, on the average $(Na_1^2/4)f(E)dE$ or none at all will enter the counter I according as the primary energy $(\frac{8}{3})(Q-E)$ is greater than or less than the bias B_1. The secondaries will be distributed in energy uniformly between the limits of Eq. (7) and will therefore give a contribution $2(Na_1^2/4)f(E)dE$ if the bias is below the lower limit, 0 if it is above the upper limit, and

$$2(Na_1^2/4)f(E)dE\{Q/6+E/3 +(E/3)^{\frac{1}{2}}(Q-E)^{\frac{1}{2}}-B_1\}/2(E/3)^{\frac{1}{2}}(Q-E)^{\frac{1}{2}},$$

if intermediate. The sum of the effects of primaries and secondaries, integrated over all values of the excitation energy E, will determine the number of counts Z_1 to be expected in counter I when it is set at a given bias, and similarly for counter II.

The intermediate nucleus Be^8 will have an excitation in the interval E to $E+dE$, the primary will enter counter I, and a secondary will enter counter II with a certain probability so that on the average such coincidences will occur to the number

$$(Na_1^2/4)2(a_2^2/4)(v_2+v_1/v_1)^2f(E)dE, \quad (13)$$

provided that the energy of the primary exceeds the bias B_1 and that the bias B_2 is less than the energy, $Q/6+E/3+(E/3)^{\frac{1}{2}}(Q-E)^{\frac{1}{2}}$, of a secondary thrown off just opposite to the primary. The factor $2(a_2^2/4)(v_2+v_1/v_1)^2$, according to Fig. 1, represents the solid angle within which the line of disintegration of Be^8 must lie if the secondary is to deviate by a small angle a_2 or less from the prolongation of the course of the primary. To (13) has to be added a similar expression allowing for coincidences where the primary enters counter II. Coincidences caused by one secondary entering each counter are negligible in number because they also can only occur when the excited Be^8 disintegrates nearly parallel to the direction of the primary, and then both have simultaneously appreciable energy only if the Be^8 is highly excited, which happens only rarely.

The number C of coincidences, and its ratio to the number Z_2 of pulses in counter II, can be calculated analytically when the excitation function for Be^8 is given by expression (6). The fraction of a sphere covered by counter I and II, respectively, being $a_1^2/4=1/440$ and $a_2^2/4=1/740$, and each experiment of Fink having been continued until 2000 particles entered

TABLE I. *Comparison of coincidences in counters I and II. The observed values in the last two columns are the number of counts in counter I and number of coincidences between I and II observed by Fink when 2000 counts were registered in II.*

Bias in Mev		Chance of Event		Calc.		Obs.	
B_1	B_2	$4Z_1/Na_1^2$	$16C/a_1^2a_2^2$	C	Z_1	Z_1	C
5.44	3.29	0.091	0.00	0	207	76	0
5.15	3.29	0.114	0.30	1	260	114	2
4.85	3.29	0.164	2.05	6	374	—	3
4.51	3.29	0.299	5.25	16	682	—	10
4.19	3.29	0.562	7.37	23	1280	—	16
3.84	3.29	1.060	10.21	31	2420	—	21
3.29	3.29	1.478	11.77	36	3370	3410	20
3.68	3.68	1.202	10.02	38	3370	—	19
4.04	4.04	0.785	5.82	34	3370	—	16
4.23	4.23	0.520	2.22	19	3370	—	26
4.40	4.40	0.366	0.00	0	3370	—	(1)
4.56	4.56	0.270	0.00	0	3370	—	0

[21] Relation (11) on the distribution function makes it possible to estimate fairly straightforwardly the distribution function below 1.5 Mev, where Oliphant, Kempton and Rutherford did not observe.

counter II, we can compute the numbers Z_1 and C to be expected and compare them with his results, as in Table I.

The hypothesis of Dee and Gilbert is seen to lead to results which by no means disagree by an order of magnitude with the observations of Fink. Details of the calculations which led to his contrary conclusions are not given in his very interesting paper, but the discrepancy presumably arose through identification of solid angle and circular angle as in the work by him and Laaff which was reanalyzed in Section 2. Even with proper allowance for geometry, predictions are not in complete accord with the observations, for at least one simple reason. In the first seven entries of Table I, counter II is used with constant bias and can be considered as monitoring counter I; so far as the measurement of Z_1 is concerned, Fink is to that extent repeating the observations of Oliphant, Kempton and Rutherford on the over-all distribution in energy of emergent alpha-particles. The fact that the first two entries of Z_1 do not agree thus only reemphasizes our earlier conclusion that expression (6) for the law of excitation of Be^8 does not fall off sufficiently rapidly outside the resonance region proper; the incomplete agreement is no argument against the disintegration theory proper of Dee and Gilbert. The *real* consequence of their hypothesis, the calculated number of coincidences, checks in order of magnitude with the observations. The discrepancies are outside the statistical errors only when the smaller values of bias are used. These discrepancies are certainly due in part to the oversimplified form assumed for the excitation function. Also allowance should be made in the calculation of the coincidences for possible asymmetry of the distribution in direction of the primary alpha-particles from the compound nucleus C^{12}. A recalculation is prevented by lack of information about the distribution for the primaries in which we are interested. It is known well only for the primaries from the reaction giving normal Be^8. That reaction, however, is responsible for no coincidences, and for a negligible number of single counts, in the above experiments.

We conclude that the hypothesis of Dee and Gilbert is consistent with all available observations when the limits of our information are taken into account. Knowledge that Be^8 has a well-defined resonance level at an excitation of about 3 Mev allows a unique analysis[11] of the scattering of alpha-particles in helium, with the result that the level in question possesses zero angular momentum.

4. Excited State with Two Units of Angular Momentum

Beta-ray decay of normal Li^8 leads to a broad unstable excited level of Be^8, according to Breit and Wigner,[22] who thus accounted qualitatively for the continuous distribution in energy of alpha-particles observed to accompany the electron emission. This explanation became more definite when Dee and Gilbert gave evidence for an excited level at about 2.8 Mev with a breadth of the order of 1 Mev. On the other hand, analysis in the preceding paper of observation on the scattering of 6-Mev to 7-Mev alpha-particles in helium indicates that Be^8 may possess a very broad resonance level with two units of angular momentum at an excitation of 4 or 5 Mev. Does either state furnish a satisfactory account of the observed distribution in energy of alpha-particles?

The electron and neutrino taking away a total energy between B and $B+dB$, the Be^8 nucleus will be left with an excitation in the interval dB at an energy given by $E=Q-B$. Here $Q=16$ Mev corresponds to the difference in mass between Li^8 and two free alpha-particles at rest. The probability per second that such a process shall occur will be nearly proportional to B^5, according to Fermi's theory of beta-decay, multiplied by the sum of the squares of the matrix elements between the initial state and all states in the interval E to $E-dB$. The behavior of the latter factor near a well-defined resonance level will follow the standard dispersion formula. Thus, the number of alpha-particles in a unit energy interval at $E/2$ will be expected to vary with E approximately as

$$B^5/[(E-E_0)^2+(\tfrac{1}{2}\Gamma)^2]. \qquad (14)$$

This formula, with $E_0=2.8$ Mev, $\Gamma=0.8$ Mev,

[22] G. Breit and E. Wigner, Phys. Rev. **50**, 1191 (1936); **51**, 593 (1937).

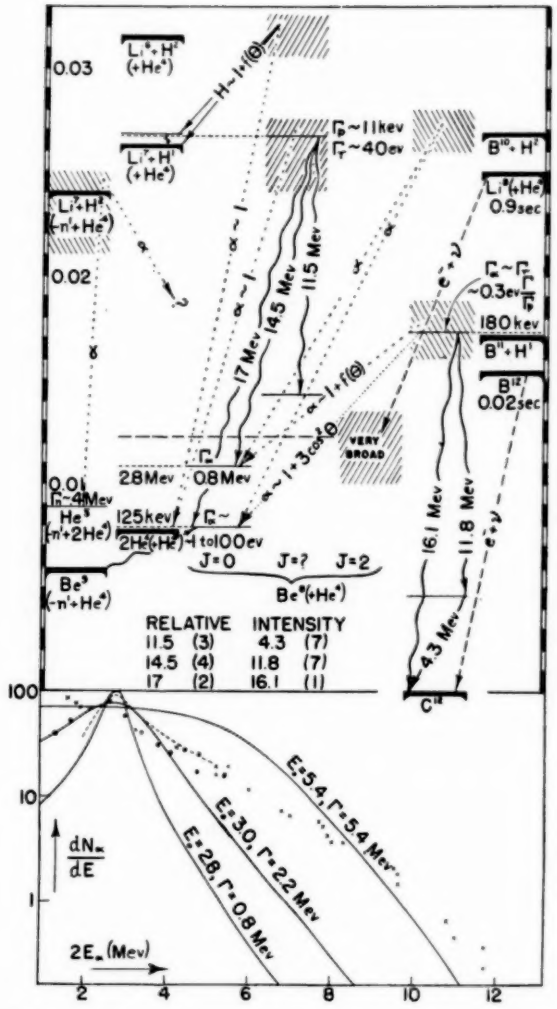

FIG. 3. The upper diagram summarizes certain transformations which lead to the nucleus Be^8. In the lower chart the circles and crosses represent observations of Rumbaugh, Roberts and Hafstad, reference 23, on the distribution in energy of alpha-particles which follow the decay of Li^8, and the dashed curve is based on the results of Fowler and Lauritsen. Disagreement between the measurements and the lower smooth curve shows that the end state of the decay process cannot be the 2.8-Mev level of Be^8.

gives a variation with energy in definite disagreement with the observations[23] (Fig. 3). Therefore we conclude that the beta-ray decay of Li^8 leads to a state of Be^8 which possesses a different angular momentum, and has much greater breadth, than the 2.8-Mev level. Assignment to the final state of an angular momentum of two units is most reasonable in view of analysis of the scattering of alpha-particles in helium. It is found impossible to assign to the end level a single energy E_0 and width Γ such that expression (14) will fit the observations. This situation, while at first sight unsatisfactory, is in the last analysis reasonable; the dispersion formula will not apply, and no satisfactory definition of level width and energy will in general be possible, when the "level" has a breadth comparable with its own excitation. To go further in such a case one would in principle have to solve a many-body problem and then carry through a calculation of matrix elements like that given by Kittel.[24]

On the above view the failure of Li^8 to decay with observable probability into either the 2.8-Mev level or the 0.12-Mev state of Be^8 is to be understood as caused by the action in each case of the same selection rule. Except for changing the role of the 2.8-Mev level we therefore come back to the interpretation of Breit and Wigner: The ground level of Li^8 is the component of highest angular momentum in the triplet $^3P_0$, $^3P_1$, $^3P_2$ predicted by Feenberg and Wigner[16] as lowest states of Li^8; a beta-ray transition in which the angular momentum changes by two units will be of negligible importance in comparison with a transition of the type 2→2. Absence of transitions to the 2.8-Mev level support the conclusion drawn from the alpha-particle scattering that this state has zero angular momentum.

Although the transition 2→2 is observed, the absolute value of the decay probability is, according to Kittel,[24] of the order of a hundredth what would off-hand have been expected from the lifetimes of nuclei of nearly that same mass. As explanation he suggests the change in spin (triplet→singlet) involved in the transformation, a change which is associated with the completely different symmetry character predicted for the two levels in question by Feenberg and Wigner.

5. SUMMARY: THE PROBLEM OF THE BORON REACTION

Analysis of observations on the scattering of alpha-particles in helium and of certain coincidence experiments has led to information about the first three levels of the nucleus Be^8. Figure 3

[23] W. A. Fowler and C. C. Lauritsen, Phys. Rev. **51**, 1103 (1937); L. H. Rumbaugh, R. B. Roberts and L. R. Hafstad, Phys. Rev. **51**, 1106 (1937); **54**, 672 (1938).

[24] C. Kittel, Phys. Rev. **55**, 515 (1939).

summarizes these results, together with some features of transformations in which Be^8 is involved. Satisfactory interpretations already given in the literature[25] for yields and angular distributions in most of these reactions need be changed only little, and in a fairly obvious manner, to take account of the new conclusions. However, to understand the selection rules for the reaction $B^{11}+H^1$ is at least as difficult now as when Oppenheimer and Serber treated the question[26] on the assumption that the 2.8-Mev level was of the type $^1D_2$. The evidence from the alpha-particle scattering has forced us to assign to this state the same angular momentum and parity as the $^1S_0$ ground level of Be^8, and the distribution of alpha-particles following the decay of Li^8 has indirectly helped to confirm this reassignment. Yet the disintegration of B^{11} leads to the ground state with a probability which shows a sharp resonance for 180-kev protons, while there is no apparent resonance in the much greater yield of Be^8 nuclei excited to the 2.8-Mev level. The intensity of both groups has been studied by various observers, particularly by Williams, Wells, Tate and Hill.[27] Still no available observations make it clear whether the apparent selection rule is absolute: (1) Does that state of the compound nucleus C^{12} which emits long (short) range alpha-particles also emit a few of short (long) range? If further observation shall reveal that the selection rule is not absolute, then we will have to ask, (2) why the probabilities are so different for C^{12}, in a given level, to break up into two states of Be^8 of the same angular momentum and parity; and (3) what must be the properties of the resonance level of C^{12} that it gives rise to a distribution in angle of long range alpha-particles approximately proportional to $1+3\cos^2\theta$.[28] If on the other hand, the selection rule shall be shown to be absolute, then an extremely difficult problem will arise, and it will be necessary to ask: (4) What is the possibility that the observations on the scattering of alpha-particles in helium, analyzed in the previous article, are in error by an amount much more than the limits stated in the original experimental papers? Further progress appears to depend on answering some of the above-mentioned questions. *Note added in proof.*—In contrast to the results of Neuert,[28] Jacobs and Whitson[29] now find that the angular distribution of both long and short range alpha-particles is spherically symmetric. They have kindly reported to the author that the curve for yield as a function of proton energy for *each* group of alpha-particles shows a resonance superposed on an exponentially increasing background. This result speaks against the operation of any absolute selection rule in the boron reaction and is consistent with the conclusion that the 2.8-Mev level of Be^8 has zero angular momentum. Moreover, the resonance and nonresonance processes, respectively, can now be interpreted in terms of singlet and triplet states of C^{12} formed by protons incident in s states. As principal problem there appears to remain only the explanation for the intensity difference between long and short range groups.

[25] Summarized in H. A. Bethe, Rev. Mod. Phys. **9**, 69 (1937); M. S. Livingston and H. A. Bethe, Rev. Mod. Phys. **9**, 245 (1937).

[26] J. R. Oppenheimer and R. Serber, Phys. Rev. **53**, 634 (1938).

[27] J. H. Williams, W. H. Wells, J. T. Tate and E. L. Hill, Phys. Rev. **51**, 434 (1937).

[28] H. Neuert, Ann. d. Physik **36**, 447 (1939).

[29] J. A. Jacobs and W. L. Whitson, Phys. Rev. **59**, 108A (1941).

Interaction of Alpha-Particles

HENRY MARGENAU
Sloane Physics Laboratory, Yale University, New Haven, Connecticut
(Received November 8, 1940)

The properties of the forces between alpha-particles are discussed on the basis of a Heitler-London analysis augmented by a "van der Waals" calculation. The results are in some respects unfavorable to the alpha-particle model of the nucleus inasmuch as they contradict the assumptions often made when this model is applied. Thus, for instance, it is pointed out that there are no attractive van der Waals forces beyond the range of the exchange forces, the range of the second-order forces being no greater than that of the first-order forces. The forces between alpha-particles are not additive. The range of the forces is approximately equal to that of the forces between elementary nuclear particles. The Heitler-London forces are repulsive if the usual choice of a symmetric Hamiltonian is made. The details of the forces are first worked out in connection with a simple fictitious example (§1) in terms of which these various features are most easily discussed. Calculations for the alpha-particle, for which a ψ-function of the Gauss type is assumed, are made in §§2 and 3. Finally (§4) the results are used in an examination of the problem of the scattering of alpha-particles in helium. It appears that the scattering of the S waves can be explained only partially by means of the present interaction, its fault being the failure to produce resonance at the correct energy.

THE attempts to understand the properties of nuclei have led to the invention of a number of models which are thought to represent, in an approximate fashion, the significant details of nuclear structure. The earliest of these, the independent particle or Hartree model, has been discussed so frequently that its merits, and more particularly its faults, are now commonly recognized. Of more recent interest has been the alpha-particle model[1] which springs from the consideration that the alpha-particle is a tightly bound group, and likely, as such, to have a fairly permanent identity within a nucleus. In agreement with this picture it is sometimes supposed that alpha-particles interact in a manner typical of the constituent parts of a molecule; indeed the machinery of molecular theory is then brought into action and a number of qualitative results are obtained. But the detailed manner of interaction of two alpha-particles, about which apparently plausible but totally *ad hoc* assumptions are made in such calculations, has not been investigated with due thoroughness. Even the simple question as to the attractive or repulsive nature of these supposed building blocks of nuclei does not seem to have been satisfactorily answered, nor is there any evidence that the scattering of alpha-particles in helium can or cannot be understood in terms of basic postulates about forces between primary nuclear constituents. The present paper deals with these questions.

A common argument relative to the alpha-particle interaction relies on the analogy with the molecular problem: At close distances of approach, it is pointed out, there must be strong exchange forces, and these are repulsive because the interaction occurs between closed shells; at larger distances of separation, attractive van der Waals forces come into play, and finally the Coulomb force alone remains active. In addition to this, one often assumes these forces to be additive.

A little reflection shows, however, that these conclusions may not be taken for granted, for there are, after all, essential differences between the molecular and the nuclear case. For example, the exchange repulsion between two H atoms which occurs at small distances when they approach each other in the triplet state, depends quite definitely upon the character of the Coulomb force; it might well turn into an attraction if the force between electrons were itself of an exchange nature. The force between nuclear elementary particles is of this type; hence a special investigation is needed to ascertain the direction of the force acting between alpha-particles. Secondly, to speak of a van der Waals force is in this instance almost meaningless; for this terminology implies that there exists a

[1] Cf., for instance, L. R. Hafstad and E. Teller, Phys. Rev. **54**, 681 (1938). For a general discussion of the various aspects of particle groups in nuclei see J. A. Wheeler, Phys. Rev. **52**, 1083 (1937). Here the limitations of the simple alpha-particle picture are recognized.

region in which second-order forces are large compared to the first-order forces. In molecular interactions this is true because, as one may easily see, the Coulomb force has a range which is much larger than the diameter of a molecule—an alpha-particle, however, has dimensions of the same order of magnitude as the range of the elementary nuclear forces. It will also be seen that the assumption of the additivity of inter-alpha-forces is quite untenable.

A simplified quantitative calculation of the interaction in question has been made by Heisenberg.[2] He assumes that the centers of mass of the alpha-particles are not exactly localized but distributed in space with Gaussian probability. This artifice has the advantage of obviating an explicit calculation of the kinetic energy of the particles, and furthermore respects the uncertainty principle in more adequate measure than the formalism of fixed alpha-centers would. However, it makes the results obtained more difficult to interpret.[3] Heisenberg's calculation differs from the one presented in this paper in several other respects: It neglects forces between like particles and assumes only Majorana forces between unlike particles, restrictions which are no longer permissible; finally, in the calculation of the exchange integrals, terms which arise from double transpositions of coordinates in the ψ-function are omitted. The latter approximation is a valid one when the overlap integral is small, but this condition is strongly violated in the present case over the entire region of the interaction.

The method to be employed in the present paper and its results may be discussed most simply in connection with a fictitious two-particle problem which bears a certain resemblance to the interaction of two deuterons. The ψ-functions used, however, are very poor approximations to the deuteron functions, so that the results have only qualitative significance. But the essential differences between the nuclear and the molecular problem can be seen very clearly.

[2] W. Heisenberg, Zeits. f. Physik **96**, 473 (1935).

[3] Cf. H. Bethe and R. F. Bacher, Rev. Mod. Phys. **8**, 82 (1936). The result stated in footnote 67 of this paper is not valid since Heisenberg's Eq. (14) holds only for small η.

1. Two-Particle Problem. Comparison Between Exchange and van der Waals Forces

Let us assume a particle to be bound to a fictitious center by simple harmonic forces. Its state function corresponding to the lowest energy will then be

$$u=(q/\pi)^{3/4}\exp\left[-\tfrac{1}{2}qr^2\right], \tag{1}$$

q being a parameter which measures the strength of binding. If an identical particle is situated with its center of force a distance $\mathbf{R}$ from that of the first particle, the ψ-function for this system may be written in the Heitler-London approximation:

$$\psi(1,2)=(2-2\delta^2)^{-\frac{1}{2}}\times[u(1)v(2)-v(1)u(2)]\alpha(1)\alpha(2). \tag{2}$$

The spins are here taken to be parallel; $v(r)$ stands for $u(\mathbf{r}-\mathbf{R})$, and

$$\delta=\int uv\,d\tau=\exp\left[-\tfrac{1}{4}qR^2\right].$$

Suppose that particles 1 and 2 interact, their classical potential energy being V. The first-order energy between the two is then given as the sum of two terms:

$$\Delta_1E=\bar{V}+\Delta E_{\text{kin}},$$

where $\bar{V}=\int\psi^*V\psi\,d\tau$ and ΔE_{kin} is the difference between the mean of $-(\hbar^2/2M)(\nabla_1^2+\nabla_2^2)$ taken with the function ψ, and the kinetic energy of the two oscillators at infinite separation. Turning our attention first to the computation of ΔE_{kin} we find

$$\int\psi\nabla_1^2\psi\,d\tau=\int\psi\nabla_2^2\psi\,d\tau$$

$$=(1-\delta^2)^{-1}\left[\int u\nabla^2u\,d\tau-\delta\int u\nabla^2v\,d\tau\right]$$

$$=-3q/2-\tfrac{1}{4}q^2R^2\delta^2/(1-\delta^2).$$

The first term of this expression, when multiplied by $-\hbar^2/2M$, is just the kinetic energy of one particle not interacting with the other, that is, $-(\hbar/2M)\int u\nabla^2u\,d\tau$. Hence

$$\Delta E_{\text{kin}}=(\hbar^2/4M)q^2R^2\delta^2/(1-\delta^2). \tag{3}$$

It is perhaps noteworthy that in the limit $R\to0$, ΔE_{kin} becomes $\hbar^2q/2M=\frac{1}{2}h\nu$, ν being the classical

frequency of the oscillator. Now the kinetic energy of an oscillator in its ground state is $\frac{3}{4}h\nu$, one-half its total energy; in the next excited state, the kinetic energy is $(\frac{3}{4}+\frac{1}{2})h\nu$. Thus our value of ΔE_{kin} indicates a promotion of one of the oscillators to an excited state as $R\to 0$. The same result may be read from the function (2) which becomes

$$\psi_{R\to 0}=q^{\frac{1}{2}}(\mathbf{r}_2-\mathbf{r}_1)\cdot\mathbf{R}u(1)u(2)/|R|$$

and this represents the $(1s)(2p)$-configuration of two (isotropic) oscillators.

As to V, two different suppositions will be made. First we take it to be an ordinary potential energy: $V=-Ae^{-r^2/a^2}$. Evaluation of the integrals (cf. formulas 15) leads to

$$\bar{V}=-A\tau^{\frac{3}{2}}(1-\delta^2)^{-1}$$
$$\times(\exp[-\tau R^2/a^2]-\exp[-\tfrac{1}{2}\sigma R^2/a^2]). \quad (4)$$

Here σ and τ are two parameters which occur throughout this work:

$$\sigma\equiv qa^2; \quad \tau\equiv\sigma/(\sigma+2). \quad (5)$$

Second, we may choose for V a Majorana potential: $V=-Ae^{-r^2/a^2}P_{12}$. In that case $\bar{V}$ is given by (4) but with its sign reversed. Collecting these results we obtain for the first-order energy (using the notation 5)

$$\Delta_1E=\frac{\hbar^2}{4Ma^2}\sigma^2\frac{R^2}{a^2}\frac{\delta^2}{1-\delta^2}\pm\bar{V}. \quad (6)$$

For $R\to 0$, this expression takes the form $\hbar^2\sigma/2Ma^2 \pm A\tau^{5/2}\sigma$; as R increases Δ_1E changes in monotone fashion. Clearly, if V is a Majorana (or Heisenberg) potential, Δ_1E represents a repulsion at all distances, while an ordinary potential may, for suitable values of A and a, produce attraction.

Next we consider the second approximation, Δ_2E, which is given by $-\langle V^2\rangle_{Av}/E_m$. The quantity E_m is some mean of all the excited energies of the system, the exact value of which can be ascertained by performing the summation appearing in the expression for the second-order perturbation energy. For the present purposes no exact attempt to evaluate it will be made. In molecular problems, it is in general sufficient to calculate $\langle V^2\rangle_{Av}$ with the function $u(1)v(2)$, a procedure which neglects exchange. To test the validity of this simplification let us first compute $\langle V^2\rangle_{Av}$ with exchange, that is with the use of the function $\psi(1, 2)$ given by (2). The result is easily seen to be

$$\langle V^2\rangle_{Av}=A^2\left(\frac{\sigma}{\sigma+4}\right)^{\frac{3}{2}}(1-\delta^2)^{-1}$$
$$\times\left(\exp\left[-\frac{2\sigma}{\sigma+4}\frac{R^2}{a^2}\right]-\exp\left[-\frac{\sigma}{2}\frac{R^2}{a^2}\right]\right). \quad (7)$$

If $\langle V^2\rangle_{Av}$ had been calculated with the use of $u(1)v(2)$ alone, the bracket appearing here would have contained only the first item, and the factor $(1-\delta^2)$ would be replaced by 1. Thus we identify the first term in the bracket as the "direct" one, the second as the exchange term.

The range of the nuclear force is a, the "radius" of the ψ-functions of each particle is $q^{-\frac{1}{2}}$. Hence $q^{\frac{1}{2}}a\equiv\sigma^{\frac{1}{2}}$ is the ratio of these two lengths. Now it is seen from (7) that, if σ is large, the exchange term decreases very rapidly in comparison with the direct term as R increases. This provides the justification for neglecting the exchange term in ordinary molecular problems. In the nuclear problem, however, σ is of order unity, and the exchange term must be retained.

It is equally instructive to compare the range of the first-order forces with that of the second-order forces. If σ is large, only the constituent $\bar{V}$ of Δ_1E remains ($\delta^2=\exp[-\frac{1}{2}\sigma R^2/a^2]$), and the exchange term in $\bar{V}$ (second term in the bracket of (6)) becomes small in comparison with the other; hence the dominating part of Δ_1E is $\exp[-\tau R^2/a^2]$ and this becomes e^{-R^2/a^2}. The leading term of $\langle V^2\rangle_{Av}$ in this case is

$$\exp\left[-\frac{2\sigma}{\sigma+4}\frac{R^2}{a^2}\right]\to\exp\left[-2\frac{R^2}{a^2}\right].$$

Thus the first-order forces have the *longer* range even for large σ. This is indeed characteristic of the nuclear situation. The fact that in the molecular case the reverse is true is conditioned by the nature of the Coulomb force and by the circumstance that each molecule has as many attracting as repulsive constituents. In the interaction of two H atoms, for example, the direct term (corresponding to $\exp[-\tau R^2/a^2]$ in (6)) becomes zero as soon as the atoms cease to overlap, whereas the direct term of (7) continues

to be appreciable and furnishes the van der Waals attraction.

These considerations illuminate the marked differences which exist between nuclear interactions and those between molecules. They prepare for an understanding of the results which will now be deduced for the interaction between alpha-particles.

2. Alpha-Particles. First-Order Forces

The energy of an alpha-particle is given variationally with good approximation by a product of Gauss functions of the type (1),[4] which yields more than 90 percent of the true energy if the range of the nuclear forces is 2.25×10^{-13} cm.[5] The value of q will depend on this range; indeed the lowest value of the energy is obtained by choosing

$$qa^2=\sigma=2.60.$$

Let the particles composing the first alpha-particle be labeled 1256, those composing the second 3478; 1, 2, 3, and 4 are protons. At large separation the first alpha-particle will have the state function

$$\tfrac{1}{2}\cdot\begin{vmatrix}u(1)\alpha(1) & u(1)\beta(1)\\ u(2)\alpha(2) & u(2)\beta(2)\end{vmatrix}\cdot\begin{vmatrix}u(5)\alpha(5) & u(5)\beta(5)\\ u(6)\alpha(6) & u(6)\beta(6)\end{vmatrix}, \quad (8)$$

the second a similar one with u replaced by v. α and β are spin functions. The system of two will be represented by the product of these, that is, by a product of four 2-rowed determinants. Such a function neglects the exchange of particles between the alpha-groups. The function which includes this exchange, and which will serve as the basis for the present calculation, is the following:

$$\psi=N_pU(1234)\cdot N_nU(5678) \quad (9)$$

with $N_p=N_n=(4!)^{-\frac{1}{2}}(1-\delta^2)^{-1}$, and

$$U(1234)=\begin{vmatrix}u_+(1) & u_-(1) & v_+(1) & v_-(1)\\ u_+(2) & u_-(2) & v_+(2) & v_-(2)\\ u_+(3) & u_-(3) & v_+(3) & v_-(3)\\ u_+(4) & u_-(4) & v_+(4) & v_-(4)\end{vmatrix} \quad (10)$$

$u_+(1)$ means $u(1)\alpha(1)$ etc., δ is again $\exp[-\frac{1}{4}qR^2]$, and $v(i)=v(\mathbf{r}_i)=u(|\mathbf{r}_i-\mathbf{R}|)$. $\mathbf{R}$ is the vector from the center of the first to that of the second alpha-particle. This coordinate will here be treated as a fixed parameter in conformity with molecular methods. The justification for such a procedure is not nearly so good in nuclear problems as it is in the molecular one, where the individual moving particles (electrons) are very much lighter than the nuclei. Our results will therefore be in error on this account; but this error will hardly affect the conclusions we wish to draw. To avoid it would require the use of more complicated methods such as that of Wheeler.[1]

The calculation of the first-order forces proceeds as follows: From the function ψ [Eq. (9)], $\bar{V}$ is computed, V being the total potential energy of the particles 1 to 8. From this must be subtracted the internal potential energy, V_0, of two alpha-particles which are not interacting, and finally ΔE_{kin}, the kinetic energy of promotion of 2 neutrons and 2 protons and the mutual Coulomb energy, E_c, are to be added. V is the sum over all 28 particle pairs of the elementary interaction V_{ij}, and this will here be taken as the sum of 3 exchange potentials and one ordinary potential with coefficients to be discussed later. Thus

$$V_{ij}=-AJ_{ij}(w+mP_{ij}+bQ_{ij}+hP_{ij}Q_{ij}) \quad (11)$$

with $J_{ij}=\exp[-r_{ij}^2/a^2]$. The operator P permutes space coordinates, Q permutes the spins. This form of V_{ij} no longer appears consistent in detail with recent developments in nuclear physics, meson potentials being now generally favored. The latter differ from (11) chiefly in two respects: They depend on r_{ij} in a slightly different way and they vary with the angle between $\mathbf{r}_i$ and $\mathbf{r}_j$. This last feature is not likely to be important in the present problem because the alpha-particles, being closed shells, will not exhibit polar forces even if the elementary particles do. As to the dependence on r_{ij}, the meson potential introduces a singularity at the origin which must be meaningless and is avoided by some cutting-off process. It is not yet known whether the radial function of the meson potential is more satisfactory than that of (11).

[4] H. Margenau and W. A. Tyrrell, Phys. Rev. **54**, 422 (1938).

[5] According to Breit, Thaxton and Eisenbud, Phys. Rev. **55**, 1018 (1939) the range is smaller. The degree of approximation by Gauss functions is then poorer.

V consists of 12 like-particle terms and 16 unlike-particle terms. Typical of the first class is V_{34}, of the second, V_{48}. We first establish the fact that all like-particle $\bar{V}_{ij}$ are equal, and similarly that all unlike-particle $\bar{V}_{ij}$ are equal, so that

$$\bar{V}=12\bar{V}_{34}+16\bar{V}_{48}. \tag{12}$$

The first follows immediately from the indistinguishability of like particles in the determinants U which compose the function ψ. Equality of unlike-particle interactions may be proved as follows: Since ψ is antisymmetrical with respect to (1234) and also to (5678), we have, for instance,

$$\int\psi V_{17}\psi d\tau=\int(14)(78)\psi(14)(78)\,V_{17}(14)(78)\psi d\tau=\int\psi V_{48}\psi d\tau.$$

(The numbers in parentheses indicate transpositions of coordinates to be performed in the function, ψ or V, which follows; and integrals include summations over spins.) Thus $\bar{V}_{17}=\bar{V}_{48}$ etc., and this establishes (12). In calculating the like-particle interaction we note that

$$\int\psi J_{34}P_{34}Q_{34}\psi d\tau=-\int\psi J_{34}\psi d\tau \quad\text{and}\quad \int\psi J_{34}P_{34}\psi d\tau=-\int\psi J_{34}Q_{34}\psi d\tau.$$

Therefore

$$\bar{V}_{34}=-A\left\{(w-h)\int\psi J_{34}\psi d\tau+(b-m)\int\psi J_{34}Q_{34}\psi d\tau\right\}. \tag{13}$$

The calculation of the integrals which appear here involves first an integration over particles (5678). There will then be left in ψ only one determinant, and this may be decomposed in a suitable way to form the products ψ^2 and $\psi\cdot Q_{34}\psi$. The final integrations are all elementary and can be performed with the use of the single formula

$$\int\int_{-\infty}^{\infty}\exp\,(-ax_1^2-bx_2^2+cx_1+dx_2+ex_1x_2)dx_1dx_2=\pi\left(ab-\frac{e^2}{4}\right)^{-\frac{1}{2}}\exp\left(\frac{ad^2+bc^2+cde}{4ab-e^2}\right). \tag{14}$$

The following basic integrals occur:

$$\left.\begin{aligned}
&\lambda_1\equiv\int u^2(1)u^2(2)J_{12}d\tau_1d\tau_2 &&=\int v^2(1)v^2(2)J_{12}d\tau_1d\tau_2 &&=\tau^{\frac{1}{2}}\\
&\lambda_2\equiv\int u^2(1)v^2(2)J_{12}d\tau_1d\tau_2 &&&&=\tau^{\frac{1}{2}}\exp\,[-\tau\rho^2]\\
&\lambda_3\equiv\int u(1)v(1)u(2)v(2)J_{12}d\tau_1d\tau_2 &&&&=\tau^{\frac{1}{2}}\exp\,[-\tfrac{1}{2}\sigma\rho^2]\\
&\lambda_4\equiv\int u(1)v(1)u^2(2)J_{12}d\tau_1d\tau_2 &&=\int u(1)v(1)v^2(2)J_{12}d\tau_1d\tau_2 &&=\tau^{\frac{1}{2}}\exp\,[-\tfrac{1}{4}(\sigma+3)\tau\rho^2]\\
&\delta\equiv\exp\,[-\tfrac{1}{4}\sigma\rho^2]
\end{aligned}\right\} \tag{15}$$

with $\sigma=qa^2$, $\tau=\sigma/(\sigma+2)$, $\rho=R/a$. One then obtains

$$\left.\begin{aligned}
&\int\psi J_{34}\psi d\tau=\tfrac{1}{3}(1-\delta^2)^{-2}\{\lambda_1+2\lambda_2-\lambda_3-4\delta\lambda_4+\delta^2(3\lambda_3-\lambda_2)\},\\
&\int\psi J_{34}Q_{34}\psi d\tau=\tfrac{1}{3}(1-\delta^2)^{-2}\{-\lambda_1+\lambda_2-2\lambda_3+4\delta\lambda_4-2\delta^2\lambda_2\}.
\end{aligned}\right\} \tag{16}$$

Turning now to the unlike-particle interaction, $\bar{V}_{48}$, we note first that

$$\int \psi J_{48} Q_{48} \psi d\tau = \tfrac{1}{2} \int \psi J_{48} \psi d\tau \quad \text{and} \quad \int \psi J_{48} P_{48} Q_{48} \psi d\tau = \tfrac{1}{2} \int \psi J_{48} P_{48} \psi d\tau.$$

The factor $\frac{1}{2}$ on the right side of these equations results because half the terms in the expanded determinants drop out on account of spin orthogonality after the Q permutations have been carried out. Thus

$$\bar{V}_{48} = -A \left\{ (w + \tfrac{1}{2}b) \int \psi J_{48} \psi d\tau + (m + \tfrac{1}{2}h) \int \psi J_{48} P_{48} \psi d\tau \right\}, \tag{17}$$

and the integrals are

$$\begin{aligned} \int \psi J_{48} \psi d\tau &= \tfrac{1}{2}(1-\delta^2)^{-2}\{\lambda_1 + \lambda_2 - 4\delta\lambda_4 + 2\delta^2\lambda_3\}, \\ \int \psi J_{48} P_{48} \psi d\tau &= \tfrac{1}{2}(1-\delta^2)^{-2}\{\lambda_1 + \lambda_3 - 4\delta\lambda_4 + \delta^2(\lambda_2 + \lambda_3)\}. \end{aligned} \tag{18}$$

From (13), (16), (17), and (18) $\bar{V}$ can be compounded in accordance with Eq. (12). The internal potential energy of two alpha-particles, V_0, is easily seen to be

$$V_0 = -12A(w+m)\lambda_1.$$

Thus

$$\begin{aligned} \bar{V} - V_0 = -4A(1-\delta^2)^{-2}\{w[(4-\delta^2)\lambda_2 + (5+4\delta^2)\lambda_3 - 12\delta\lambda_4] + m[(4\delta^2-1)\lambda_2 + (10-\delta^2)\lambda_3 - 12\delta\lambda_4] \\ + 2(b-h)(1-\delta^2)(\lambda_2 - \lambda_3)\}. \end{aligned} \tag{19}$$

The remaining λ's are all exponential functions of $-R^2$, but have different ranges. The expression is finite at $R=0$ and tends to the limit

$$-4A\tau^3\sigma^{-2}\{w[4(\sigma-\tau)^2 + \tfrac{1}{2}\tau^2] + m[11\tau^2/2 - (\sigma-\tau)^2] + 2(b-h)\sigma^2\tau\}. \tag{20}$$

The coefficients of w, m, b, and h in (19) are plotted in Fig. 1. It is to be noted that ordinary forces produce strong attraction, spin exchange forces half as strong attraction, while Majorana and Heisenberg forces produce repulsion between alpha-particles, results which are seen to be closely related to the saturation properties of these forces.

To evaluate Eq. (19) it is necessary to fix the nuclear constants w, m, b, and h. Fortunately, the interaction is almost independent of the particular choice as long as it satisfies the relations[6]

$$\left.\begin{aligned} w+m+b+h &= 1 \\ m+h &\geqq 2w+2b, \\ m+2h &\geqq 4w+2b. \end{aligned}\right\} \quad \begin{matrix} \\ \text{(a)} \\ \text{(b)} \end{matrix}$$

In addition to these, let us impose: $b+h=0.2$, a value which seems to be in agreement with most facts known about light nuclei. One can then plot h as a function of w, first in accordance with relation (a) taken as an equality and disregarding (b), then in accordance with equality (b) disregarding (a). To eliminate all ambiguity we now select that value of h, for any given w, which makes the repulsion smallest; that is, the smaller of the two permitted values of h. The locus of these is very nearly

$$h = 1.25w - 0.1.$$

[6] N. Kemmer, Nature **140**, 192 (1937); G. Breit and E. Feenberg, Phys. Rev. **50**, 850 (1936).

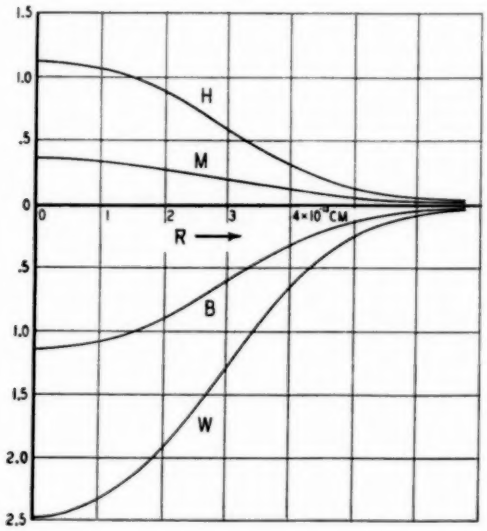

FIG. 1. Contributions to the potential energy of two alpha-particles, as functions of separation between their centers, from the different constituents of V. Heisenberg and Majorana forces (H, M) produce repulsion, the others attraction.

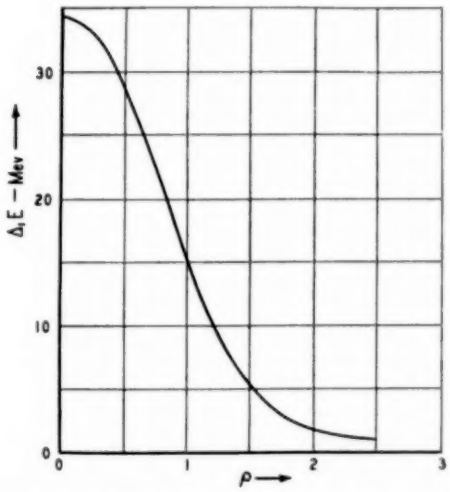

FIG. 2. Total first-order interaction between alpha-particles as function of ρ, the distance of separation in units a, the range of the nuclear force [cf. Eq. (11)].

This allows the parameters appearing in $\bar{V}-V_0$ to be expressed in terms of w: $m=0.80-w$, $b-h=0.40-2.50w$. Now, as mentioned before, minimization of the alpha-particle energy requires σ to be 2.60, hence $\tau=0.565$. It is seen from Fig. 1 that the ratio of the coefficients of w, m, b, h is approximately constant at all values of R, so that the value of $\bar{V}-V_0$ at any particular R, and most conveniently at $R=0$, is a measure of this interaction. Let us, therefore, evaluate $\bar{V}-V_0$ at $R=0$ as a function of w. Equation (20) gives

$$-60.5 \text{ Mev } [2.47w-0.35m+1.13(b-h)],$$

if A is taken to be 35.6 Mev in conformity with the theory of light nuclei. When the above values are inserted here, it turns out that w cancels almost exactly and the result is -10.4 Mev. We conclude, therefore, that the first-order interaction between alpha-particles is almost independent of the choice of force parameters. The potential energy is negative, but it will be seen that $\Delta_1 E$, which includes also the kinetic energy of promotion and the Coulomb energy E_C, is everywhere positive.

The total kinetic energy is

$$-\frac{\hbar^2}{2M}\langle\sum_i \nabla_i^2\rangle_{Av}=-\frac{4\hbar^2}{M}(1-\delta^2)^{-1}\int[u\nabla^2 u-\delta u\nabla^2 v]d\tau=\frac{4\hbar^2}{M}(1-\delta^2)^{-1}\{\tfrac{3}{2}q-(\tfrac{3}{2}q-\tfrac{1}{4}q^2R^2)\delta^2\}.$$

From this must be subtracted $(8\hbar^2/2M)(3q/2)$, the kinetic energy at infinite separation. Thus

$$\Delta E_{\text{kin}}=\frac{\hbar^2}{Ma^2}\sigma^2\rho^2\frac{\delta^2}{1-\delta^2}.$$

The Coulomb energy is most conveniently calculated in the "two center" system of coordinates familiar from the theory of the hydrogen molecule. If exchange is neglected, the result is very simple:

$$E_C=(4e^2/R)\text{ erf }[(\tfrac{1}{2}q)^{\frac{1}{2}}R].$$

Inclusion of exchange makes the expression more complicated for small values of R, but the modifications are hardly of interest because in this region E_C is much smaller than the other constituents of

the interaction. It takes the value 3.27 Mev at $R=0$ if we take for a the value 2.25×10^{-13} cm. When ΔE_{kin} and E_C are added to (19) and the λ-integrals are introduced, the result is

$$\Delta_1 E=\frac{\exp\left[-\frac{1}{2}\sigma\rho^2\right]}{1-\exp\left[-\frac{1}{2}\sigma\rho^2\right]}\left\{\frac{\hbar^2}{Ma^2}\sigma^2\rho^2-\frac{4A\tau^{\frac{1}{2}}}{1-\exp\left[-\frac{1}{2}\sigma\rho^2\right]}\left[w(5+4\exp\left[-\tfrac{1}{2}\sigma\rho^2\right]+4\exp\left[\tfrac{1}{2}\sigma\tau\rho^2\right]\right.\right.$$
$$-\exp\left[-\tau\rho^2\right]-12\exp\left[-\tfrac{1}{4}\tau\rho^2\right])+m(10-\exp\left[-\tfrac{1}{2}\sigma\rho^2\right]+4\exp\left[-\tau\rho^2\right]-\exp\left[\tfrac{1}{2}\sigma\tau\rho^2\right]$$
$$\left.\left.-12\exp\left[-\tfrac{1}{4}\tau\rho^2\right])+2(b-h)(1-\exp\left[-\tfrac{1}{2}\sigma\rho^2\right])(\exp\left[\tfrac{1}{2}\sigma\tau\rho^2\right]-1)\right]\right\}+(4e^2/R)\operatorname{erf}\left[(\tfrac{1}{2}\sigma)^{\frac{1}{2}}\rho\right]. \quad (21)$$

This expression is plotted in Fig. 2 for $b+h=0.2$, a choice which, as noted, makes $\Delta_1 E$ practically independent of w. The largest component of (21) is ΔE_{kin} which represents the energy of promotion of 4 particles to p states. It is to be remarked, however, that the function ψ of (9), while approaching the correct configuration $(1s)^4(2p)^4$ as $R\to0$, does not acquire the proper symmetry of a ^1S-state but contains an admixture of ^1D and ^1G as well. This implies increasing poorness of the approximation to the energy as $R\to0$, a defect which did not arise in the two-particle problem discussed in the foregoing section. The range of the first-order forces is seen to be practically the same as that of the nuclear forces themselves.

3. Second-Order Forces

An exact calculation of the second-order forces would be extremely tedious. We shall use here the method outlined in §1 and compute $-\langle V^2\rangle_{\text{Av}}$, leaving aside the constant factor $1/E_m$, since our interest concerns chiefly the range of the second-order forces. Furthermore, $\langle V^2\rangle_{\text{Av}}$ will be calculated *without* exchange. The effect of this neglect may be understood by examining Eq. (7) again. With the value of σ for the alpha-particle, the exchange term in that expression is $e^{-1.30\rho^2}$, the direct term is $e^{-0.79\rho^2}$. The latter persists at larger distances. Our procedure will therefore yield the constituent of the second-order forces which has the longer range. Finally, we shall avoid the complications arising from the fact that V is a mixture of different exchange terms and calculate $\langle V^2\rangle_{\text{Av}}$ for ordinary, pure Majorana, etc., interactions. After making all these simplifications, no quantitative inferences may be drawn from the results of this section, but several characteristic features become evident. The calculations need not be given in detail. Suffice it to say that, when

$$V=\sum_{i\neq j}V_{ij}{}^7$$

is squared and the integrations are performed, there result three groups of terms: 2-particle integrals like $\langle J_{15}{}^2\rangle_{\text{Av}}$, 16 in number; 3-particle integrals like $\langle J_{15}J_{16}\rangle_{\text{Av}}$, 96 in number; 4-particle integrals, 144 in number. The integrals are in general different for the different types of interactions. For spin-dependent interactions, the numbers of integrals will be effectively reduced by orthogonality of spin functions which fail to match after permutation. This explains the different coefficients in the expressions which follow. We find

$V_{ij}=J_{ij}$:

$$\langle V^2\rangle_{\text{Av}}=16\left(\frac{\sigma}{\sigma+4}\right)^{\frac{1}{2}}\exp\left[-\frac{2\sigma}{\sigma+4}\rho^2\right]+96\left[\frac{\sigma^2}{(\sigma+1)(\sigma+3)}\right]^{\frac{1}{2}}\exp\left[-\frac{2\sigma}{\sigma+3}\rho^2\right]$$
$$+144\left(\frac{\sigma}{\sigma+2}\right)^3\exp\left[-\frac{2\sigma}{\sigma+2}\rho^2\right],$$

$V_{ij}=J_{ij}P_{ij}$:

$$\langle V^2\rangle_{\text{Av}}=16\left(\frac{\sigma}{\sigma+4}\right)^{\frac{1}{2}}\exp\left[-\frac{2\sigma}{\sigma+4}\rho^2\right]+96\left[\frac{\sigma^2}{(\sigma+1)(\sigma+3)}\right]^{\frac{1}{2}}\exp\left[-\frac{\sigma+4}{\sigma+3}\cdot\frac{\sigma}{2}\rho^2\right]$$
$$+144\left(\frac{\sigma}{\sigma+2}\right)^3\exp\left[-\sigma\rho^2\right].$$

[7] The summation here is to be extended only over pairs not belonging to the same alpha-particles.

$V_{ij}=J_{ij}Q_{ij}$:

$$\langle V^2\rangle_{Av}=16\left(\frac{\sigma}{\sigma+4}\right)^{\frac{1}{2}}\exp\left[-\frac{2\sigma}{\sigma+4}\rho^2\right]+48\left(\frac{\sigma}{\sigma+2}\right)^{3}\exp\left[-\frac{2\sigma}{\sigma+2}\rho^2\right],$$

$V_{ij}=J_{ij}P_{ij}Q_{ij}$:

$$\langle V^2\rangle_{Av}=16\left(\frac{\sigma}{\sigma+4}\right)^{\frac{1}{2}}\exp\left[-\frac{2\sigma}{\sigma+4}\rho^2\right]+48\left(\frac{\sigma}{\sigma+2}\right)^{3}\exp\left[-\sigma\rho^2\right].$$

$\rho\equiv R/a$.

As an example, $\langle V^2\rangle_{Av}$ and $\bar{V}$ have been plotted for the case of pure Majorana forces in Fig. 3, the ordinates having been so adjusted as to make the two equal at $R=0$. $\langle V^2\rangle_{Av}$, which corresponds to the van der Waals force in molecular interactions, falls off much more rapidly than the exchange force $\bar{V}_{\text{exch}}$. To suppose that there exists a "van der Waals minimum" beyond the range of the repulsive first-order forces would be fallacious.

This result has also an important bearing on the additivity of the interaction between alpha-particles. In molecular problems, and in nuclear problems as well, additivity holds for second-order forces, but not for first-order exchange forces. Inasmuch as there exists for molecules a range in R in which only second-order forces are present, additivity holds within this range. The absence of such a range in nuclear interactions destroys additivity completely. It is clear, therefore, that attempts to calculate energies of complex nuclei based on the assumption of unique and additive inter-alpha forces must fail.[8] On the other hand, the validity of considerations respecting symmetries, multiplicities and the general topology of levels of complex nuclei is not impaired by the results here obtained, even though these considerations involve the concept of alpha-particles as constituent and relatively stable groups.

Apart from this general conclusion, there is reason to wonder if an interaction composed of the first- and second-order forces deduced above is applicable to the two-body problem, in which additivity is of no concern.

4. The Scattering of Alpha-Particles in Helium

The question thus arises as to whether and to what extent the interactions derived in the foregoing sections will explain the scattering of alpha-particles in helium. A very careful analysis of the experimental scattering data has been made by Wheeler,[9] who has also deduced phase shifts which account for the experimental results. These will here be used as a basis for comparison with expectations to be derived from the present model.

To be sure, this model is very indefinite because the second-order forces have not been calculated completely. It is certain, however, that whatever modifications these latter would introduce in the calculated Δ_1E, they are confined to the region $R<4.5\times10^{-13}$ cm. Somewhere in this region there must be a minimum which produces the level corresponding to the ground state of Be^8. To fix one parameter, the fact will be used that the energy of this level is very nearly zero[10] with respect to the energy of two alpha-particles at infinite separation. In the calculation of phase shifts, we shall, therefore, use a scattering potential indicated by the solid line in Fig. 4. For $R>R_0=4.5\times10^{-13}$ cm, the potential will be appreciably Coulombian. The potential trough occurring at smaller distances will be considered to have a fixed outer radius R_0, and the internal radius R' will be adjusted so that there will

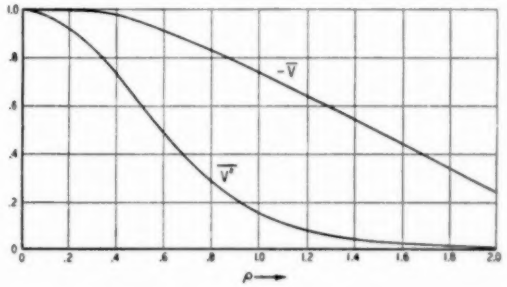

FIG. 3. Comparison of $\bar{V}$ and $\langle V^2\rangle_{Av}$. Ordinates are arbitrarily adjusted to make the two equal at $\rho=0$.

[8] Cf. in this connection also the conclusions of B. O. Grönblom and R. E. Marshak, Phys. Rev. **55**, 229 (1939).

[9] J. A. Wheeler, Phys. Rev. **59**, 16 (1941).

[10] S. K. Allison, L. S. Skaggs and N. M. Smith, Jr., Phys. Rev. **57**, 550 (1940).

exist but one level, and this at zero energy. The depth of the trough, D, will then be a function of R'. (Cf. Fig. 5.)

This model is highly idealized. The results for a smooth potential with sloping walls, however, differ insignificantly from those of this simple model. Even a potential having the form of the dashed curve in Fig. 4, which is not excluded by the previous analysis, yields results for the phase shifts which are qualitatively the same as

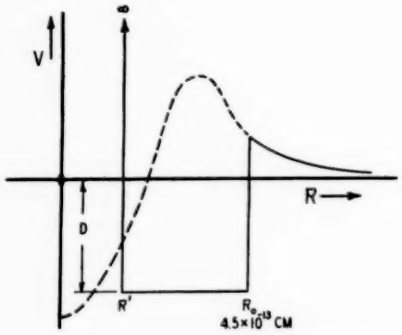

FIG. 4. Potential assumed in scattering calculations.

the ones here discussed. Details would change the local curvature of the phase shifts plotted in Fig. 6 but do not alter appreciably the region of the diagram to which the values of K_0 are confined.

The phase shift K_0, corresponding to the alpha-wave of zero angular momentum, is taken to be zero for scattering in a pure Coulomb field. For the potential of Fig. 4, it is computed by fitting the wave function inside the hole, $\sin k'(r-R')$ with $k'^2=(2\mu/\hbar^2)(D+E)$, to a proper function in the Coulomb field at $r=R_0$. This work is greatly abbreviated if use is made of the tables published by Wheeler.[11] In Fig. 6, K_0 is plotted against the energy of the incident alpha-particles for different values of R'. The lowest of these graphs corresponds to an infinitely deep trough of zero width at $R=R_0$, the highest to the absence of all repulsion near the origin. It may be noticed that all curves converge to the value $K_0=\pi$ at $V=0$. This feature is, of course, independent of our assumptions about the potential; it is a consequence solely of the existence of a stable ^1S level at zero energy.

[11] J. A. Wheeler, Phys. Rev. **52**, 1123 (1937).

The K_0 curve which Wheeler, in an adjoining paper, has deduced from scattering data and found compatible with the facts known about Be^8, is also plotted in Fig. 6. At lower energies it is seen to lie in a region permitted by the simple alpha-particle model under discussion, but it rapidly moves out of this region as the energy increases. The reason for this behavior is the resonance occurring in the S wave at an energy of about 3 Mev according to Wheeler's analysis. The potential deduced in this paper will not yield a resonance level at so low an energy.

The existence of an excited level in the neighborhood of 3 Mev above the lowest state of Be^8 and of width ≈ 0.8 Mev is quite definitely indicated in the observations by Dee and Gilbert[12] on the disintegration of B^{11} by protons, and in the scattering experiments of Devons.[13] Previously it had been identified as a $^1D_2$ state, but Wheeler[9] shows it to be a ^1S level. One can easily see that the simple alpha-particle model is incompetent to account for these facts inasmuch as it gives too small a range for the non-Coulombian forces. The difficulty is with the spacing of the levels, which comes out too large. Let us adjust the parameter R' so that the

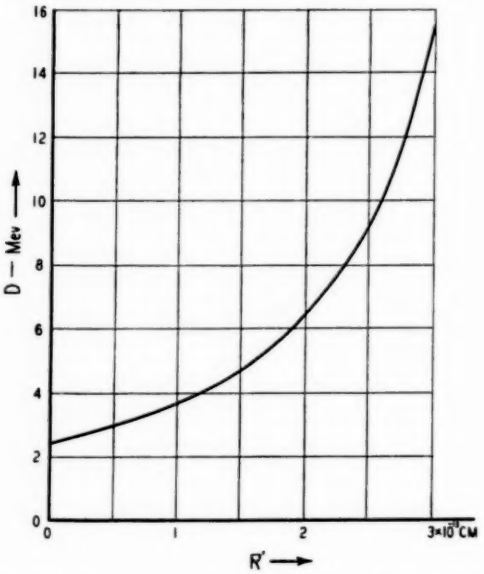

FIG. 5. Relation between D (cf. Fig. 4) and R' which will produce the lowest level in Be^8 at zero energy.

[12] P. I. Dee and C. W. Gilbert, Proc. Roy. Soc. **A154**, 279 (1936).
[13] S. Devons, Proc. Roy. Soc. **A172**, 559 (1939).

energy levels have the closest possible spacing, that is, let $R'=0$. One can then compute the position of the first ^1S resonance in the continuum[14] and it is found to lie about $6D$ above zero. Its width is of the order of the level spacing, that is, around $3D$. Now to obtain the lower ^1S level at zero energy, D must be 2.4 Mev. Hence the lowest position obtainable for the ^1S resonance would be 14 Mev, and the width would be of that order of magnitude, all of which disagrees with experience. The state in question can obviously not be understood on the basis of the simple alpha-particle model; it must involve a considerable rearrangement of elementary particles and seems to be much better described by the Hartree model.[15]

To produce the resonance at the correct place one must assume a force range far greater than is compatible with our former conclusions, and one would then encounter difficulties in explaining the initial trend of Wheeler's K_0 curve at low energies. The inconsistency attaching to the width of the excited level has already been pointed out by Rosenthal[16] who, using a Morse curve for the potential, finds the resonance to be too diffuse for consideration.

Conclusion

The application to the interaction between alpha-particles of methods similar to those which describe successfully the forces between atoms, leads to results which leave no basis for the supposition that the forces are describable as a superposition of repulsive first-order and attractive second-order effects. There is indeed no indication that the various orders of the perturbation scheme converge, and the forces are not additive. It is possible, however, to fix their range with reasonable certainty if detailed assumptions are made regarding the interaction between elementary particles. This range is approximately equal to that of the elementary forces.

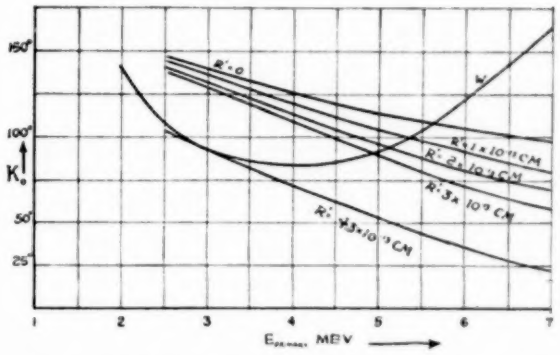

FIG. 6. *Solid lines:* Phase shift of S wave, K_0, as calculated on the basis of the model of Fig. 4, for different values of R'. *Curve marked W:* K_0 values derived from scattering data by Wheeler.

When the positive results of this study are incorporated in a simple model, the scattering of alpha-particles in He can be discussed. The computed phase shifts for the wave of zero angular momentum are in accord with observations at low energies of the incident particles, but fail to explain the resonance observed at higher energy.

The results definitely discredit the early alpha-particle model which endowed these groups with fairly permanent existence in higher nuclei and sought to explain nuclear structure by assuming unique and sometimes additive forces between them. They indicate in addition that even the interaction of two alpha-particles cannot be treated successfully by methods familiar from the theory of molecular forces. On the other hand they do not dispute the legitimate rôle which these alpha-groups may play in determining symmetries and multiplicities of nuclear states.

The author records with gratitude the privilege of using Professor Wheeler's results before their publication. His thanks are likewise extended to the Institute for Advanced Study which permitted him a most stimulating stay in Princeton.

[14] H. Margenau, Phys. Rev. **46**, 613 (1934).
[15] E. Feenberg and E. Wigner, Phys. Rev. **51**, 95 (1937).
[16] J. E. Rosenthal, Phys. Rev. **54**, 315 (1938).

Excited States of Nuclear Particles in the Meson-Pair Theory

CHARLES L. CRITCHFIELD*
Princeton University and The Institute for Advanced Study, Princeton, New Jersey
(Received October 14, 1940)

A meson-pair theory of nuclear forces is considered in which it is not necessary to use perturbation calculations. Former results in this theory are improved. New considerations are found necessary if the interaction between heavy particle and meson field is large enough to form bound meson states. For such large interactions, discrete stationary states of neutron and proton exist some of which have higher or lower charge and spin than the normal states. The energy required to excite the higher discrete states is of the order of the rest energy of the meson.

THERE is, as yet, no conclusive estimate of the true value of the spin of the meson or of the statistics which the meson obeys. Theoretical work on nuclear forces in which both possibilities for statistics were used, i.e., Einstein-Bose and Fermi-Dirac, has been done on the assumption that nuclear particles can emit and absorb a meson or a pair of mesons and has met with some measure of success in both cases. In these theories it is necessary to cut off the integrations at small lengths which are of the same order of magnitude as the range of nuclear forces. A better understanding of this result which essentially equivocates the existence of a field may perhaps be available if the perturbation method which is usually used can be foregone. It is the further development of a more exact theory of meson-pair (spin $\frac{1}{2}$) forces that this paper has to report.

Previous calculations of nuclear forces in which it was assumed that neutrons and protons can emit and absorb pairs of particles having spin $\frac{1}{2}$ have been made without using the perturbation method. The first of these papers[1] deals only with those cases in which Coulomb energies, the kinetic reaction of neutron and proton and the rest mass of the emitted particles can be neglected safely. That work assumed the field particles to be electrons and positrons and in it is a detailed discussion of the pair production and destruction process involved by the interaction used. The types of interaction which avoid an accumulation of charge about nuclear particles in their lowest states are also found. A second step in this theory[2] takes into account the rest mass of the field particles so that the results can be applied to meson pairs. The validity of the formula obtained is limited, however, to interaction energies which are not strong enough to form discrete stationary states in which one or more mesons are bound to the neutron or proton. The present paper investigates the properties of these discrete states and indicates under what conditions the former calculations must be supplemented.

The meson-pair theory of nuclear forces is based on the assumption that mesons have charge $\pm e$, mass $\sim 1/10$ proton mass and spin $\frac{1}{2}h$ obeying the exclusion principle. Interaction between the field described by the Dirac wave functions belonging to these mesons and a nuclear particle fixed at the origin of coordinates is assumed to be of the form

$$J=-\eta\int d\mathbf{x}\int d\mathbf{x}'\psi(\mathbf{x}')^{+}\beta\psi(\mathbf{x})u(x)^{*}u(x') \quad (1)$$

in which η is a constant giving the strength of the interaction, $\psi(\mathbf{x})^{+}$, $\psi(\mathbf{x})$ are quantized wave functions of the meson field having four components on which β operates in the usual way and $u(x)$ is an arbitrary spherically symmetrical function replacing the δ-function (which would be required by relativistic invariance). β is the operator which transforms as a scalar. The state of the heavy particle is assumed to be unchanged by this interaction.

By transforming J to momentum space and adding it to the Hamiltonian of free mesons one obtains the Hamiltonian for the mesons in which electromagnetic interactions and the kinetic

* National Research Fellow.
[1] Wigner, Critchfield and Teller, Phys. Rev. **56**, 530 (1939).
[2] C. L. Critchfield and W. E. Lamb, Jr., Phys. Rev. **58**, 46 (1940).

reaction of the nuclear particle are neglected. This Hamiltonian leads, by commutation with the quantized wave function and subsequent separation, to the equation for the wave function of a single meson, $\phi(\mathbf{p})$, of energy E:

$$[E-c(\boldsymbol{\alpha},\mathbf{p})-\beta]\phi(\mathbf{p})$$
$$+\eta v(p)\beta\int v(p')^*\phi(\mathbf{p}')dp'=0. \quad (2)$$

The rest energy of the meson, μc^2, is taken as unity. $v(p)$ is the normalized Fourier transform of $u(x)$. Solutions of Eq. (2) which take the rest mass into account have been found[2] for all eigenvalues $|E|>1$. The eigenvalues, E, are determined by the condition that a certain operator on the spin vector have the eigenvalue -1, *viz.*

$$4\pi\beta\eta\int_0^\infty \frac{E+\beta}{E^2-1-c^2p^2}v(p)^2p^2dp=-1, \quad (3)$$

which is considered to be the limit of the sum

$$\frac{4\pi^2\hbar\eta}{L}\sum_{n=1}^{\infty}\frac{\beta E+1}{(E^2-1)-c^2p_n^2}v(p_n)^2p_n^2=-1, \quad (4)$$

where L is the radius of a sphere in which p_n is considered to be quantized: $p_n=n(\pi\hbar/L)$, and the limit is taken by allowing the radius, L, to become indefinitely large. It is then evident that if $v(p)$ has no zeros, the left-hand side of Eq. (4) as a function of E becomes infinite at every $E^2=1+c^2p_n^2$ the sign of the infinity being opposite for opposite directions of approach. The first differential quotient of Eq. (4) with respect to E yields

$$-\frac{4\pi^2\hbar}{L}\eta\beta\sum_{n=1}^{\infty}\frac{c^2p_n^2+(E+\beta)^2}{(E^2-1-c^2p_n^2)^2}v(p_n)^2p_n^2.$$

For a given eigenvalue of β, either 1 or -1, the differential quotient is either positive or negative, respectively, for all values of E. There is then only one solution of Eq. (4) between two successive singularities.

Eigenvalues E satisfying $|E|>1$ can, according to the above arguments, differ only by an infinitesimal amount, $\sim\hbar c/L$, from the values $\pm(1+c^2p_n^2)^{\frac{1}{2}}$ and only by summing over all occupied energy levels in the "negative sea" comprising an infinite number of states can the order of the total energy change become of finite or perhaps infinite order. This summation has been presented in explicit form for one heavy particle and implicitly for two heavy particles in reference 2. It is found that the change in $q\equiv(1/c)(E^2-1)^{\frac{1}{2}}$ from its force-free value, p_n, is $x(\pi\hbar/L)$ where

$$\tan\pi x=2\pi^2q(E+\beta)v(q)^2/[-\eta^{-1}-(E+\beta)f(q)],$$
$$f(q)\equiv\frac{4\pi}{c^2}\int_0^\infty[p^2v(p)^2-q^2v(q)^2](q^2-p^2)^{-1}dp.$$

For very small η, $x\to0$ as $\eta\to0$; this is the case if we take the arctg near zero for small η. The two results for x, obtained with different values of β can be added and the total change in energy in all negative levels for which $|E|>1$ is

$$\Delta E_{\text{con}}=-\frac{2}{\pi}\int_0^\infty\frac{c^2qdq}{(c^2q^2+1)^{\frac{1}{2}}}\operatorname{arctg}\frac{4\pi^2q^2v(q)^2[qf(q)-(c^2\eta q)^{-1}]}{\eta^{-2}-c^2q^2f(q)^2+4\pi^4q^4v(q)^4/c^2+2f(q)/\eta} \quad (5)$$

in which, also, the arctg is to be taken on that branch of the curve which becomes zero as η becomes very small.

In the "hole-theory" which is assumed here the energy of the lowest state (all negative energy levels filled) is negative infinity with or without interaction with nuclear particles. Any finite result which may be obtained from the expression for ΔE_{con} is a finite difference between the infinities in the two cases which is made definite by summing over the same *number* of mesons in each. This procedure is consistent with the conservation of total charge under the interaction.

Although it has been assumed that $v(p)$ has no zeros each exception to this assumption will change the argument for only four states counting

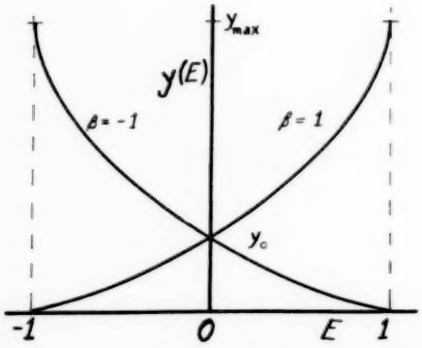

FIG. 1. Sketch of the function $y(E)$. Eigenvalues of E less than one (μc^2) in absolute value are determined by the intersection of this function with a horizontal line at $1/\eta$.

positive and negative energies and both spins and the error made by neglecting this change is infinitesimal. It need be postulated, therefore, that $v(p)$ have only a finite number of zeros in order that the summation over all energy levels obtained before be correct.

The preceding discussion applies to the energy levels for which $|E|>1$. We now consider the possibility of energy levels for which $|E|<1$. For this range of E Eq. (3) presumably has no singularities on the real E axis and there is no need to resort to a summation. Solutions of Eq. (3) are values of E satisfying

$$y(E)=1/\eta \tag{6}$$

$$y(E)\equiv\int_0^\infty \frac{1+\beta E}{c^2p^2+1-E^2}4\pi v(p)^2p^2dp,$$

$$y(E)'=\beta\int_0^\infty \frac{c^2p^2+(E+\beta)^2}{(c^2p^2+1-E^2)^2}4\pi v(p)^2p^2dp.$$

Clearly there is no solution of Eq. (6) for $-1<E<1$ when $\eta<0$. It is, therefore, sufficient to consider only positive values of η. The sign of the derivative of $y(E)$ is the sign of the particular eigenvalue of β that is being considered for the whole range of E. This shows that the extreme values of $y(E)$ are approached as $|E|\to1$; beyond these extreme values the eigenvalues of E must lie infinitesimally close to $E=\pm1$. The maximum values of $y(E)$ are equal and are obtained by taking β and E of the same sign

$$y_{max}=\frac{8\pi}{c^2}\int_0^\infty v(p)^2dp,$$

which is presumed to be finite. The minimum value of $y(E)$ is then obtained by taking β and E of opposite sign and is seen to be zero. Intersection of the two branches of $y(E)$ corresponding to two eigenvalues of β takes place at $E=0$

$$y(0)=4\pi\int_0^\infty \frac{v(p)^2}{1+c^2p^2}p^2dp.$$

A qualitative sketch of the function $y(E)$ is shown in Fig. 1.

Let E_k be the energy at which the function $v(p)$ has its maximum; then $y_{max}\sim\mu c^2/E_k^2$. "Discrete states" may then arise if the interaction energy η is of the order of, or larger than, $E_k^2/\mu c^2$. If it be so that the particular choice of η and $v(p)$ is such that η falls in this range ($\eta\gtrsim\sim E_k^2/\mu c^2$), calculation of the total energy change in the meson field must include the finite energy changes in states between $-\mu c^2$ and μc^2. When spin is taken into account there are four such states, two of negative energy and two of positive energy in general. The lowest state of the system, one heavy particle plus meson field, differs in energy from the lowest state without interaction by

$$\Delta E=\Delta E_{con}+2(\mu c^2-|E_y|), \tag{7}$$

where E_y is the value of $|E|<1$ which satisfies Eq. (6) and ΔE_{con} is the total energy change in the continuum given by Eq. (5).

The appearance of discrete bound states of a system of particles for sufficiently large interactions is well known from the theory of the deuteron. In the present theory discrete states appear only if $\eta\gtrsim1/y_{max}$.

A straightforward extension of the procedure given for one heavy particle can be made for two heavy particles along the line pursued in the previous work. Such a calculation would be important for the forces between the two heavy particles if the interaction energy were of the correct magnitude to give discrete states. The formula for this calculation will not be developed in this paper.

It is the purpose of the present note rather to investigate the states of heavy particle plus meson field which are characterized by the presence of additional mesons or meson pairs. Suppose the interaction between a neutron and

the meson field to be that considered above with $y_{max}>1/\eta>0$ so that we have the most general case. Then the lowest state of the system, in which the neutron is considered fixed at a point, is the state in which all negative energy levels of mesons are occupied and all positive levels empty. All levels having $|E|>1$ belong to the continuum and are changed only infinitesimally by the interaction and in addition there are two levels (of opposite spins) at E_y and two at $-E_y$, $|E_y|<1$ which are different from μc^2 by a finite amount.

The charge distribution in the lowest state has been proved in an earlier work[1] to be uniform for the interaction that has been used. In higher states of neutron plus meson field the charge distribution is not necessarily uniform. Let us start with the lowest state and create one pair of mesons by removing a meson from the state $-E_1$ and placing it in a state E_2 by supplying the energy E_1+E_2. If E_1 and E_2 (both positive) are larger than μc^2 there will be only an infinitesimal change in charge density, for, these eigenfunctions of the individual mesons differ only infinitesimally from plane waves and give a uniform charge distribution. Consequently, any finite number of pairs produced in which the energy levels involved are not $\pm E_y$ will not produce a change in the neighborhood of the neutron.

Let us now consider the special case that the pair is produced by a transition from $-E_1$ to E_y. The level at E_y is different by a finite amount from the level at μc^2 and will change the charge density in the proximity of the neutron. Departure from a uniform distribution will be entirely the result of the level at E_y being occupied. It is then necessary to calculate $|\psi(\mathbf{x})|^2$ for the state at E_y. According to the former work the eigenfunction belonging to energy E is

$$\phi(\mathbf{p})=\frac{E+\beta+c(\boldsymbol{\alpha},\mathbf{p})}{E^2-1-c^2p^2}Cv(p),$$

$$\psi(\mathbf{x})=(2\pi\hbar)^{-\frac{3}{2}}\int\phi(\mathbf{p})e^{-i\mathbf{p}x}d\mathbf{p},$$

where C is a constant spinor and normalizing factor.

As a special example: If $v(p)$ approach zero more rapidly than p^{-2} as $p\to\infty$ in all parts of the negative half-plane $\psi(\mathbf{x})$ can be estimated by Cauchy's theorem to contain, in linear combination, $u(x)$ and $\exp[-x(1-E_y^2)^{\frac{1}{2}}/hc]$. The radius of the charge concentration found under this assumption is essentially the larger of the radii of $u(x)^2$ or $\exp[-2r(1-E_y^2)^{\frac{1}{2}}/hc]$. Such a charge accumulation gives the states of the neutron in question the characteristics of discrete states. There are evidently five distinct types of these discrete states and we shall enumerate the lowest levels of each type together with the net charge and possible spins in each level. All negative levels except those having energy $-E_y$ are tacitly assumed to be filled and the number of mesons having energy $\pm E_y$ are given. The meson is assumed to have unit charge. This enumeration appears in Table I.

There is evidently no possibility of interpreting these discrete states so that they may include the proton and neutron as eigenstates of the same system because of the connection between spin and statistics and the fact that protons have unit charge. A rearrangement of levels can be brought about by introducing a spin dependence of potential between meson and nuclear particle; and in this connection it may be observed that if the interaction constant is large enough to form discrete meson states the device[3] previously found necessary to obtain spin dependence of forces in the deuteron may not be required, namely that both a spin-dependent and a spin-independent interaction had to be postulated. Discrete states can be formed only for one eigenvalue of the spin interaction so that the symmetry of the previous calculation (which was

TABLE I. *States of the meson.*

Energy of Excitation	Number in E_y	Number in $-E_y$	Net Charge	Total Spin
zero	0	2	0	$\frac{1}{2}$
E_y	0	1	−1	0, 1
	1	2	1	
$2E_y$	0	0	−2	$\frac{1}{2}$
	1	1	0	$\frac{1}{2}$, $\frac{3}{2}$
	2	2	2	$\frac{1}{2}$
$3E_y$	1	0	−1	0, 1
	2	1	1	
$4E_y$	2	0	0	$\frac{1}{2}$

[3] C. L. Critchfield, Phys. Rev. **56**, 540 (1939).

for electrons) is destroyed and the possibility of a tensor-tensor interaction alone is open. Furthermore it has been pointed out by Heitler[4] that the existence of discrete states would be very important in the scattering of mesons by nuclei.

In conclusion we may sum up the status of the "exact" solution of the meson-pair theory of nuclear forces as follows: Coulomb interaction and motion of heavy particles are neglected; neutron and proton are assumed to interact with mesons in a particular state $v(p)$ and if the interaction constant η is equal to or greater than

$$\left\{8\pi\mu\int_0^\infty v(p)^2dp\right\}^{-1}$$

discrete states are formed. If η is less than the critical value it is sufficient to consider the effect of the nuclear particle on the continuum of filled meson levels of negative energy.

The author would like to express his thanks to Professor Eugene Paul Wigner for suggesting an investigation of excited states of nuclear particles.

[4] W. Heitler, Nature **145**, 29 (1940).

JANUARY 1, 1941 PHYSICAL REVIEW VOLUME 59

Branching Ratios in the Fission of Uranium (235)*

H. L. ANDERSON, E. FERMI AND A. V. GROSSE
Pupin Physics Laboratories, Columbia University, New York, New York

(Received October 14, 1940)

A survey has been made of the percentages of slow neutron-induced uranium fissions that give rise to the formation of various radioactive series. These percentages were obtained by measuring the number of β-disintegrations of a suitable member of the series after an irradiation under specified geometrical conditions and a quantitative chemical separation. The percentages found for the series thus far investigated vary from about 0.1 percent to 10 percent.

A LARGE number of radioactive series found among the fission products of uranium have been reported. Thus far, however, the work has been confined mostly to the identification and the genetic relationships of the radio-elements which arise from uranium fission. The present work is part of a systematic attempt to determine in a quantitative way the probability that when uranium fission occurs a given radioactive series will appear. We shall call this probability the branching ratio of the radioactive series.

In Table I† are listed those radio-elements which have been found to date with indication, wherever possible, of their genetic relationships and atomic weights. In compiling this table we have relied mainly on the critical survey of Livingood and Seaborg,[1] supplemented by data which have appeared subsequently. In Table I the fission fragments have been arranged in two groups; a light group having atomic weights in the range from 82 to 100 and a heavy group with weights ranging from 127 to 150. To date, 10 radioactive chains have been identified in the light group and 12 in the heavy group. Because of greater analytical ease we have concentrated our effort on the heavy group and have determined the branching ratios of 9 out of 12. The sum of these heavy group fission series amounts to only about 50 percent, (see Table I) indicating that our present knowledge of fission fragments is still incomplete.

The presence of a variety of series may be interpreted by assuming that the original splitting may take place into different fragments. The emission of one or more neutrons further increases the number of possibilities. If no neutrons were emitted the sum of the weights of the two fragments ought to be equal to 236, in the case of fission produced by slow neutrons in U^{235}. If

* Publication assisted by the Ernest Kempton Adams Fund for Physical Research of Columbia University.

† *Note added in proof.*—The 22-hour and the 6.6-hour iodines have now been assigned to atomic weights 133 and 135, respectively, by C. S. Wu, Phys. Rev. **58**, 126 (1940).

[1] J. J. Livingood and G. T. Seaborg, Rev. Mod. Phys. **12**, 30 (1940).

TABLE I. *Radioactive series from uranium fission. S indicates a stable isotope.*

HEAVY GROUP

	127	128	129	130	131	132	133	134	135	136	137	138	139	140	—	—	—	—	—	—	—
Sb 51	80 hr.		4.2 hr.												5 min.	10 min.	10 min.				
Te 52	10 hr.	S	70 min.	S	25 min.										77 hr.	60 min.	43 min.	15 min.			
I 53	S				8 day										24 hr.	22 hr.	54 min.	6.6 hr.			
Xe 54		S	S	S	S	S		S		S			30s	short		5 day		9.4 hr.	15 min.		
Cs 55							S						6 min.	40s?					32 min.		
Ba 56				S		S		S	S	S	S	S	86 min.	300 hr.						14 min.	1 min
La 57													S	40 hr.						2.5 hr.	18 min
%	0.18		0.34		1.6								6.4	8.4	5.2	7.6	12	9(?)			

LIGHT GROUP

	82	83	84	85	86	87	88	89	90	—	—	—	—	—	—	—
Br 35		2.3 hr.								40 min.	3.8 hr.					
Kr 36	S	1.9 hr.	S		S		3 hr.	5 min.								
Rb 37		S		S		S	18 min.	15 min.								
Sr 38			S		S	S	S	51 day				6 hr.	7 min.			
Y 39								S				3.3 hr.				
Zr 40									S					17 hr.	70 day	
Cb 41														75 min.		
Mo 42																67 hr.
— 43																6.6 hr.
%														6.1		

neutrons are emitted this sum is correspondingly less. Since, presumably, the same number of neutrons is not always emitted, we need not expect that when a given series in the heavy group occurs it will always be accompanied by the same series in the light group. Very little information is available as to the relative probability of the formation of the various fission products. We have, therefore, undertaken a study of these probabilities. Since we shall be unable to continue this research for some months because of the rebuilding of the Columbia cyclotron now in progress, it was thought worth while to report on the results obtained thus far.

EXPERIMENTAL METHOD

In each measurement we irradiated a solution containing 50 grams of uranium element inside a paraffin block placed in a fixed position near the cyclotron. Usually, uranyl nitrate was used, but the sulphate was employed for the antimony determination. Neutrons were produced in the cyclotron by the bombardment of Be with 6-Mev protons. These neutrons have an energy up to about 2 Mev and our geometrical arrangement was such that practically only slow neutrons were effective in producing fission. Our results, therefore, refer to the fission of U^{235}. The intensity of irradiation was monitored by means of a gold foil placed in a fixed position inside the paraffin block. The activity of the gold foil was compared to that of a standard uranium plaque by means of an ionization chamber. In a few cases a Rn+Be source was used for the irradiation instead of the cyclotron.

For the investigation of each element a known amount of the element in a suitable chemical form was added as a carrier to the uranium solution, together with smaller quantities of all other known fission products. The desired element was subsequently purified and separated. A weighed fraction of the added amount was painted on a thin aluminum strip, covered with Scotch cellulose tape and wrapped around a thin-walled silvered-glass counter.[2] The strip was held by means of a suitable aluminum container so as to insure the reproducibility of its disposition relative to the counter. Taking into account the absorption of the β-rays, the geometrical efficiency of the counting arrangement, and the finite time of irradiation, as explained below, the number of β-disintegrations per second at saturation of the element in question was obtained. The branching ratio, i.e., the fraction of fissions giving rise to a particular radioactive series, was calculated from the formula,

$$R = I\eta/gfMFN.$$

[2] Made by Eck and Krebs, New York City.

I is the observed initial activity of the preparation measured in counts per minute; f is the ratio of the weights of carrier element used for the activity measurement to that added to the irradiated solution; M is the intensity of irradiation as measured in arbitrary units with the gold monitor; F is the fraction of saturation of the activity in question accumulated during the time of irradiation; η is the correction factor for the absorption of the β-rays. For its determination an aluminum cylinder of thickness 0.043 g/cm², equivalent to the combined thickness of the counter wall and the Scotch tape, was inserted between the sample and the counter. If an exponential law of β-ray absorption is assumed, η is the ratio of the measured activity without the aluminum to that with it. Values of η are given in Table II. The thickness of the counter wall was found by comparing, with a second counter as detector, the absorption for β-rays of radium E of the counter used with an aluminum cylinder of known thickness under the same geometrical conditions. In this way the thickness of the counter wall was found to be equivalent to 0.029 g/cm² of aluminum. The Scotch tape had a thickness equivalent to 0.012 g/cm². A small increment was added to take into account the absorption in the average sample measured.

The symbol g is the geometrical efficiency of the counting arrangement. It was determined by measuring in our standard way the β-activity of a weighed amount of U_3O_8 and was found to be $\frac{1}{3}$. Differences in this efficiency caused by possible differences in the back-scattering of the various β-rays were neglected. The measurement of g was repeated several times with varying amounts of U_3O_8 and was found to give the same result to within a few percent.

N is the number of fissions per minute taking place in the uranium solution for unit intensity of irradiation. In order to determine N we proceeded in the following way: In place of the uranium solution we used 140 cc of a solution of $MnSO_4$. In order to alter the distribution of neutrons as little as possible the concentration of this solution was adjusted so that the number of neutron captures per second would be roughly the same as in the uranium case. The activity of a known fraction of these manganese atoms was then determined with the counter in our standard way. The number of fissions per uranium atom is equal to the number of disintegrations per manganese atom times the ratio of the fission cross section of uranium to the capture cross section of manganese for thermal neutrons. We found that for unit intensity of irradiation 960,000 fissions took place in our uranium solution per minute.

On the assumption that a series of radio-elements has no branchings we chose for each radioactive series one convenient radio-element for determining the percentage of fissions of the series. The chemical elements investigated were I, Sb, Ba and Zr. The series investigated are those of Table I for which the percentages are given.

Iodine

Iodine was separated by the following method: A standard solution of 5 KI+1 KIO_3 was added to the uranium solution and acidified with dilute H_2SO_4 to free all of the iodine. The free iodine was then steam distilled into a flask containing water and converted into iodide ion by titrating with $NaHSO_3$; the iodine was then precipitated as either PdI_2 or AgI.

Originally, our practice was to paint PdI_2 precipitated in the presence of Br ion on the aluminum strip. Since on several occasions the PdI_2 reacted with the aluminum with some loss of iodine, these measurements could be relied on for giving only relative branching ratios of the various iodine isotopes. For absolute determinations we used a precipitate of AgI. Bromine is not separated in this case, but since the bromine products are short-lived the determinations could be made on the longer-lived iodines. For these last measurements we used a Rn+Be source.

Separation of iodine has permitted us to

TABLE II. *Absorption factors η for 0.043 g/cm² of aluminum.*

Element	Half-Life	η	Element	Half-Life	η
$_{51}Sb^{129}$	4.2 hr.	1.67	$_{53}I$	22 hr.	1.85
$_{52}Te^{129}$	70 min.	1.81	$_{53}I^{131}$	8 days	4.9
$_{51}Sb^{127}$	80 hr.	1.61	$_{56}Ba^{139}$	86 min.	1.26
$_{52}Te^{127}$	10 hr.	1.66	$_{56}Ba^{140}$	300 hr.	1.52
$_{53}I$	54 min.	1.60	$_{57}La^{140}$	36 hr.	
$_{53}I$	2.4 hr.	1.60	$_{40}Zr$	17.2 hr.	1.39
$_{53}I$	6.6 hr.	2.0	$_{41}Cb$	75 min.	

investigate the following series,[3]

(1) Te^{131} (30 min.) or (30 hr.)→I^{131} (8 day),

(2) Sb (10 min.)→Te (60 min.)
→I (22 hr.)→Xe (5 day),

(3) Te (~15 min.)→I (6.6 hr.)→Xe (9.4 hr.),

(4) Sb (5 min.)→Te (77 hr.)→I (2.4 hr.),

(5) Sb (<10 min.)→Te (43 min.)→I (54 min.).

In one experiment iodine was separated 24 hours after the end of a 7-hour irradiation. The decay curve was readily analyzed into an 8-day and a 22-hour activity; no evidence for the presence of the 5-day Xe could be found and it was assumed that this gas escaped from the sample during measurement.

We were able to determine that the 8-day iodine arises principally from the 30-minute rather than the 30-hour isomer of tellurium. This was done by irradiating for 2 hours and separating the iodine after 22 hours and again after 89 hours. If the 8-day iodine arose from the 30-hour tellurium the ratio of its activity from the second separation to that from the first would be 1.1. If instead, it arose from the 30-minute tellurium this ratio would be zero. A ratio of 0.1 was found which indicates that the 8-day iodine arises principally from the 30-minute tellurium.

The branching ratio of the 2.4-hour activity was obtained as follows. The parent substance of this radio-element has a much longer life (77 hours) than the parent elements of all other radio-iodines produced in the fission. It follows that the 2.4-hour radio-iodine is the only radio-iodine which can be regenerated in an irradiated uranium solution from which iodine has been removed once one or two days after irradiation. We therefore irradiated a solution and after about one day performed a first iodine separation. The collected iodine has a decay curve in which all the following periods were represented: 8 days, 2.4 hours, 66 hours and 22 hours. The solution was then allowed to stand for about one more day; the 77-hour tellurium, which was still present in the solution, reproduced during this time the 2.4-hour iodine; a second iodine separation collected, therefore, the 2.4-hour iodine almost pure.

The activity of the 54-minute iodine could easily be distinguished from all other activities because of the large difference in period from the other activities and the fact that a separation of iodine soon after a short irradiation yields this activity with a much greater intensity than any other.

We were, however, not able to get a very convincing decay curve of the 6.6-hour iodine, perhaps because the daughter substance (9.4-hour Xe) was occluded only in part in our sample. The corresponding branching ratio given in the table is somewhat doubtful. The branching ratios in the case of the 22-hour and the 2.4-hour iodines were measured using AgI precipitation. The branching ratios of the other isotopes were obtained by analyzing decay curves of PdI_2 precipitations and comparing initial activities of the 22-hour and 2.4-hour activities with the others. Irradiations of various lengths of time gave reasonably consistent results.

Antimony

Antimony and some tellurium were added to the uranium sulphate solution in the form of a solution of $SbCl_3$ in 50-percent H_2SO_4 and reduced with granulated zinc and sulphuric acid in a hydrogen generator to SbH_3, and absorbed in a $AgNO_3$ solution. The silver antimony precipitate was filtered, decomposed with concentrated HCl and antimony precipitated with H_2S from the solution in the usual way and weighted as Sb_2S_3 after drying in a stream of CO_2.

The activity of the Sb samples was analyzed in order to determine the branching ratios of the following series:[3]

(1) Sb^{127} (80 hr.)→Te^{127} (10 hr.)→I^{127},

(2) Sb^{129} (4.2 hr.)→Te^{129} (70 min.)→I^{129}.

The decay curves show evidence of the growth of the two radio-telluriums (10 hours and 70 minutes) out of the chemically separated samples of antimony. The branching ratios of these two series are considerably smaller than any other found so far. This fact may perhaps be related to the circumstance that these series are at the low atomic weight end of the heavy group.

[3] P. H. Abelson, Phys. Rev. **56**, 1 (1939).

Barium

This element was separated from the irradiated solution by first eliminating most of the $UO_2(NO_3)_2$ by ether extraction and precipitating Ba and Sr as sulphates in the aqueous extract. These sulphates were melted with $KNaCO_3$ in the presence of the oxides of Te, Mo and Cb, the washed carbonates dissolved in dilute HCl and precipitated, in the presence of Th (to eliminate UX), for a second time as sulphates. After converting these to carbonates Ba was separated from Sr as $BaCrO_4$ in acetic acid solution and reconverted into $BaSO_4$.

From the activity of the barium samples we determined the branching ratios of the two series:[4]

(1) Xe^{139} (<30 s)→Cs^{139} (6 min.)
→Ba^{139} (86 min.)→La^{139},

(2) Xe (short)→Cs (40 s?)
→Ba (300 hr.)→La (40 hr.).

A first barium sample was separated from a uranium solution irradiated for many hours. Special care was taken to purify the sample as thoroughly as possible from UX contamination. Since this purification process took several days only the 300-hour activity was found in the decay curve. Actually, the lifetime appeared from our measurements to be somewhat longer. The first part of the decay curve shows evidence of the growth of the 40-hour lanthanum. This growth was, however, not sufficiently intensive for a reliable separate determination of the absorption factors of Ba and La. In determining the branching ratio we used the average absorption factor of the complex radiation of Ba and La. This procedure may of course introduce some additional error into this determination.

The activity of the 86-minute barium was measured on a $BaCrO_4$ sample separated from a uranium solution irradiated about one hour. Because of the short time available for the purification an appreciable UX background was observed in this sample. The 86-minute activity was, however, much more intensive and could be analyzed without difficulty.

Zirconium

For the chemical separation of zirconium the U solution was acidified with concentrated HCl to about 25 percent, the Zr precipitated as a phosphate and the ZrP_2O_7 purified as previously described[5] and finally converted into ZrO_2.

The chain investigated was:

Zr (17.2 hr.)→Cb (75 min.).

A zirconium oxide sample separated from a solution irradiated about two hours was measured. The decay curve showed an initial rise caused by the growth of the 75-minute columbium and then a decay with the 17.2-hour period of zirconium. A rather small background, presumably caused by a long-living zirconium was also observed. We were unable to separate the two absorption factors of 17.2-hour zirconium and 75-minute columbium from these curves and we used, therefore, an average absorption coefficient. Two irradiations, one of 2 hours and another of 10 hours, gave, in good agreement, 5.9 and 6.3 for the branching percentages.

Assuming that one radioactive fragment in the light group and one radioactive fragment in the heavy group are produced in each fission, we would expect the sum of the branching percentages to be 100 for each of the two groups. The percentages for the nine series analyzed in the heavy group add to about 50. Apart from possible errors, especially in the determination of the number of fissions, this low result is partly caused by incomplete analysis (9 out of 12) of the known series and probably also by series not yet discovered.

In conclusion the authors wish to express their indebtedness to the Research Corporation for financial aid. One of us (AVG) is also indebted to the John Simon Guggenheim Memorial Foundation for the grant of a fellowship.

[4] O. Hahn and F. Strassmann, Naturwiss. **27**, 529 (1939); G. N. Glasoe and J. Steigman, Phys. Rev. **58**, 1 (1940).

[5] A. V. Grosse and E. T. Booth, Phys. Rev. **57**, 664 (1940).

Photo-Fission of Uranium and Thorium

R. O. HAXBY,*† W. E. SHOUPP,* W. E. STEPHENS,*‡ AND W. H. WELLS
Westinghouse Research Laboratories, East Pittsburgh, Pennsylvania

(Received August 30, 1940)

Fission of uranium and thorium has been observed to be produced by irradiation with γ-rays. The cross section for this photo-fission produced by the γ-ray from fluorine bombarded with protons has been measured and found to be:

$$\sigma_U = 3.5 \pm 1.0 \times 10^{-27} \text{ cm}^2,$$
$$\sigma_{Th} = 1.7 \pm 0.5 \times 10^{-27} \text{ cm}^2.$$

INTRODUCTION

SOON after neutron-induced fission of uranium and thorium was discovered it was pointed out that sufficient excitation of the heavier nuclei by γ-rays might also cause fission.[1, 2] A search was made in several laboratories for fission caused by γ-rays, but no effect was observed.[3, 4] The failure to observe fission of this type was thought to be caused by insufficient γ-ray intensities, as calculated from the yields of the $F(p, \gamma)$ and $Li(p, \gamma)$ reactions given by Livingston and Bethe.[5] However, we looked for and discovered photo-fission. This was made possible by the fact that the yield of γ-rays from $F(p, \gamma)$ is actually much greater than quoted[5] and increases rapidly with proton energy. A preliminary report[6] has been published, and this paper gives a full account of our experiments.

APPARATUS

The arrangement of apparatus used to observe photo-fission is shown in Fig. 1. High energy protons from the Westinghouse pressure electrostatic generator were magnetically analyzed and directed on to a CaF_2 target in a Faraday cage. This proton current was measured by a current integrator and on a microammeter connected to ground through a 45-volt battery; the Faraday cage being made negative. Gamma-rays produced in the fluorite crystal target irradiated a 12-cm² piece of uranium metal, placed on the high voltage plate of the ionization chamber. The ionization pulse of the fission recoils was amplified and observed on an oscilloscope. The pulses greater than twice the α-particle background were observed visually, and counted with a hand counter. The ionization chamber filled with air at atmospheric pressure was 1 cm deep, and 2000 volts were applied to the collector plate. The intense γ-ray background made it necessary to ground the grid of the first tube of the amplifier through a resistance of 20 megohms, so that the background would not change the grid bias, and consequently the gain of the amplifier. With thick uranium samples in the ionization chamber, the α-particle intensity was high enough to give α-coincidences, and hence only kicks greater than twice the highest observed coincidence kick were counted as fissions. It was determined that the

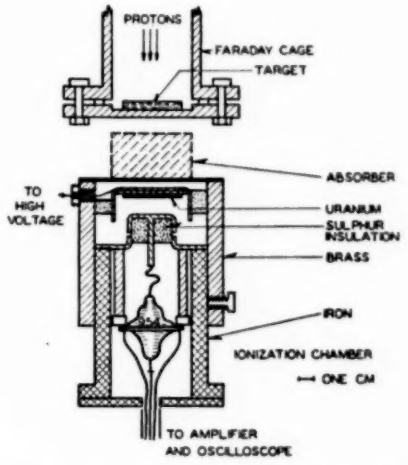

FIG. 1. Arrangement for detecting photo-fission.

* Westinghouse Research Fellow.
† Now with the Sperry Gyroscope Company.
‡ Now at Stanford University.
[1] E. Feenberg, Phys. Rev. **55**, 504 (1939).
[2] N. Bohr and J. A. Wheeler, Phys. Rev. **56**, 426 (1939).
[3] Roberts, Meyer and Hafstad, Phys. Rev. **55**, 417 (1939).
[4] Heyn, Aten and Bakker, Nature **143**, 516 (1939).
[5] M. S. Livingston and H. A. Bethe, Rev. Mod. Phys. **9**, 316 (1937).
[6] Haxby, Shoupp, Stephens and Wells, Phys. Rev. **58**, 92 (1940).

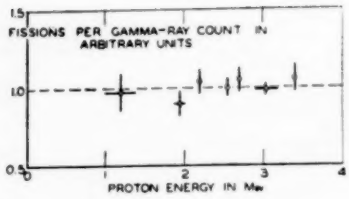

FIG. 2. Fissions per γ-ray count *vs.* proton energy.

presence of intense γ-radiation did not change the distribution of α-kicks. With thin layers of uranium, practically all the fission pulses were of a maximum height determined by saturation of the linear amplifier.

The γ-ray intensity was measured with a Geiger counter shielded with one inch of lead, except for a window over which was placed only $\frac{1}{8}$ inch of lead in the direction of the target. The counting was done with either a scale-of-four and Cenco recorder or a counting rate meter. The counter tube was placed at a distance of 3 to 8 feet from the target to prevent the counter from saturating. To correct for that fraction of the counts due to radiation scattered by the lead shield, a 4-cm plug of lead was inserted in the window and the difference with and without this plug was taken to be proportional to the intensity of γ-rays coming from the target.

EXPERIMENTS

To establish that the fission recoils observed were due to γ-rays and not to neutrons, we have found that: (1) Too few neutrons were given off from the target to cause the observed fissions; (2) the fission rate was proportional to the γ-ray intensity, the latter being varied by changing the proton energy or the proton current, and (3) the absorption of the fission-producing radiation was similar to that for high energy γ-rays and not like that for neutrons.

A few neutrons were observed to come from the CaF_2 target when it was bombarded with protons. These neutrons were detected by means of a BF_3 ionization chamber coupled to a linear amplifier, and the voltage excitation curve was measured. The threshold for neutron production of these neutrons was approximately $E_p = 1.8$ Mev, and the yield was of the order of 1/800 that previously observed from Li (p, n).[7] The (p, n) reaction responsible for this background was not identified, but is reasonably ascribed to either Ca (p, n), whose excitation curve it resembles, or to lithium contamination. The intensity of neutrons from the bombardment of CaF_2 is approximately half that from calcium metal, and has, approximately, the same threshold. However, no fissions were observed when uranium was exposed to irradiation from calcium metal bombarded with protons, all other conditions being identical with the experiment in which CaF_2 was bombarded and fission observed. This proves definitely that the phenomenon we attribute to photo-fission is not caused by neutrons from the calcium (p, n) reaction. Furthermore, fissions have been observed at proton energies as low as 1 Mev, at which energy no neutrons more than the natural background were observed. As a further check, the expected number of fissions were observed when the target was changed to AlF_3, but no fissions occurred when a target of aluminum metal was used.

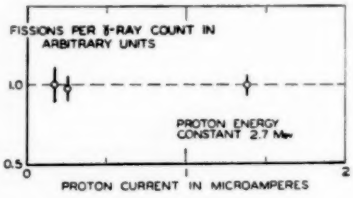

FIG. 3. Fissions per γ-ray count *vs.* proton current.

Although the γ-ray intensity, and hence the fission rate, is very low at lower proton energies, we were able to observe fissions down to proton energies of 1 Mev, and to measure the fission rate per unit of γ-ray intensity. A curve showing fissions per γ-quantum in arbitrary units as a function of proton energy from 1 to 3.4 Mev is given in Fig. 2. The γ-ray yield changes by about a factor of 70 in going from 1 Mev to 3.4 Mev. Part of this increase was compensated by increasing the proton current at lower proton energies. The points in Fig. 2 are averages of several runs, and the vertical lines through the points indicate the statistical uncertainty. The number of fissions per unit of γ-ray intensity was measured as the proton current was changed. These results are given in Fig. 3.

The absorption of the fission-producing radiation from the target was measured by interposing various absorbers between the target and the

[7] Haxby, Shoupp, Stephens and Wells, Phys. Rev. **57**, 348A (1940).

uranium. The geometry used is shown in Fig. 1. The Geiger counter and shield used to measure the γ-ray intensity were at right angles to the proton beam, and were 228 cm away. The γ-ray intensity readings registered by the Geiger counter, were not corrected for radiation scattered by the lead shield as the γ-ray intensity remained practically constant. The presence of the various absorbers placed between the target and the fission counter caused no change in γ-ray intensity. The number of fissions per unit of γ-ray intensity, in this case per Geiger count, is plotted in Fig. 4 for different absorbers and different thicknesses of lead absorber. These readings were taken with a proton beam current of 0.5 μa of 3.4-Mev protons. The absorption coefficients taken from the curves of Fig. 4 are tabulated in the second column of Table I. In the third column the absorption coefficients calculated for 6-Mev γ-rays are tabulated. The agreement between columns two and three is quite satisfactory. In contrast, similar absorption measurements with the neutrons from Li (p, n) to cause fissions, were made. The absorption coefficients determined in the same way for lead, iron, and paraffin, were 0.23 ± 0.05, 0.13 ± 0.05 and 0.13 ± 0.05 cm^{-1}, respectively. The vast difference in absorption shows conclusively that the observed fissions are caused by γ-rays.

It seems unlikely that a secondary reaction such as the photo-disintegration of the plate on which the uranium was mounted should give enough neutrons to cause an appreciable number of the observed fissions. We observed no change in fission rate when the backing plate was doubled in thickness, or when it was changed from brass to aluminum. Furthermore, the experiment which measured the neutrons produced when CaF_2 was bombarded with protons should likewise have measured neutrons produced by photo-disintegration or brass or aluminum since

TABLE I. *Absorption coefficient of fission-producing radiation.*

Absorber	Absorption Coefficients (cm^{-1}) Obs.	Calc. for 6 Mev γ-Rays
Paraffin	0.01 ± 0.07	0.04
Aluminum	0.14 ± 0.07	0.07
Iron	0.28 ± 0.07	0.26
Lead	0.53 ± 0.08	0.50

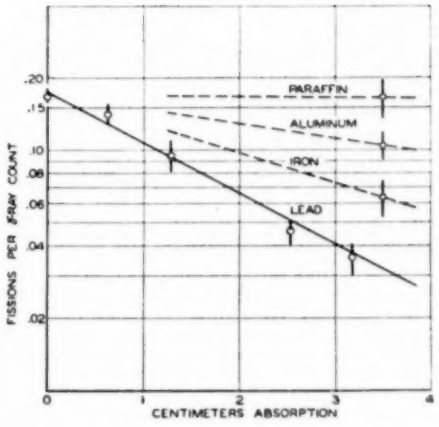

FIG. 4. Fissions per γ-ray count *vs.* thickness of γ-ray absorber.

the BF_3 counter contained large quantities of both substances. The fact that approximately half as many neutrons were observed from CaF_2 as from Ca indicates that the fluorine γ-rays do not cause appreciable photo-disintegration in aluminum or brass. Therefore, the fission observed cannot be caused by photo-neutrons from these substances.

When uranium was removed from the ionization chamber there were no observed fission kicks. Likewise, with the proton beam hitting a quartz plate instead of the fluorite target, no fissions were ever observed. Occasional pulses induced from switch transients, sparking in the high voltage, or spray voltage were observed, but since the counting was visual, these could easily be distinguished from fission kicks by their wave form and were, consequently, not counted.

Cross Section for Photo-Fission

The cross section for the photo-fission process was measured by using a uranium film thin enough so that every fission process could be observed in the ionization chamber. Since each fission produces a *pair* of recoil atoms having roughly the same mass, one of the particles will be in a direction to be recorded by the ionization, while the other will be absorbed in the backing plate on which the uranium is deposited. The evaporated films we used contained approximately 1 mg/cm², which is roughly $\frac{1}{4}$ cm air equivalent in stopping power.[8]

[8] We wish to thank Dr. E. D. Wilson of these laboratories for preparing the films for us.

If such a film contains N atoms of uranium and if it is traversed by a γ-ray beam of δ quanta/cm²-sec., and if σ is the cross section for the fission process in cm², then the number of fissions per second, f, is

$$f=\sigma N\delta. \quad (1)$$

To find N for the thin films of uranium, we measured the weight of the film and also the number of α-particles emitted from it. The first film was gray, and was assumed to be U_3O_8, while the second was black, assumed to be UO_2. The weight of the first film was 4.06 mg, giving $N=0.87\times10^{19}$. The uranium used was separated chemically about 10 years ago; consequently it does not contain an appreciable amount of ionium, and the U II should be in approximate equilibrium. Actino-uranium should be present in the normal ratio. Using Nier's disintegration constants[9] we calculate a total α-emission per second per atom of uranium to be 9.76×10^{-18}. The observed number of α-particles was assumed to be half the total number, although actually, because of the geometry, it will be somewhat less. For the first film the observed number of α-particles per second was 40, giving $N=0.82\times10^{19}$. This is in good agreement with the estimate made from the weight of the film. The second, black, film (UO_2) weighed 5.75 mg, giving 1.27×10^{19} atoms from the weight. It emitted 57 α-particles per second, giving 1.17×10^{19} atoms from the activity.

We were unable to get such a good check in the analogous procedure for a thin evaporated film of thorium. Therefore, the cross section for thorium was obtained by comparing the fission yields from thick targets of uranium and thorium. In each case the same exposed area of freshly sandpapered metal was used. The relative yield gives:

$$\sigma_U/\sigma_{Th}=2.0\pm0.1. \quad (2)$$

This is the average of several runs at different proton energies. The uncertainty arises mainly from the statistical fluctuations involved. The thorium used was spectroscopically free of uranium, and the uranium had less than a few percent of thorium contamination.

Next we consider the factor δ in Eq. (1). Let Γ be the total number of quanta/sec. from the target. Then $\delta=\Gamma/4\pi r^2$, where r is the distance from the uranium to the γ-ray source. We have

$$\Gamma=pqy, \quad (3)$$

where p is the number of protons per second striking the fluorite crystal, y is the yield in quanta per proton at 1-Mev proton energy, and q is the ratio of the yield at the energy used to that at 1 Mev.

With a Geiger counter cylinder 1×5 cm located 82 cm from the fluorite target, we observed 7.4 γ-counts/sec. when the proton current was 1.4 μa (8.7×10^{12} proton/sec.) at 1 Mev. Assuming the counter efficiency to be 2 percent[10] this gives roughly 7.3×10^{-7} γ-quanta/proton at 1 Mev. This yield has been independently and more carefully measured by Lauritsen, Fowler, and Streib to be 7.6×10^{-7} γ-quanta/proton at 1 Mev.[11] The agreement between our rough Geiger counter measurements and this more accurate electroscope measurement is reassuring. However, the number of quanta per proton we obtain *is about 1000 times greater* than the value given by Livingston and Bethe.[5] That value is presumably derived from Hafstad's[12] comparison of the lithium and fluorine γ-ray intensities, together with a rough guess for the Li (p, γ) yield. Hence, the value for Li (p, γ) must also be much too low. In the calculations which follow, we will use $y=7.6\times10^{-7}$ quanta/proton.

We have taken many excitation curves to determine the value of q in Eq. (3). Some runs were taken with protons, mass 1; others were taken by comparing the yield from mass 1 at 3 Mev with mass 3 at 3 Mev (effectively 1 Mev per proton). The averages of several runs are given in Table II. These are probably not accurate to better than 10 percent. The value $q=10.5$ at 2.0 Mev checks with that obtained at Wisconsin[13] where they obtained $q=11$.

TABLE II. *Yield of quanta/proton as a function of proton energy*

E_p (MEV)	1.5	2.0	2.9	3.0	3.2	3.4
q	3.4	10.5	52	55	63	70

The notation F (p, γ) is a convenient but in-

[9] A. O. Nier, Phys. Rev. **55**, 152 (1939).

[10] J. V. Dunworth, Rev. Sci. Inst. **11**, 167 (1940).

[11] We wish to thank Dr. Fowler for informing us of this result before publication.

[12] Hafstad, Heydenburg and Tuve, Phys. Rev. **50**, 504 (1936).

[13] Herb, Kerst and McKibben, Phys. Rev. **51**, 691 (1937).

exact designation for the γ-rays from fluorine bombarded with protons, since it has been shown[14] that most of the high energy rays are emitted from an excited state of O^{16} derived from $(Ne^{20})^*$ by emission of an α-particle. The energy of the γ-rays has been measured to be 6.3 Mev[14] and the character of the γ-rays does not seem to change when the proton energy is varied from 0.33 to 1.36 Mev. Since we observed fission at 1-Mev proton energy it seems probable that the 6.3-Mev quanta cause the fissions. Also since the fissions/(γ-quantum) remain constant with increase of proton energy from 1 Mev to 3.4 Mev, it seems probable that there is no marked change in the γ-ray spectrum over this range. For the cross-section calculation we assume as equally effective all the quanta recorded on the counter (through $\frac{1}{8}$ inch of lead). This assumption neglects the possibility that the γ-rays consist of several close lines or have weak high energy components.

Fifteen runs were taken in the determination of the fission rate per proton current. Two uranium films were used, the proton energy and current were varied as well as the distance of the uranium to the target. In a sample run, 41 fissions were observed in 295 seconds from a uranium film containing 1.22×10^{19} atoms placed so that $1/4\pi r^2$ was 0.0134 cm^{-2} when the CaF_2 target was bombarded with 0.91 μa of 3.0-Mev protons. The mean value of these fifteen determinations of the uranium cross section is $\sigma=3.47\times10^{-27}$ cm^2. The distribution of the individual values gives a root-mean-square deviation from the mean of 0.81×10^{-27}, most of which arises from the fluctuation statistics caused by the finite number of fissions in each run. Other sources of error are such that this value of the cross section may well have a probable error of 30 percent. Coupled with the result already cited for the ratio of σ_U to σ_{Th}, we get $\sigma_{Th}=1.73\times10^{-27}$ cm^2 also with a probable error of about 30 percent.

We have also observed fission in both uranium and thorium produced by the 17-Mev γ-rays from lithium bombarded with protons. The effect is quite weak, because of the smaller number of quanta available, but the cross sections seem to be at least of the same order of magnitude as with the fluorine γ-rays, and are being studied further. We have also observed neutrons emitted when thorium is irradiated with fluorine γ-rays. These are probably released in the fission process, and are being investigated further. We have observed no fission in bismuth, thallium, or mercury, with either lithium or fluorine γ-rays. However, the intensity of lithium γ-rays used was relatively small.

[14] W. A. Fowler and C. C. Lauritsen, Phys. Rev. **56**, 840 (1939).

Discussion

Bohr and Wheeler[2] predicted a cross section for photo-fission of 10^{-27} and 10^{-28} cm^2 for uranium and thorium, respectively, on the basis of Bothe and Gentner's[15] photo-disintegration cross section of 5×10^{-26} cm^2 and estimates of the partial widths of nuclear levels caused by fission and by neutron emission founded partly on theoretical considerations, partly on the observational material available at that time.

Additional experiments performed in the meantime make it possible to give in the present instance a somewhat more detailed treatment of the balance of energy which, according to Weisskopf[16] and Bohr and Wheeler[2] determines the partial widths of nuclear levels.

In particular, in view of our recent measurements of the neutron fission thresholds[17] it seems that Bohr and Wheeler's curve of the critical energy of fission should have its ordinate scale lowered by about $\frac{1}{2}$ Mev. The critical energy for fission E_f is the sum of the neutron binding energy E_n and the neutron energy necessary to produce fission, Q_n. Since Bohr and Wheeler have calculated E_n to be 5.1 Mev for U^{239} and 5.2 Mev for Th^{233} and our measurements suggest Q_n is 0.3 and 1.1 Mev,[17] then E_f should be 5.4 and 6.3 Mev, respectively. These values are just 0.5 Mev less than those estimated by Bohr and Wheeler.[18] This revision of their E_f curve gives for U^{238} and Th^{232} (the nuclei concerned in photo-fission) critical energies of fission of 5.2 and 6.1 Mev. The neutron binding energies of these same nuclei

[15] W. Bothe and W. Gentner, Zeits. f. Physik **106**, 236 (1937).

[16] V. F. Weisskopf and D. H. Ewing, Phys. Rev. **57**, 472 (1940).

[17] Haxby, Shoupp, Stephens and Wells, Phys. Rev. **57**, 1088A; **58**, 199A (1940).

[18] This revision makes slow neutron fission of Pa to be expected. The cross section may, however, be small enough to have been missed at Columbia.

calculated as in Bohr and Wheeler's paper are 6.1 (U^{238}) and 6.2 Mev (Th^{232}).[19] Excitation of U^{238} by a 6.3-Mev γ-ray, then, raises the nuclear energy to 1.1 Mev above the critical fission energy but only 0.2 Mev above the energy necessary to emit a neutron. Hence the Γ_f as read from Bohr and Wheeler's Fig. 5 is certainly larger than Γ_n and Γ_r. For Th^{232}, on the other hand, the 6.3-Mev γ-excitation raises the nucleus to an energy 0.2 Mev above the critical fission energy and 0.1 Mev above the energy necessary to emit a neutron. Since these energies are not accurately known, and since Γ_n, especially, depends very critically on the excess energy in this region, all we may say is that Γ_f, Γ_n, and Γ_r may be of the same order of magnitude.

The cross section for the ejection of neutrons from various heavy nuclei by γ-rays of 17 Mev energy has been measured by Bothe and Gentner[15] to be 5×10^{-26} cm^2. In these experiments the nuclei are raised to excited states of such energy that neutron emission is overwhelmingly more probable than radiative de-excitation. This will no longer necessarily be the case when the excitation is produced by the fluorine γ-rays and when, as in our experiments, fission provides an additional means of disposing of excited nuclei. The cross section will be reduced below the figure of Bothe and Gentner by the fraction $\Gamma_f/(\Gamma_f+\Gamma_n+\Gamma_r)$ on this account. It will be further reduced because the probability of radiative excitation of the normal nucleus varies (in the region of continuous level distribution with which we are concerned) approximately as the cube of the quantum energy.[20] Thus we have as the cross section for the radiative production of fission

$$\sigma\sim\Gamma_f/(\Gamma_f+\Gamma_n+\Gamma_r)5\times10^{-26}(6.3/17)^3$$
$$=\Gamma_f/(\Gamma_f+\Gamma_n+\Gamma_r)2.5\times10^{-27}\text{ cm}^2.$$

As we have seen, Γ_f for U^{238} is larger than Γ_n and Γ_r, so that $\Gamma_f/(\Gamma_f+\Gamma_n+\Gamma_r)$ is approximately one. This gives $\sigma_U=2.5\times10^{-27}$ cm^2 in agreement with the observed value 3.5×10^{-27} cm^2. For Th^{232}, on the other hand, since Γ_f, Γ_n and Γ_r may all be of the same order of magnitude, we can say only that the fraction, $\Gamma_f/(\Gamma_f+\Gamma_n+\Gamma_r)$ is between 0 and 1, giving $\sigma_{Th}=0$ to 2.5×10^{-27} cm^2. Whether competition from neutron emission, or radiation, or both, is the cause of the lower cross section for thorium will have to be decided by more accurate knowledge of the energies involved and the partial widths, or by more experimental information on the neutrons emitted. As Dr. Wheeler suggests, there seems to be more chance that neutron emission is the competing mechanism since there is more likelihood that the neutron width will exceed rather than fall below the radiation width.

We wish to thank Dr. F. W. Stallman for assistance with some of the measurements, and Dr. E. U. Condon for his help and encouragement throughout all these experiments.

[19] We are indebted to Dr. Wheeler for these calculations and for his emphasis that these values are accurate to 0.2 Mev because of the use of accurately known natural disintegration energies to calculate the packing fractions. We also wish to thank him for his help in revising this section.

[20] We wish to thank Dr. Weisskopf for suggesting these considerations.

Positrons from Light Nuclei

M. G. WHITE, E. C. CREUTZ, L. A. DELSASSO AND R. R. WILSON
Palmer Physical Laboratory, Princeton University, Princeton, New Jersey

(Received November 14, 1940)

Four nuclei of the type discussed by Wigner, containing one more proton than neutron, have been produced. The nuclei, their half-lives and positron energies are: P^{29}, 4.6 seconds, 3.63 Mev; S^{31}, 3.2 seconds, 3.85 Mev; Cl^{33}, 2.4 seconds, 4.13 Mev; and A^{35}, 2.2 seconds, 4.38 Mev. These energies are in excellent agreement with the calculated values and indicate that (1) the $\pi-\pi$ force is equal to the $\nu-\nu$ force plus the Coulomb repulsion, (2) the nuclear volumes are proportional to the atomic weights, and (3) the nuclear charge is distributed uniformly through the volume. The half-life-energy relation is in good agreement with the Fermi theory. Deviations are in the direction anticipated by the Gamow-Teller modification.

INTRODUCTION

THE difference in binding energy of isobars which differ only in the interchange of the protons with the neutrons has been supposed on theoretical grounds to consist almost entirely of the extra Coulomb energy of the nucleus with the higher charge. Assuming that the $\pi-\pi$ force exceeds the $\nu-\nu$ force only by the Coulomb repulsion, and that the charge on the nucleus is distributed uniformly through a volume proportional to the mass number, one may calculate within a multiplicative constant this binding energy difference, and hence the maximum energy of the positrons emitted in the transition to the lighter nucleus.[1,2] The constant in this proportion, and consequently the nuclear radius, may be evaluated from the experimental data on the energies of beta-rays from nuclei of this particular type, i.e., nuclei which contain one more proton than neutron. We have produced four more of these positron emitting isotopes, which are discussed separately in the following paragraphs.

P^{29}

The production of this isotope, as well as of the others to be discussed, was made possible by increasing our available proton energy from $\sim$6.3 to >8.6 Mev. Silicon crystals were pressed into clean lead sheet and bombarded in an atmosphere of hydrogen for times averaging about 3 seconds, with $\sim$0.5 μA of protons. Silicon exists as three stable isotopes, $Si^{28,29,30}$. We believe the short period activity produced is P^{29} rather than P^{28} because of the agreement of the half-life and energy with the predictions of theory. However, since P^{30} is also produced when silicon is bombarded with protons, it was necessary to keep the bombardment time to a minimum to eliminate as much as possible of this 2.5-minute activity. The β-ray spectrum was obtained in a cloud chamber filled with helium and alcohol vapor, and with a magnetic field of 714 oersteds. Only one photograph per bombardment was made. The proton

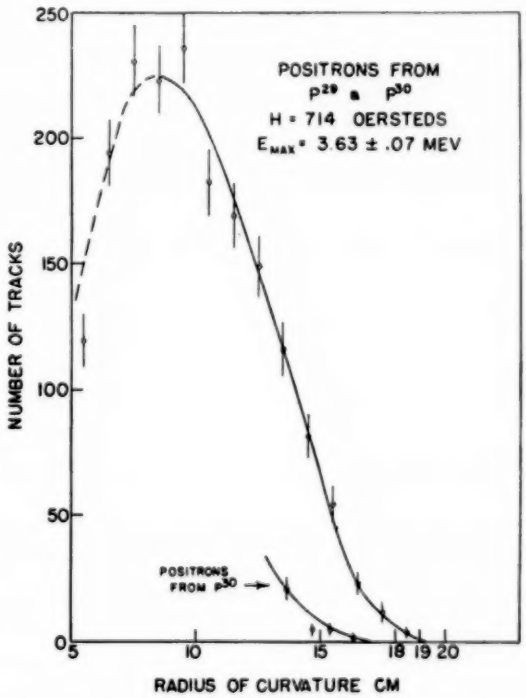

FIG. 1. Positrons from P^{29} and P^{30}. Vertical lines through the points estimate the probable error, as the square root of the numbers of tracks.

[1] E. Wigner, Phys. Rev. **56**, 519 (1939).
[2] White, Delsasso, Fox and Creutz, Phys. Rev. **56**, 512 (1939).

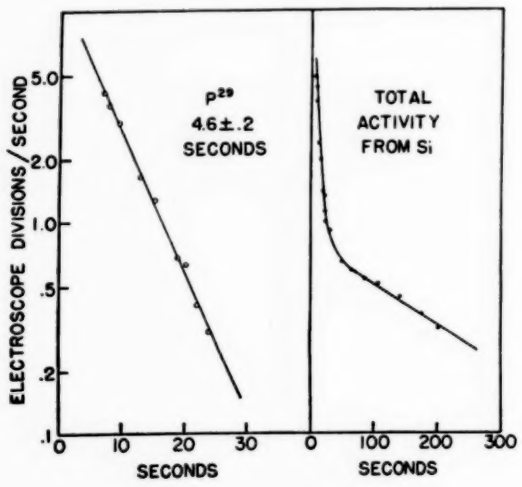

FIG. 2. Decay curve of P^{29}.

beam was shut off during expansion by a cam controlling the ion source, thus eliminating the gamma-ray background of the cyclotron. Targets were placed manually in a well in the chamber within three seconds after bombardment stopped. A large number of targets were used in rotation so that the P^{30} activity would not build up after repeated short exposures to the beam. It was hoped that the energy of P^{29} would be sufficiently higher than that of P^{30} so it could be distinguished. That this was possible may be seen from Fig. 1, where the momentum spectrum of all positrons from the two reactions $Si^{29,30}(p, n)P^{29,30}$ is plotted as well as the upper end of the spectrum of positrons from P^{30} alone, the latter being obtained when the proton energy was below the threshold for production of P^{29}. (The total number of tracks in the two cases was closely the same.) After adding the energy lost in the foil window of the cloud chamber, the upper limit for P^{29} positrons is 3.63 ± 0.07 Mev.

The half-life was obtained by repeatedly photographing a stop watch dial and the image of the fiber of a projection-type Lauritsen electroscope on which the activated target was placed; the cyclotron being turned off after the bombardment was completed. Unfortunately the P^{30} background always had to be subtracted from the decay curves, thus increasing the probable error of the measurement. The half-life, as is seen in Fig. 2, is 4.6 ± 0.2 seconds.

S^{31}

After bombarding iron for various times and finding no appreciable activity, iron-phosphorus alloy was chosen as the target for the production of this isotope. The experimental method was the same as for P^{29}, except that here the problem was much simpler; since P^{31} is the only stable isotope of phosphorus, S^{31} is the only likely radioactive nucleus produced by proton bombardment. From Fig. 3 the upper limit of the positrons is seen to be 3.85 ± 0.07 Mev. Figure 4 shows a typical decay curve, giving a half-life of 3.2 ± 0.2 seconds[3] as the mean of several such curves.

To be certain that the electroscope method is a valid one for the measurement of these short half-lives, in spite of the finite collection time of the ions produced in the instrument, a check was made in the following way. A 15-mC radium source was suspended over the electroscope window by a cord passing over a pulley and thence to a drum whose speed of rotation was proportional to the velocity of a chronograph tape on which the passage of the electroscope fiber over the scale divisions could be recorded. Readings of the activity were first made with the radium stationary at various heights above the

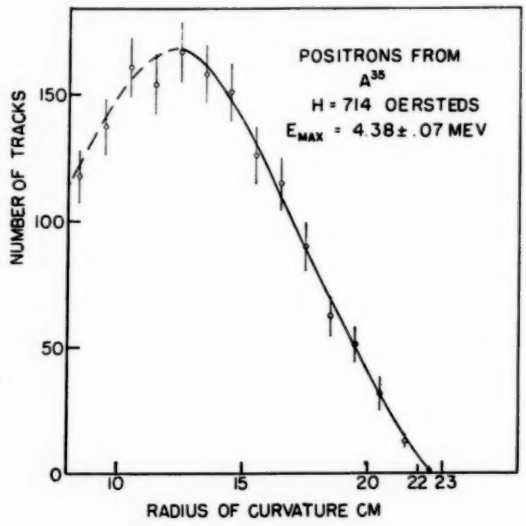

FIG. 3. Positrons from S^{31}.

[3] Since completion of this work the half-life of this isotope, produced by $Si^{28}(\alpha, n)S^{31}$, was reported by King and Elliott at the Chicago meeting of the American Physical Society, November, 1940 (Phys. Rev. **59**, 108A (1941)), as 3.18 seconds. Although their method of measurement was different from ours, their value agrees well with ours.

electroscope. A plot of activity against height was then made. This plot was compared with that obtained when the radium source was in constant motion away from the window. The second case corresponds roughly (insofar as the rate of change of ionization in the electroscope is concerned) to a decaying source. Comparison of the two curves shows whether or not the rate of decrease of activity measured by the electroscope actually corresponds to the rate at which the incident radiation is decaying. The agreement was excellent up to speeds corresponding to half-lives of three seconds and was within 5 percent for a half-life of 1.6 seconds. This fact has been considered in estimating our probable errors.

Cl^{33}

This isotope was reported by Hoag,[4] produced by $S^{32}(D, n)Cl^{33}$. In our laboratory sulfur was melted onto lead strips and bombarded with protons to obtain the reaction $S^{33}(p, n)Cl^{33}$. This activity, like the preceding, was a "clean" one, i.e., no other periods were produced in any quantity. Sufficient proton energy is not available* to produce $S^{32}(p, n)Cl^{32}$, while Cl^{34} and Cl^{36} gave no difficulty because of their long lifetimes. An additional possibility is that the isotope produced is P^{29} by $S^{32}(p, \alpha)P^{29}$, and that the supposed P^{29} obtained when we bombard Si is actually P^{28}. These two coincidences with the

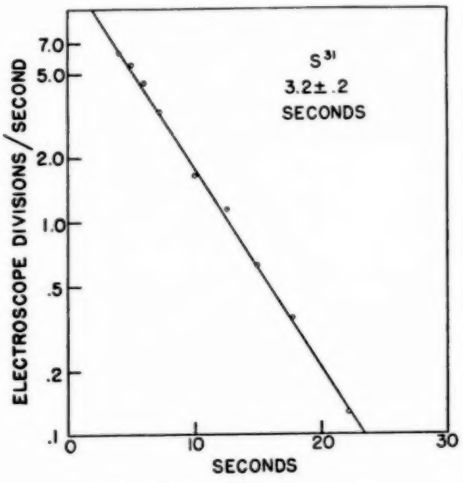

FIG. 4. Decay curve of S^{31}.

[4] J. Barton Hoag, Phys. Rev. **57**, 937 (1940).

* From Barkas' masses, the threshold for this reaction is ~13 Mev.

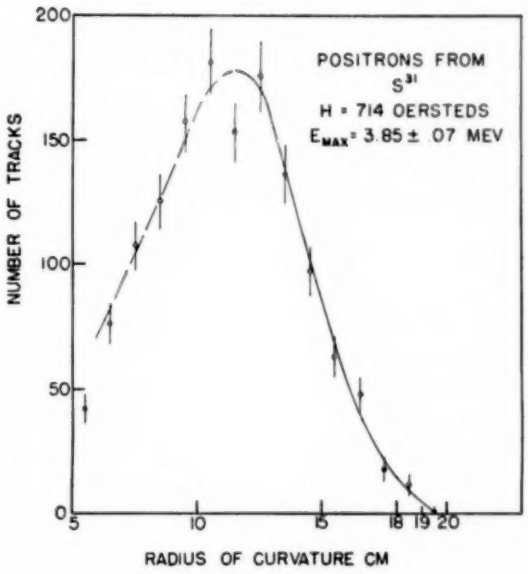

FIG. 5. Positrons from Cl^{33}.

energies expected from Cl^{33} and P^{29} (see discussion) would, however, seem very improbable. The upper limit of the positrons is seen from Fig. 5 to be 4.13 ± 0.07 Mev. Figure 6 shows a half-life curve. The value is 2.4 ± 0.2 seconds.

As in all experimental work, the accurate determination of the upper limits of beta-ray spectra by the cloud-chamber method requires that extreme precautions be taken to guard against subjective errors. It was expected, before these experiments were made, that the energies would increase with the atomic number of the element concerned. Since the same cloud-chamber magnetic field was used for all four elements, it would be very easy unconsciously to "look for" tracks of slightly higher radius of curvature with each successive element. A very large percentage of the tracks photographed are not measured because they are diffuse, scattered, too short, or do not clearly originate in the target. Therefore whether or not a track is counted is necessarily very much a matter of personal choice in deciding whether or not it is a "good" one. Probably the best way to insure against any unintentional cheating would be to mix all the pictures of all the elements before measuring them, so that the observer would not know whether he "ought" to find high energy tracks on a certain film or not. This was not done, but various other precautions were taken. The reprojected tracks were com-

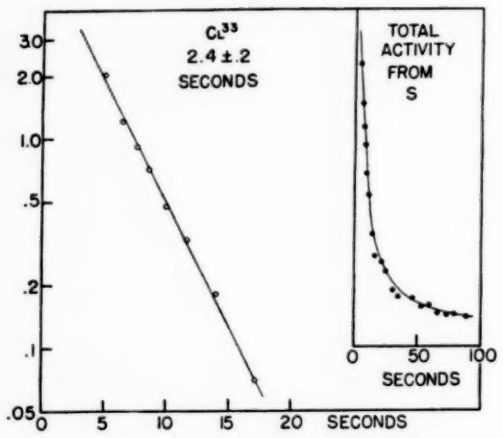

FIG. 6. Decay curve of Cl^{33}.

pared with arcs of circles printed in black ink on white cards, each card having un-numbered arcs of radii from 5 cm to 25 cm in ½-cm steps. When a track was found to fit a certain arc better than the next one on either side, a pencil mark was made on that arc. As soon as enough marks had been made on one card so that the observer began to be aware of any "shape" to their distribution, a new card was taken. Thus for any spectrum, from 15 to 30 cards were used. Furthermore, it is quite difficult, if not impossible, to tell from looking at a track whether its radius is 18, 20, or 22 cm for instance, until it is compared with a measured arc. All distributions were plotted before the theoretical energies were calculated. The curves were finally drawn in through the points on sheets with the abscissae un-numbered and the spectra un-named. Under these conditions different people well within the probable error obtained the same upper limit from the data.

A^{35}

Since bombardment of lead has not shown appreciable activity, lead chloride was used as the target material to produce the reaction $Cl^{35}(p, n)A^{35}$. The only contaminating activity was of long period, possibly A^{37}. The momentum spectrum of the positrons accompanying the decay back to Cl^{35} is shown in Fig. 7, giving an upper limit of 4.38±0.07 Mev. The half-life, as averaged from curves such as that given in Fig. 8, is 2.2±0.2 seconds.[5] In this case, as well as in

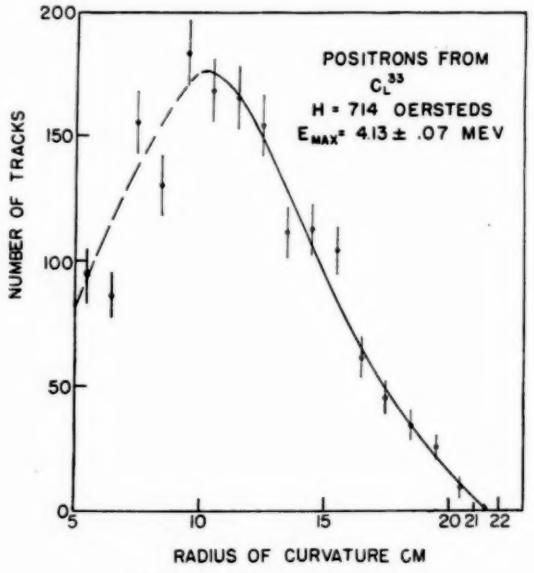

FIG. 7. Positrons from A^{35}

the preceding, consideration must be made of the failure of the electroscope to follow such rapidly decaying activity. This correction has been made, amounting to about 0.1 second.

DISCUSSION

All nuclei of this type which can be made by (p, n) reactions, with the exceptions of Na^{21} and Ca^{39} have now been studied.[6] The half-life but not the energy of Na^{21} has been measured.[7] In Fig. 9 the measured positron energy of these

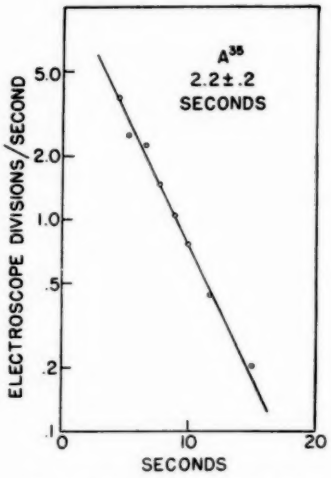

FIG. 8. Decay curve of A^{35}.

[5] L. D. P. King and D. R. Elliott, reference 3, quote 1.91 seconds for the half-life of this nucleus, as produced by $S^{32}(\alpha, n)A^{35}$.

[6] L. D. P. King and D. R. Elliott, reference 3, report 0.87 second for the half-life of Sc^{41}, made by $Ca^{40}(D, n)$.

[7] Creutz, Fox and Sutton, Phys. Rev. **57**, 567 (1940).

nuclei is plotted against that calculated on the assumptions stated in the introduction, namely that (1) the $\pi-\pi$ force is equal to the $\nu-\nu$ force plus the Coulomb repulsion, (2) the charge is uniformly distributed throughout the volume, and (3) the nuclear volume is proportional to the mass number. The theoretical values are calculated under the assumption that the nucleus has Coulomb energy[1]

$$E=\tfrac{1}{2}\times 2.35\times z(z-1)A^{-\frac{1}{3}}mc^2.$$

The difference in this quantity for two nuclei of charge z and $z-1$ is then

$$\Delta E=2.35(z-1)A^{-\frac{1}{3}}mc^2.$$

The constant was chosen to give the best visual fit to the data. To obtain the expected upper limit of these beta-ray spectra, one must subtract from this available energy two electron masses and the neutron-proton mass difference. Converting to Mev this gives for the upper limit, since $A-1=2(z-1)$,

$$E_{\max}=6.0(A-1)A^{-\frac{1}{3}}-1.78 \text{ Mev},$$

provided the decay is to the ground state of the final nucleus. This is assumed since in previous work on similar nuclear types no gamma-radiation was definitely found.[2,8] Deviation from a straight line would indicate that these assumptions are invalid. The agreement in most cases is good enough to make another investigation of the worst cases (15, 25, 27) worth while.

The transition probability for β-decay, according to Fermi's theory,[9] is given by

$$\lambda=GI(\omega),$$

where G depends on the matrix element for the transition and ω is the maximum total positron energy. I is roughly $\omega^5/30$. For this reason the half-lives should be about proportional to ω^{-5}. In Fig. 10 are plotted the observed half-lives to the minus one-fifth power, against the observed ω. $I(\omega)$ has actually been more accurately calculated from formulas 1(a) and (2) of reference (1), and in Table I are given values of this quantity as well as the observed half-lives multiplied by $I(\omega)$. Figure 11 shows a plot of $I(\omega)\cdot t$ against z. It may be of some interest to point out that the proton and neutron form an isobaric pair of this series. If we assume the Fermi theory to hold for the decay of the neutron by electron emission, using an average value of It from Fig. 11 with the neutron-proton mass difference of $1.5mc^2$, we estimate the half-life of the neutron to be roughly one-half hour.

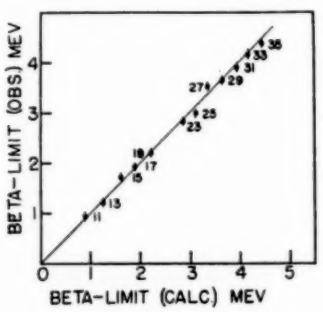

FIG. 9. Observed and calculated energies of positrons from nuclei with one more proton than neutron. Vertical lines estimate the probable error.

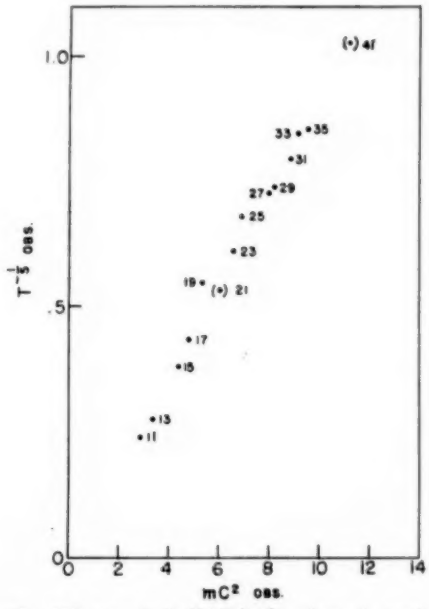

FIG. 10. (Observed half-life)$^{-1/5}$ plotted against the observed total positron energy. Calculated energies were used at points 21 and 41.

The following discussion was written by Professor Wigner.

The fact that the quantity in the last column in Table I is essentially constant can be most simply interpreted by assuming that the matrix element of the transition to the normal state of

[8] Richardson presented cloud-chamber evidence for gamma-radiation from N^{13} (Phys. Rev. **53**, 610 (1938); **55**, 609 (1939)). Valley, using a magnetic spectrograph, failed to find such radiation (Phys. Rev. **56**, 839 (1939)).

[9] E. Fermi, Zeits. f. Physik **60**, 320 (1934).

the product nucleus is essentially constant throughout the series and that this transition determines at least the order of magnitude of the lifetime. Both these assumptions follow from Fermi's theory of β-decay and also from Gamow and Teller's modified form if one assumes, in the latter case, that the effect of the spin-dependent forces on the wave functions is small.

There are several phenomena which seem to support and others which appear to contradict the above theories. *We shall discuss them here only insofar as the experiments have a bearing on them.*

Fermi's original theory would require that the numbers in the last column be all exactly equal if the $\pi-\pi$, $\nu-\nu$ and $\pi-\nu$ interactions are all equal. The variations within the last column must be interpreted then on the Fermi theory as being caused by modifications of the wave function resulting from differences between the above forces. The variation within the last column is perhaps somewhat bigger than one would expect on this basis. In this theory, from the normal state of any of the radioactive nuclei of this series, only the transition into the normal state of the product nucleus is "allowed."

In the Gamow-Teller modification of Fermi's theory one has to consider the doublet structure of the normal states. From a $^2P_{3/2}$ normal state of, say, C^{11}, not only the transition into the $^2P_{3/2}$ normal state of B^{11} is "allowed" but also the transition into the $^2P_{1/2}$ state of this nucleus. The situation is similar in the other cases. The matrix elements of both transitions can be calculated.

TABLE I. *Values of $I(\omega)$ and of $I(\omega)\times t$.*

Z	$(\omega)_{OBS}$ (mc^2)	$I(\omega)$	t_{OBS} (SEC.)	$I(\omega)\times t_{OBS}$
11	2.86	3.46	1230	4330
13	3.37	10.2	630	6430
15	4.37	42.1	125	5260
17	4.78	66.3	64	4230
19	5.31	116	20.3	2360
21	6.00*	222	23	6920
23	6.52	351	11.6	4070
25	6.85	452	7	3160
27	7.93	967	4.9	4730
29	8.16	1100	4.6	5060
31	8.75	1590	3.2	5080
33	9.14	2010	2.4	4680
35	9.57	2550	2.2	5610

* Calculated.

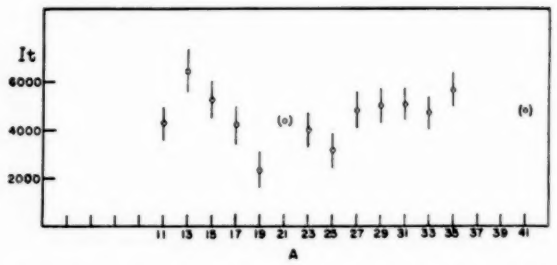

FIG. 11. Fermi's $I(\omega)$ calculated from observed values of ω (=total positron energy), multiplied by the observed half-life. The calculated ω was used for the points at 21 and 41.[10]

Since the energy of transition into the normal state of the product nucleus is measured, the transition probability into this state can also be calculated. Since, however, the energy of transition into the upper state is, in general, not known, the transition probability into this state cannot be evaluated. As the lifetime of the radioactive nucleus is the reciprocal of the sum of both transiton probabilities, it cannot be evaluated exactly. However, in most cases, the transition into the normal state will play a predominant role and one will expect, therefore, that the total transition probability will be relatively largest where the matrix element of the transition into the normal state is largest.

This appears to be in agreement with observation. The matrix element is largest ($\frac{3}{4}$) in the case of a $^2S_{1/2}-{}^2S_{1/2}$ transition. One has reason to suppose that this takes place in the case of the $Ne^{19}-F^{19}$ transition, and, in fact, the last column (which is inversely proportional to the transition probability) is smallest in this case. The matrix element is smallest ($\frac{1}{12}$) in the case of the $^2P_{1/2}-{}^2P_{1/2}$ transition, which is assumed to take place for $n=13$ and $n=15$. The last column shows large values in these cases. In case of the other transitions the matrix element has intermediate values.

[10] References for Fig. 11: $A=11$, Delsasso, White, Barkas and Creutz, Phys. Rev. **58**, 586 (1940); $A=13$, Kikuchi, Watasi, Itoh, Takeda and Yamaguchi, Proc. Phys. Soc. Japan **21**, 52 (1939) and Lyman, Phys. Rev. **51**, 1 (1937); $A=15$, Fowler, Delsasso and Lauritsen, Phys. Rev. **49**, 561 (1936); $A=17$, Curie, Richardson and Paxton, Phys. Rev. **49**, 368 (1936); $A=19$, 23, 25, White, Delsasso, Fox and Creutz, Phys. Rev. **56**, 512 (1939); $A=21$, Creutz, Fox and Sutton, Phys. Rev. **57**, 567A (1940); $A=27$, McCreary, Kuerti and Van Voorhis, Phys. Rev. **57**, 351 (1940), Barkas, Creutz, Delsasso, Sutton and White, Phys. Rev. **58**, 383 (1940).

The Paschen-Back Effect

VII. Configuration Interaction

J. B. GREEN
Mendenhall Laboratory of Physics, Ohio State University, Columbus, Ohio
(Received October 23, 1940)

The spectrum of krypton furnishes a very fine example of the effect of configuration interaction. The levels $3s_5$ and $4d_2$, belonging to configurations of the same parity are less than 1 cm^{-1} apart, and the Zeeman patterns of lines arising from them show large perturbations, both as regards positions and relative intensities of the components. A semiempirical theory is discussed which leads to excellent agreement with experiment.

THE problem of determining the positions and relative intensities of the components of a Paschen-Back pattern when the perturbing levels belong to the same configuration has been discussed in V.[1] It was possible, in those cases, to calculate the problem accurately, because the wave functions of the energy levels could be completely specified in terms of LS wave functions. When two configurations of the same parity lie close together, this is no longer possible. Each of the levels of each configuration partakes of the nature of the other configuration. This means that the transformation matrix given in V, Eq. (2a), contains nondiagonal elements between terms of the two different configurations. The calculation of this matrix for particular cases, while it may be possible, would be exceedingly laborious. It is the purpose of this paper to present a semiempirical method of carrying out these calculations and to apply it to the particular case of the interaction between $3s_5$ (configuration $4p^5 7s$) and $4d_2$ (configuration $4p^5 5d$) of krypton. Both of these configurations being odd, they are capable of perturbing each other.

In the general case, in the absence of a magnetic field, the energy matrix is diagonal in J; in the presence of a magnetic field, it is diagonal in M. If we confine our attention to these two quantum numbers, we see that the nondiagonal elements in V, Eq. (4a), can be divided into two classes: (1) those for which $\Delta J=0$, when the element is proportional to M; and (2) those for which $\Delta J=1$, when the element is proportional to $(J^2-M^2)^{\frac{1}{2}}$, where J is the larger of the two J's. The diagonal elements contain terms proportional to Mg', where g' is the weak-field g factor. The important thing to notice is that the factor of proportionality is the same[2] for all values of M.

The portion of the energy matrix for two perturbing levels for a given value of M would therefore be

$$\begin{array}{c|cc} & J-1 & J \\ J-1 & A+Mg_1\omega & K\omega(J^2-M^2)^{\frac{1}{2}} \\ J & K\omega(J^2-M^2)^{\frac{1}{2}} & B+Mg_2\omega \end{array} \qquad (1)$$

where g_1 and g_2 are the weak-field g factors of $(J-1)$ and J, respectively; A and B their respective field-free positions; ω the normal Lorentz separation; and K a constant depending on the LS parameters of the two levels. Setting each of the determinants of this matrix equal to zero for each value of M enables us to determine the positions of the two levels in the magnetic field in terms of the constant K. K is then determined from the experimentally determined energy levels. Having determined K, we may then proceed to find the transformation matrix in V, Eq. (8a), which is necessary for the calculation of the intensities of the components. It is not possible, however, to determine the sign of K definitively from the experimentally determined energy levels. K appears in these calculations only as K^2. A similar uncertainty with respect to sign therefore occurs also in the transformation matrix of V, Eq. (8a), and we must resort to the

[1] J. B. Green and J. F. Eichelberger, Phys. Rev. **56**, 51 (1939).

[2] This fact is not clearly brought out by Roberson and Mack, Phys. Rev. **57**, 1074 (1940), who find the result experimentally. The problem has also been discussed for a simpler case by Mack and Laporte, Phys. Rev. **51**, 291 (1937), who, however, have not considered the problem of calculating the intensities.

TABLE I. *Data for the pattern of λ7493.*

Transition	$2p_8-3s_5$ Position	Intensity $K>0$ $\gamma>0$	Int. $K<0$ $\gamma=0.8$	$2p_8-4d_2$ Position	Intensity $K>0$ $\gamma>0$	Int. $K<0$ $\gamma=0.8$
2→1	3.20	2	2			
1→0	2.26	$(0.74\sqrt{3}+0.67\gamma)^2$	0.50	2.83	$(0.67\sqrt{3}-0.74\gamma)^2$	3.10
0→−1	1.77	$(0.96\sqrt{3}+0.29\gamma\sqrt{3})^2$	1.54	2.94	$(0.29\sqrt{3}-0.96\gamma\sqrt{3})^2$	3.42
−1→−2	1.15	$(0.99\sqrt{2}+0.14\gamma\sqrt{6})^2$	1.19	3.17	$(0.14\sqrt{2}-0.99\gamma\sqrt{6})^2$	4.76
−2→−1	−3.20	2	2			
−1→0	−2.57	$(0.99\sqrt{3}-0.14\gamma)^2$	3.38	−0.55	$(0.14\sqrt{3}+0.99\gamma)^2$	0.25
0→1	−1.95	$(0.96\sqrt{3}-0.29\gamma\sqrt{3})^2$	4.32	−0.78	$(0.29\sqrt{3}+0.96\gamma\sqrt{3})^2$	0.66
1→2	−1.46	$(0.74\sqrt{2}-0.67\gamma\sqrt{6})^2$	5.57	−0.89	$(0.67\sqrt{2}+0.74\gamma\sqrt{6})^2$	0.22
2→2	1.34	8	8			
1→1	0.40	$(0.74\sqrt{2}+0.67\gamma\sqrt{6})^2$	0.08	0.97	$(0.67\gamma\sqrt{2}-0.74\gamma\sqrt{6})^2$	5.72
0→0	−0.09	$(0.29\gamma\sqrt{8})^2$	0.46	1.08	$(-0.96\gamma\sqrt{8})^2$	4.70
−1→−1	−0.71	$(-0.99\sqrt{2}+0.14\gamma\sqrt{6})^2$	2.92	1.31	$(-0.14\sqrt{2}-0.99\gamma\sqrt{6})^2$	2.92
−2→−2	−1.34	8	8			

experimentally determined intensity pattern to resolve this difficulty. The (strength)$^{\frac{1}{2}}$ of a particular component could be expressed as in V, Eq. (9a),

$$(A''jm|S^{\frac{1}{2}}|H''j'm')=[a_1'S_1^{\frac{1}{2}}+\gamma a_2'S_2^{\frac{1}{2}}],$$

where $S_1^{\frac{1}{2}}$ and $S_2^{\frac{1}{2}}$ are the (strengths)$^{\frac{1}{2}}$ of the individual transitions of the two components without perturbation, but reduced to the same scale so that the sum of the strengths of the components for each of the lines is the same; and γ^2 is the relative strength of the two lines in the absence of a magnetic field. A theoretical calculation of γ would be an almost hopeless task, involving, as it would, the relative transition probabilities of two different configurations, which, moreover, perturb each other.* The relative signs of a_1' and a_2' depend on the sign of K and on the selection rules given by Condon and Shortley.[3]

With respect to the particular case of the interaction between $3s_5$ and $4d_2$ of krypton, three lines were available for study:

λλ6904–5 $2p_{10}-4d_2$, $3s_5$
λλ7486–7 $2p_9-(4d_2)$, $3s_5$
λλ7493–4 $2p_8-4d_2$, $3s_5$.

Careful measurements were made of the positions of the components, and having previously determined the g factors of $2p_{10}$, $2p_9$, and $2p_8$ from other lines, the relative positions of the levels of $3s_5(J=2)$ and $4d_2(J=1)$ were calculated. Since the levels corresponding to $M=2$ and $M=-2$ for $3s_5$ are unperturbed, their midpoint was called the zero position and all levels were referred to it. In a field for which $\omega=1.69$ cm^{-1}, the following levels were determined:

	$M=-2$	−1	0	1	2
$3s_5$	−5.06	−2.57	−0.09	2.26	5.06
$4d_2$		−0.55	1.08	2.84	

Knowing the unperturbed positions of

$3s_5$	−5.06	−2.53	0	2.53	5.06

we find that the levels of $3s_5$ have been shifted

−0.04	−0.09	−0.27

so that the levels of $4d_2$ must have been shifted

+0.04	+0.09	+0.27

making their unperturbed positions

−0.59	0.99	2.57

which yields a g value of 0.935. Putting these values back into (1) we find $K=0.098$ for all values of M with an accuracy of 0.01 cm^{-1}. This value of K substituted in (1) yields the following results:

	$M=-2$	−1	0	1	2
$3s_5$	−5.06	−2.57	−0.10	2.27	5.06
$4d_2$		−0.55	1.09	2.83	

* While it might be possible to determine the sign of γ by assuming that the radial functions of the configurations are nearly hydrogenic, and that the angular functions can be determined by assuming that the configurations are separate, we are still faced with the problem of determining the sign of K. The nondiagonal terms in the matrix (1) arise only because the configurations *are* mixed and this spoils our first assumption.

[3] E. U. Condon and G. H. Shortley, *Theory of Atomic Spectra* (Cambridge, 1935), 9³(11).

These values determine the following transformation matrices (the upper sign for $K>0$, the lower for $K<0$)

$M=-2$

	s_5
s_5'	1.00

$M=-1$

	s_5	d_2
s_5'	0.99	± 0.14
d_2'	0.14	∓ 0.99

$M=0$

	s_5	d_2
s_5'	0.74	± 0.67
d_2'	0.67	∓ 0.74

$M=1$

	s_5	d_2
s_5'	0.96	± 0.29
d_2'	0.29	∓ 0.96

$M=2$

	s_5
s_5'	1.00

Let us now consider the calculation of a particular pattern. The line λ7493 has been chosen, for it affords several opportunities for the determination of the sign of K. The average g value of $2p_8$ had already been fixed as 1.10, so that the pattern for $\omega=1.69$ cm^{-1} may be calculated from

	$M=-2$	-1	0	1	2
$2p_8$	-3.72	-1.86	0	1.86	3.72.

Within a given Zeeman pattern, the relative intensities depend only on J, and we find that for $J=2\rightarrow J=2$ they are

2, 3, 3, 2; (8), (2), (0), (2), (8); 2, 3, 3, 2;

while for $J=1\rightarrow J=2$ they are

1, 3, 6; (6), (8), (6); 6, 3, 1

the intensity 6 belonging to the transitions $M=\pm 1\rightarrow M=\pm 2$. Each of these groups yield a total sum of 40, so that they are already reduced to the same scale. If we now assume that

$$\frac{\text{Int. } (p_8 d_2)}{\text{Int. } (p_8 s_5)}=\gamma^2,$$

the data for the pattern of λ7493 are given in the third and sixth columns of Table I for positive γ and K.

It is to be noted that reversing the sign of K produces the same effect as reversing the sign of γ in Table I. Really, only the relative sign of γ and K is of importance.

From estimates on the field-free intensities of the lines above, we come to the conclusion that

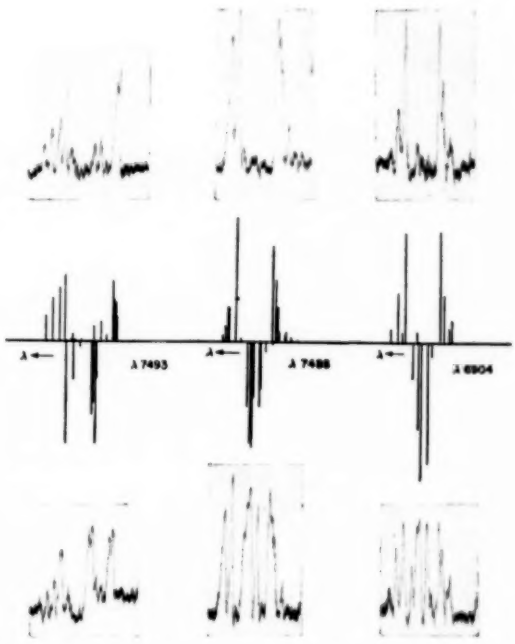

FIG. 1. Comparison of calculated and observed patterns for λ7493, λ7486, λ6904. At the top are the microphotometer traces for the perpendicular polarization. In the middle are the calculated patterns with the perpendicular polarization above and parallel polarization below. At the bottom are the microphotometer traces of the lines including both polarizations.

$\gamma \doteq 0.8$. Comparing then the intensities of components $1\rightarrow 0$ and $1\rightarrow 2$ of $2p_8-3s_5$ we find that if γ(or K) is taken with the positive sign, $1\rightarrow 0$ will be greater in intensity than $1\rightarrow 2$ whereas $1\rightarrow 0$ is missing, and $1\rightarrow 2$ is very strong. Again, comparing $1\rightarrow 0$ and $1\rightarrow 2$ of $2p_8-4d_2$ we find a similar result. We therefore use γ with the sign reversed and arrive at columns 4 and 7. The results are plotted in Fig. 1.

Proceeding in the same way with λ6904 we find that $\gamma=0.2$ fits the experimentally determined pattern quite accurately. In the case of λ7486, the procedure is much simpler, for $2p_9-4d_2$ is a "forbidden" transition. The calculated and observed patterns of these three lines are depicted in Fig. 1. The agreement is seen to be excellent.

The author wishes to express his thanks to Drs. D. W. Bowman and E. H. Hurlburt for their assistance.

The Zeeman Effect of Xenon

J. B. GREEN, E. H. HURLBURT* AND D. W. BOWMAN†
Mendenhall Laboratory of Physics, Ohio State University, Columbus, Ohio
(Received November 13, 1940)

Measurements of the Zeeman effects of about 125 lines in the spectrum of XeI have been made. The g sum rule is violated by both of the completely known configurations, and in some cases may be accounted for by configuration interaction. For other configurations, where only the lower levels are known, the J of the core is shown to be a "good" quantum number.

PRELIMINARY classifications in the spectrum of xenon were first given by Meggers *et al.*[1] and were later extended by Gremmer[2] and Rasmussen.[3] The subsequent improvement in photographic techniques enabled Humphreys and Meggers[4] to list further lines and classifications.

Measurements of the Zeeman effect of a few lines of XeI were first carried out by Pogány,[5] and were later supplemented by the addition of fifteen more lines by Lörinczi.[6] The present investigation covers the measurements on about 125 lines, of which those associated with transitions involving the $5p^5mf$ configurations will be discussed at a later date, because of their bearing on a problem of some theoretical importance. Our experimental results are in many cases at considerable variance with Lörinczi's, more so than in the case of krypton[7] and we are unable to account for these discrepancies. Only one error in Humphreys and Meggers'[4] classification has been found, an inversion of the classification of $8d_5$ and $8d_6$. Zeeman effect data clearly show that the H-M $8d_6$ has $J=1$. This modification inverts the usual order of the d_5 and d_6 levels, which also occurs in the case of $5d_5$ and $5d_6$.

The apparatus was the same as that used in our previous work.[7] A mixture of 5 percent Xe and 95 percent He was employed in the discharge tube. Eastman Special Spectroscopic plates were used for wave-lengths greater than 6800A. Eastman 40's were used from λ3200–λ4800; Eastman IG from λ4800–λ5800 and Eastman Superpanchromatic Press were found especially suitable in the region λ5800–λ6800. All plates except the 40's were presensitized by bathing for one minute in a cold 4-percent aqueous ammonia solution.

Exposures varied from 48 hours to 100 hours and in all cases one discharge tube served for a complete exposure.

Table I is a summary of the measurements with the exception of those involving the $5p^5mf$ levels which are indicated by the notation PB (beginning Paschen-Back effect). Parallel polarizations are enclosed in parentheses, mixed polarizations in square brackets; in the fourth column, bold face indicates strongest components, in the last two columns, italics indicate assumed values obtained from other lines.

Table II is a summary of the averages of the g values taken from the last two columns of Table I. Whenever possible, these averages represent only resolved patterns.

Only two configurations of XeI are completely known, $5p^56s$ and $5p^56p$. The comparisons between experiment and theory are given in Tables III and IV. An inspection of these tables shows that XeI is the bad boy of the rare gas spectra. Even the lowest configurations are perturbed enough so that the g sum rule is violated. In all of the other rare gas spectra the g sum rule is accurately verified for all of the low configurations for all values of J. In the XeI spectrum, only $J=2$ of $5p^56p$ satisfies this rule.

The discrepancy in the $5p^56s$ configuration is real and is probably caused by the near presence of the upper levels of $5p^55d$. Pogány's[5] results are based on an assumed value of 1.50 for $1s_5$, and while this appears to be correct, no independent

* Now at Fenn College, Cleveland, Ohio.
† Now at Hendrix College, Conway, Arkansas.
[1] Meggers, de Bruin and Humphreys, Bur. Stand. J. Research **3**, 731 (1929).
[2] W. Gremmer, Zeits. f. Physik **59**, 154 (1930).
[3] E. Rasmussen, Zeits. f. Physik **73**, 779 (1932).
[4] C. J. Humphreys and W. F. Meggers, Bur. Stand. J. Research **10**, 139 (1933).
[5] B. Pogány, Zeits. f. Physik **93**, 364 (1934).
[6] K. Lörinczi, Dissertation, Budapest (1937).
[7] Green, Bowman and Hurlburt, Phys. Rev. **58**, 1094 (1940).

TABLE I. *Observed Zeeman patterns in xenon.*

WAVE-LENGTH	COMBINATION	J VALUES	OBSERVED ZEEMAN PATTERN	g_a	g_b
*3685.90	$1s_5 - 5p_6$	2, 2	(0.225), 1.448	1.510	1.386
*3693.49	$1s_5 - 5p_8$	2, 3	(0.000), 1.113	*1.500*	1.307
3809.84	$1s_4 - 5p_5$	1, 0	(0.000), 1.200	1.200	0/0
*3950.925	$1s_5 - 4p_6$	2, 2	(0.210), 1.451	1.509	1.392
*3967.541	$1s_5 - 4p_8$	2, 3	(0.000), 1.044	*1.500*	1.272
3974.417	$1s_5 - 4p_9$	2, 2	(—), [0.767], **1.103**, **1.490**, 1.876	1.490	1.103
3985.202	$1s_5 - 4p_{10}$	2, 1	(**0.000**), (0.301), **1.193**, 1.493, —	1.493	1.794
4078.821	$1s_4 - 4p_5$	1, 0	(0.000), 1.205	1.205	0/0
*4109.709	$1s_4 - 4p_6$	1, 2	(0.000), 1.495	*1.204*	1.398
*4116.115	$1s_4 - 4p_7$	1, 1	(0.166), 1.120	1.203	1.036
*4135.134	$1s_4 - 4p_9$	1, 2	(0.000), 0.992	*1.204*	1.062
4193.01	$1s_5 - 4V$	2, 2	(PB)**	*1.502*	0.86
4193.530	$1s_5 - 4U$	2, 3		*1.502*	1.18
*4500.977	$1s_5 - 2p_2$	2, 1	(0.000), 1.481	*1.500*	1.537
4524.681	$1s_5 - 2p_3$	2, 2	(—), (**0.601**), 0.878, **1.195**, **1.501**, 1.823	1.502	1.195
4582.747	$1s_4 - 2p_1$	1, 0	(0.000), 1.206	1.206	0/0
4611.890	$1s_5 - 3p_7$	2, 1	(**0.000**), (0.601), —, 1.502, **2.098**	1.501	0.902
4624.276	$1s_5 - 3p_6$	2, 2	(0.122), (**0.302**), 1.186, **1.341**, **1.512**, 1.664	1.509	1.345
4671.226	$1s_5 - 3p_8$	2, 3	(**0.000**), (0.177), (0.437), **0.976**, 1.170, 1.348, 1.516, —	1.516	1.348
4690.971	$1s_5 - 2p_4$	2, 1	(**0.000**), (0.719), —, 1.498, **2.202**	1.494	0.786
4697.020	$1s_5 - 3p_9$	2, 2	(0.378), (**0.750**), —, **1.123**, **1.497**, 1.866	1.498	1.124
*4734.152	$1s_4 - 2p_2$	1, 2	(0.000), 1.183	*1.205*	1.190
4792.619	$1s_5 - 3p_{10}$	2, 1	(**0.000**), (0.215), **1.268**, 1.517, —	1.500	1.732
4807.019	$1s_4 - 3p_5$	1, 0	(0.000), 1.207	1.207	0/0
4829.709	$1s_4 - 3p_7$	1, 1	(0.300), 0.903, 1.198	1.202	0.900
‡4843.294	$1s_4 - 3p_6$	1, 2	(**0.000**), (0.152), —, 1.344, **1.508**	1.192	1.350
4916.508	$1s_4 - 2p_4$	1, 1	(0.417), 0.797, 1.204	1.206	0.794
*4923.152	$1s_4 - 3p_9$	1, 2	(0.000), 1.078	*1.204*	1.120
5028.280	$1s_4 - 3p_{10}$	1, 1	(0.522), 1.203, 1.722	1.203	1.723
[a]5392.795	$1s_3 - 6X$	0, 1	PB	0/0	0.50
5394.738	$2p_{10} - 8d_5$	1, 1	(0.550), 1.311, 1.851	1.853	1.308
*5488.555	$2p_9 - 9d_4$	2, 3	(0.000), 1.059	*1.106*	1.082
5552.385	$2p_{10} - 7d_3$	1, 2	(**0.000**), [0.607], **1.302**, 1.847	1.847	1.302
5566.615	$2p_{10} - 7d_5$	1, 1	(0.629), 1.217, 1.845	1.845	1.217
5581.781	$2p_{10} - 7d_6$	1, 0	(0.000), 1.859	1.859	0/0
*5618.878	$2p_9 - 8d_4$	2, 3	(**0.000**), 1.056	1.106	1.081
5688.373	$1s_2 - 6V$	1, 2	PB	*1.321*	0.87
*5722.14	$2p_9 - 6s_4$	2, 1	(0.000), **1.065**	*1.106*	1.188
[b]5823.89	$1s_3 - 5X$	0, 1	PB	0/0	0.50
*5824.80	$2p_9 - 7d_4$	2, 3	(0.000), 1.050	*1.106*	1.078
5894.988	$2p_{10} - 6d_5$	1, 1	(0.181), 1.185, 1.835	1.855	1.185
5931.241	$2p_{10} - 6d_6$	1, 0	(0.000), 1.852	1.852	0/0
*5934.172	$2p_8 - 7d_4'$	3, 4	(0.000), 1.088	*1.336*	1.237
*5998.115	$2p_9 - 5s_4$	2, 1	(0.000), 1.081	1.109	1.164
*6111.759	$2p_7 - 7d_1''$	1, 2	(0.000), 0.959	*1.022*	0.980
*6152.069	$2p_9 - 6d_1'$	2, 3	(0.000), 1.424	*1.106*	1.265
6163.935	$1s_2 - 5V$	1, 2	PB	*1.32*	0.87
6178.302	$1s_2 - 5Y$	1, 2	PB	1.326	1.10
6179.665	$1s_2 - 5X$	1, 1			0.50
*6182.420	$2p_9 - 6d_4$	2, 3	(0.000), 1.041	1.110	1.076
6189.10	$2p_{10} - 4s_4$	1, 1	(0.712), 1.154, 1.839	1.845	1.148
6198.260	$2p_{10} - 4s_5$	1, 2	(**0.000**), (0.360), **1.140**, 1.499, 1.852	1.854	1.497
6200.890	$2p_6 - 7d_1'$	2, 3	(**0.000**), (—), (—), **0.916**, —, —, —, —	*1.379*	1.225
*6206.297	$2p_9 - 6d_5$	2, 1	(0.000), 1.071	*1.106*	1.176
*6224.169	$2p_8 - 7d_3$	2, 2	(0.153), 1.333	1.376	1.290
*6261.212	$2p_8 - 6d_1'$	3, 3	(0.283), 1.283	1.338	1.228
6265.301	$1s_3 - 4p_{10}$	0, 1	(0.000), 1.808	0/0	1.808
6292.649	$2p_8 - 6d_4$	3, 3	(—), [0.528], [**0.790**], **1.077**, **1.339**, 1.596, 1.856	1.337	1.076
*6294.45	$2p_8 - 6d_3$	3, 2	(0.000), 1.357	*1.336*	1.316
*6314.97	$2p_7 - 5s_4$	1, 1	(0.144), 1.092	1.020	1.164
*6318.062	$2p_8 - 6d_4'$	3, 4	(0.000), 1.085	*1.336*	1.236
*6430.155	$2p_8 - 5s_5$	2, 2	(0.220), 1.450	1.389	1.512
†6469.705	$2p_{10} - 5d_3$	1, 2	(**0.000**), **0.459**, (0.703), 1.192, 1.849	1.849	1.192
6472.841	$2p_{10} - 5d_2$	1, 1	0.812, (1.040), 1.852	1.852	0.812
6487.765	$2p_{10} - 5d_1''$	1, 2	(**0.000**), **0.300**, (0.780), 1.080, 1.863	1.860	1.080
*6498.718	$2p_7 - 6d_1''$	1, 2	(0.000), 0.969	*1.022*	0.987
6500.37	$2p_8 - 7d_2$	0, 1	(0.000), 0.899	0/0	0.899
6521.508	$2p_7 - 6d_3$	1, 2	(**0.000**), (0.269), —, 1.290, **1.573**	1.020	1.296
*6533.159	$2p_9 - 4s_4$	2, 1	(0.000), 1.080	*1.106*	1.158
6543.360	$2p_9 - 4s_5$	2, 2	(0.401), (**0.767**), **1.098**, **1.495**, 1.887	1.098	1.495
6668.920	$2p_{10} - 5d_5$	1, 0	(0.000), 1.862	1.862	0/0
6728.008	$2p_{10} - 5d_6$	1, 1	(0.581), 1.273, 1.853	1.854	1.273
6827.315	$1s_3 - 4X$	0, 1	(0.000), 0.505	0/0	0.505
‡*6846.613	$2p_9 - 5d_3$	2, 2	(0.167), 1.211	*1.106*	1.199
‡6850.13	$2p_9 - 5d_2$	2, 1	(**0.000**), (0.280), —, —, **1.383**	1.103	0.823
6863.20	$2p_8 - 6d_2$	0, 1	(0.000), 0.914	0/0	0.914
*6866.838	$2p_9 - 5d_1''$	2, 2	(0.066), 1.089	1.107	1.071
*6882.155	$2p_9 - 5d_4$	2, 3	(0.000), 0.947	*1.106*	1.026
*6910.82	$2p_7 - 4s_4$	1, 1	(0.142), 1.111	*1.022*	1.164
6925.53	$3d_3 - 6U$	2, 3	PB	*1.376*	1.17
6935.62	$3d_3 - 6Y$	2, 2	PB	*1.376*	1.09
*6976.182	$2p_9 - 5d_1'$	3, 3	(0.198), 1.301	1.339	1.263
*6982.05	$2p_9 - 5d_3$	3, 2	(0.000), 1.596	*1.336*	1.076
7019.02	$2p_9 - 5d_4$	3, 3	(0.290), (0.566), (0.860)	*1.336*	1.026
*7047.37	$2p_8 - 4s_5$	2, 2	(0.217), 1.426	1.365	1.486
*7119.598	$2p_8 - 5d_4'$	3, 4	(0.000), 1.039	*1.336*	1.217
*7257.94	$3d_4 - 6Z$	3, 4	PB	(1.01)	(*1.02*)
‡7262.54	$2p_7 - 5d_3$	1, 2	(**0.000**), (0.178), —, —, **1.379**	1.023	1.201
7266.49	$2p_7 - 5d_2$	1, 1	(0.198), 0.822, 1.029	1.026	0.824
*7285.301	$2p_7 - 5d_1''$	1, 2	(0.000), 1.092	*1.022*	1.069
††7316.272	$1s_2 - 4Y$	1, 2	(**0.000**), (0.232), **0.885**, 1.115, 1.35	1.342	1.110
7321.452	$1s_2 - 4X$	1, 1	0.506, (0.814), 1.316	1.318	0.504
*7336.480	$2p_9 - 3s_1'''$	2, 3	(0.000), 1.151	*1.106*	1.128
[c]7355.58	$3d_6 - 5X$	0, 1	PB		0.50
7386.002	$2p_{10} - 3s_5$	1, 2	(**0.000**), (0.383), **1.084**, 1.464, 1.851	1.848	1.465
7400.41	$2p_6 - 5d_3$	2, 2	(0.181), (**0.379**), 1.002, **1.189**, **1.388**, 1.579	1.384	1.194
7424.05	$2p_8 - 5d_1''$	2, 2	(0.320), (**0.629**), (—), **1.068**, **1.376**, 1.673	1.376	1.068
7451.00	$3d_5 - 5V$	1, 2	PB	1.40	0.85
7472.01	$3d_5 - 5Y$	1, 2	PB	1.395	1.10
7474.01	$3d_5 - 5X$	1, 1	PB		0.50
7492.23	$2p_8 - 3s_1'''$	3, 3	(0.176), (0.413), (**0.636**), 0.910, **1.125**, **1.339**, 1.549, 1.754	1.338	1.125
7501.13	$2p_8 - 3s_1''''$	2, 2	(—), (**0.338**), 0.934, **1.101**, **1.278**, 1.442	1.105	1.274
7514.54	$2p_7 - 5d_6$	1, 0	(0.000), 1.022	1.022	0/0
7642.025	$1s_3 - 2p_2$	0, 1	(0.000), 1.553	0/0	1.553
7643.91	$3d_3 - 5U$	2, 3	PB	*1.376*	1.17
7664.56	$3d_3 - 5Y$	2, 2	PB	1.376	1.10
*7802.651	$2p_9 - 3s_4$	2, 1	(0.000), 1.068	*1.106*	1.182
‡7887.395	$1s_2 - 2p_1$	1, 0	(0.000), 1.313	1.313	0/0
7967.314	$1s_3 - 3p_7$	0, 1	(0.000), 0.906	0/0	0.906
8206.341	$1s_2 - 2p_4$	0, 1	(0.000), 0.790	0/0	0.790
8266.519	$1s_2 - 2p_2$	1, 1	(0.232), 1.324, 1.549	1.321	1.551
8280.116	$1s_4 - 2p_5$	1, 0	(0.000), 1.206	1.206	0/0
8346.823	$1s_2 - 2p_3$	1, 2	(**0.000**), (0.146), **1.060**, 1.201, —	1.345	1.201
‡8409.190	$1s_5 - 2p_7$	2, 1	(**0.000**), (0.474), 1.043, 1.493, **1.961**	1.497	1.034
8819.412	$1s_5 - 2p_8$	2, 3	(**0.000**), (0.171), (0.347), **1.014**, 1.164, 1.332, 1.493, 1.657	1.499	1.330
9045.446	$1s_5 - 2p_9$	2, 2	(0.394), (**0.776**), —, —, —, —	*1.500*	1.109

* Pattern was not resolved.
** PB Pattern unsymmetrical due to Paschen-Back effect.
† Almost symmetrical patterns whose separations were badly disturbed by beginning PB effect.
‡ Pattern was partly obscured by other lines (i.e., Xe spark line or He line or ghost of He line).
[a] Forbidden line $1s_3 - 6Y$ also appeared.
[b] Forbidden line $1s_3 - 5Y$ also appeared.
[c] Forbidden line $3d_4 - 5Y$ also appeared.

TABLE II. *Average g values of* XeI.

j	TERM	1	2	3	4	5	6	7	8	9
2	s_5	1.500		1.465	1.496	1.512*				
1	s_4	1.204		1.182*	1.154	1.164	1.188			
1	s_2	1.321								
0	s_3	0/0								
3	p_8		1.336	1.348	1.272*	1.307*				
2	p_9		1.106	1.123	1.103					
2	p_6		1.379	1.347	1.395*	1.386*				
2	p_3		1.195							
1	p_{10}		1.852	1.728	1.801					
1	p_7		1.022	0.903	1.036*					
1	p_4		0.790							
1	p_2		1.552							
0	p_5		0/0	0/0	0/0	0/0				
0	p_1		0/0							
4	d_4'					1.217	1.236	1.237*		
3	d_4			0.01		1.026	1.076	1.078*	1.081*	1.082*
3	d_1'					1.263*	1.246*	1.225*		
3	s_1'''			1.126						
2	d_3			1.376†		1.196	1.303	1.298		
2	d_1''					1.073	0.987*	0.980*		
2	s_1''									
2	s_1''''			1.274						
1	d_5			1.395†		1.273	1.180*	1.217	1.308	
1	d_2					0.819	0.914	0.899		
1	s_1'									
0	d_6			0/0		0/0	0/0	0/0		
3	U				1.18†	1.17†				
2	Y				1.11†	1.10†	1.09†			
2	V				0.86†	0.87†	0.87†			
1	X				0.504†	0.50†	0.50†			

* Obtained only from unresolved patterns.
† Obtained only from perturbed patterns.

TABLE III. *g values for* Xe $5p^5 6s$.

J	LEVEL	OBSERVED (POGÁNY)	OBSERVED (AUTHORS)	CALCULATED (HOUSTON)[8]
1	$1s_4$	1.20	1.204	1.221
	$1s_2$	1.30	1.321	1.279
Σg		2.50	2.525	2.500
2	$1s_5$		1.500	1.500

measures of $1s_2$ and $1s_4$ are indicated. Lörinczi's[6] results also appear to be unreliable as indicated by the large error in $2p_{10}$.

Partial g sums based on jj-coupling may be obtained for several configurations, and these are listed in Table V.

Inspection shows that except for the case of $5p^5 7p$ $(J=1)$, the spectrum of XeI is remarkably close to jj-coupling, at least insofar as we may

[8] W. V. Houston, Phys. Rev. **33**, 297 (1929).

TABLE IV. *g values for* Xe $5p^5 6p$.

J	LEVEL	OBSERVED (POGÁNY)[5]	OBSERVED (LÖRINCZI)[6]	CALCULATED (LÖRINCZI)[6]	CALCULATED (GREEN)[9]	OBSERVED (AUTHORS)
1	$2p_2$			1.424	1.494	1.552
	$2p_4$		0.781	0.733	0.639	0.790
	$2p_7$	1.02	1.009	1.099	1.029	1.022
	$2p_{10}$		1.75	1.689	1.838	1.852
	Σg			4.945	5.000	5.216
2	$2p_3$	1.183	1.178	1.169	1.178	1.195
	$2p_6$	1.402	1.381	1.407	1.391	1.379
	$2p_9$	1.113	1.113	1.096	1.098	1.106
	Σg	3.698	3.672	3.672	3.667	3.680
3	$2p_8$				1.333	1.336

TABLE V. *Partial g sums in* XeI.

CONFIGURATION	J	jj COUPLING	OBSERVED
$5p^5 7p$	1	2.833	2.631
$5p^5 8p$	1	2.833	2.837
$5p^5 7p$	2	2.500	2.470
$5p^5 8p$	2	2.500	2.498
$5p^5 5d(s_1''')$	3	1.111	1.126
$5p^5 5d(s_1'''')$	2	1.289	1.274
$5p^5 7d$	1	2.167	2.092
$5p^5 8d$	1	2.167	2.094
$5p^5 9d$	1	2.167	2.116
$5p^5 7d$	2	2.277	2.269
$5p^5 8d$	2	2.277	2.290
$5p^5 9d$	2	2.277	2.278
$5p^5 7d$	3	2.306	2.289
$5p^5 8d$	3	2.306	2.322
$5p^5 9d$	3	2.306	2.303

say that the J of the core is a "good" quantum number. In the particular case of $5p^5 7p$ $(J=1)$ both of the levels $3p_{10}$ and $3p_7$ have g values smaller than the neighboring $5p^5 6p$ and $5p^5 8p$ levels, their sum being 0.202 less than for jj-coupling, while $5p^5 6p$ $(J=1)$ has a g sum 0.217 in excess of the theoretical g sum. The energy levels concerned are:

$2p_2$ 8555	$3p_{10}$ 9907
$2p_4$ 9455	$3p_7$ 9089

so that both configuration interaction and the sharing of g values by the two configurations are extremely probable.

[9] J. B. Green, Phys. Rev. **52**, 736 (1937).

Work Function and Temperature*

SAMUEL SEELY†
Pupin Physics Laboratories, Columbia University, New York, New York
(Received November 2, 1940)

The change in height of the potential energy barrier at the surface of a metal with the expansion of the metal due to heating is investigated. Also, the change of the normal maximum energy of an electron in a metal is calculated as a function of the temperature of the metal. These calculations show that the work function of a metal is a linear function of its temperature. These results, when combined with the thermionic emission equation, show that the thermionic emission constant is a characteristic of the metal, and is no longer the same for all pure metals. The calculated results for the thermionic emission constants for several metals show fair agreement with the experimentally determined values.

SEVERAL suggestions have been offered in an attempt to resolve the difference that is found to exist between the thermionic emission constant, A_0, predicted by theory and the value which is obtained by experiment. According to modern statistical theory, this constant, which appears in the Dushman equation relating the thermionic emission current density, J_{Th}, with the temperature

$$J_{Th}=A_0T^2\epsilon^{-(E_B-E_M)/E_T}=A_0T^2\epsilon^{-E_w/E_T} \quad (1)$$

has a value of 120 amperes·cm^{-2}·degrees^{-2} for all pure metals. Actually, however, a value approximately one-half of this theoretical value has been found to apply for many pure metals, although values which are widely different from 60 amperes·cm^{-2}·degree^{-2} have been reported for several metals. In this expression E_B denotes the height of the potential barrier at the surface of the metal, E_M is a quantity which is characteristic of the metal (and will be considered in some detail below), E_w (defined as the difference between E_B and E_M) is the work function of the metal, all in electron volts, E_T is the electron volt equivalent of temperature ($=kT/e\cdot 10^7=T/11{,}600$; with k=Boltzmann's constant, e=charge of the electron in coulombs), and where T is the temperature in degrees Kelvin.

In order to verify this equation experimentally, a graph based on the logarithm of this equation is plotted. That is, since

$$\log_{10}(J_{Th}/T^2)=\log_{10}A_0-0.434(11{,}600E_w)/T, \quad (2)$$

then a plot of $\log_{10}J_{Th}/T^2$ *versus* $1/T$ should be a straight line having a slope equal to $-0.434(11{,}600E_w)$ and an intercept equal to $\log_{10}A_0$. Logarithmic plots of this type yield the low values mentioned.

A careful analysis by Nordheim[1] showed that Eq. (1) should actually have the form

$$J_{Th}=A_0(1-r)\epsilon^{-E_w/E_T}, \quad (3)$$

where r is a reflection coefficient. This factor expresses the ratio of the number of electrons reflected back into the body of the metal at the surface to the total number of electrons which are moving in the escape direction. However, calculations show that the reflection factor is less than 0.07 for the type of potential variations which exist at the surface of the metal. A physical argument by Becker and Brattain[2] likewise leads to the conclusion that r must be very small. The presence of the reflection coefficient in Eq. (3) does not, therefore, resolve the difference.

More recently Herzfeld[3] and Becker and Brattain[2] concluded from thermodynamic considerations that the work function, E_w, appearing in Eq. (1) is not a constant, but is a quantity that varies with the temperature. This conclusion has received experimental confirmation.[4] The magnitude of the variation observed for tungsten is just of the right order to resolve completely the difference between the theoretical value and the

* Publication assisted by the Ernest Kempton Adams Fund for Physical Research of Columbia University.
† Now at the College of the City of New York, New York.

[1] L. Nordheim, Proc. Roy. Soc. **121**, 626 (1928).
[2] J. A. Becker and W. H. Brattain, Phys. Rev. **45**, 694 (1934).
[3] K. F. Herzfeld, Phys. Rev. **35**, 248 (1930).
[4] A. L. Reimann, Proc. Roy. Soc. **163**, 499 (1937); J. G. Potter, Phys. Rev. **58**, 622 (1940); F. Krüger and G. Stabenow, Ann. d. Physik **22**, 713 (1935).

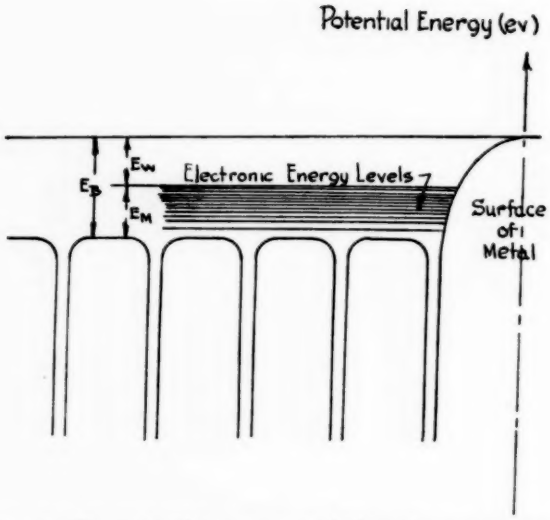

FIG. 1. The potential energy variation along a row of atoms in a metal.

experimental value of the thermionic emission constant.

THE VARIATION OF E_M WITH TEMPERATURE

That E_w cannot be a constant, independent of the temperature, follows from the definition of E_w in terms of E_B and E_M, and the fact that both E_M and E_B can be shown to be temperature dependent functions. According to the electron theory of metals,

$$E_M = E_0\left[1-\frac{\pi^2}{12}\frac{E_T^2}{E_0^2}\right] \text{(electron volts)}, \quad (4)$$

where E_0 may be shown to have the form

$$E_0 = \frac{h^2}{8em10^7}\left(\frac{3N}{\pi}\right)^{\frac{2}{3}} \text{(electron volts)}. \quad (5)$$

The symbols have the following meanings: h is Planck's constant, e is the electronic charge in coulombs, m is the mass of the electron in grams, and N denotes the concentration of free electrons per cc of the metal. By inserting the known values of the constants in this expression, E_0 may be written in the form

$$E_0 = 3.62\times10^{-15}N^{\frac{2}{3}} \text{(electron volts)}. \quad (6)$$

As pointed out both by Herzfeld and by Becker and Brattain, the quantity N depends upon the temperature because the density of the material is temperature dependent. By making use of the fact that the linear expansion of most metals can be written with good approximation by an expression of the form

$$l = l_0(1+\alpha T), \quad (7)$$

where α is the coefficient of linear expansion, it follows that $N = N_0/(1+\alpha T)^3$. By combining this expression with (6)

$$E_0 = 3.62\times10^{-15}[N_0/(1+\alpha T)^3]^{\frac{2}{3}}$$

which may be written in the form

$$E_0 = E_{00}/(1+\alpha T)^2, \quad (8)$$

where the quantity

$$E_{00} = 3.62\times10^{-15}N_0^{\frac{2}{3}} \quad (9)$$

is a constant, independent of the temperature.

Equation (4) may then be written in the form

$$E_M = \frac{E_{00}}{(1+\alpha T)^2}\left[1-\frac{\pi^2}{12}\frac{E_T^2}{E_{00}^2}(1+\alpha T)^4\right],$$

which reduces to the approximate form

$$E_M = E_{00}\left\{1-2\alpha T+\left[3\alpha^2T^2-\frac{\pi^2}{12}\frac{E_T^2}{E_{00}^2}\right]\right\}.$$

The third term in this expression is very small compared with the second term over the normal range of temperatures, and so may be neglected. Thus to a good approximation

$$E_M = E_{00}(1-2\alpha T). \quad (10)$$

THE VARIATION OF E_B WITH TEMPERATURE

Herzfeld first pointed out that E_B should be temperature dependent. However, his calculations of E_B and dE_B/dT, based upon an approximate method due to Bethe[5] leads to incorrect results. This calculation predicts a greater variation in the term dE_B/dT than in the term dE_M/dT. The net result is a greater value for the thermionic emission constant than 120 amperes·cm^{-2}·degree^{-2}. This contradicts the facts for all metals.

The explicit dependence of E_B on the temperature may be investigated in two ways. One way makes use of considerations dictated by the modern theory of solids. The other is based on the image law for the force on an electron near the surface of a metal. The results are the same, to the approximation in which we are interested.

[5] H. Bethe, Ann. d. Physik **87**, 55 (1928).

According to considerations of the theory of solids, the potential energy distribution in a metal has the general form illustrated in Fig. 1. The presence of the potential energy barrier at the surface of the metal results from the lowering of the potential energy in the region within the metal by the contributions of the ions which are tightly bound to fixed points of the crystal lattice, and by the lack of such lowering at the surface of the metal because of the lack of ions in the region outside of the metal. The effective potential energy at any point in the metal will consist of the sum of the contributions to the potential energy of all of the ions in the immediate neighborhood of the point in question. This is so because the potential at any point due to any ion decreases rapidly with the distance from the position of the ion.

In any event, the potential energy at any point in the body of the metal with respect to the exterior will be, if we consider the contributions of all of the ions to this potential energy, of the form

$$U_0 = -e \sum \frac{(Z-S)e}{r},$$

where Z is the atomic number of the atom, S is the atomic screening factor, and r is the distance from the position of each ion to the reference point. The screening factor gives a measure of the effectiveness of the orbital electrons surrounding the nucleus in reducing the nuclear charge. It is, therefore, a function of the distance from the nucleus of the atom. However, as indicated in Fig. 1, the potential energy in the metal is substantially constant throughout the major portion of its volume, except for the rather intense local variations which exist in the immediate neighborhood of the nuclei.

If it is assumed that $(Z-S)$ does not change appreciably when the interionic distances are slightly altered because of the expansion of the metal when its temperature is raised, then

$$U = -e \sum \frac{(Z-S)e}{r(1+\alpha T)}.$$

By expanding the term in the denominator and retaining only the first-order term in the temperature, the result may be written in the form

$$E_B = E_{B_0}(1-\alpha T), \tag{11}$$

where the term E_B gives the height of the potential energy barrier in electron volts. This expression shows that the height of the potential barrier at the surface of the metal is decreased slightly as a result of the expansion of the metal caused by heating.

According to considerations of the image law of force on an electron at the surface of the metal, the height of the potential barrier is related to the force function by the expression

$$eE_{B_0} \cdot 10^7 = -\int_0^\infty f(x)dx, \tag{12}$$

where $f(x)$ is the functional form of the force function, which has the general shape illustrated in Fig. 2. That the image law for the force on the electron is essentially the correct one for thermionic phenomena is shown by the calculations of Schottky[6] in which the effect of an accelerating field at the surface of a thermionic cathode is successfully explained in terms of this law of force.

Because of the expansion resulting from the heating, it is necessary to calculate the value of

$$eE_B \cdot 10^7 = -\int_0^\infty f(x+\Delta)dx, \tag{13}$$

where, from Eq. (7)

$$\Delta = \alpha T x. \tag{14}$$

By expanding the integrand in a Taylor's series, and integrating the series term by term, the result is that given by (11) if we retain only the first-order term in αT.

General Results

By combining Eqs. (11) and (10) with the definition of E_w,

$$E_w = E_B - E_M = E_{B_0}(1-\alpha T) - E_{00}(1-2\alpha T)$$
$$= (E_{B_0} - E_{00}) - \alpha T(E_{B_0} - 2E_{00}).$$

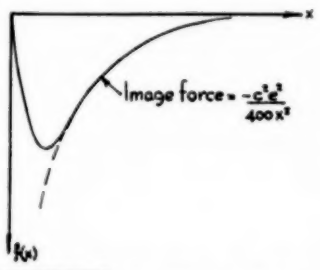

FIG. 2. The image force function at the surface of a metal.

[6] W. Schottky, Physik. Zeits. **15**, 872 (1914).

TABLE I. *Comparison of experimental and calculated values of thermionic emission constants.*

MATERIAL	MEASURED A	E_{w0}	$\alpha\times10^{6}$*	CALCULATED E_{00}	C	CA_0
C [7]	30	4.3	7.9	13.5	0.432	52
Ca [8]	60	2.2	25	4.7	0.485	58
Mo [8]	55	4.1	5.5	9.4	0.715	86
Ni [8]	27	2.8	18.2	11.7	0.153	18
Pt [9]	32	5.3	11	9.5	0.585	70
W [8]	60	4.5	7.3	9.1	0.671	80

* From *International Critical Tables.*

It follows from this that

$$E_w = E_{w0} + \alpha(E_{00} - E_{w0})T \text{ (electron volts)} \quad (15)$$

where, by definition $E_{w0} = E_{B0} - E_{00}$. It is observed that this expression predicts a linear dependence of the work function on the temperature. The quantity E_{w0} is independent of the temperature, and may be called the "work function at absolute zero" or the "true work function" of the metal.

For the case of tungsten (based upon the assumption that each tungsten atom supplies 2 free electrons) $E_{00} = 9.1$ ev, and, from experimental measurements, $E_{w0} = 4.5$ ev. These quantities, together with the experimental value of $\alpha = 7.3\times10^{-6}$ per degree in Eq. (15) yield

$$E_w = E_{w0} + 3.4\times10^{-5}T \text{ (electron volts)}. \quad (16)$$

This result is in fair agreement with the results of Potter,[4] Reimann[4] and Krüger and Stabenow who found the values 6.3×10^{-5}, 7.1×10^{-5} and 6×10^{-5} ev/degree, respectively, for the coefficient of T.

By combining Eq. (15) with Eq. (1), the thermionic emission equation may be written in the form

$$J_{Th} = CA_0T^2\epsilon^{-E_{w0}/ET}, \quad (17)$$

where the term

$$C = \exp\left[-\frac{\alpha(E_{00}-E_{w0})T}{E_T}\right]$$

$$= \exp\left[-\alpha(E_{00}-E_{w0})\times11{,}600\right] \quad (18)$$

is independent of the temperature, and depends only on the value of E_{00}, E_{w0}, and the coefficient of linear expansion of the metal. Because of this correction coefficient, one no longer expects the thermionic emission constant in Eq. (17) to be the same for all metals.

The values predicted by this expression for CA_0, and the values obtained experimentally for the thermionic emission constants of several metals are contained in Table I. In columns two, three and four are contained the experimentally determined values of the thermionic emission constants A, the work function, and the coefficient of linear expansion of the material. In columns five, six and seven are contained the calculated values of E_{00} (based on the assumption of 2 electrons/atom), the correction factor C, and the thermionic emission constant CA_0.

CONCLUSIONS

Based on the foregoing considerations, it appears that the slope of the thermionic emission logarithmic plot should be associated with the true work function of the metal, E_{w0}. This is a quantity which is constant and independent of the temperature. The effect of the temperature on the values of E_M and E_B results in the appearance of a correction term in the thermionic emission equation which lowers the thermionic emission constant below 120 amperes/cm^2/degree^2. Furthermore, the value of the thermionic emission constant will depend upon the metal considered, and will vary from metal to metal. This yields values which are more nearly in agreement with the values determined experimentally.

It must be kept in mind that E_{00} appears in the correction term expressed by Eq. (18). Since the calculation of this quantity requires a knowledge of the number of free electrons per atom of the metal, an unknown error may result from the assumption of two electrons per atom. However, the experiments of Rupp[10] on the diffraction of electrons in passing through matter furnish evidence which, for Mo, Ni and W, removes the uncertainty in this number.

The author wishes to express his thanks to his colleague at the City College, Dr. Jacob Millman, for interesting and helpful discussions of this problem.

[7] A. L. Reimann, Proc. Phys. Soc. London **50**, 496 (1938).
[8] S. Dushmann, Rev. Mod. Phys. **2**, 381 (1930).
[9] L. V. Whitney, Phys. Rev. **50**, 1154 (1936).
[10] H. Rupp (see R. H. Fowler, *Statistical Mechanics*, (Macmillan, 1936), second edition, p. 355.

Photoconductivity of a Natural Willemite Crystal*†

ROBERT C. HERMAN,** *Palmer Physical Laboratory, Princeton University, Princeton, New Jersey*

AND

ROBERT HOFSTADTER, *Randal Morgan Laboratory of Physics, University of Pennsylvania, Philadelphia, Pennsylvania*

(Received November 13, 1940)

This paper deals with the dependence of the photoconductivity of a natural single crystal of willemite on the wave-length of exciting light, temperature and time. The ultraviolet absorption spectrum of this crystal has been obtained.

INTRODUCTION

THE mineral willemite (zinc orthosilicate—Zn_2SiO_4) has played an important role in the development of luminescent materials. The behavior of zinc orthosilicate phosphors under electron bombardment as well as irradiation with ultraviolet light has been the subject of many investigations.[1] Until recently, the excitation spectrum for fluorescence of willemite was said to lie in the spectral range between 2200 and 3000A,[2] although it has been reported that excitation can be caused by irradiation with the neon resonance lines[3] as well as by Hg 3650A.[4] The work of Kroger,[1b] shows that the excitation spectra of zinc orthosilicate phosphors extend from about 2100A to beyond 5000A. Recently, Beese found willemite phosphors to fluoresce when irradiated with ultraviolet light in the spectral range from 3150 to 1400A.[5]

Some time ago, one of the authors (R. H.) found that both natural polycrystalline willemite and a willemite phosphor (1 percent Mn) prepared artificially exhibited photoconductivity in the spectral range from about 2500 to 3650A.[6] Since that time, the authors have studied the photoconductivity of a natural single crystal of willemite in the hope that some correlation might be found between it and the excitation spectrum. Recently, Hill and Aronin,[7] have reported photoconductivity in the case of pure and Mn activated zinc orthosilicate phosphors.

It is the purpose of the present paper to report results obtained on the dependence of photoconductivity on the wave-length of the exciting light, temperature and time as well as on the ultraviolet absorption of a natural single crystal of willemite.

EXPERIMENTAL

Figure 1 is a schematic diagram of the apparatus employed. Both the crystal and a calibrated thin window Na photo-cell (kindly lent to us by the General Electric Company) were mounted in vacuum. Electrical connections were made through leads sealed in Pyrex glass tubes. The photo-currents from the crystal (5×10^{-14} to 5×10^{-11} amp.) and the photo-cell (10^{-12} to 2×10^{-11} amp.) were amplified by separate FP-54 electrometer tube circuits so that it was possible to make simultaneous, independent measurements of photoconductivity and incident energy.[8] In this manner any fluctuations of the ultraviolet source (Hanovia Uviarc) were eliminated. The amplified currents from photo-cell and crystal were read by a Moll microgalvanometer (0.2-sec. period) and Moll galvanometer (1.5-sec. period), respectively. When absorption measurements

* This work was done while the authors were at Princeton University.

† A preliminary account of this work was given at the Princeton Meeting of the American Physical Society, June 1939. See Phys. Rev. **56**, 212 (1939).

** Now at the Moore School of Electrical Engineering, University of Pennsylvania, Philadelphia, Pennsylvania.

[1] For example, see (a) R. P. Johnson, Am. J. Phys. **8**, 143 (1940) and (b) F. A. Kroger, Physica **6**, 764 (1939).

[2] (a) J. W. Marden, N. C. Beese, and G. Meister, Trans. I. E. S. **34**, 55 (1939); (b) C. G. Found, Trans. I. E. S. **33**, 161 (1938), see p. 187.

[3] (a) A. Ruttenauer, Physik. Zeits. **37**, 810 (1936); (b) H. G. Jenkins and J. N. Botwell, Trans. Faraday Soc. **35**, 155 (1939); (c) M. Schon, reference 3(b), p. 162.

[4] A. Ruttenauer, Zeits. f. tech. Physik **19**, 148 (1938).

[5] N. C. Beese, J. Opt. Soc. Am. **29**, 278 (1939).

[6] R. Hofstadter, Phys. Rev. **54**, 864 (1938).

[7] A. G. Hill and L. R. Aronin, Phys. Rev. **57**, 1090 (1940).

[8] No corrections have been made for the loss of energy by reflection from the crystal in measuring both photoconductivity and absorption. In all but the absorption measurements the crystal was thick enough so that all the incident light not reflected was absorbed completely.

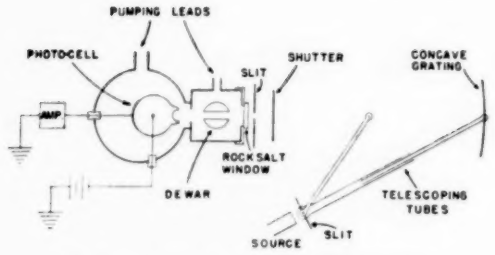

FIG. 1. Schematic diagram of apparatus.

were made a readjusted Zernicke type Ze galvanometer (1.3-sec. period) was employed. The ultraviolet source was mounted behind a slit which could be moved along the arc of a circle, in such a way that the source always pointed to the concave grating, by means of the arrangement shown in Fig. 1.[9] The optical system was such that the upper part of any mercury line fell on the crystal while the lower part fell on the photocell. Since the intensity along the height of the mercury lines varied in a different complicated manner for each line, it was necessary to make appropriate corrections. It was not realized at first that the intensity varied in this manner. This effect was probably caused by the fact that the concave grating was aluminized.[10] Related effects have been reported by Strong[11] who found that Wood anomalies[12] of spectral energy distribution were frequently developed by evaporating certain metallic films on gratings. So far as we know the particular effect we mention has not been reported in the literature. The necessary corrections mentioned above might have introduced an error of about ten percent only in the curves showing the dependence of photoconductivity on wave-length. All other curves shown in this paper do not depend upon this correction.

Figure 2 shows how the crystal was mounted in the Dewar vessel during part of these experiments. Temperature measurements were made with a calibrated copper-Eureka thermocouple mounted close to the crystal and connected to a Leeds and Northrup type K potentiometer. The voltage supplies for both the crystal and photocell were batteries contained in metal boxes, and were insulated from ground by means of Lucite supports standing on a layer of paraffin. All sensitive leads were insulated from ground by the use of Lucite plugs and were electrically shielded.

The single crystal of willemite, kindly given to us by the Geology Department of Princeton University, came from Franklin, New Jersey. It was uniformly pale green in color, transparent, uncracked and gave a green body fluorescence when irradiated with ultraviolet light or bombarded with electrons. The crystal was about 14 mm long and had four well-defined crystal faces whose dimensions were about 14×3 mm. Certain spectroscopic analyses on portions of the crystal have been made but the results are not entirely conclusive. However, it is certain that Mn, Mg and Fe are present. A microchemical analysis, kindly performed by Dr. E. H. Winslow, of the General Electric Company, gave the following data: Mn—0.70 percent, Fe—0.27 percent, Cu and Ni—less than 0.001 percent, if any.

Two parallel crystal faces, 2.0 mm apart, were polished and then sputtered with gold before mounting. The electric field was applied perpendicular to the long axis of the crystal and the direction of the light was perpendicular to both throughout these experiments. No attempt was made to study the effect of different crystal orientations. In order to make absorption measurements the crystal was ground and polished to a thickness of 0.3 mm. The absorption spectrum at room temperature was obtained in air by moving the crystal in and out of the light beam next to the exit slit of the ultraviolet monochro-

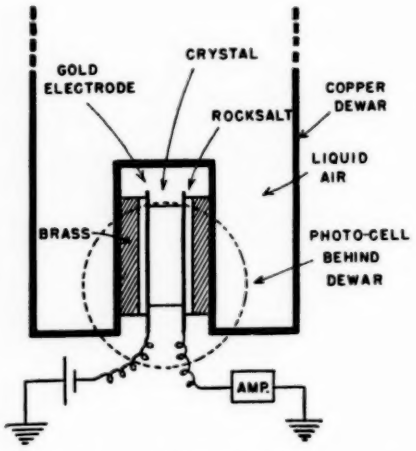

FIG. 2. Mounting of crystal in Dewar.

[9] A similar arrangement was employed previously by one of the authors and Mr. F. B. Quinlan of the General Electric Company.

[10] This was kindly suggested to us by Professor Shenstone.

[11] J. Strong, Phys. Rev. **49**, 291 (1936).

[12] R. W. Wood, Phil. Mag. **4**, 396 (1902); **23**, 310 (1912).

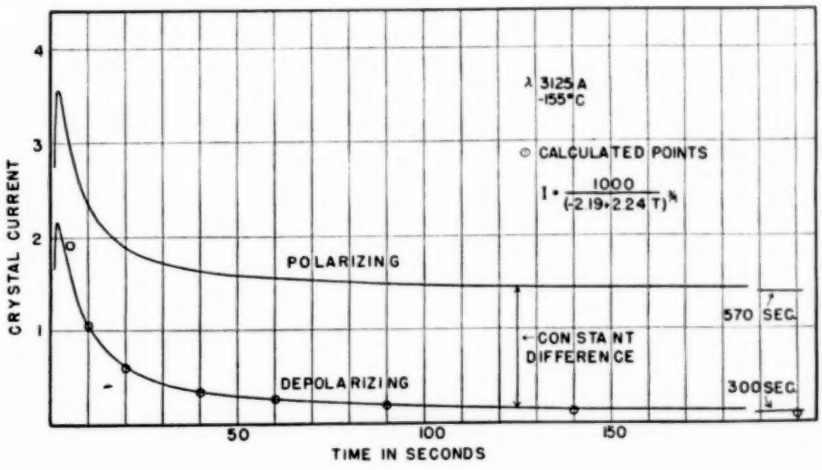

FIG. 3. Dependence of crystal current (in arbitrary units) on time.

mator. In obtaining the absorption spectrum at low temperatures (−145°C) the crystal was mounted on a fixed copper slit in contact with the Dewar vessel in order to avoid moving the specimen at low temperatures. By means of a shutter the energy transmitted through the crystal was measured as well as the energy in that part of the line that passed through the open slit below the crystal. This was repeated at room temperature. If the ratio of the two transmissions is taken, the result is a relative transmission spectrum. Since the room temperature transmission spectrum had been determined "absolutely," this relative transmission spectrum at low temperature could be converted into percentage transmission. Absorption spectra at room temperature were obtained photographically also.[13] Ultraviolet light from a hydrogen arc was focused on the crystal mounted in front of the slit of a Jobin and Yvon spectrograph. Eastman No. 33 plates were employed. The transmission of the crystal was obtained by comparing crystal transmission with intensity marks put on the plate by varying the exposure time. The plates were measured by means of a densitometer.

The procedures followed in making the other measurements reported in this paper will be discussed in the next section. All electrical measurements were made at different times with gold electrodes. These experiments were repeated in rough fashion with Aquadag electrodes and qualitative agreement was obtained in all cases.

[13] We wish to thank Dr. A. M. Chase of the Biology Department of Princeton University for allowing us to use his apparatus for these measurements.

RESULTS AND DISCUSSION

In order to find the dependence on time of the crystal current the procedure was the following: Initially the crystal was illuminated while its electrodes were grounded through the amplifier in order to put it in a "depolarized" state, that is to say, one in which the crystal is free from all charge. Red light approximately up to 1μ was not effective in releasing the charge, while ultraviolet light was highly efficient. The next step was to put the electric field on while the crystal was in the dark. The crystal was then illuminated with light of a given wave-length. On opening a shutter the crystal current was observed to rise very rapidly to a maximum and then drop off slowly to some equilibrium value. At intervals of one second (determined by a metronome) and less frequently as time went on, positions of the galvanometer spot were marked off and subsequently plotted. After equilibrium had been attained the electrodes were grounded through the amplifier with the crystal in the dark. If the crystal was again illuminated without delay (in our experiments this was done well within 30 seconds) a reverse current was caused to flow. This was measured in the manner already described. In all cases the current fell to zero immediately when the illumination was cut off.

It was found for various mercury lines that the current rises rapidly after illumination has begun and then decreases to a saturation value because a reverse field is set up in the crystal caused by polarization. The ratio of the maximum current to its saturation value was found to be about 2.5.

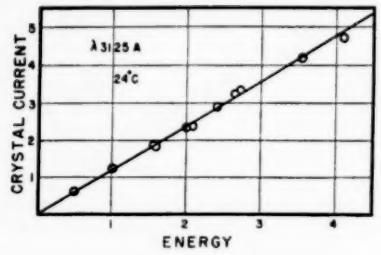

FIG. 4. Behavior of crystal current with respect to incident energy for constant voltage gradient.

These results are similar to those obtained for sulphur by Kurrelmeyer.[14] When the crystal is grounded through the amplifier and light is allowed to fall on it, a reverse current flows which has the same dependence on time as the photocurrent with the field on. Typical results are shown in Fig. 3. It is to be noted that the difference in the ordinates of these two curves is constant except at the beginning. These curves can be fitted best by the formula shown in the figure. Similar results have been obtained for different mercury lines and at different temperatures. If a set of such curves is taken for a given wave-length by varying the intensity of illumination, it is found that the difference between the ordinates is a constant for any pair of curves except during the first two or three seconds. Figure 4 shows how the crystal current varies as a function of intensity of illumination at constant voltage gradient. In this curve we have plotted the maximum crystal current, the crystal having been initially "depolarized." A straight line relationship is obtained also if one plots the saturation currents instead of the maximum currents. Figure 5 shows how the crystal current varies as a function of voltage gradient at constant intensity of illumination. The linearity of the curves shown in Figs. 4 and 5 furnishes evidence that we are dealing with primary currents. No signs of secondary currents were observed up to our maximum voltage gradient of 900 volts/cm for different wave-lengths and different temperatures. The dark current was found usually to be less than 10^{-13} amp. So far as we know the dark current did not vary (except for varying surface conditions). Therefore, we believe that no "excitation current" exists in willemite as it does in sulphur.[14]

We have obtained curves of photoconductivity per unit incident energy *versus* wave-length by measuring the maximum crystal current, the crystal having been freed initially of all charges, for each wave-length setting. However, similar curves using equilibrium currents gave the same spectral dependence except for a constant numerical factor. The results obtained are shown in Figs. 6 and 7 at the temperatures indicated and a constant voltage gradient of 900 volts/cm. Each curve shown has been obtained by averaging several runs. These curves have been drawn in each case so that the crystal current per unit incident energy at λ3022A is arbitrarily taken as unity. We should like to call attention to the fact that the crystal current per unit incident energy decreases as the temperature decreases and at different rates for different wave-lengths in such a way that the region of photoconductivity becomes narrower. For example at λ3022A the response decreases by a factor of about three in going from 93°C to −155°C, while at λ2537A this factor is about twenty-five.

Some structure is observed in all these curves, which we believe to be real. However, the corrections which had to be made might have exaggerated the structure.[15] In the room temperature curve of photoconductivity *versus* wave-length a peak appears near λ2753A. Hofstadter also has found such a peak while studying a natural polycrystalline sample of willemite obtained from Franklin, New Jersey, as well as with an artificially prepared phosphor activated with Mn.[6] Examination of Beese's fluorescent response curves for various types of willemite and a Mn activated phosphor shows a peak in this

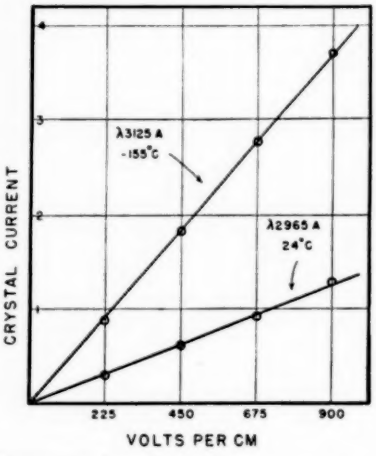

FIG. 5. Variation of crystal current (in arbitrary units) with voltage gradient at constant intensity of illumination.

[14] B. Kurrelmeyer, Phys. Rev. **30**, 893 (1928).

[15] See the experimental part of this paper.

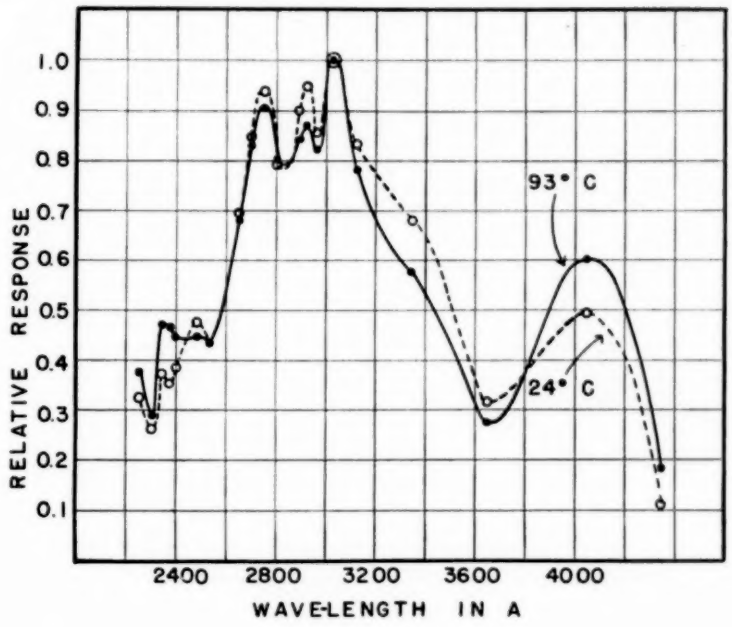

FIG. 6. Crystal current per unit incident energy (at constant voltage gradient) plotted against wave-length.

same neighborhood.[5] Both Beese and ourselves find a peak near λ2925A of which there was a slight indication in Hofstadter's curve *A*. Other coincidences seem to occur in the shorter wave-length region in Beese's and our own work, although Beese has not indicated that the structure in this part of the spectrum is real. We also find peaks of photoconductivity in the longer wave-length region which do not occur in Hofstadter's or in Beese's work. Their curves drop off sharply near 3000A. Perhaps the presence of different impurities accounts for this difference. However, Kroger's[1b] excitation spectra for Zn_2SiO_4-Mn phosphors also exhibit structure in the longer wave-length region. It is necessary to point out that there is no clearcut agreement between the data of Kroger and those of Beese and ourselves in this region.

It is well known that there is a close connection between photoconductivity and light absorption in a crystal. We wished to see whether there was some simple relation in the case of willemite. The absorption of the willemite crystal was obtained as described in the experimental section. Figure 8 shows the absorption spectrum obtained photographically and by direct transmission measurements made with a photo-cell. These absorption spectra agree qualitatively (the spectrum obtained by means of the photo-cell is more accurate) and differ from the absorption spectrum of pure Zn_2SiO_4 which has an absorption edge at about λ2200A as reported by Kroger.[1b] According to our results the absorption edge of our crystalline sample (0.70 percent Mn) lies in a very different position from the edge found for a willemite phosphor (1 percent Mn) by Kroger. We note that there is a side band on the long wave-length side of the absorption edge at about 3000A which is probably due to the 0.70 percent Mn or other impurities present in the natural willemite crystal. Kroger has also found such side bands in the absorption spectra of willemite phosphors activated with Mn. However, the absorption spectra we have obtained photographically do not exhibit the structure evident in his curves in the spectral range between 3500 and 4500A. The absorption spectrum of a natural willemite crystal discussed by Marden, Beese and Meister[2a] apparently does not show the band on the long wave-length side of the absorption edge.

An absorption spectrum was obtained also at low temperatures but is not given here because of its uncertainty. However, the low temperature spectrum is quite similar to that at room temperature except that both the absorption edge and the side band seem to shift to shorter wave-lengths. Until further studies are made on the effect of impurities on both photoconductivity

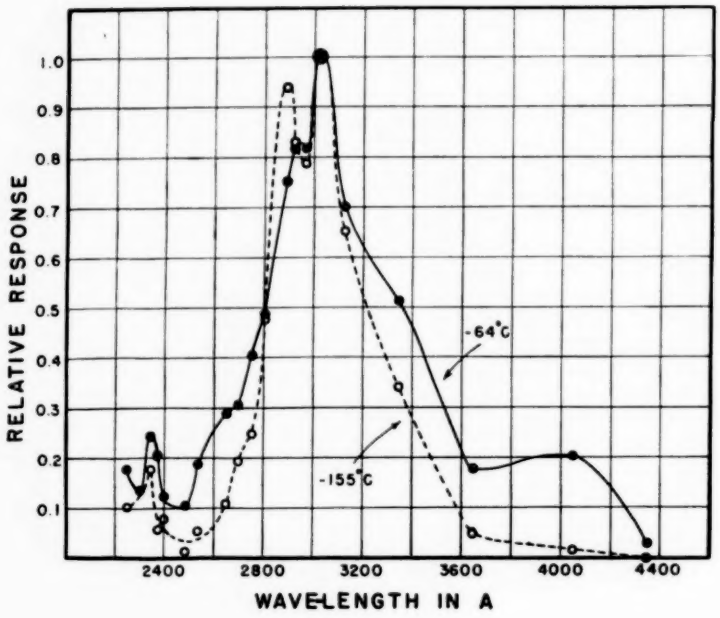

FIG 7. Photoconductivity at lower temperatures. See Fig. 6.

and absorption it is not possible for us to draw definite conclusions regarding relations between them.

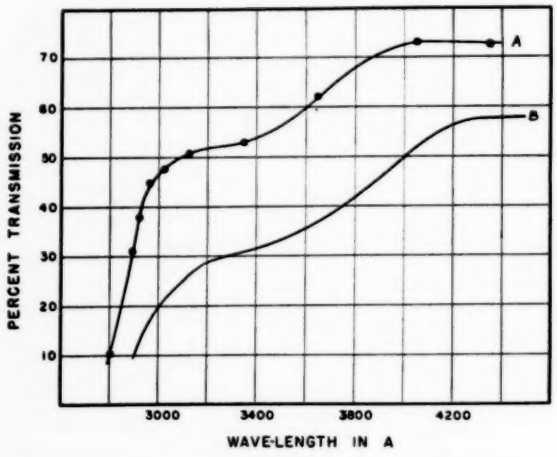

FIG. 8. Transmission of thin sample of crystal. Curve *A* —photo-cell. Curve *B*—photographic. Points on curve *B* were obtained generally at intervals of 10A. No interval was larger than 25A.

Some results on the dependence of the dark current on temperature have been reported previously.[16] At the present time we have nothing to add to the account already given.

ACKNOWLEDGMENT

We wish to thank the members of the Geology Department at Princeton University for their kind cooperation in many respects. We also wish to extend our appreciation to the General Electric Company for the interest they have taken in this work and for the aid they have given us. The Radio Corporation of America has kindly helped us in the analysis of our sample. It is a pleasure to thank Mr. W. Duryea and Mr. C. Grove for aid in building the apparatus and technical assistance. Finally, we appreciate the encouragement given us by Professor Shenstone.

[16] R. C. Herman and R. Hofstadter, Phys. Rev. **57**, 936 (1940).

Dynamical Determination of the Elastic Constants and Their Temperature Coefficients for Quartz

JOHN V. ATANASOFF AND PHILIP J. HART
Iowa State College, Ames, Iowa

(Received August 28, 1940)

A mathematical theory is presented giving the relations between the elastic constants and the frequencies of piezoelectric vibration for an infinite plate of homogeneous but aeolotropic material. Since no such theory is known for finite plates it is, strictly speaking, impossible to determine the elastic constants of the material from measurements on such plates. However, the viewpoint of perturbation theory indicates that certain frequencies of vibration of finite plates asymptotically approach the frequencies of vibration of infinite plates of the same material, orientation and thickness as the harmonic order increases. The experimental results confirm that this is an excellent method of eliminating edge effects and accurate data that are seemingly quite independent of mother crystal and proportions of the plate are obtained. However, in the evaluation of the elastic constants and their temperature coefficients from these data it is found that there is a small but not easily explained discrepancy between these results and the classical elastic theory for substances of the symmetry class D_3 generally accepted for quartz. Detailed observations have been made in the temperature interval from 0° to 80°C but additional results enable the calculation of the values of certain of the elastic constants at higher temperatures up to the alpha-beta transition point.

INTRODUCTION

THE mathematical relationship existing between the elastic constants of a homogeneous aeolotropic substance and the velocities of propagation of waves with different orientations of the phase planes has been known for many years.[1] Koga[2] seems to have been the first to develop an accurate theory of the frequencies of vibration of infinite plates when the phase surfaces are planes parallel to the surfaces of the plate. The harmonic frequencies of an infinite plate are exact integral multiples of the fundamental frequencies.

A rigorous solution has never been obtained for the vibrational frequencies of a plate of finite dimensions and in any study of such vibrations one must proceed by approximate methods. Strictly speaking, in order to be able to infer the elastic constants from measurements of the frequencies of vibration of a finite plate, a solution for this case would be needed, and this objection can be made to most, if not all, of the dynamical determinations of the elastic constants that have been made. In this paper, a method of procedure will be used which removes this necessity and permits the calculation of the elastic constants directly from the theory for infinite plates.

[1] A. E. H. Love, *A Treatise on the Mathematical Theory of Elasticity* (Cambridge University Press, 1934), pp. 298, 299.

[2] I. Koga, Physics **3**, 70–80 (1932).

GENERAL ELASTIC THEORY

1. Thickness vibrations of an infinite anisotropic plate

If, in an anisotropic elastic substance; u is the displacement vector, ϕ is the second-rank stress tensor,[3] θ is the second-rank strain tensor,[3] c is the fourth-rank elastic tensor,[3] and F is the volume rate of force developed by the stress tensor, we have from elastic theory the fundamental equations

$$\theta_{ij}=\frac{1}{2}\left(\frac{\partial u_i}{\partial x_j}+\frac{\partial u_j}{\partial x_i}\right), \tag{1}$$

$$\phi_{ij}=c_{ijk\beta}\theta_{\alpha\beta}, \tag{2}$$

$$F_j=\partial\phi_{ij}/\partial x_i. \tag{3}$$

In this paper the usual convention that repeated subscripts are to be summed is used.

The mathematical description of the free vibrations of a portion of homogeneous but anisotropic material is easily derived from these equations. By combining (1), (2) and (3) with Newton's equations of motion and making use of the symmetry[3] there results the wave equation

[3] Many tensor quantities used in elastic theory possess a certain symmetry thus $\phi_{ij}=\phi_{ji}$, $\theta_{ij}=\theta_{ji}$, $c_{ijab}=c_{ijba}=c_{jiab}=c_{abij}$ and $e_{iab}=e_{iba}$. This symmetry reduces the number of independent terms in the tensor and permits the use of the common notation with fewer subscripts. For instance, $c_{2223}=c_{24}$ since $11=1$, $22=2$, $33=3$, $23=4$, $13=5$, $12=6$. From the symmetry, we also have $31=4$ etc.

for this type of material

$$\rho\ddot{u}_j = c_{ij\alpha\beta}\partial^2 u_\alpha/\partial x_i \partial x_\beta \tag{4}$$

in which ρ is the density of the substance. The boundary condition at a free surface of the material where the unit normal is the vector ν is easily found from (1) and (2) to be

$$c_{ij\alpha\beta}\left(\frac{\partial u_\alpha}{\partial x_\beta}+\frac{\partial u_\beta}{\partial x_\alpha}\right)\nu_i = 0. \tag{5}$$

In searching for a normal mode of vibration the substitution of

$$u_i = \psi_i e^{i\omega t} \tag{6}$$

in (4) and (5) is permitted and there results the simpler characteristic system

$$c_{ij\alpha\beta}\frac{\partial \psi_\alpha}{\partial x_i \partial x_\beta}+\rho\omega^2\psi_j = 0, \tag{7}$$

$$c_{ij\alpha\beta}\left(\frac{\partial \psi_\alpha}{\partial x_\beta}+\frac{\partial \psi_\beta}{\partial x_\alpha}\right)\nu_i = 0. \tag{8}$$

The problem at hand is to obtain a solution of the system (7), (8) for an infinite plate. Let the infinite bounding surfaces be the planes $x_1 = 0$ and $x_1 = s$. Then it is easy to see that a solution of the form

$$\psi_j = A_j \cos(n\pi x_1/s) \tag{9}$$

in which the A's are constants, satisfies the boundary condition (8). The condition that (9) satisfy (7) is the linear secular system

$$c_{1j\alpha 1}A_\alpha - \kappa^2 A_j = 0 \tag{10}$$

in which

$$\kappa^2 = 4\rho s^2 f^2/n^2, \quad f = \omega/2\pi. \tag{11}$$

This secular system determines the frequencies and modes of vibration in the usual way. The secular equation

$$\begin{vmatrix} c_{1111}-\kappa^2 & c_{1121} & c_{1131} \\ c_{1211} & c_{1221}-\kappa^2 & c_{1231} \\ c_{1311} & c_{1321} & c_{1331}-\kappa^2 \end{vmatrix} = 0 \tag{12}$$

has three roots in κ^2 and hence there are three independent fundamental modes and, in general, three different fundamental frequencies of vibration for each orientation of the infinite plate. The harmonic frequencies of an infinite plate are exact integral multiples of the fundamental frequencies.

If one wishes to find the frequencies and modes of vibration for an infinite plate with arbitrary orientation it is convenient to introduce a transformation of coordinates which makes the new x_1 axis normal to plate. The effect of such a transformation on the c's is determined by the fact that they form a tensor of the fourth rank.

If the elastic constants are to be determined, the resonant frequencies of several plates having various orientations with respect to the natural axes of the material may be required. One must measure the frequencies of at least as many independent modes of vibration as there are constants to be evaluated.

2. Excitation of vibrations

A complete treatment of piezoelectric vibrations would require the introduction of certain forces arising from the piezoelectric effect in the wave equation (4) and the solution of this modified equation with the boundary condition (5). However, the excitation of a resonance mode of vibration can be simplified by the following considerations. Because the damping forces of a vibrating quartz crystal are small, considerable amplitude is reached with a given driving force. Consequently, the elastic forces in the crystal are large compared with the piezoelectric driving forces, and the mode of vibration is not much perturbed by the driving force. If one assumes the mode of vibration as known from calculations on the free undamped case, the driving energy due to a field E can be calculated from the integral

$$\int_\tau\int E_i dP_i d\tau \tag{13}$$

in which

$$P_i = e_{i\alpha\beta}\theta_{\alpha\beta}, \tag{14}$$

where the e's form the third-rank piezoelectric tensor.[3] In certain special cases this integral will be zero, indicating that it is impossible to drive the given mode of vibration with the given field arrangement. Thus it is impossible to drive the even harmonics of an infinite plate with a field which is independent of position in space. In the specific case of quartz only the terms e_{11}, e_{12}, e_{14},

e_{25}, and e_{26} of the piezoelectric tensor are not zero. This indicates a further reason why the integral (13) may vanish and driving of the cut become impossible.

3. Secular equations for certain infinite plates of quartz

Since quartz belongs to the crystal class D_3 it has the following nonzero elastic constants c_{11}, c_{12}, c_{13}, c_{14}, $c_{22}=c_{11}$, $c_{23}=c_{13}$, $c_{24}=-c_{14}$, c_{33}, c_{44}, $c_{55}=c_{44}$, $c_{56}=c_{14}$, $c_{66}=\frac{1}{2}(c_{11}-c_{12})$ if it is placed in the coordinate system so that the x_3 and x_1 axes correspond to the threefold and the twofold axes of the crystal, respectively. Two angles are used to designate the orientation of the quartz plates. The first angle, the azimuth, is the angle between the projection of the normal to the plate on the x_1x_2 plane and the x_1 axis. The second angle, the altitude, is the angle between the normal to the plates and its projection on the x_1x_2 plane.

By the use of Eq. (12), the equation relating the elastic constants to the frequencies of vibration for a (0°, 0°) plate, is found to be

$$[c_{1111}-\kappa^2][(c_{1221}-\kappa^2)(c_{1331}-\kappa^2)-c_{1321}c_{1231}]=0.$$

The linear factor in the equation represents a purely longitudinal mode of vibration excited by an alternating electric field in the x_1 direction, and the quadratic factor represents two more complicated modes involving shear vibrations, and excited by a field in the x_2 direction.

Similarly, by replacing the 1's by 2's in the first and fourth subscripts of the c's in Eq. (12), the equation for the (30°, 0°) plate can be obtained:

$$[c_{2112}-\kappa^2][(c_{2222}-\kappa^2)(c_{2332}-\kappa^2)-c_{2322}c_{2232}]=0.$$

Hence, the secular equation of this plate also contains a linear factor representing a pure shear mode of vibration excited by an electric field in the x_2 direction. The other two modes of vibration can be excited by a field in the x_1 direction.

In a similar manner, the equation for the (0°, 90°) plate is found to be

$$(c_{3113}-\kappa^2)(c_{3223}-\kappa^2)(c_{3333}-\kappa^2)=0,$$

the equation being completely factorable. The first and second factors represent pure shears which should be excited by alternating electric fields in the x_2 and x_1 directions, respectively. The third factor represents a purely longitudinal mode of vibration which cannot be excited by piezoelectric methods since there is no piezoelectric constant corresponding to the θ_{33} strain.

The equation for plates of these three orientations, written in terms of the principal elastic constants, are, for a 0°, 0° plate,

$$\kappa^2-c_{11}=0, \qquad \text{(I)}$$

$$\kappa^4-(c_{44}+c_{66})\kappa^2+c_{66}c_{44}-c_{56}^2=0 \qquad \text{(III)}$$

for a (30°, 0°) plate

$$\kappa^2-c_{66}=0, \qquad \text{(II)}$$

$$\kappa^4-(c_{11}+c_{44})\kappa^2+c_{11}c_{44}-c_{24}^2=0 \qquad \text{(IV, V)}$$

and for a (0°, 90°) plate,

$$(\kappa^2-c_{33})(\kappa^2-c_{44})(\kappa^2-c_{44})=0.$$

The equation for an R plate, obtained by a transformation of the elastic constants is factorable, as are the equations for all orientations that may be expressed by (30°, x°). The mode of vibration defined by the first factor is a mode composed of the shear strains θ_{12} and θ_{13}, and thus capable of being excited by a field having a component in the x_2 direction. The second factor defines two more complicated modes of vibration involving the strains θ_{22}, θ_{33}, and θ_{23}, these vibrations being excited by a field in the x_1 direction.

The equation for a (0°, 45°) or a (0°, −45°) plate is found by similar methods to be nonfactorable. The three complicated modes of vibration for this plate involve strains such that the resulting polarization has components in both the x_1 and x_2 directions.

The equation for the R plate, written in terms of the principal elastic constants, are

$$\kappa^2-0.38260c_{44}-0.97205c_{56}-0.61740c_{66}=0, \quad \text{V(I)}$$

$$\begin{aligned}\kappa^4-[&0.61740c_{11}+0.97205c_{24}+0.38260c_{33}\\&+c_{44}]\kappa^2-0.23622c_{13}^2-0.60014c_{13}c_{24}\\&-0.47245c_{13}c_{44}+0.23622c_{11}c_{33}\\&+0.14638c_{33}c_{44}+0.37191c_{33}c_{24}\\&+0.38118c_{11}c_{44}-0.38118c_{24}^2=0. \qquad \text{(VII)}\end{aligned}$$

The equation for the (0°, 45°) plate is

$$8\kappa^6-[4c_{11}+4c_{33}+12c_{44}+4c_{66}]\kappa^4-[2c_{14}^2+4c_{14}c_{56}+4c_{56}^2-4c_{11}c_{44}-2c_{11}c_{66}-4c_{44}^2-4c_{44}c_{66}+2c_{13}^2+4c_{13}c_{44}-2c_{11}c_{33}-2c_{33}c_{66}-4c_{33}c_{44}]\kappa^2-c_{13}(-c_{13}c_{66}-c_{13}c_{44}+2c_{14}c_{56}+2c_{56}^2-2c_{44}c_{66}-2c_{44}^2)-c_{33}(c_{11}c_{44}+c_{44}^2+c_{44}c_{66}+c_{11}c_{66}-c_{14}^2-2c_{14}c_{56}-c_{56}^2)-c_{44}(c_{11}c_{44}+c_{11}c_{66}-c_{14}^2)+c_{11}c_{56}^2=0. \quad \text{(VIII, IX, X)}$$

In Eqs. (III) to (X), inclusive, the constant ordinarily written c_{14} is written as c_{14}, $-c_{24}$, or c_{56}, depending upon its position in the stress-strain table. The reason for splitting this constant will be explained later. The Roman numerals indicate the secular factor associated with each of the ten modes of vibration used in determining the elastic constants.

4. Finite plates

Since no easy exact theory of the vibrations of a finite plate is possible, it seems best, for the present purposes, to use the following perturbation point of view.

Imagine the finite plate as being formed by moving the lateral surfaces of the plate in from infinity. One result of this change is to introduce new frequencies corresponding to the new finite lateral dimensions of the crystal. The perturbing effect of these finite boundaries on the "thickness" modes of vibration of the infinite plate (i.e., those modes of vibration with phase planes parallel to the surfaces of the plate) is twofold. The first is a shift in frequency caused by the presence of the boundaries. The second effect is the coupling which the existence of these lateral boundaries introduces between the given frequency and others which may be in the same neighborhood. One would expect theoretically, from the principle of Saint Vernant, that these perturbations of the thickness frequencies of an infinite plate of given thickness by the finite lateral boundaries in an actual physical plate of the same thickness would decrease rapidly as the wave-length becomes small compared with the lateral dimensions of the crystal. We shall see that this result is confirmed experimentally, and it is a principal precaution of the present paper that the conditions of infinite plates be closely approximated by using very high harmonics of the thickness modes of vibration and hence a wave-length very small compared with the lateral dimensions. This procedure is much better than an attempt to use plates of large lateral dimensions which attempt, of course, is limited by the size of the specimens available as well as by the size that is convenient to cut and use. The use of very thin plates is also undesirable because it is very difficult to cut such plates with a high relative accuracy and without introducing surface scratches which have a significant effect.

Experimental Methods

Two large, relatively flaw-free natural quartz crystals having well-developed, reflecting facets, were selected for use, and only those portions of the crystals distant from any twinning visible by means of polarized light were used to make the plates. The surfaces of all the plates were etched with hydrofluoric acid and were found to exhibit no traces of twinning. Plates were cut from each of the natural crystals (hereafter designated as crystals 1 and 2) having the following orientations: (0°, 0°) the so-called x cut; (30°, 0°) or (90°, 0°) a y cut; (30°, −38° 12½′), an R cut, and (0°, 45°). A(0°, 90°) or z cut was also made from crystal 1. The dimensions of all the plates were approximately 2.2×2.2×0.45 cm, all being accurate rectangular parallelepipeds in shape and having unrounded edges free from nicks.

Optical methods, making use of the reflecting facets of the crystals, were used to orient the plates. The orientations of all the plates were checked by x-ray methods which revealed no measurable error of orientation for any plate. Opposite surfaces of the plates were ground parallel to each other to within 0.0001 cm and the National Bureau of Standards determined the average thicknesses of these plates, their measurements being accurate to 0.00001 inch.

The plates were made to vibrate piezoelectrically as a filter between a variable frequency, stable oscillator and a sensitive vacuum tube voltmeter for detecting resonance frequencies of the plates. An audioamplifier was

used for the approximate location of the resonance points and for obtaining beat notes between the oscillator and a frequency meter. By this method, frequencies of higher order harmonics of the plates were determined to an absolute accuracy of about one part in twenty-five thousand.

The quartz plates were mounted in a vertical position with their weight resting on a lateral face so as to leave the main surfaces as nearly as possible free of external stresses. Two sets of plane parallel electrodes were used, one for applying the alternating electric field parallel to the thickness of the plate, and the other for applying the field perpendicular to the thickness. A small air gap was left between the plate and each electrode. The electrodes and plates were contained in a constant temperature chamber, the temperature being measured to within 0.05°C by means of a thermocouple and potentiometer. The constant temperature chamber was arranged so that the air could be evacuated from it to prevent the air from damping or shifting the frequencies of the plates. However, it was found, for all harmonics except the lowest, that there was no detectable frequency change produced by the presence of the air, and so, for most of the work, the chamber was not evacuated.

Preliminary Investigation

In a preliminary study with the quartz plates previously described, the frequency "spectra" of all the plates were rather fully investigated, the temperature being maintained at 35°C. It was found that in the lower frequency region (the region up to approximately 5000 kilocycles per second for the particular plates used) there were literally many hundreds of frequencies to which a crystal plate would react, these responses, however, having a great range of amplitudes. The presence of so many frequencies of response can be explained by the fact that a finite plate in the form of a rectangular parallelepiped was used, and lateral modes of vibration and couplings between modes made possible a great multiplicity of vibrational frequencies. In general, however, the harmonics of the main modes of vibration were excited more strongly than the other frequencies and could be recognized by their greater intensity.

The measurable frequency "spectrum" became progressively simpler with higher frequencies until harmonics of only the main modes, and in some cases harmonics of certain lateral modes of vibration, were detectable, the latter much more faintly than the former. Beyond about 20,000 kilocycles per second, the harmonics of only the main modes of vibration were detectable.

The frequencies of the odd harmonics of the main modes of vibration were determined from the fundamental up to the 87th harmonic in some cases, and harmonic frequencies of certain lateral modes (those modes whose phase planes are parallel to the small lateral surfaces of the plate) were measured up to the 263rd harmonic. It was found that there was a relatively large variation in the frequency of the harmonic divided by the order of the harmonic, i.e., f/n, in the lower frequency region because of coupling between modes and because of edge effects of the plates. As the order of the harmonic was increased, coupling and edge effects decreased until variations from the mean of f/n for all harmonics above about the 31st for the main modes of vibration, with very few exceptions, amounted to less than 0.01 percent. These experimental results, therefore, confirm the basic assumption of the method employed that the higher the order of the harmonic of a finite plate, the closer the value of f/n should approach the fundamental frequency of a theoretical infinite plate of the same thickness. In general, it was also found that f/n for the lateral modes of vibration approached the theoretical value more slowly with increase in n than it did for the main modes.

As an example of the sort of data obtained for each of the quartz plates, there is presented in Fig. 1 the values of f/n for four modes of vibration of one of the (30°, 0°) plates. Mode III in the figure is a lateral mode of vibration. Here, the general asymptotic approach of f/n to its final value may be attributed to edge effects of the plate, and individual often stronger variations of f/n to coupling between modes. The vertical lines connecting resonance points of approximately the same frequency indicate possible coupling between modes, but it must be remembered, of course, that there are many natural modes of vibration of this plate whose frequencies were not

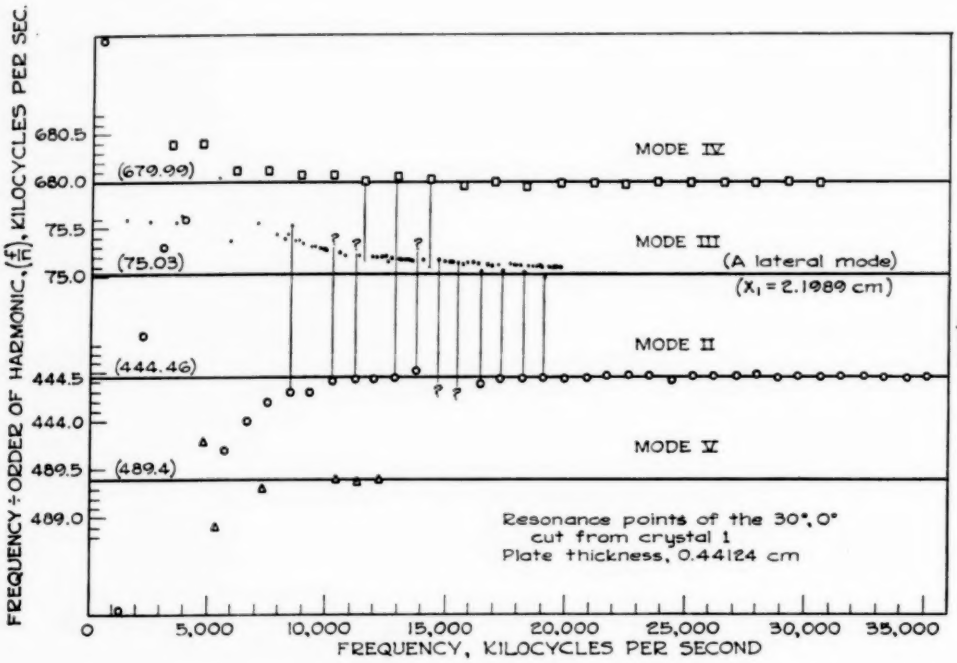

FIG. 1. Values of f/n as a function of frequency for several modes of vibration.

measured, which could be responsible for coupling.

In the experimental investigation, most of the modes of vibration defined by Eqs. (I) to (X) were excited by the appropriate alternating electric field. Only one of the two modes of vibration defined by Eq. (III) for the (0°, 0°) plates, however, was observed, the other mode probably being too weak to detect. However, both modes defined by Eq. (IV, V) for the (30°, 0°) plates were obtained, the mode designated as (V) being much the weaker of the two. Only one of the R modes defined by Eq. (VII) was observed. The modes of vibration for the (0°, 90°) plate were not excited strongly above the very lowest frequencies, possibly because of the close coupling and damping occurring between the two essentially equal modes of vibration. The three modes of vibration, (VIII), (IX), and (X) for the (0°, 45°) plates were obtained with approximately equal intensity by an electric field in the direction of the thickness of the plate. A field in the x_2 direction also excited all three of these modes of vibration, the frequencies for the higher order harmonics for the x_2 field being the same within the experimental error as the frequencies for the field in the (0°, 45°) direction, thus providing experimental evidence that the air gap width is not of consequence for high frequencies.

The values of κ^2 calculated by Eq. (7) for corresponding modes of vibration of the plates made from the natural quartz crystals 1 and 2, proved to be identical within the limits of error allowed by the thickness measurements of the plates for all the different modes of vibration. This fact is an indication of the uniformity of all flaw-free quartz.

DATA FOR ELASTIC CONSTANTS AND THEIR TEMPERATURE COEFFICIENTS

In order to be able to determine both the elastic constants and their temperature coefficients frequency measurements of the various modes of vibration were made between the approximate temperatures of 0° and 80°C. Frequencies of five consecutive harmonics were determined in the frequency region between 22,000 and 30,000 kilocycles per second for each mode of vibration, the variation of f/n from the mean value of the five f/n's seldom being greater than 0.005 percent. An average value of f/n was found for each mode of vibration at each temperature for which temperature measurements were made, for the plates from both crystals 1 and 2,

these data being presented in Figs. 2 to 10. In the figures, the curves for the plates from crystals 1 and 2 are plotted close together so that the slopes may be compared. The change of frequency with temperature of mode of vibration (V) (this mode being very weak) was not measured. However, the value of f/n at 35°C for this mode was evaluated, but less precisely, by harmonics up to the 25th (see Fig. 1), this value being 489.4 kc/sec.

Since the curves of change of frequency with temperature show but small experimental error, it is possible to determine the value of f/n accurately for any desired temperature, the values of f/n used here in the evaluation of the elastic constants of quartz being determined in this way for the temperature of 35°C. It is also possible to determine accurately the slopes of these curves, (and in some cases, perhaps, even the second derivative of frequency with respect to temperature), the temperature coefficients of the elastic constants being here determined by the use of the slopes of these curves at 35°C.

In Table I are presented the selected values of f/n and of $d(f/n)/dT$ (T being temperature in °C) at 35°C for the plates from crystal 1. Also presented are the calculated values of Sf/n, of κ^2, and of $S\cdot d(f/n)/dT$, the latter three values being constants which do not depend on plate thickness. A Roman numeral in column 1 refers to the mode of vibration which is defined by the equation of the same number. The density of quartz was taken as 2.648 g/cc at 35°C.

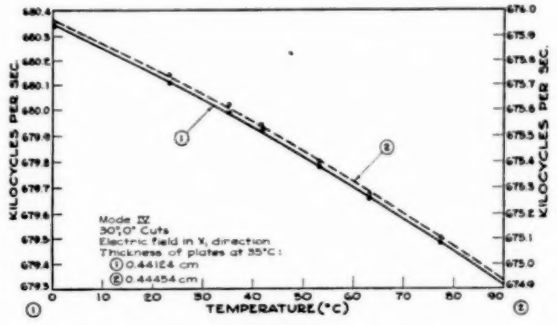

FIG. 2. Frequency of mode (I) vibration as a function of temperature.

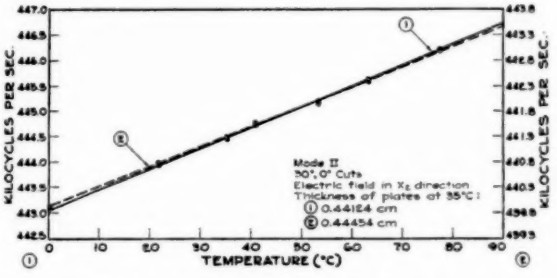

FIG. 3. Frequency of mode (II) vibration as a function of temperature.

CALCULATION OF THE ELASTIC CONSTANTS

Substitution of the values of κ^2 from Table I into Eqs. (I) and (II) gives directly, $c_{11}=87.55$ and $c_{66}=40.74$, the units being 10^{10} dynes per square centimeter. Since $c_{66}=\frac{1}{2}(c_{11}-c_{12})$, c_{12} is found to be 6.07. However, the solution of Eqs. (III) to (X) with the assumption that $c_{14}=-c_{24}=c_{56}$ (a direct consequence of the trigonal axis generally accepted for quartz), offers difficulties because of the fact that these equations are found to be inconsistent to a degree not explainable by known experimental errors. In fact, substitution of the numerical values of c_{11} and c_{66} into Eqs. (III) and (VI) and the simultaneous solution of

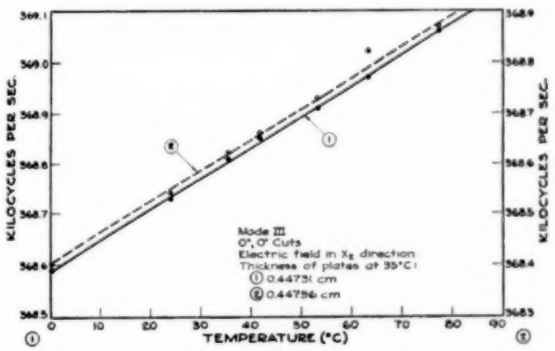

FIG. 4. Frequency of mode (III) vibration as a function of temperature.

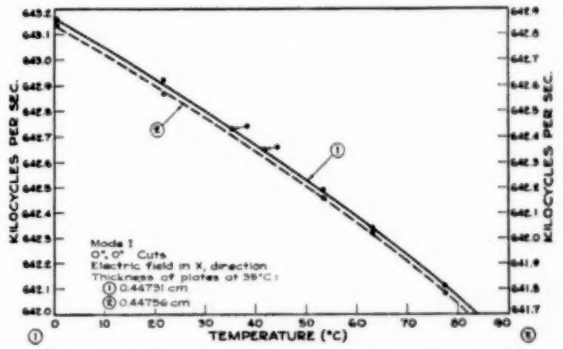

FIG. 5. Frequency of mode (IV) vibration as a function of temperature.

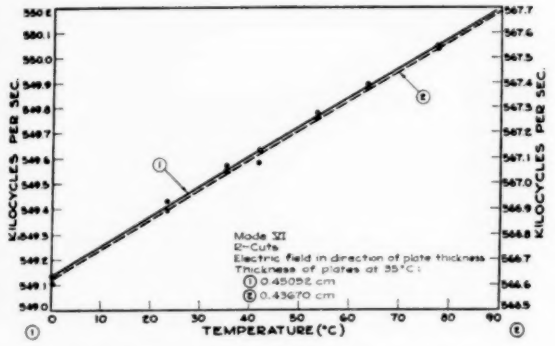

FIG. 6. Frequency of mode (VI) vibration as a function of temperature.

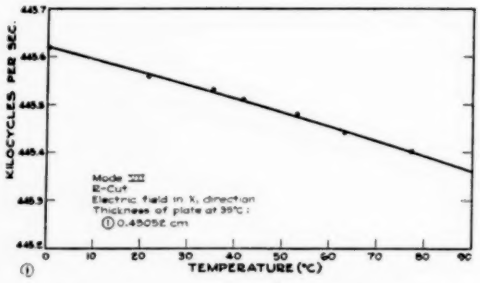

FIG. 7. Frequency of mode (VII) vibration as a function of temperature.

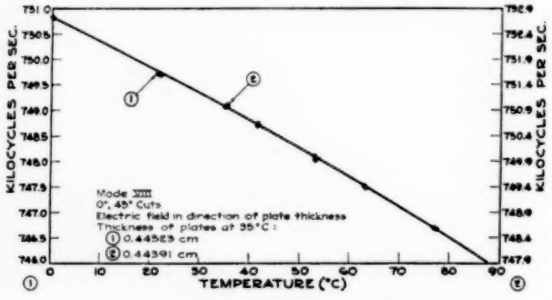

FIG. 8. Frequency of mode (VIII) vibration as a function of temperature.

these equations gives $c_{44}=57.19$ and $c_{56}=18.40$. Similarly, solution of Eqs. (IV) and (V) gives $c_{44}=\kappa_{IV}^2+\kappa_V^2-c_{11}=57.19$ and $-c_{24}=17.25$. Since the c_{44}'s in these two cases prove to be identical, and since c_{11} and c_{66} are determined directly, one has either to doubt the fact that $-c_{24}$ should be equal to c_{56} or to attempt to find some error of theory or measurement leading to this peculiar result. The data for the independent equations (VII) to (X) would be expected to present more evidence on this question.

Values of c_{11}, c_{66}, c_{44}, c_{14}, c_{24}, and c_{56} substituted into Eqs. (VII) to (X) give four equations in the two unknowns, c_{13} and c_{33}. Simultaneous solution of each possible pair of these equations should give the same set of values for c_{13} and c_{33}, provided the values of the substituted constants are correct. Average values of the four constants determined by any combinations of Eqs. (I) to (VI), inclusive, with the assumption that $-c_{24}=c_{56}$, substituted into Eqs. (VII) to (X), make the latter equations highly inconsistent. It should be mentioned that, because of the form of Eqs. (VII) to (X), the coefficients of c_{13} and c_{33} often involving differences between numbers of almost equal magnitude, the values of the known constants substituted into these equations must be very nearly correct before the equations show any great degree of consistency.

By assuming that $-c_{24}=c_{56}$, and with the values determined from Eqs. (I) to (VI), Eqs. (VII) to (X) can be solved, first, with the assumption that $c_{14}=c_{56}$, and second, with the assumption that $c_{14}=-c_{24}$. The first assumption makes the last four equations much more consistent than does the substitution of any values of the constants obtained from Eqs. (I) to (VI) by setting $-c_{24}=c_{56}$. The second assumption, however, makes the equations more consistent yet, the inconsistency in the latter case being of such small value that it can be attributed, possibly entirely, to experimental error. The experimental data, therefore, give evidence that $c_{14}=-c_{24}\doteq c_{56}$.

An analysis of Eqs. (I) to (VI) shows that, in

TABLE I. *Summary of results. The data are from the plates from crystal 1 at 35°C. The values of κ^2 for the plates from crystal 2 checked so closely with the values from crystal 1 that it did not seem necessary to include the data from crystal 2 in the table. Comparative examples of the results obtained from crystals 1 and 2 are, for mode of vibration I, $\kappa^2=87.55$ for crystal 1 and $\kappa^2=87.56$ for crystal 2. Similarly, for mode II, $\kappa^2=40.74$ for crystal 1 compares with $\kappa^2=40.76$ for crystal 2, and for mode III, $\kappa^2=28.82$ compares with $\kappa^2=28.83$, etc.*

Mode of Vibration No.	f/n, kc/sec.	Plate Thickness, s, cm	sf/n cm·kc/sec.	$\kappa^2=4\rho s^2(f/n)^2$ 10^{10} dynes/cm^2	$d(f/n)/dT$ cycles/sec.·°C	$s\cdot d(f/n)/dT$ cm·cycle/sec.·°C
I	642.73	0.44731	287.50	87.55	−13.4	−5.99
II	444.46	0.44124	196.11	40.74	+39.3	+17.46
III	368.80	0.44731	164.97	28.82	+6.1	+2.73
IV	679.99	0.44124	300.04	95.35	−11.0	−4.89
V	489.4	0.44124	215.94	49.39		
VI	549.55	0.45052	247.58	64.92	+11.8	+5.15
VII	445.53	0.45052	200.72	42.67	−2.8	−1.26
VIII	749.06	0.44523	333.50	117.81	−53.2	−23.60
IX	489.29	0.44523	217.85	50.27	−12.5	−5.55
X	410.74	0.44523	182.87	35.42	−12.6	−5.59

order to make these equations consistent assuming $-c_{24}=c_{56}$, certain of the experimentally determined κ^2's must be raised in value and others lowered. If the absolute value of this rise or drop is assumed to be equal for each mode of vibration to be changed, the magnitude of this change can be calculated. Its value is much too large to be attributed to experimental error.

If we follow the empirical lead indicated above and assume $c_{14}=-c_{24}\mp c_{56}$, the adiabatic elastic constants of quartz are found to have the values presented in Table II.

TABLE II. *The adiabatic elastic constants of quartz at 35°C.*

$c_{11}=87.55\times10^{10}$	$c_{14}=-c_{24}=17.25\times10^{10}$ dynes/cm²
$c_{66}=40.74$	$c_{56}=18.40$
$c_{12}=6.07$	$c_{13}=13.3$
$c_{44}=57.19$	$c_{33}=106.8$

The authors are well aware of the grave difficulties inherent in the assumption that $c_{14}=-c_{24}\mp c_{56}$ in quartz. If confirmed, this result would force the relinquishment of the seemingly well-established trigonal axis and cause a change in its classification from D_3 to C_2 thus making quartz a monoclinic crystal. The following paragraphs indicate the rather extended effort that has been made to find another explanation of these experimental results.

The first suggestion is that quartz may not be a uniform substance even when it passes the optical and other tests previously described. One might then ascribe the results obtained to the fact that macroscopically quartz does not belong to the class D_3, being distorted by irregularities due to impurities or other causes. However, the excellent agreement between the wave velocities for similarly oriented plates cut from different mother crystals argues against this explanation. Furthermore, below, there will be described results obtained from cubes cut from the same two crystals, and these results agree, to within experimental error, with those obtained from the plates. Previous experimenters have obtained somewhat discordant results for the elastic constants of quartz but it cannot be said with certainty that these results indicate non-uniformity of tested quartz. On the contrary, it may be that difficulties of the type being outlined here have played a part in making the values of the elastic constants uncertain.

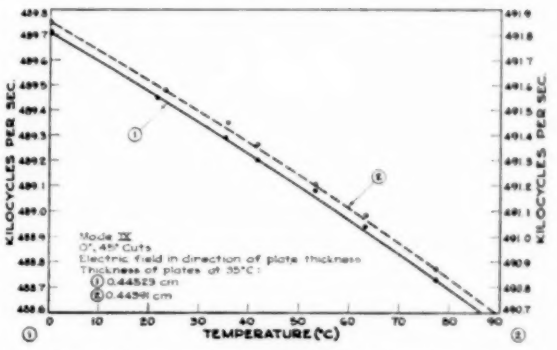

FIG. 9. Frequency of mode (IX) vibration as a function of temperature.

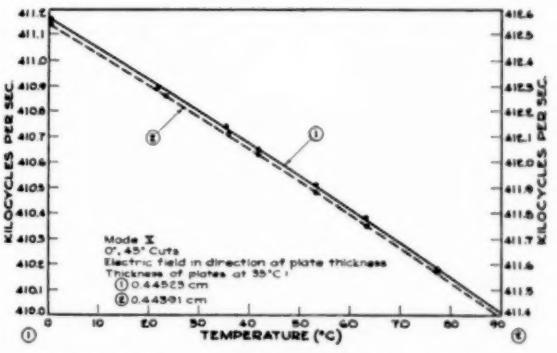

FIG. 10. Frequency of mode (X) vibration as a function of temperature.

The only likely source of error in the cutting of the plates would be in their orientation, since it is a simple matter to grind the surfaces until they are parallel and measure them. However, an examination of the modes involved will indicate that the measurement of the X, Y, and R cut plates is sufficient to furnish an inconsistent set of equations and these cuts are easy to orient with the crystal faces and to test with x-ray Laue photographs.

There are a variety of other possibilities. Since quartz is as good a conductor of heat as some of the metals the possibility that the wave motion is no longer adiabatic for the shortest waves used was examined. Isothermal wave motion should yield consistent secular equations for the determination of the elastic constants, but it was thought that the hybrid case might result in such inconsistencies. However, dimensional analysis, as well as more exact calculations, shows that the heat conductivity for the range of frequencies used is entirely negligible.

It was suggested that the inconsistencies might

TABLE III. *Values of differential coefficients. The units are 10^{10} dynes/cm²/°C.*

MODE OF VIBRATION NO.	$\frac{\partial\kappa^2}{\partial f}\frac{df}{dT}$	+ $\frac{\partial\kappa^2}{\partial s}\frac{ds}{dT}$	+ $\frac{\partial\kappa^2}{\partial\rho}\frac{d\rho}{dT}$	= $\frac{d\kappa^2}{dT}$
I	−0.00365	+0.00234	−0.00304	−0.00435
II	+0.00725	+0.00109	−0.00141	+0.00693
III	+0.00095	+0.00077	−0.00100	+0.00072
IV	−0.00311	+0.00255	−0.00331	−0.00387
V		+0.00132	−0.00172	
VI	+0.00270	+0.00147	−0.00225	+0.00192
VII	−0.00054	+0.00096	−0.00148	−0.00106
VIII	−0.01666	+0.00251	−0.00408	−0.01823
IX	−0.00256	+0.00107	−0.00175	−0.00324
X	−0.00217	+0.00076	−0.00123	−0.00264

be due to surface effects or to nearly plane standing waves not parallel to the faces of the crystal. Since these effects should be sensitive to changes in the thickness and relative proportions of the crystal plates, respectively, a further investigation was made with crystal blocks approximately cubical in proportion. One such cube was cut from each of the mother crystals, with its edges parallel to the coordinate axes, and, of course, such a block could be regarded as either a (0°, 0°) or as a (30°, 0°) plate. The method of investigation was the same as that previously used except that very high harmonics (up to the 263rd) had to be used in order to eliminate the perturbing effects of the edges. Without giving details, it may be stated that calculation of κ^2 from the constant value of f/n approached by the modes of vibration (I), (II), (III), and (IV) gave values which were identical, within experimental error, with the values obtained by means of the plates previously used. It thus appears that effects of these two types cannot be responsible for the observed inconsistency existing between the equations of vibration.

There remains the interesting question of the adequacy of the theoretical treatment. The mathematical theory of elasticity which forms the basis of this treatment has not, in the main, been experimentally verified to any high degree of accuracy because the irregularities of most materials tend to cloud the results. Only the more perfect crystals, of which quartz is one, offer material of sufficient uniformity to make such a verification possible and experiments of the type discussed probably constitute one of the best experimental procedures. On the mathematical side, it must be said that the tensor-invariant point of view used in constructing mathematical elasticity leaves its structure so secure that it is not easy to imagine any simple modification that will be an improvement. There are, of course, certain restrictions in the use of the theory of elasticity, the principal one being due to the fact that Hooke's law is only valid for small values of the strains but the present method is admirably suited to work within this limit.

To summarize, there seem to be three alternatives to account for contradictory secular equations: (a) There has been some systematic error of experimentation in spite of the consistency of the data; (b) the classical theory of vibrations is inadequate; or (c) macroscopically, quartz does not possess a trigonal axis, at least the two mother crystals examined show a common deviation from the class D_3. The third choice has been adopted in calculating the elastic constants presented but this is done from a heuristic point of view. If quartz is really monoclinic, the observations made are insufficient to determine the thirteen elastic constants which it would possess and one can only say that the wave velocities obtained are in good agreement with those of a monoclinic crystal with the elastic constants which are not zero having the values indicated in the table. There may be some justification for this arbitrary assumption that certain of the constants are zero since, if quartz is not of trigonal symmetry, it must be very nearly so.

CALCULATION OF THE TEMPERATURE COEFFICIENTS

Values of the temperature coefficients of the elastic constants of quartz obtained by various investigators differ greatly in magnitude, probably because of experimental errors involved in measuring a small change in rigidity or frequency. It is also a difficult task to design a quartz plate of finite dimensions whose lower harmonics will not be distorted by coupling with other modes of vibration. The consistency obtaining in the data here presented for frequency *versus* temperature, indicates that the use of harmonics of higher order for frequency measurements provides a very successful method for eliminating the perturbations of the frequency caused by edge effects.

In the equation of vibration for the plates (Eqs. (I) to (X)), the elastic constants and the κ^2's involved are all functions of temperature. Furthermore, in Eqs. (VI) to (X), the coefficients of the c's are direction cosines of the plate orientations which are also functions of temperature. From the manner in which the κ^2's and the direction cosines vary with temperature, it is possible to differentiate Eqs. (I) to (X) with respect to temperature, and to solve the resulting equations for the dC_{ij}/dT's, T being temperature.

By Eq. (11)

$$\kappa^2 = 4\rho s^2 f^2, \quad (f = \lim f_n/n \text{ as } n \to \infty)$$

f here being the theoretical fundamental frequency of the plate. Since the density, thickness, and frequency, are all functions of temperature, then

$$\frac{d\kappa^2}{dT} = \frac{\partial \kappa^2}{\partial f}\frac{df}{dT} + \frac{\partial \kappa^2}{\partial s}\frac{ds}{dT} + \frac{\partial \kappa^2}{\partial \rho}\frac{d\rho}{dT}$$

$$= 8\rho s^2 f \frac{df}{dT} + 8\rho s f^2 \frac{ds}{dT} + 4 s^2 f^2 \frac{d\rho}{dT}.$$

All the quantities on the right side of this equation are determined (see Table I) except the quantities ds/dT and $d\rho/dT$ which can be calculated from the accepted coefficients of expansion of quartz, so it is possible for $d\kappa^2/dT$ to be determined. These data are presented in Table III. It may be pointed out that the term $(\partial\kappa^2/\partial f)(df/dT)$, column 2, and not $d\kappa^2/dT$, is the term which must be zero in order for a quartz plate to have a zero temperature coefficient.

By use of the derivatives of Eq. (I) and (II), dC_{11}/dT and dC_{66}/dT are found to be equal to -0.00435 and $+0.00693$, respectively, the units being 10^{10} dynes/cm^2/°C. Similarly, by use of Eqs. (III), (V), and (VI), the quantities dC_{44}/dT, dC_{24}/dT, and dC_{56}/dT can be determined, and these values substituted in the remaining equations for the determination of dC_{13}/dT and dC_{33}/dT.

TABLE IV. *The temperature coefficients of the elastic constants of quartz.*

c_{ij}	$\frac{dc_{ij}}{dT}$	$\delta c_{ij} = \frac{dc_{ij}}{dT} \Big/ c_{ij}$	δc_{ij} As Determined by Bechmann[1, 2]	δc_{ij} As Determined by Mason[3]	δc_{ij} As Determined by Koga[4]
c_{11}	-0.00435	-49.7×10^{-6}	-48×10^{-6}	-54×10^{-6}	-61.1×10^{-6}
c_{66}	$+0.00693$	$+170.1$	$+144$	$+161$	$+199$
c_{12}	-0.01821	-3000	-2115	-2350	
c_{44}	-0.00965	-169	-151	-160	-199
c_{14}	$+0.00184$	$+107$	$+82$	$+96$	$+110$
c_{25}	$+0.00143$	$+78$			
c_{13}	-0.00765	-580	-530	-687	
c_{33}	-0.0227	-213	-208	-251	

[1] R. Bechmann, Hoch: tech. u. Elek: akus. **44**, 145 (1934).
[2] A. Scheibe, *Piezoelektrizität des Quarzes* (Theodor Steinkopff, Dresden, 1938), p. 54.
[3] W. P. Mason, Bell Sys. Tech. J. **19**, 85 (1940).
[4] I. Koga, Rep. Radio Research, Japan **6**, 1 (1934).

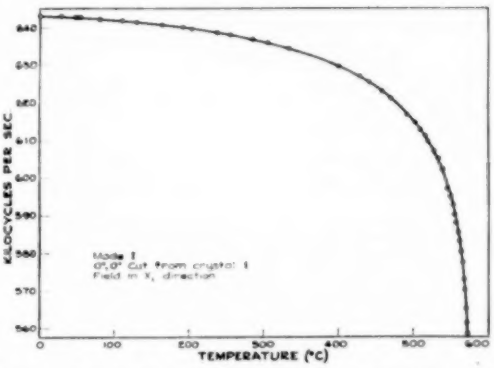

FIG. 11. Variation of the fundamental frequency of mode (I) with temperature.

In the differentiation of the equations, the direction cosines occurring in Eqs. (VI) and (VII) were taken as variables, the effect of the variation of these cosines with temperature being found to be small but not negligible. In Eqs. (VIII), (IX), and (X), however, because of the extreme complexity of these equations, the direction cosines were assumed to be constants. It was found, however, that the two unknowns, dC_{13}/dT and dC_{33}/dT, obtained by solving the different possible combinations of pairs of the differentials of the four equations (VII) to (X), were surprisingly consistent. Table IV contains the experimentally determined values of the rates of change of the elastic constants with respect to temperature, and also the values of the temperature coefficients of the elastic constants, δc_{ij}, the latter being the quantities dc_{ij}/dT divided by the corresponding c_{ij}'s. For purposes of comparison, the table also contains values of the temperature coefficients obtained by other investigators.

THE ELASTIC CONSTANTS AT HIGHER TEMPERATURES

In a further investigation, the resonance frequencies of certain of the (0°, 0°) and (30°, 0°) plates were investigated up to and beyond the critical point of quartz. In Figs. 11 to 14 are

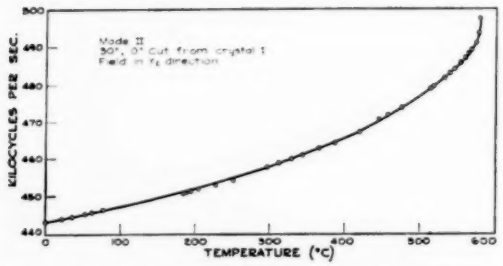

FIG. 12. Variation of the fundamental frequency of mode (II) with temperature.

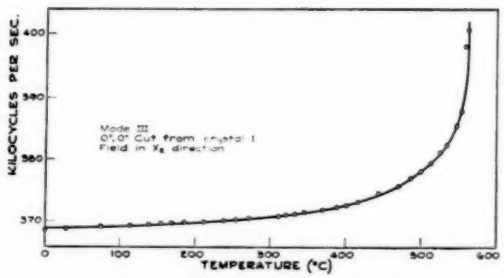

FIG. 13. Variation of the fundamental frequency of mode (III) with temperature.

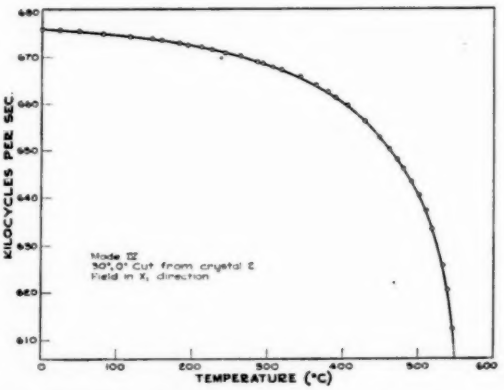

FIG. 14. Variation of the fundamental frequency of mode (IV) with temperature.

presented the fundamental frequencies of modes of vibration (I), (II), (III), and (IV), as a function of the temperature. The data for these curves were obtained by following the 17th, 27th, 27th, and 15th plate harmonics, respectively, in the above modes of vibration as the temperature was changed. The thickness of the plates at 35°C for modes (I) to (IV) were, 0.44731 cm, 0.44124 cm, 0.44731 cm, and 0.44454 cm, respectively.

If it be assumed that $-c_{24}=c_{56}=c_{14}$, it is possible to solve Eqs. (I) to (IV) simultaneously for the evaluation of four of the elastic constants at temperatures approaching the critical point. While the previous evidence given here indicates that $-c_{24}$ may not equal c_{56}, still such calculations may yield useful information on the behavior of the elastic constants at higher temperatures, although the values of c_{44} and c_{14} obtained will not agree with those obtained before because of the assumption here that $-c_{24}=c_{56}$. In Table V are presented the elastic constants obtained by Eqs. (I) to (IV) through the use of the data given in Figs. 11 to 14, the elastic constants being corrected for the change in thickness and density of the plates with temperature.

Since modes (III) and (IV) became too weak to measure as the critical point was approached, c_{44} and c_{14} cannot be evaluated at that point through these data. However, the trend of the data indicates that c_{44} approaches a minimum of about 30 at the transition point, while c_{14} seems to fall to zero, c_{14} for β-quartz being equal to zero. It will be noticed that c_{14} first exhibits a positive temperature coefficient and that this coefficient later becomes negative.

Mode of vibration (II) seems to have continued being excited for a short time after the transition point (probably indicated by the sudden change in slope in Fig. 12) was reached, thus determining the value of c_{66} for β-quartz at 580°C, although this latter point may be somewhat in doubt.

The frequencies of vibration of modes (I) to (IV) were all carefully checked at 35°C both before and after being heated beyond the critical point, and these frequencies were found to coincide exactly. Therefore, although the piezoelectric strength was observed in certain cases to have been changed by the heating, the elastic constants evidently were not altered.

In conclusion we wish to thank Professor G. L. Clark and Dr. S. T. Gross of the University of Illinois for making the Laue photographs to check the orientations of the plates and for several helpful discussions.

TABLE V. *Four of the elastic constants of quartz at various temperatures.*

	0°C	100°	200°	300°	400°	500°	540°	550°	562°	573°	580°
c_{11}	87.7	87.3	86.6	85.5	83.6	79.6	76.3	74.6	71.6	65.7	
c_{66}	40.5	41.2	42.0	43.1	44.5	46.7	47.8	48.2	48.7	49.3	50.6
c_{44}	55.9	55.0	53.7	51.8	49.2	44.1	38.0	37.4	<33.8		
c_{14}	17.8	17.9	18.0	17.9	17.4	15.2	12.4	10.1			

A Determination of the c_{44} Elastic Constant for Beta-Quartz

JOHN V. ATANASOFF AND ERWIN KAMMER
Iowa State College, Ames, Iowa
(Received August 28, 1940)

A careful determination of the elastic constant c_{44} of beta-quartz has been made using the method of Atanasoff and Hart. The results obtained, $c_{44}=35.75\times10^{10}$ dynes/cm², differs by a factor of nearly two from the only other published value. A study of the behavior of this constant in the range 0° to 650°C, the consistency in the value obtained from different cuts from different crystals and other facts seem to justify the value of the constant here determined.

THE work described here is an outgrowth of several researches which have been performed at this laboratory in the past few years. Wilson[1] has investigated the piezoelectric oscillations of quartz plates. Atanasoff and Hart[2] later calculated the elastic constants of quartz from measurements of the frequencies of the piezoelectric vibrations of plates cut from the crystal at specific orientations. This work has demonstrated the advantage of using high order harmonics in measuring the wave velocity to avoid edge effects. Since these researches had been confined to alpha-quartz, it was proposed to apply this technique to the determinations of the elastic properties of beta-quartz. The only measurements of the elastic properties of beta-quartz are those of Osterberg and Cookson[3] who used an interference method with monochromatic light to determine whether the crystal was oscillating and, if so, the mode of oscillation.

A detailed derivation of the mathematical expressions applicable to alpha-quartz plates of any orientation with regard to the crystallographic axes is given in the work of Atanasoff and Hart.[2] However, we are interested in a different crystal structure, that of beta-quartz, and these expressions need some modification. Since the work of Bragg and Gibbs[4] and also that of Wyckoff[5] has established the symmetry class of beta-quartz to be C_6 rather than D_3 as in alpha-quartz, the matrix of the elastic constants, using Voigt's[6] notation, becomes:

$$\begin{matrix} c_{11} & c_{12} & c_{13} & 0 & 0 & 0 \\ & c_{11} & c_{13} & 0 & 0 & 0 \\ & & c_{33} & 0 & 0 & 0 \\ & & & c_{44} & 0 & 0 \\ & & & & c_{44} & 0 \\ & & & & & \tfrac{1}{2}(c_{11}-c_{12}). \end{matrix}$$

The c_{14} constant which is present in the matrix for alpha-quartz is zero here. An expansion of the secular equation (see Eqs. (I) and (III) of reference 2) for an infinite X cut plate will now be:

$$(c_{11}-\kappa^2)(c_{11}/2-c_{12}/2-\kappa^2)(c_{44}-\kappa^2)=0, \quad (1)$$

where κ^2 has the value, $4\rho s^2 f^2/n^2$, ρ being the density, s the thickness of the plate, and f is the frequency of the nth harmonic. An expansion of the secular equation for a Y cut plate (see Eqs. (II) and (IV) of reference 2) takes the following form:

$$(c_{11}/2-c_{12}/2-\kappa^2)(c_{22}-\kappa^2)(c_{44}-\kappa^2)=0. \quad (2)$$

To ascertain which modes of vibration will be excited when the crystal has the symmetry of beta-quartz, an examination of the piezoelectric tensor is necessary. In Voigt's[6] notation it has the components:

$$\begin{matrix} 0 & 0 & 0 & e_{14} & 0 & 0 \\ 0 & 0 & 0 & 0 & -e_{14} & 0 \\ 0 & 0 & 0 & 0 & 0 & 0. \end{matrix}$$

The term e_{14} implies the subscripts e_{123} or e_{132} being a term of a third-rank tensor. Hence an alternating electric field applied in the x_1 direction excites vibrations involving strain compo-

[1] R. G. Wilson, "A study of the piezoelectric oscillation of quartz plates," unpublished Thesis, Library, Iowa State College, Ames, Iowa, 1936.
[2] J. V. Atanasoff and P. J. Hart, Phys. Rev. **59**, 85 (1941), preceding paper.
[3] H. Osterberg and J. W. Cookson, J. Frank. Inst. **220**, 361–371 (1935).
[4] W. Bragg and R. E. Gibbs, Proc. Roy. Soc. London **A109**, 414 (1925).
[5] R. W. G. Wyckoff, Am. J. Sci. **11**, 112 (1926).
[6] W. Voigt, *Lehrbuch der Kristallphysik* (Teubner, Leipzig, 1928), 585–586 and 830–831.

TABLE I. *Dimensions of the plates.*

CRYSTAL 1	X	Y	Z
X cut	0.4472	1.305	2.238
Crystal 2			
Y cut	2.198	0.4445	2.180

nents θ_{23}. These excited vibrations are therefore shear modes. Hence the factor,

$$c_{44}-\kappa^2=0 \tag{3}$$

is the part of the secular equations (1) and (2) for both X and Y cuts with which we are concerned and c_{44} the elastic constant here determined.

The quartz plates used in this investigation were chosen from those used by Atanasoff and Hart[2] in their work on elastic constants. The orientations of the plates were accurate to within three minutes of arc as checked by Clark and Gross at the University of Illinois from Laue x-ray patterns. Twinned portions were in each case eliminated after examination in polarized light. Etching of these crystals also verified the uniformity of the material. The dimensions (in centimeters) of the plates used are listed in Table I. The experimental method used was identical with that of Atanasoff and Hart.[2]

Typical data obtained near the temperature of 600°C are exhibited in Tables II and III. From the term involving c_{44} in Eqs. (1) and (2), the elastic constant for beta-quartz at 600°C is:

$c_{44}=4\rho s^2 f^2/n^2=35.75\times10^{10}$ dynes/cm² from the X cut plate

$c_{44}=4\rho s^2 f^2/n^2=35.78\times10^{10}$ dynes/cm² from the Y cut plate.

By means of linear interpolation, the value of the frequency at 600°C has been estimated from Tables II and III for use in the above calculation. The value for the density of quartz used is that of Day, Sosman and Hostetter,[7] namely 2.517 g/cm³ at 600°C. To calculate the value of the new thickness at the high temperature from that measured at room temperature, the change in linear dimension was estimated from the work of Le Chatelier as reproduced in Vigoreux.[8]

[7] A. L. Day, R. B. Sosman and J. C. Hostetter, Am. J. Sci. **37**, 16 (1914).

[8] P. Vigoreux, *Quartz Resonators and Oscillators* (His Majesty's Stationery Office, London, 1931).

In Fig. 1 there is plotted the value of c_{44} throughout the range from 0°C to 650°C. The values below the transition point are those of Atanasoff and Hart.[2] The point at 562°C is not known accurately because of a lack of knowledge of the elastic constant c_{24} involved in the secular equation (IV) as given in the paper of Atanasoff and Hart.[2] However, the curve at this temperature must be above the point plotted, otherwise the values of c_{24} would be imaginary. On the other hand, the crystal class of beta-quartz requires this constant to be zero. The shape of the dotted portion of the curve is suggested by direct observations of elastic coefficients near the critical temperature.[9] For some reason, the electrical response of a crystal in the neighborhood of the critical point is very weak and this accounts for the absence of data in that region. The cause of this weak response is uncertain, but it is unlikely that the piezoelectric constant involved falls to a small value near the critical point. It may be that irreversible changes induced by the vibrations absorb their energy. This explanation is supported by the observed fact that the oscillations can be followed closer to the critical point when approaching it from the high temperature side.

The value of the elastic constant c_{44} calculated above is in sharp disagreement with the value of 19.36×10^{10} dynes/cm² given by Osterberg and Cookson[3] at the same temperature. In determining this constant for beta-quartz, Osterberg and Cookson[3] have employed a theory

TABLE II. *The frequency f/n of the Y cut beta-quartz plate. Frequencies are given in kilocycles per second and temperature in degrees centigrade.*

TEMPERATURE	OBSERVED FREQUENCY f	HARMONIC OF CRYSTAL n	f/n
587	9582.8	23	416.64
592	10422	25	416.88
594	11259	27	417.00
598	10433	25	417.32
603	10440	25	417.60
606	10446	25	417.84
592	2917.4	7	416.77
598	2921.0	7	417.28
602	2922.6	7	417.52
606	2924.7	7	417.82

[9] R. B. Sosman, *The Properties of Silica* (Chemical Catalog Company, New York, 1927), p. 466.

which is closely related to one given by Mason,[10] yielding an expression of the form:

$$F_{np}=\tfrac{1}{4}(c_{44}/\rho)^{\frac{1}{2}}(n^2/y^2+p^2/z^2)^{\frac{1}{2}}$$

or

$$F_{mp}=\tfrac{1}{4}(c_{44}/\rho)^{\frac{1}{2}}(m^2/x^2+p^2/z^2)^{\frac{1}{2}},$$

where F is the observed frequency of oscillation, c_{44} is the elastic constant calculated for beta-quartz, ρ is the density, while x, y and z are the half-dimensions of the rectangular parallelepiped quartz specimen along the indicated axes. This theoretical treatment was admittedly an approximation, but some such approximation was found necessary. A more exact theory of vibration is required to permit the calculation of the elastic constants with any accuracy for the lower modes. Their theory seems to stand in the following relation to an accurate theory of finite plates for which their treatment is proposed. (A) Certain body constraints are assumed which simplify the differential equation describing the problem. (B) Certain boundary conditions are left unsatisfied by the solution chosen for this differential equation.

TABLE III. *The frequency f/n of the X cut beta-quartz plate. Frequencies are given in kilocycles per second and temperature in degrees centigrade.*

TEMPERATURE	OBSERVED FREQUENCY f	HARMONIC OF CRYSTAL n	f/n
611	2910.0	7	415.71
598	2902.8	7	414.69
592	2899.3	7	414.19
618	8738.1	21	416.10
618	7072.5	17	416.03
618	6240.5	15	416.03
618	5409.7	13	416.13
618	3746.0	9	416.22
618	2912.0	7	416.00
618	2083.2	5	416.65

[10] W. P. Mason, Bell Sys. Tech. J. **13**, 446–448 (1934).

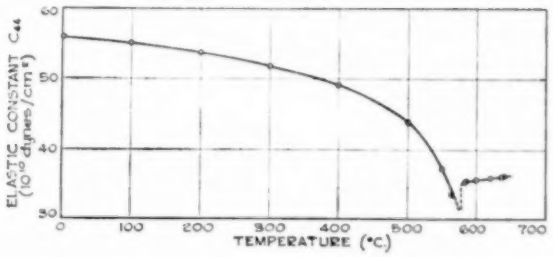

FIG. 1. Variation of the elastic constant c_{44} with temperature.

The imposition of constraints upon a vibrating system, as in *A*, has the effect of raising the frequency of vibration.[11] Hence, if a measured frequency of vibration is inserted into either formula above, the elastic constant c_{44} so calculated would have a value lower than it would for the case in which no constraint was supposed in the theoretical development. Leaving some boundary conditions unsatisfied, as in *B*, however, has the effect of removing constraints upon the vibrating system. This would cause the frequency of vibration to be decreased.[10] Thus the mathematical treatment of the problem used by Osterberg and Cookson is open to question. In fact, the elastic constant c_{44} as calculated by them has a different value for each type of vibration studied. Also the values obtained for this constant on crystals of different dimensions do not agree. This certainly indicates that the mathematical methods used in deriving these results are not adequate and it may even be that there has been an error in the identification of the modes of vibration.

It is a pleasure to thank Dr. Philip J. Hart for considerable assistance in the experimental part of this paper.

[11] R. Courant and D. Hilbert, *Methoden der Mathematischen Physik* (Julius Springer, Berlin, 1931), Part II, p. 244.

Protons of Double Charge and the Scattering of Mesons

H. J. BHABHA
Indian Institute of Science, Bangalore, India
(Received November 16, 1940)

THE purpose of this note is to give a new formula for the scattering of mesons and to draw the attention of experimental physicists* to the consequences of a theory recently put forward by the present author[1] which predicts the existence of protons of charge $2e$ and $-e$ so that a proper search might be made for these particles.

On the old theory the cross section for the scattering of longitudinally polarized *charged* mesons by a proton or neutron caused by the charge of the heavy particles (g_1 interaction) was of the form

$$\text{constant } (g_1^2/\mu c^2)^2 p^4/\mu^2 E^2. \tag{1}$$

E denotes the energy, p the momentum and μ the rest mass of a meson. For high energies this cross section increases as E^2 and therefore completely robs the meson of its penetrating power. The corresponding cross section for the scattering of longitudinally polarized *neutral* mesons was calculated in a previous paper[2] (formula (43)) and correct to 1 percent it may be written in the simpler form

$$6\pi\frac{\mu^2c^4}{E^2}\left(1+\frac{1}{2}\frac{\mu^2c^4}{E^2}\right)\frac{1}{(3Mc^2/2g_1^2)^2+\{(E/hc)^2\}}. \tag{2}$$

Even without the term in curly brackets which expresses the effects of radiation reaction, (2) would decrease as E^{-2} and is less than (1) by an order of magnitude caused by the appearance of M (the proton mass) instead of μ in the denominator. This difference between (1) and (2) is entirely caused by the fact that whereas on the accepted theory a positive meson can only be absorbed by a neutron and emitted by a proton, a neutral meson can be absorbed and emitted by both.[2] There are thus twice as many states leading to the scattering of neutral as of charged mesons and these largely cancel each other, reducing the cross section (1) to the magnitude (2). To avoid this difficulty I put forward the idea[1] that the heavy particles could exist in states of all integral charge positive and negative with different rest energies, of which only the two of lowest energy (rest mass), namely the proton and neutron, appear normally in nature. This idea was communicated to Dr. Heitler[3] and has been adopted by him to recalculate the scattering of charged mesons. It reduces the cross section (1) to a magnitude of the order (2). Further arguments in favor of this idea are given in my paper.[1]

A definite consequence of this assumption is that protons of charge $2e$ and $-e$ must also occur in nature. The processes leading to the production of these particles and the circumstances under which they might be expected to occur have been investigated in the above paper.[1] The most probable process for the production of these particles is the collision of two protons or two neutrons, thus

$$\begin{aligned} P+P &\rightarrow P_2+N \\ N+N &\rightarrow P_-+P \end{aligned} \tag{3}$$

where P_2 and P_{-1} denote the protons of charge $2e$ and $-e$, respectively. The process (3) only takes place if the kinetic energy of the colliding particles is at least twice the mass excess of a doubly charged proton over an ordinary proton, i.e., about 35 Mev. The cross section for the process (3) is of the order 10^{-25} cm^2, so that a very energetic proton would produce a proton of charge $2e$ after some 5 g/cm^2 of hydrogen. The doubly charged proton would not, however, emerge as frequently as an ordinary proton from heavy nuclei because at least 17 Mev goes to its

* At my suggestion Professor H. J. Taylor made a search last May in photographic plates suitably treated to show the tracks of heavy particles and exposed on the Himalayas to cosmic radiation at a height of 18,000 feet. It is Professor Taylor's opinion that this method is not sensitive enough to distinguish between a proton, a proton of charge $2e$ and an α-particle. The search is therefore best made with a Wilson chamber.

[1] H. J. Bhabha, Proc. Ind. Acad. Sci. **A11**, 347–368, 468 (1940).

[2] H. J. Bhabha, Proc. Roy. Soc. **A172**, 384–409 (1939).

[3] W. Heitler, Nature **145**, 29 (1940).

creation and the double charge makes the penetration of the Coulomb barrier more difficult. The cross section for the creation of the new particles by fast mesons or γ-rays is of the order 10^{-29} cm^2. For mesons which have come to rest, the capture probability of a negative meson resulting in the conversion of a nuclear neutron into a negative proton is of the order 10^{11} per second, while for positive mesons it is negligible on account of the Coulomb repulsion.[4]

The new particles are unstable, the mean lifetime for spontaneous β-decay into an ordinary proton or neutron being $\frac{1}{6}$ sec., while the lifetime for annihilation of a negative proton by a reverse of the process (3) is $3\times10^{-5}/Z$ second in gases, Z being the atomic number of the gas.

The above assumption of new particles does not diminish the scattering of mesons caused by the *spin* of the heavy particles (g_2 interaction), which still remains of the order (1). I have now extended the classical theory of spinning particles moving in a Maxwell field[5] to cover a meson field. The resulting cross section for the scattering of *transversely polarized* mesons caused by the *spin* of the heavy particles on this theory can be written correctly to within 2 percent in the simple form

$$4\pi\frac{p^4}{(3\mu c^2/4g_2'^2)^2\mu^2E^2+p^6h^{-2}} \qquad (5)$$

The scattering is a large angle scattering, so that whenever it takes place, the meson is removed from the beam. The smooth curve in Fig. 1 shows the dependence of this cross section on energy, plotted for $g_2'^2/hc=1/13.3$. For low energies the cross section is of the order (1) and agrees with the old quantum-mechanical cross section, as shown by the broken curve. It is a maximum at $E\sim3.5\mu c^2$, its value at the maximum being $\sim3\times10^{-26}$ cm^2 if we take $\mu c^2=85\times10^6$ ev. In spite of its largeness, the above cross section does not deprive the meson of its penetrating power since it decreases for high energies as p^{-2} due to the p^6 term in the denominator which expresses the effects of radiation reaction. The

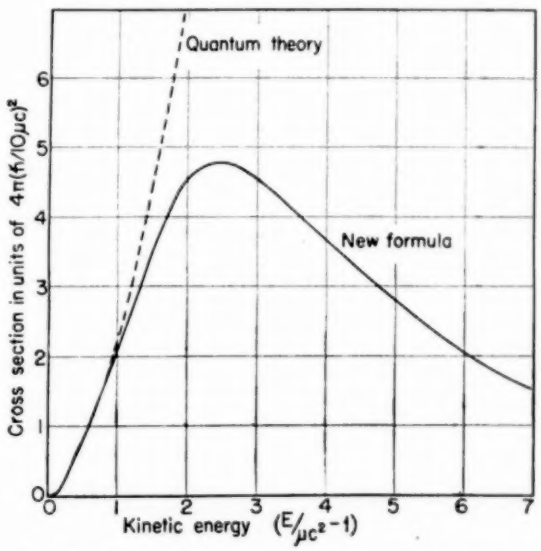

FIG. 1. The variation of cross section with energy.

main scattering takes place for energies near $3\mu c^2$, and still further accentuates the cutting off of the energy spectrum of mesons for energies *below* $3\mu c^2$, as calculated by Euler and Heisenberg.[6] This agrees better with the observations of Blackett.[7]

Longitudinally polarized mesons are not scattered by the rotation of the spin and hence their scattering is of the order (2). This is less than (5) by a factor $(g_1^2/hc)^2(\mu/M)^2<1/20{,}000$. *Thus longitudinally polarized mesons are very much more penetrating than transversely polarized mesons.*

[4] Cf. S. Tomonaga and G. Araki, Phys. Rev. **58**, 90 (1940) for ordinary capture.

[5] H. J. Bhabha, Proc. Ind. Acad. Sci. **A11**, 247–267, 467 (1940); Nature **145**, 819 (1940).

[6] H. Euler and W. Heisenberg, Ergeb. d. exakt. Naturwiss. **17** (1938).

[7] P. M. S. Blackett, Proc. Roy. Soc. **A165**, 11–31 (1938).

Letters to the Editor

PROMPT publication of brief reports of important discoveries in physics may be secured by addressing them to this department. Closing dates for this department are, for the first issue of the month, the eighteenth of the preceding month, for the second issue, the third of the month. Because of the late closing dates for the section no proof can be shown to authors. The Board of Editors does not hold itself responsible for the opinions expressed by the correspondents.

Communications should not in general exceed 600 words in length.

Capture Cross Sections for C Neutrons

R. D. O'NEAL AND M. GOLDHABER
Department of Physics, University of Illinois, Urbana, Illinois
December 16, 1940

The total and scattering cross sections for slow neutrons have been measured reasonably well for most elements, but the capture cross sections are known for a few elements only. Lapointe and Rasetti,[1] simplifying the well-known "neutron density method" of Frisch, Halban and Koch,[2] have measured a number of capture cross sections for thermal neutrons. Their method, however, is valid only for capture cross sections $>10^{-24}$ cm². For smaller cross sections the "method of induced radioactivity" has recently been applied by Rasetti[3] and by the authors.[4] Though this method does not allow of any great accuracy it yields some valuable information which would be difficult to obtain in any other way.

This method can be employed for nuclei where the capture of a slow neutron leads to the formation of a radioactive isotope. By exposing an element of unknown capture cross section (σ_c) to slow neutrons, and comparing its activity with that produced under the same conditions in an element of known capture cross section one can calculate σ_c. A convenient standard for such measurements is Mn ($\sigma_c = 9.4\times10^{-24}$ cm²). Though our procedure was different from Rasetti's, as far as the geometrical arrangement is concerned, the agreement between his and our values is as good as can be expected for β-ray measurements. On the whole, we used thicker samples, of the order of one to two β-half-value thicknesses. To avoid several corrections, especially those caused by the difference in scattering and stopping power of different elements for β-rays, mixtures of Mn and the element under investigation, or an element close to it in atomic number, were exposed to slow neutrons. The largest errors are introduced by the somewhat uncertain corrections for the difference in the β-ray energies of the isotopes investigated and the standard element Mn. The effect caused by resonance neutrons was obtained in every case by repeating the measurement with samples exposed inside Cd. Only for the Sb and Ga isotopes was this contribution large. Just one-half of the light elements with $Z\leq20$ have properties which allow their investigation with a 100-mg Ra$-\alpha-$Be source. We have studied all these, and a few heavier ones.

Our results, somewhat revised and extended since our first report, are summarized in Table I. For K, which is difficult to investigate because of its natural radioactivity, we had previously reported $\sigma_{\text{eff}}<0.05\times10^{-24}$ cm². A repetition of the measurement under improved conditions gave a value in agreement with Rasetti's.

We wish to thank Professor Rasetti for informing us of his results before publication.

TABLE I. *Summary of results for capture cross sections for C neutrons. T = half-lifetime of radioactive isotope, σ_{eff} = effective cross section per "average" atom, σ_c = capture cross section corrected for abundance of isotope. The values marked (p) signify partial cross sections, as these isotopes may partially decay by β-emission and partially by K-electron capture. For comparison we give in the last two columns Rasetti's values and those measured by Manley, Haworth and Luebke,[5] with the help of a strong D+D neutron source.*

ELEMENT	T	σ_{eff} 10^{-24} CM²	ABSORBING ISOTOPE	σ_c IN 10^{-24} CM² AUTHORS	R	M, H AND L
$_{7}$N*	8 sec.	—	N^{15}	<0.2		<0.01
$_{9}$F	12 sec.	<0.05	F^{19}	<0.05		0.01
$_{11}$Na	14.8 hr.	0.4	Na^{23}	0.4	0.35	
$_{12}$Mg	10.2 min.	0.03	Mg^{26}	0.3		
$_{13}$Al	2.4 min.	0.2	Al^{27}	0.2	0.21	
$_{14}$Si	170 min.	<0.02	Si^{30}	<0.5		
$_{15}$P	14.3 days	0.3	P^{31}	0.3	~0.2	
$_{17}$Cl	37 min.	0.07	Cl^{37}	0.3		
$_{19}$K	12.4 hr.	~0.1	K^{41}	~1.5	~1.4	
$_{20}$Ca	2.5 hr.	<0.01	Ca^{48}	<5		
$_{28}$Ni	2.6 hr.	0.03	(Ni^{62})	(0.8)		
$_{29}$Cu	5 min.	0.8	Cu^{65}	2.4	1.8	
$_{31}$Ga	20 min.	0.6	Ga^{69}	1 (p)		
	14 hr.	1	Ga^{71}	2.6		
$_{51}$Sb	2.8 days	2	Sb^{121}	3.6 (p)	3.3	
	60 days	1	Sb^{123}	2.3 (p)		
$_{81}$Tl	4.2 min.	<1	Tl^{205}	<3.3 (p)		0.17
$_{83}$Bi	5 days	<0.1	Bi^{209}	<0.1		

* Through the courtesy of Professor Urey we were able to use ammonium nitrate enriched in N^{15} for this experiment.

[1] C. Lapointe and F. Rasetti, Phys. Rev. **58**, 554 (1940).
[2] O. R. Frisch, H. v. Halban and J. Koch, Proc. Danish Acad. **15**, 10 (1938).
[3] F. Rasetti, Phys. Rev. **58**, 869 (1940).
[4] M. Goldhaber and R. D. O'Neal, Phys. Rev. **59**, 109A (1941).
[5] J. H. Manley, L. J. Haworth and E. A. Luebke, Phys. Rev. **59**, 109A (1941).

The Abundance Ratio Ni^{61} : Ni^{64}

HENRY A. STRAUS
Ryerson Physical Laboratory, University of Chicago, Chicago, Illinois
December 3, 1940

The published values of the isotopic constitution of nickel have for some time shown strong discrepancies with respect to the ratio Ni^{61} : Ni^{64}. Aston[1] found Ni^{61} to be 1.7 percent of the total and failed to detect Ni^{64}. De Gier and Zeeman,[2] using the parabola method, failed to find Ni^{61} and found Ni^{64} to be 0.9 percent of the total. Lub,[3] using a similar apparatus, found Ni^{64} to be 0.9 percent of the total but found Ni^{61} to constitute 0.1 percent. Dempster[4] found Ni^{61} to be approximately equal in abundance to Ni^{64}.

These results were obtained photographically. Dempster used a spark between nickel electrodes as an ion source. The others used a discharge tube containing nickel carbonyl. In the latter case, the organic compounds present in the source may lead to entirely erroneous estimates of intensity because of their superposition on the lines of the substance under study.

In this work a new double-focusing mass spectrograph was used to separate the ions of the different isotopes. The ions were produced in the type of source developed by Dempster, in which an oscillating spark between nickel electrodes 1.5 mm in diameter is used. A collector system consisting of a pair of Faraday chambers whose apertures were large enough to collect all the ions of one mass was used. The separation of the collectors could be varied so that they would simultaneously collect the current caused by a pair of isotopes. The currents to the Faraday chambers were measured by two electrometers, with a null method of comparison in which the collected charges were balanced out by induced charges. This method reduces errors caused by leakage, makes the measurement less dependent on electrometer sensitivity, and reduces errors caused by fluctuations of source intensity.

The ratio of abundance of Ni^{61} : Ni^{64} was determined by setting the collector separation for three mass units and comparing the currents carried by the ions at the mass numbers 61 and 64. Then the collectors were set to a separation corresponding to two mass units and the ratio of the current at 59 and at 63 to the current at 61 was determined. This enables one to estimate the strength of the scattered background of ions at 61 due to 60 and 62, since the ratio of Ni^{58} to Ni^{60} has been determined. The corrected ratio of Ni^{61} : Ni^{64} was found to be 1.3. A more extended report of this work is to appear in the near future.

[1] F. W. Aston, Proc. Roy. Soc. **149**, 396 (1935).
[2] J. de Gier and P. Zeeman, K. Akad. Amst. Proc. **38.8**, 810 (1935).
[3] W. A. Lub, K. Akad. Amst. Proc. **42.3**, 253 (1939).
[4] A. J. Dempster, Phys. Rev. **50**, 98 (1936).

Production of He^3

R. D. Hill
University of Melbourne, Melbourne, Australia
November 8, 1940

Since no He^3 is known to be evolved naturally it seems feasible that its presence[1] in the atmosphere may be explained by means of transmutations involving cosmic rays. Of these reactions, it would appear that the Li^6 slow neutron reaction is the most probable. An estimate of the He^3 yield by this reaction has been made as follows.

The number of neutrons which would have been captured by Li^6 in the earth's crust has been calculated from the expression:

$$\frac{f\rho SAT}{k}\left(1+\frac{e^{-kX_0}}{kX_0}-\frac{1}{kX_0}\right) \quad \text{where} \quad f=\frac{\sigma_{Li^6}N_{Li^6}}{\Sigma\sigma N},$$

σ and N being the relative capture cross sections and relative abundances of the various atoms in the earth's crust, ρ the density of crust, S the area of the continental land, A the number of neutrons per g per sec. produced at the upper surface of crust by cosmic rays (it is assumed that the neutrons do not diffuse great distances from their place of production), T the period over which the He^3 atoms have collected on the earth, k the absorption coefficient of the neutron-producing cosmic rays and X_0 the depth of denudation during the time T. These quantities have the following estimated values: $f\sim 3\times 10^{-3}$ (thermal neutrons), $\rho=2.7$ g cm^{-3}, $S\sim 1.5\times 10^{18}$ cm^2, $A\sim 10^{-4}$ g^{-1} sec.$^{-1}$ at sea level,[2] $k\sim 1.8\times 10^{-2}$,[2] $X_0\sim 2\times 10^4$ cm, $T\sim 2\times 10^9$ yr.* Since κX_0 is large, the number of Li^6 atoms disintegrated is $f\rho SAT/k\sim 4.5\times 10^{30}$. Assuming a He^3/He^4 ratio of 10^{-7},[1] the number of He^3 atoms observed to be present in the air is $\sim 4\times 10^{31}$.

While this estimate of the production of He^3 appears to be slightly too low, it may be possible to explain a higher yield as caused by a higher intensity of neutrons. The value of A is probably larger on account of (1) a distribution of land having altitudes greater than sea level (2) the depth of the atmosphere being significantly less throughout the earth's age than it is today. The absorption of Li atoms present in sea water can give only a slight increase in He^3 yield because of the large capture of thermal neutrons by hydrogen and chlorine.

According to the present explanation of the existence of He^3, the lower concentration of He^3 in gas-well helium[1] may be a consequence of its evolution mainly in the upper layers of the earth's crust.

[1] L. W. Alvarez and R. Cornog, Phys. Rev. **56**, 379, 613 (1939).
[2] S. A. Korff, Rev. Mod. Phys. **11**, 211 (1939); Bethe, Korff and Placzek, Phys. Rev. **57**, 573 (1940); C. G. Montgomery and D. D. Montgomery, Rev. Mod. Phys. **11**, 255 (1939).

* *Editorial Note.* In connection with the choice of the value of T, Dr. H. Goldhaber to whom the author sent this letter for criticism remarks that a better value might be 3×10^7 years. As was first recognized by Jeffreys, the amount of He^4 in the atmosphere is much smaller than might be expected from the amount generated through α-particle decay during 2×10^9 years. This has been ascribed to loss of helium atoms at the top of the atmosphere, presumably through collisions of the second kind. (See H. N. Russell, *The Solar System and Its Origin* (New York, 1935), p. 76.) The average time which a helium atom spends in the atmosphere has been estimated to be about 3×10^7 years. It would appear that this value, rather than the age of the earth, should be inserted for T in Mr. Hill's formula. This would lead to a still smaller value for the He^3 content of the atmosphere. However, an estimate of this type must necessarily remain somewhat uncertain, since several of the values appearing in the formula, as well as the He^3 content of the atmosphere, are only roughly known at present.

Correction: Isotope Shift in Boron

(Phys. Rev. **58**, 879 (1940))

John P. Vinti
Worcester Polytechnic Institute, Worcester, Massachusetts
December 11, 1940

A mistake was made in quoting Mrozowski's[1] results on the shift of the line λ3451 of B II. In his plates this line was actually fully resolved, so that the shift was measured directly and not by decomposition into two Doppler curves as in the cases λ2497, 2498 of B I. Numerical data on breadths of the components of λ3451 are not given in Mrozowski's paper, but he has kindly informed me by letter that the observed separation of the components (0.877 cm^{-1}) was about $4\frac{1}{2}$ times their half-widths. The half-widths thus amount to 0.2 cm^{-1}, or about 6 times the predicted spread due to nuclear spin of 0.031 cm^{-1}; the conclusion as to the unobservability of the latter thus remains valid.

[1] S. Mrozowski, Zeits. f. Physik **112**, 223 (1939).

Hyperfine Structure of Ionized Mercury Lines

S. MROZOWSKI
Ryerson Physical Laboratory, University of Chicago, Chicago, Illinois
December 8, 1940

In connection with my work on the "hyperfine structure of the quadrupole line 2815A and some other lines of ionized mercury,"[1] Dr. L. Sibaiya published a letter[2] in a recent issue of *The Physical Review* in which he refers to a paper on the "hyperfine structure of some Hg II lines" published by Venkatesachar and himself[3] several years ago. I regret very much that I had overlooked this interesting paper and did not refer to it in my article. The structure of the line 3984A observed by me deviates much less from their findings than from the data reported in papers of several authors referred to in my article. Nevertheless, I disagree with other statements of Dr. L. Sibaiya and I should like to make here a few remarks on this matter.

Although Venkatesachar and Sibaiya[3] found the correct correlation of components to the Hg isotopes in the line 3984A they were able to determine from the observed structure only the difference of separations in the two levels $6^2P_{3/2}$ and $5d^96s^2\,{}^2D_{5/2}$. Therefore, they calculated the splittings from the formula of Goudsmit.[4] As the calculated difference of separations did not agree closely with the measured value, for the $6^2P_{3/2}$ level they adopted the theoretical value without further explanation and then estimated the separation in the $^2D_{5/2}$ level from their experimental results. In contradistinction to this, all spin separations (Hg^{199}) and isotope shifts reported in my paper are purely experimental. On photographs with overexposed main components, a very weak component at about $+1.000$ cm^{-1} was observed which might permit the evaluation of the separations in each level independently. But, on account of the low accuracy of the measurements under these circumstances, this component was not reported in my paper and the analysis was carried out by using the separation of the $^2D_{5/2}$ level found from the measurements of the structure of the line 2815A. Since the separations found experimentally by me agree very closely with those expected from Goudsmit's formula, it is not surprising that they agree so perfectly with the value reported by Venkatesachar and Sibaiya in the case of the level $6^2P_{3/2}$ and less perfectly in the case of the level $^2D_{5/2}$.

My report[1] on the analysis of some allowed lines of Hg II (3984A and 2848A) was incidental, since the main purpose of my paper was the analysis of the forbidden quadrupole line 2815A. In the case of the line 2848A the structure observed by me[1] differs from the results of Venkatesachar and Sibaiya.[3] The last line investigated by Venkatesachar and Sibaiya[3] and mentioned in Dr. L. Sibaiya's letter,[2] namely the line 2262A, has also been analyzed by me, among many other lines of Hg II. My pictures show that the structure reported by Venkatesachar and Sibaiya is incomplete and is due to overlapping of orders (they used only one Lummer-Gehrcke plate for the analysis). Contrary to their conclusion, the odd isotopes have a quite considerable total spin separation in the upper state $5d^96s6p\,{}^2\bar{D}_{5/2}$ (about 0.7 cm^{-1}), which is in agreement with the presence of an unpaired $6s$ electron in this state. The correlation of the even isotopes is opposite to that adopted by Venkatesachar and Sibaiya. It leads to a considerably smaller isotope shift in the level $^2\bar{D}_{5/2}$ (0.3 cm^{-1}) than the value reported by them (0.68 cm^{-1}). The smaller shift is also in agreement with the presence of only one $6s$ electron (two $6s$ electrons give a shift of 0.5 cm^{-1} in the levels $5d^96s^2\,{}^2D_{3/2,\,5/2}$). I hope to report the results of the analysis of a considerable number of lines (about 130) of Hg II soon.

[1] S. Mrozowski, Phys. Rev. **57**, 207 (1940).
[2] L. Sibaiya, Phys. Rev. **58**, 925 (1940).
[3] B. Venkatesachar and L. Sibaiya, Proc. Ind. Acad. Sci. **1**, 8 (1934).
[4] S. Goudsmit, Phys. Rev. **43**, 636 (1933).

Isotopic Weights of Ni Isotopes by the Doublet Method

T. OKUDA, K. OGATA, H. KURODA, S. SHIMA AND S. SHINDO
Department of Physics, Faculty of Science, Osaka Imperial University, Osaka, Japan
November 10, 1940

There are five isotopes for Ni, their relative abundance being estimated as follows:[1]

MASS NO.	58	60	61	62	64
RELATIVE ABUNDANCE	68.0	27.2	0.1	3.8	0.9

While Aston[2] had reported the value of 57.9116 ± 0.0020 for the isotopic weight of Ni^{58}, we obtained the following values for mass differences of these five doublets by photographing all five doublets of Ni isotopes by the electric discharge through the vapor mixture of $Ni(CO)_4$ and $n-C_7H_{16}$ with a mass-spectrograph of Bainbridge-Jordan type.

DOUBLET	NUMBER OF DOUBLETS MEASURED	DIFFERENCE OF MASS ($\Delta M\times10^3$)
$C^{12}{}_4H_{10}-Ni^{58}$	16	137.12 ± 0.39
$C^{12}{}_5-Ni^{60}$	10	69.59 ± 0.31
$C^{12}{}_5H-Ni^{61}$	3	$73.5\ \pm1.5$
$C^{12}{}_5H_2-Ni^{62}$	7	86.07 ± 0.37
$C^{12}{}_5H_4-Ni^{64}$	3	104.48 ± 0.54

By employing these results as well as $H^1=1.008131\pm0.033\times10^{-4}$ and $C^{12}=12.003871\pm0.33\times10^{-4}$,[3] the isotopic weights of Ni isotopes were obtained as follows:

ISOTOPIC WEIGHT	PACKING FRACTION
$Ni^{58}=57.95967\pm4.1\times10^{-4}$	-6.97 ± 0.07
$Ni^{60}=59.94977\pm3.5$	-8.37 ± 0.06
$Ni^{61}=60.9540\ \pm15.$	$-7.5\ \pm0.3$
$Ni^{62}=61.94955\pm3.9$	-8.14 ± 0.06
$Ni^{64}=63.94740\pm5.6$	-8.22 ± 0.09

With both these results and aforementioned relative abundance, we calculated chemical atomic weight of Ni as 58.69, adopting the Smyth's conversion factor 1.000275. This value shows perfect agreement with the international chemical atomic weight of Ni 58.69.

[1] O. Hahn, S. Flügge, J. Mattauch, Physik. Zeits. **41**, 1 (1940).
[2] F. W. Aston, Nature **141**, 1096 (1938).
[3] K. Ogata, Proc. Phys.-Math. Soc. Japan **22**, 486 (1940).

Proceedings of the American Physical Society

Minutes of the Chicago, Illinois Meeting

November 22–23, 1940

THE 237th regular meeting of the American Physical Society was held at Chicago, Illinois, on Friday and Saturday, November 22 and 23, 1940 at the University of Chicago. The attendance at the meeting was about three hundred.

On Friday evening the Society held a dinner in Judson Court, at which members of the Chicago Physics Club were guests. The attendance was one hundred and fifty-six. Professor John Zeleny presided and the after-dinner speakers were Professor Arthur H. Compton, Dr. Karl K. Darrow, Dean Henry G. Gale, and Professor Robert A. Millikan. Preceding the dinner a reception was held in the lounge.

Meeting of the Council. At the meeting of the Council held on Friday, November 22, 1940 the deaths of two Fellows (Morris B. Crawford and James S. Stevens) and of two Members (William E. Harper and Clement Moran) were reported. One candidate was transferred from Membership to Fellowship and one hundred and fifty-six candidates were elected to Membership. *Transferred from Membership to Fellowship:* Howard A. Robinson. *Elected to Membership:* Lawrence H. Aller, A. Eugene Anderson, Wm. Alan Andrews, Edgar L. Armi, Gabrielle Asset, Melvin Avrami, Norman J. Bailey, Judd O. Baker, James C. Barnes, Walter M. Barss, Lowell C. Beers, M. F. Behar, Frederick D. Bennett, Rose Berger, George C. Bladwin, T. Robert Burnight, G. A. Burton, Wallace C. Caldwell, Britton Chance, William R. Clark, Norman D. Coggeshall, Arthur V. Cohee, Clifford H. Colpitts, Clarence M. Connelly, C. Sharp Cook, Jesse B. Coon, Eugene P. Cooper, Bruce B. Cork, Ernest D. Courant, William A. Crouse, Gordon A. Davis, Irvine H. Dearnley, Robert W. DeMonte, Dominic d'Eustachio, Charles F. DeVoe, John W. DeWire, P. J. Donovan, Ray L. Doran, Daniel R. Elliott, Louis D. Ellsworth, Richard M. Emberson, John C. Evvard, William Feldman, Gilbert H. Fett, Robert J. Finkelstein, R. E. Fox, Philipp G. Frank, William E. Frye, Duncan M. Gage, Herman B. Galvin, Ronald Geballe, John J. Gilvarry, Alvin Glassner, Ralph A. Goodwin, Robert B. Gray, Wilbur E. Gross, Andrew Guthrie, Frederick T. Haddock, Jr., Everett M. Hafner, William W. Havens, Jr., Ralph Heller, Stuart C. Hight, Robert C. Hilliard, James R. Hooper, Jr., Isidore Hudes, Charles L. Hutchinson, Edwin C. Hutter, Ludolph Jacobs, Robert L. Kamm, Kathleen M. Kane, H. Paul Koenig, Andrew P. Kruper, Satoshi Kusakabe, Eugene E. Lampi, John L. Laverty, Jr., Elliott Lawton, John G. Leschen, Leonard M. Liebermann, Milton Lipnick, Arnold N. Lowan, Robert F. McCune, Raymond H. McFee, Wayne L. McKusick, Edward B. Meservey, J. L. Michiels, Donald J. Middlehurst, Charles G. Miller, Leonard C. Miller, Francis M. Millican, Ferdinand H. Mitchell, Eugene Mittelmann, Lloyd Motz, Charles J. Mullin, Lloyd G. Mundie, Effraim A. Nahum, Henry W. Newson, Myron H. Nichols, John J. Oberly, Charles L. Oxley, George R. Paine, James P. Parker, Josephus O. Parr, Jr., Frederick W. Paul, Joseph A. Pearce, Gilbert J. Perlow, J. R. Perkins, Jr., Joseph E. Perry, Jr., Bernard Peters, Leroy E. Peterson, John R. Platt, Harry D. Polster, Albert F. Prebus, Victor Ragosine, James Rainwater, William L. Rast, Victor H. Regener, Herbert S. Ribner, John S. Rinehart, Nathan Rosen, Pearl J. Rubenstein, Henri S. Sack, Francis J. Safford, Aaron Sayvetz, Otto H. Schmitt, Raemer E. Schreiber, Elmer J. Scott, Robert W. Scott, Glenn T. Seaborg, Alex Shesterkin, John W. L. Shork, Stanley Siegel, John A. Simpson, Jr., Charles S. Smith, Jr., Ronald N. Smith, Donald O. Sproule, Philip M. Stehle, Joseph W. Straley, Lawrence J. Strohmeyer, Hubert E. Tanis, Jr., J. Earl Thomas, Roy Thomas, Robert W. Thompson, Luke V. Titone, William D. Townes, Anthony Turkevich, Katherine M. Van Horn, William S. Van Horne, Bob E. Watt, Paul K. Weimer, William L. Whitson, Carl P. Wiedow, John P. Woods, R. Edwin Worley, J. Howard Wright, Hubert P. Yockey and Paul A. Zahl.

The regular scientific program of the Society consisted of forty-nine contributed papers of which five, numbers 24, 27, 29, 32 and 49, were read by title. The abstracts of these papers are given in the following pages. An Author Index will be found at the end.

HAROLD W. WEBB, *Acting Secretary*
Columbia University, New York, N. Y.

ABSTRACTS OF CONTRIBUTED PAPERS

1. Low Terms in Co VII and Ni VIII. E. E. ANDERSON AND J. E. MACK, *University of Wisconsin.*—Bowen's work on the low levels in the scandium-like isoelectronic sequence up to Fe VI has been supplemented by the identification of the levels $3d^3\ {}^4FP\ {}^2GH$ (also Bowen's "*A*") and $3d^24p\ ({}^3F)\ {}^{4,2}GFD\ ({}^3P)\ {}^4DPS\ ({}^1G)\ {}^2HG$ in Co VII and Ni VIII. (There is doubt as to the reality of the proposed Ni VIII $d^3\ {}^2H_{5\frac{1}{2}}$, $d^2p\ ({}^3F)\ {}^2D\ ({}^3P)\ {}^4P\ ({}^1G)\ {}^2H_{5\frac{1}{2}}$.) The identification of appreciably more lines, especially intercombinations, here than in lower spectra in the sequence, may be attributed to the gradual change in coupling as well as the high excitation from our 2 μf, 60,000-volt sparks. Work is progressing on the comparison of the separations in $3d^3$ with Marvin's equations (for Co I d^7s^2, including *ls* interaction). Heretofore, among isoelectronic sequences in this neighborhood, no configuration $3d^{z-1}4p$ has been identified beyond stage VI. Undoubtedly the correct explanation of this limitation is Bowen's, that $3p^53d^{z+1}$ is expected to cross, and therefore disturb, $3d^{z-1}4p$ at about that stage. (At present a level in this neighborhood can hardly be expected to be found unless it can be predicted with fair accuracy.) Although some small irregularities remain to be explained, the general smoothness of the curves $\nu(Z)$ throughout this sequence indicates that $3p^53d^4$ is probably still well above $3d^24p$ in Ni VIII.

2. On the Spectrum of Hg II. S. MROZOWSKI, *University of Chicago* (*Introduced by R. S. Mulliken*).—The previously found[1] complex structures of many lines in the singly ionized mercury spectrum have been critically examined and the isotope shifts in 49 energy levels and the hyperfine structure splittings in 10 of them have been roughly determined. The isotope shifts and hyperfine splittings are very small for levels of the configurations $5d^{10}nx$ (excluding the ground state formerly studied[1]), and quite considerable for levels of the type $5d^96snx$. In the latter case shifts of about 0.3 cm^{-1} (between consecutive even isotopes) and hyperfine splittings amounting to from 0.4 to 1.3 cm^{-1} have been found. A few perturbations are present in both sets of levels. The analysis shows further the necessity of rejecting the existing classification of some lines. Nearly a half of the lines studied are not yet classified, and serious difficulties are encountered in the classification of a part of them.

[1] S. Mrozowski, Phys. Rev. **57**, 207 (1940).

3. The Zeeman Effect of Xenon. E. H. HURLBURT, D. W. BOWMAN, AND J. B. GREEN, *Ohio State University.*—Measurements of about 125 lines in the spectrum of Xe I yield *g*-values for the only two completely known configurations of Xe I. The results are partially in disagreement with those published by Lörinczi.[1] For a number of configurations, partial *g*-sums indicate that the *J* of the core is a "good" quantum number, while the extra electron represents an interesting case of intermediate coupling. This is especially true for the p^5f configurations.

[1] Lörinczi, Diss. Budapest, 1937.

4. The Paschen-Back Effect. VIII. Configuration Interaction. J. B. GREEN, D. W. BOWMAN AND E. H. HURLBURT, *Ohio State University.*—The spectrum of krypton furnishes a very fine example of the effect of configuration interaction. The levels $3s_5$ and $4d_2$, belonging to configurations of the same parity, are less than 1 cm^{-1} apart, and the Zeeman patterns of lines arising from them show large perturbations, both as regards positions and relative intensities of the components. A semi-empirical theory is discussed which leads to excellent agreement with experiment.

5. A Rotational Analysis of Some CS_2 Bands in the Near Ultraviolet. LEONARD N. LIEBERMANN, *University of Chicago* (*Introduced by R. S. Mulliken*).—The rotational structure of six bands in the region 3450A–3700A has been analyzed.[1] Alternate *J* values are missing as is expected from the zero spin of the sulphur nuclei. The band lines follow the formula: $\nu = A + Bm + Cm^2 - sm^4$. The m^4 term in this formula is not related to the centrifugal expansion, but to the triangular shape of the molecule in its excited electronic state. The value of *s* as a function of the apex angle can be derived from asymmetrical top theory and leads to 120° for the apex angle of CS_2 in its excited state. This value is confirmed by the results of an analysis of a band with a *Q* branch. An equation has been derived relating the separation of the upper state rotational levels of this band to the apex angle. Two bands show a perturbation which is attributed to their common upper Σ state being perturbed by a neighboring Π state. A partial vibrational analysis could be made because some bands have states in common. The frequency for the bending vibration ν_2 for the lower state is 401 cm^{-1}, while that for the deformation vibration ν_2 in the upper state is probably 275 cm^{-1}.

[1] A preliminary report has been published. See Phys. Rev. **58**, 183 (1940).

6. Explanation of the Rotational Structure of the λ3800 Band System of SO_2. N. METROPOLIS, *University of Chicago.*—Photographs of the rotational structure of the absorption bands of SO_2, taken in first and second order with our 30-ft. grating spectrograph, show a remarkable shading to both sides. This is true of about twelve individual bands, whose vibrational analysis has been reported.[1] Exposures taken at various temperatures have intensity distributions corresponding to a band origin approximately

at the center of the band. The rotational structure of the absorption bands exhibits a coarse structure degraded toward higher frequencies. These transitions are associated with the component of angular momentum along the symmetry axis and are called the K structure. A much finer J structure extends and fades out toward lower frequencies. These characteristics indicate that $C_K' > C_K''$ and $B_J' < B_J''$, where B and C are coefficients of the J and K structure, respectively. In terms of dimensional changes in the transition, it means that an increase of the apex angle, $\alpha' > \alpha''$, is a necessary condition and is here more significant than a change of the bond distances. This result is in agreement with the intensity distribution of the vibrational structure. A general treatment of the dimensional changes and their effect on the patterns of the rotational bands of polyatomic molecules has been carried through.

[1] N. Metropolis and H. Beutler, Phys. Rev. **57**, 1078 (1940).

7. Raman Spectra of Some Ethers Containing One or More Phenyl Groups. FORREST F. CLEVELAND AND M. J. MURRAY, *Illinois Institute of Technology.*—Raman frequencies, estimated intensities and depolarization factors have been obtained for *n*-propylphenyl, *n*-butylphenyl, ethylbenzyl, *n*-butylbenzyl and dibenzyl ethers by use of a spectrograph having a linear dispersion of 33 A/mm at 4500A. Characteristic monosubstituted benzene frequencies whose values were constant in the five ethers are 618(5)0.8, 1001(10)0.1, 1029(7)0.3, 1156(4)0.8, 1176(4)0.8, 1588 and 1604(6)0.7, 3058(9)0.3. In the 3000 cm^{-1} region, the line 3058(9)0.3, is attributed to a vibration involving the phenyl group hydrogens. The polarized frequency near 2860 and the depolarized frequency near 2960 seem to correspond to symmetrical and unsymmetrical vibrations of the $-CH_2-$ group, while the polarized 2930 line probably corresponds to an inner frequency of the $-CH_3$ group. A frequency 2911(6)0.6 was observed for the three ethers containing the propyl and butyl groups, but not for the other two. A weak line at 3204 in the benzyl ethers may correspond to the overtone of the 1600 frequency. The ether group $(R-O-R')$ frequencies are possibly the ones near 1125, 900 and 440 cm^{-1}.

8. Use of the Radioactive Properties of Thorium for a Quantitative Study of Phagocytosis. F. A. MAXFIELD AND O. A. MORTENSEN, *University of Wisconsin.*—Use has been made of the radioactive properties of colloidal thorium dioxide, intravenously injected into rabbits, to study the functional capacity of the reticulo-endothelial cells for phagocytosis. A mathematical analysis of the problem is presented which indicates that when the system is not overloaded, the foreign material should be removed from the blood according to the relation

$$n = n_0 e^{-at} + (b/2\alpha) n_0 e^{-bt}.$$

Here $a \gg b$ and n is the number of particles remaining in the blood at any time, t. Experiments on 13 rabbits substantiate this prediction. With a standard injection of 1 cc of colloidal thorium dioxide per kilogram of body weight, n decreases according to three distinct exponential relations. The system is apparently overloaded initially, but after n decreases to about one-sixth its initial value (at $t=0$), the fraction of the amount of material present that is removed in unit time increases and the rest of the curve follows the predicted relation. The fact that the system is initially overloaded was checked by the use of smaller amounts of thorium. In all cases more than 99 percent of the thorium was removed from the blood stream within 6 or 8 hours after the injection. The technique reported here should serve as a basis for testing many theories of phagocytosis now largely based on deduction.

9. Some Rules Concerning Isobaric Radioactive Nuclei. ARTHUR E. HAAS, *University of Notre Dame.*—Isobaric pairs of artificially produced β^--emitters obey the rule that the nucleus with odd charge number has the greater half-life. Isobaric pairs of unstable nuclei of which one is a β^-- the other a β^+-emitter, follow in general the rule that the positron-emitter has the shorter half-value period. These two rules can be explained on ground of the well-known fact that the exchange force between two neutrons is, under otherwise equal conditions, stronger than that between two protons. For light β^+-emitters the half-life is often between $\frac{1}{5}$ and $\frac{3}{4}$ that of the isobaric β^--emitter. In the case of an isobaric β^-, β^--pair the corresponding stable isobaric nucleus has always a higher atomic number than the pair. In the case of an isobaric β^-, β^+-pair, however, the stable isobaric nucleus has an atomic number between those of the pair. The last two rules may be derived from Gamow's stability diagram.

10. A Magnetic α-Particle Spectrograph. ROY RINGO, *University of Chicago (Introduced by A. J. Dempster).*—A 60° deflection magnetic spectrograph, which will measure α-particles of energies from 2 to 20 Mev, has been constructed. It is readily movable and the position of the source is 42 cm from the magnetic field. These two features make it suitable for use with apparatus for artificial disintegration. The particles are detected on photographic plates where the individual tracks are observed microscopically. This method permits the use of exposures of indefinite length. The instrument was calibrated by obtaining its dispersion with α-particle groups of known energy from natural radioactive sources. The energy of the main group of protoactinium α-particles was found to be 5.053 ± 0.007 Mev by comparison with polonium α-particles taken as 5.303 Mev.[1] In all the α-particle spectra investigated large numbers of particles with energies below the main group are found. There is apparently a continuous distribution of these energies below that of the main group; as many as 10 percent of the particles have energies 5 percent or more below. The explanation of this retardation as absorption in the source is made doubtful by the fact that a 5 percent energy loss is equivalent to that in 2 mm of air, and on the thin sources used the amount of material is insufficient to account for this even considering clumping. Scattering of the particles is not a possible explanation as that should cause some particles to appear on the high energy side of the main group and none are found there.

[1] Rutherford, Wynn-Williams, Bowden, and Lewis, Proc. Roy. Soc. **A139**, 617 (1933).

11. Voltage Distribution on a Multi-Section Accelerating Tube. L. J. HAWORTH, J. H. MANLEY, AND E. A. LUEBKE, *University of Illinois.*—Difficulty in maintaining a uniform potential distribution on a multi-section accelerating tube was encountered when using the large ion currents from a modified Zinn type source. Current measurements indicated the flow of large numbers of secondary electrons between the accelerating electrodes. Introduction of external leakage currents so large as to overload the voltage supply did not appreciably affect the potential distribution. The difficulty was overcome by an arrangement of diaphragms each of which was connected to its surrounding electrode through a resistance of 10^5 ohms. Small ion currents to and electron currents from the diaphragms thus provide sufficient potential difference to prevent the escape of all secondaries except the relatively small number possessing high initial energies.

12. The Distribution in Angle of the Alpha-Particles from Boron Bombarded with Protons. JAMES A. JACOBS AND WILLIAM L. WHITSON, *State University of Iowa.*—The distribution in angle of the alpha-particles from boron bombarded with protons has been investigated at the resonance energy (160 Kev) and just above resonance (200 Kev). The target consisted of boron trifluoride gas at a pressure of 0.3 mm of mercury. Range-number curves were obtained at five different angles for both the above energies. These curves, when corrected for the variation of range with angle, show complete spherical symmetry for both the continuous and the homogeneous groups of alpha particles. The apparent asymmetry found for this reaction by Haxby, Allen, and Williams[1] and by Neuert[2] may be due to the difficulties in applying range corrections for alpha particles produced in a thick target.

[1] Haxby, Allen, Williams, Phys. Rev. **55**, 140 (1939).
[2] Neuert, Physik. Zeits. **38**, 122, 618 (1937); Ann. der Physik **36**, 437 (1939).

13. Interaction between Two Alpha-Particles and the Properties of Be^8. JOHN A. WHEELER, *Princeton University.*—Deviations from the scattering to be expected on the basis of an inverse square law of force between alpha particles receive a satisfactory interpretation in terms of the influence on particles of zero, two and four units of angular momentum of a specific nuclear interaction having a range less than 9×10^{-13} cm. The semi-stable excited state of the compound nucleus Be^8 formed in certain disintegration experiments is found from the scattering analysis to have an energy of about 3 Mev, a mean life of 0.8×10^{-21} sec. and *zero* angular momentum. For the normal state of Be^8 various values of the energy of disintegration have been assumed and for each has been calculated the number of coincidences to be expected in the experiments of Laaff and Fink. Reasonable agreement is obtained with an energy release of 125 kev, corresponding to a half-life of the order of 10^{-16} to 10^{-17} sec. It remains difficult to understand an apparent selection rule in the formation of Be^8 from the reaction of B^{11} with protons.

14. Electrostatic Deflection Studies of Alpha-Particles; the Alphas from $Li^6(p,\alpha)He^3$. SAMUEL K. ALLISON, LEONARD C. MILLER, LESTER S. SKAGGS, AND NICHOLAS M. SMITH, JR., *University of Chicago.*—A technique is described for studying nuclear reactions in which short range alpha-particles are produced with a yield that is too small for the direct application of the electrostatic deflector. In preliminary experiments a strong polonium source is used to supply alpha-particles to the deflector, and a group of these alphas, homogeneous in energy, passes through the deflector and enters a variable pressure absorption cell and ionization chamber. Cut-off pressures determined for various alpha-particle energies result in a calibrated cell which can then be used to determine the alpha-particle energies in nuclear disintegrations. Application of this method to $Li^6(p,\alpha)He^3$ results in a Q value of 3.94 ± 0.08 Mev. The calibration, extending in alpha-particle energy from 1 to 1.8 Mev, is also used to determine the slope of the range energy curve. The average value of the slope found for this region is 200 kv per mm range.

15. The Absolute Number of Quanta from the Bombardment of Fluorine with Protons. J. A. VAN ALLEN* AND NICHOLAS M. SMITH, JR.,* *Department of Terrestrial Magnetism, Carnegie Institution of Washington.*—From the experiments of Lauritsen and associates and of Burcham and associates, it seems very probable that the 6.2-Mev quanta from the proton bombardment of fluorine are associated in one-to-one correspondence with the short range alpha-particles. This correspondence makes possible the establishment of the gamma-ray intensity by measuring the alpha-particle yield. Using a specially designed variable pressure absorption-cell ionization-chamber, to facilitate clear distinction between the short range alpha-particles and the scattered protons, we have determined the angular distribution and total yield of the alpha-particles at the lowest resonance (330 kv). The determinations were based on plateaus appearing in curves of counting rate as a function of (1) cell pressure, (2) counter bias, and (3) bombarding voltage at angles of 60°, 90°, 120°, and 150° with respect to the proton beam. Our results show that: (a) To within two percent the angular distribution of the alpha-particles is spherically symmetric; and (b) The yield over 4π steradians is $8.9\pm0.5\times10^4$ alpha-particles per microcoulomb of protons bombarding a thick crystal of CaF_2. The absolute number of quanta from the reaction is presumably the same to the same accuracy. We find the angular distribution of the gamma-rays to be spherically symmetric to within the experimental error of five percent. Knowledge of the intensity of the fluorine source greatly enhances its value in photo-nuclear and other experiments.

* Carnegie Institution Fellow.

16. Short-Lived Radioactivities of $_{14}Si^{27}$, $_{16}S^{31}$, $_{18}A^{35}$, and $_{21}Sc^{41}$. L. D. P. KING AND D. R. ELLIOTT, *Purdue University.*—Radioactive elements belonging to the series characterized by $Z-N=1$ are of theoretical importance for nuclear structure determinations.[1] In an attempt to extend this series the following new reactions have been observed:

	HALF-LIFE
$_{12}Mg^{24}(\alpha,n)_{14}Si^{27}$ [2]	4.92 sec.
$_{14}Si^{28}$ $(\alpha,n)_{16}S^{31}$	3.18 sec.
$_{16}S^{32}$ $(\alpha,n)_{18}A^{35}$	1.91 sec.
$_{20}Ca^{40}$ $(d,n)_{21}Sc^{41}$	.87 sec.

The first three reactions were produced by 16-Mev alpha-particles, the final one by 8-Mev deuterons. The bombardments were performed outside of the cyclotron which reduced the bombarding energy by 0.6 mil of aluminum. Measurements of half-lives were made by means of a multiple scale Geiger counter circuit. The dial readings of the mechanical counter were photographically recorded at regular time intervals of one-half or one second. Bombarding times varied from a fraction of a second to three seconds using beam intensities of about 0.05 microampere of deuterons and alpha-particles. All the activities obtained showed an exponential decay over at least three half-lives. Any background or weak long periods were eliminated by subtraction.

[1] E. Wigner, Phys. Rev. **56**, 519 (1939).
[2] G. Kuerti and S. N. Van Voorhis, Phys. Rev. **56**, 614 (1939); Barkas, Creutz, Delsasso, Sutton and White, Phys. Rev. **50**, 38 (1940).

17. Absorption Cross Sections for Slow Neutrons. M. GOLDHABER AND R. D. O'NEAL, *University of Illinois.*—Cross sections for radiative capture of C neutrons which are $<10^{-24}$ cm^2 are not known for many elements. In those cases where the isotope produced by slow neutron capture is radioactive the capture cross sections can be determined by comparing the induced activity with that of an element of known cross section for C neutron capture. Using Mn ($\sigma_c = 9.4\times10^{-24}$ cm^2) [1] as a standard we have measured a number of cross sections in this way with the help of a 100 mg Ra-α-Be source. The results are tabulated below. (T = half lifetime of radioactive isotope, σ_{eff} = effective cross section for average atom, σ_c = capture cross section corrected for abundance of isotope.)

ELEMENT	T	σ_{eff} IN 10^{-24} CM^2	ABSORBING ISOTOPE	σ_c IN 10^{-24} CM^2
$_7$N	8 sec.	<0.0008	N^{15} *	<0.2
$_9$F	12 sec.	<0.05	F^{19}	<0.05
$_{11}$Na	14.8 hr.	0.4	Na^{23}	0.4
$_{12}$Mg	10.2 min.	0.03	Mg^{26}	0.3
$_{13}$Al	2.4 min.	0.2	Al^{27}	0.2
$_{14}$Si	170 min.	<0.03	Si^{30}	<0.7
$_{15}$P	14.3 day	0.3	P^{31}	0.3
$_{17}$Cl	37 min.	0.07	Cl^{37}	0.3
$_{19}$K	12.4 hr.	<0.05	K^{41}	<0.7
$_{20}$Ca	2.5 hr.	<0.01	Ca^{48}	<5
$_{28}$Ni	2.6 hr.	<0.03	Ni^{62}	<0.8
$_{29}$Cu	5 min.	0.8	Cu^{65}	2.4
$_{51}$Sb	2.8 day	2	Sb^{121}	3.6
	60 day	1	Sb^{123}	2.3
$_{81}$Tl	4.2 min.	<1	Tl^{203}	<3.3
$_{83}$Bi	5 day	<0.1	Bi^{209}	<0.1

* Through the courtesy of Professor Urey we were able to use ammonium nitrate enriched in N^{15} for this experiment.
[1] Lapointe and Rasetti, Phys. Rev. **58**, 554 (1940).

18. Neutron Capture Cross Sections of F^{19}, Tl^{203}, and N^{15}. J. H. MANLEY, L. J. HAWORTH, AND E. A. LUEBKE, *University of Illinois.*—With the use of the absorbers used by Goldhaber and O'Neal, neutron capture cross sections of F^{19}, Tl^{203}, and N^{15} have been measured with neutrons produced by the D–D reaction in the Illinois linear accelerator. On the basis of a cross section for Al^{27} of 0.2×10^{-24} cm^2 as found by Goldhaber and O'Neal (preceding abstract) the values found are in 10^{-24} cm^2: $\sigma(F^{19}) = 0.01$, $\sigma(Tl^{203}) = 0.17$, $\sigma(N^{15}) < 0.01$.

19. On the Activation of Chlorine by Slow Neutrons. R. D. O'NEAL, *University of Illinois.*—An attempt was made to determine the half-life of Cl^{36} (reported by Grahame and Walke as >1 year) [1] by a method similar to that described recently for H^3.[2] For this purpose CCl_4 was irradiated inside paraffin with neutrons from a 100 mg Ra-α-Be source for 9 months. The activated chlorine was separated by a Szilard-Chalmers separation. The 37 minute Cl^{38} was found to be separated with an efficiency of nearly 100 percent. However, no long-lived chlorine could be detected in the sample. If one assumes the separations to be equally efficient for the long as for the short-lived chlorine it follows that the half-life of $Cl^{36} > 1000$ years. When chlorine is bombarded with fast neutrons the well-known 88-day activity of sulphur is produced. This has been ascribed to S^{35}. As the reaction $Cl^{35}(n,p)S^{35}$ would have a positive energy release of about 650 kev it is conceivable that it takes place also with slow neutrons. Previous attempts to find heavy particles emitted from chlorine bombarded with slow neutrons have been negative.[3] However, cross sections of $<10^{-24}$ cm^2 would probably have escaped detection in these experiments. Sulphur separated from the CCl_4 sample showed no activity which implies that the cross section of the reaction $Cl^{35}(n,p)S^{35}$ $<1/1000$ of the cross section of the reaction $Cl^{35}(n,\gamma)Cl^{36}$.[4] This result together with that of Sagane[5] who failed to obtain the 88-day sulphur isotope by bombarding sulphur with deuterons makes it appear likely that this isotope is S^{37} and not S^{35}.

[1] See J. J. Livingood and G. T. Seaborg, Rev. Mod. Phys. **12**, 30 (1940).
[2] R. D. O'Neal and M. Goldhaber, Phys. Rev. **58**, 574 (1940).
[3] J. Chadwick and M. Goldhaber, Proc. Camb. Phil. Soc. **31**, 612 (1935).
[4] C. Lapointe and F. Rasetti, Phys. Rev. **58**, 554 (1940).
[5] R. Sagane, Phys. Rev. **50**, 1141 (1936).

20. Energy Distribution of Continuous X-Rays from Nuclear Excitation. G. B. COLLINS AND B. WALDMAN, *University of Notre Dame.*—The nuclear activity of indium induced by x-rays has been used to measure the energy distribution of these x-rays near their threshold. This is possible since it is known that for energies below 1.5 Mev indium is excited only by a narrow band of x-rays at 1.1 Mev.[1] Foils of indium were excited by irradiating them with x-rays produced in a gold foil (1.2×10^{-3} cm) by monochromatic electrons with energies above 1.1 Mev. By varying the energy of these electrons, the relative intensity of the x-ray spectra at different distances from the short wave limit was determined by the activity induced in the indium foils. The intensity of the x-rays was found to have a finite value at the short wave-length limit, and near the threshold to be approximately independent of the wave-length. This is in agreement with theory (see next abstract). The over-all cross section for the excitation of indium and lead by 1.2-Mev electrons, which contains, as factors, the intensity of the x-rays near the short wave limit, the radiation width of the activation level and the branching ratio, has been estimated to be about 10^{-23} cm^2 for both elements.

[1] Phys. Rev. **55**, 1129 (1939).

21. On the Excitation of Nuclei by X-Rays. EUGENE GUTH, *University of Notre Dame.*—It is shown how values of the radiation widths of activation levels may be deduced from experimental cross sections for nuclear excitations by x-rays. In interpreting the experimental data (see pre-

ceding abstract), which were obtained using electrons for the production of the x-rays, theoretical formulae were introduced for: (a) the intensity of x-rays near the short wave limit; (b) the dependency upon the energy of the radiation multipole matrix elements. The intensity of the x-rays was found to have a finite value at the short wave limit and near the short wave limit to be approximately independent of the wave-length, or of the energy of the incident electrons. Herefrom an excitation curve with many flat plateaus follows, each plateau indicating another level. The dependency of the multipole matrix elements upon the energy gives the ratio of the transition probabilities from the activation to the ground and the metastable level. From the experimental cross sections for In^{115} and Pb, radiation widths of about a few millivolts were obtained. These values are of the same order of magnitude as the radiation widths of the excited levels of RaC′ and ThC′.

22. The Structure of Liquid Nitromethane. G. C. DANIELSON AND K. LARK-HOROVITZ, *Purdue University.*—From Fourier analyses of the x-ray diffraction pattern of liquid nitromethane, different distribution curves in the liquid have been determined. The electron and atomic distribution curves show that the first and second atomic neighbors are fixed at the distances of the atoms in the molecule which agree with the ones determined from the electron diffraction pattern of the gas. As indicated by the distribution curve, their distances are, therefore, not subject to statistical fluctuations. The number of first neighbors is 1.6 at 1.33A and the number of second neighbors is 1.6 at 2.40A which agree with electron diffraction determinations. Further concentrations of atoms are found at 3.48A, 4.28A, and at 5.26A. The molecular distribution curve gives 1.9 first neighbors at 3.48A, 2.7 second neighbors at 4.28A, and 3.6 third neighbors at 5.26A. The analyses of molecular distribution curves show that the flat shaped molecules have their first neighbors in parallel arrangement and not at random orientation.

23. Electron Distribution in Metallic Lithium as Determined from X-Ray Diffraction Measurements. R. L. GRIFFITH AND P. M. HARRIS, *Ohio State University.*—The intensity of the crystalline scattering of Cu $K\alpha$ x-rays from metallic lithium powder was determined at 300°, 195° and 90°K, respectively, using an ionization spectrometer. Values of the Debye θ were calculated from the intensity measurements. The results are not in agreement with published calorimetric measurements which are also anomalous. Values of the atomic form factor appear to be much smaller for metallic lithium than for the ion in lithium fluoride, indicating a more diffuse electron distribution in the metal. A three-dimensional Fourier series for the electron density has been evaluated in certain directions. These results show a maximum in electron density midway between two atoms along the edge of the cubic unit cell. This maximum is much more pronounced at 90°K than at room temperature. A corresponding separation of the crystal structure factors into two groups (one group for all indices even, one for two odd and one even) is apparent. These results may be accounted for by a maximum in the electron density along the three coordinate axes at distances $\pm a_0/2$ from the atom. Presumably these data may be interpreted as evidence of a metallic bond. Radial charge distribution curves were also obtained for the lithium and hydrogen in lithium hydride.

24. A Method for Obtaining Powders of Uniform Sodium Chloride Crystals in Various Size Ranges, and the Effect of Size Upon the Intensity of X-Ray Reflection. FITZ-HUGH MARSHALL, *University of Chicago* (*Introduced by S. K. Allison*).—I. A technique is presented for precipitating powders of sodium chloride crystals, uniform in size and cubical in shape, in various size ranges from 1 to 70 microns, above which the range could be extended by screening. The crystals are prepared by precipitation with absolute ethyl alcohol from a saturated solution of sodium chloride in water, but varying excess quantities of water are added to either of the solutions before combining them. Control of size range, and of crystal uniformity within a size range, is accomplished by careful attention to certain primary variables in the precipitation process, each of which produces marked changes in the character of the powder obtained. These are discussed and a simplified procedure is presented for producing any desired size. II. This technique was developed to make possible a study of the variation of intensity of x-ray lines reflected from such size-graded powders. The 200-reflection of Cu $K\alpha$ radiation has been investigated, and a curve is shown for the variation of intensity with crystal size. The intensity decreases slightly with increase of crystal size, according to a curve which indicates that the crystals are imperfect but are more perfect than large single crystals.

25. The Measurement of the Intensity of X-Rays of Wave-Length 0.14A to 1.0A by Means of an Electron Multiplier Tube. JAMES S. ALLEN, *Kansas State College.*—An electron multiplier tube has been designed for the measurement of very weak x-ray intensities. Ten of the twelve electrodes in the tube are covered with a thin layer of beryllium. Multiplication occurs at these surfaces. The beam of x-rays enters the tube through a thin bubble window and ejects photoelectrons from the first electrode. The sensitive surface is composed of a thin tantalum foil. This metal was chosen because of its high atomic number and also because of the fact that it acts as a getter. The efficiency of the tube was determined by placing it on a single crystal x-ray spectrometer. The beam of x-rays passed through an ionization chamber and then into the multiplier tube. The pulses from the tube were amplified further by a four-stage amplifier and were recorded by a scale of eight counting circuit. The efficiency of the tube was measured for radiation of wave-length 0.14 to 1.0A. From 0.5 to 1.0A the efficiency increased directly with the wave-length. At $\lambda = 0.7$A about 400 photons were required for every pulse recorded.

26. Induction Electron Accelerator. DONALD W. KERST,* *University of Illinois.*—By using a magnetic field oscillating at 600 cycles and reaching a peak value of about 1600 gauss, it has been possible to trap electrons in somewhat circular orbits which miss the injection cathode. These electrons which are trapped in usable orbits are accelerated by the electric field induced by the increasing flux to an

energy of about 2.35 Mev. During this acceleration axial and radial focusing are provided by the magnetic field which falls off approximately $1/r^{\frac{1}{2}}$. The increase in time of the flux enclosed within the orbit causes the oscillations which the focusing forces produce about ideal orbits to decrease in amplitude so that the electrons group themselves in a beam. During acceleration the orbit is held at a fixed radius of about 7.5 cm by fulfillment of the condition $\phi_r = 2\pi r^2 H_r$, where ϕ_r is the flux enclosed within the orbit at a given instant and H_r is the field at the orbit at that same instant. Saturation of a portion of the magnetic circuit feeding flux through the center of the orbit causes destruction of this condition at $r = 7.5$ cm after the electrons have been accelerated and the electrons spiral inward toward a target. The intensity of the x-radiation produced is somewhat in excess of the radiation from ten millicuries of radium.

* Now with General Electric Company.

27. Conjugate Potentials of a Grid Between Conducting Planes. DON KIRKHAM, *Utah State Agricultural College.**—The function

$$W = -q \sum_{n=-\infty}^{\infty} \log \frac{\operatorname{vers} 2\pi(z-2nhi)/a}{\operatorname{vers} 2\pi(z-2di-2nhi)/a} - i(z-di)(V_a - V_c + 4\pi qd/a)/h + V_a$$

yields the conjugate potentials appropriate to an infinite grating of equally spaced filaments situated between two infinite parallel conducting planes. The grating is distance d from the upper plane, and $(h-d)$ from the lower. The potential of the upper plane is V_a and of the lower V_c. The origin of rectangular coordinates is taken at the center of a filament with y directed upward. q is the charge density per unit length of filament. Transformations similar to the above may be used to obtain convenient solutions for a number of problems involving finite and infinite gratings. The relationship between an infinite product of versines and the quasi doubly-periodic (theta-) functions[1] has been obtained.

* To be read by title.

[1] Cf. L. Rosenhead and S. D. Daymond, Proc. Roy. Soc. **A161**, 382 (1937).

28. A Lattice Type Acoustic Filter. HAROLD K. SCHILLING, *Union College, Lincoln, Nebraska.*—Acoustic band elimination filters having a simple lattice structure have been developed. They consist of parallel grooved slats, the spaces between which function as transmission lines and the grooves as sidebranches. The grooves are parallel to the length of a slat and perpendicular to the direction of transmission. They are particularly suited to the filtration of the higher frequencies, say above 5 kilocycles. Attenuations of 40 to 70 decibels over wide bands are obtained easily. The parameters determining their characteristics are: the thickness and the width of a slat; the depth, width, distance between and number of grooves. Their effects may be understood in terms of the infinite filter theory of W. P. Mason,[1] and the finite filter theory by R. B. Lindsay.[2]

[1] W. P. Mason, Bell Tech. J. **6**, 258 (1927).
[2] R. B. Lindsay, J. App. Phys. **9**, 612 (1938).

29. Simultaneous Determination of Isothermal and Adiabatic Elasticities. H. F. LUDLOFF, *Cornell University.*—The simultaneous measurement of the isothermal and adiabatic temperature curve of an elastic modulus through the temperature region of phase transitions of higher order seems possible by any dynamical method using a proper frequency system, one part of which consists of isothermal, the other part of adiabatic proper vibrations. Therefore the following problem has been investigated: How does the adiabatic or isothermal character of a proper vibration depend on the frequency range, the vibrational type and the form of the sample? Taking into account the processes of heat conduction and heat production and inserting the boundary conditions imposed by the size of the sample we found: (*a*) If the three dimensions of the sample are all of the same order, there are no isothermal proper vibrations. (*b*) If one of the sample dimensions is small compared to the other two, one has symmetrical (compressional) and antisymmetrical (bending) proper vibrations. The former ones are adiabatic. Of the latter vibrations the first few are isothermal, the number depending on the thickness of the sample. For appropriate dimensions the fundamental tone should produce an isothermal curve and the first overtone a relatively adiabatic temperature curve of an elastic parameter.

30. Theoretical Stress-Strain Curve for Rubberlike Materials. HUBERT M. JAMES, *Purdue University*, AND EUGENE GUTH, *University of Notre Dame.*—A theoretical stress-strain curve has been derived for rubberlike materials built up from long-chain molecules connected into a network by cross bonds. This network extends throughout the material, and due to its thermal agitation exerts a pull on any bounding surface which must be balanced by external forces together with internal forces representable by an internal pressure in the quasifluid material. Treating the molecular chains as perfectly flexible and the bulk material as incompressible, one finds as the stress-strain relation for the model

$$F = KT[f(La) - L^{-3/2} f(L^{-1/2}a)].$$

Here F is the stress per unit initial cross section and L is the extended or compressed length divided by the original length. $f(x)$ is defined by

$$x = \frac{e^{2f}+1}{e^{2f}-1} - \frac{1}{f}.$$

K and a are constants characterizing the chain network, $1/a$ being the maximum value of L for the model. This stress-strain curve shows the observed downward curvature for small strains and a sharp upward curvature for larger strains. The latter effect is associated with the approach of the network to its maximum extension, and differs in its temperature dependence from the qualitatively similar effect due to the crystallization of rubber by stretching. The theory shows good agreement with observations on equilibrium stress-strain curves for rubber.

31. Electrostatic Generator with Concentric Electrodes. R. G. HERB, C. M. TURNER, A. O. HANSON, AND N. D. CRANE, *University of Wisconsin.*—Our new electrostatic generator which was described in a recent letter to *The Physical Review*[1] will be described in more detail and further results on its performance will be discussed. The generator is now equipped with an electrostatic analyzer for measur-

ing the energy of the ions. No difficulty has been experienced with the accelerating tube, either from leaks or from voltage breakdown. The ion beam is well focused, but is at present limited to a few microamperes. A discussion will be given of factors which limit the current and of possibilities for improvement.

[1] Phys. Rev. **58**, 579 (1940).

32. One-Tube Counter Quenching Circuit with Capacitative Feedback. T. N. GAUTIER, *University of North Carolina (Introduced by A. E. Ruark).*—The counter wire is connected to the control grid of the quenching tube (e.g., type 57) and the grid is connected through about 6 megohms to the grounded cathode. This resistance depends upon the counter employed. The counter cylinder is connected to the negative terminal of the counter voltage supply through about 2 megohms, and is coupled to the plate of the quenching tube through a capacitance (about 0.01 mf). Thus a positive quenching pulse is transmitted from the plate to the counter cylinder through the condenser. Alternatively, the cylinder may be connected to the grid, biased to cut-off, so that a negative pulse is applied to the counter wire. These circuits are fast and reliable. As compared with the Neher-Harper circuit, they have the advantage that the plate voltage of the quenching tube need not exceed the manufacturer's rating, and the counter voltage does not depend upon the grid bias voltage. As compared with the Neher-Pickering circuit, they have the advantage that the cathode of the quenching tube is at ground potential, obviating disturbances from the a.c. heater supply. Furthermore, the counter voltage supply does not have to furnish plate current.

33. Recurrence Pulses in Cosmic-Ray Intensity. A. H. COMPTON AND A. T. MONK, *University of Chicago.*—Daily mean cosmic-ray intensities, as given by the Carnegie Institution Model C cosmic-ray meter at Teoloyucan, Mexico, were reported* last year to show a recurrence tendency with an interval between 27 and 28 days, and with no diminution in the amplitudes of the four recurrence pulses studied. These pulses arise as follows. From each calendar month are selected the five days for which the cosmic-ray intensity is highest. The intensities are then tabulated for the n days following (and preceding) these selected days. The average intensity (for the whole range of months available) corresponding to each n value is then plotted against n, and this curve has maxima lying between n's which are integral multiples of 27 and 28. These are the *positive* pulses. When the selected days are those for which the cosmic-ray intensity is *lowest*, a negative-pulse curve results. It has now been found that these pulses persist at least as far as the eighth, but with decreased amplitude. The analysis is being extended through the tenth pulse (both preceding and following).

* Monk and Compton, Rev. Mod. Phys. **11**, 173 (1939).

34. The East-West Asymmetry of the Cosmic Radiation in High Latitudes and the Excess of Positive Mesotrons. THOMAS H. JOHNSON, *Bartol Research Foundation of the Franklin Institute.*—The slight east-west asymmetry in high latitudes, now confirmed by Seidl, is interpreted as resulting from deflections of the mesotron component in the earth's magnetic field after the rays have entered the atmosphere and have lost energy by ionization. Since this component contains about twenty percent more positive than negative rays the deflections produce an asymmetry. Orbits of rays in the range of energy where rest mass cannot be neglected have been investigated and the deflections determined. It is assumed that deflections without energy loss would have resulted in a symmetrical distribution for the ranges of energy concerned, and the asymmetry is traced to the difference between the actual deflection and that of a ray which loses no energy. In computing this difference, instead of the actual deflection, one avoids the necessity of introducing an upper boundary of the atmosphere. The deflection shifts the angular distribution so that rays which in the absence of a field would have produced an intensity proportional to $\cos^2\zeta$ at zenith angle ζ actually produce this intensity at zenith angle $\zeta+\delta$, where the deflection δ is towards the west for positive rays and towards the east for negative rays. The asymmetries calculated in this way agree with the observed values and give the correct variation of the asymmetry with zenith angle and elevation. The theory is also in accord with what little is known of the effect of absorbing material upon the asymmetry. More extensive experimental studies of the asymmetry under various thicknesses of absorbing material would provide a method alternative to the magnetic cloud chamber for studying the positive excess at various energies.

35. The Exact Solution of the Integral Equations for Cosmic-Ray Showers. M. DRESDEN, W. T. SCOTT AND G. E. UHLENBECK, *University of Michigan.*—A fundamental problem of the theory of cosmic-ray showers is the determination of the average number of particles $F(E_0, E, x)dE$ in the energy range dE which will emerge when a particle of energy E_0 enters a layer of matter of thickness x. The theory connects the function F with the known probabilities of pair formation, bremsstrahlung and ionization by means of certain integro-differential equations. We have found an exact method of solution for these equations. The method starts with a Laplace transformation in x. Using the appropriate boundary condition the resulting inhomogeneous integro-differential equation in the variable E can always be transformed into an ordinary integral equation of the Fredholm type with variable lower limit. This can be solved by standard methods. A simplified model, proposed by Furry, will be used to illustrate the solution, and the connection with the existing approximation methods will be discussed.

36. The Variation of the Intensity of Extensive Cosmic-Ray Showers with Altitude. NORMAN HILBERRY, *University of Chicago and New York University.*—The intensity of extensive cosmic-ray showers has been measured at a number of altitudes from sea level to the top of Mt. Evans. A set of four Geiger-Müller tubes, each of 200 square centimeters effective area, was mounted just below the top of a Ford station wagon. Single counters were placed at the front and at the rear of the car and the other two were placed in vertical twofold arrangement at the center; the maximum extension between the extreme counters was 2.5 meters.

The observed counting rates were:

COUNTS PER HOUR	ALTITUDE IN METERS
24.1 ±0.3	4330
20.5 ±0.5	3900
14.0 ±0.5	3240
7.3 ±0.8	2190
5.0 ±0.4	1616
1.47 ±0.15	95

The accidental counting rate was less than 0.2/hr. at 4330 m and less than 0.01/hr. at 95 m. Using a suitable power law energy distribution for the incoming particles, the cascade theory gives good agreement between the predicted variation and the experimental observations.

37. Production of Mesotrons by a Neutral Radiation. VICTOR H. REGENER, *University of Chicago*, AND BRUNO ROSSI, *Cornell University*.—An experiment was performed on Mt. Evans, Colorado (4300 m) to investigate the production of mesotrons by non-ionizing radiation. Mesotrons produced in 5 cm of lead were recorded by Geiger-Mueller counters in fourfold and fivefold coincidence arrangement. The fourfold coincidences could be operated by a single mesotron, whereas for a fivefold coincidence two or more mesotrons had to be generated in one process. By means of a counter tray above the producing layer of lead, operating in anticoincidence, only mesotrons produced by a non-ionizing radiation could be recorded. The absorption of the non-ionizing, mesotron-producing radiation was measured by placing additional layers of lead above the anticoincidence counters. Good evidence for the production of mesotrons was found. The number of mesotrons produced in 5 cm of lead (2/hr.) was about 1 percent of the total number of mesotrons entering the solid angle of the apparatus at that altitude. There is also evidence for the production of more than one mesotron in a single process. The non-ionizing, mesotron-producing radiation is not considerably absorbed by 2.5 cm of lead. This excludes photons as a producing agent and makes the production of mesotrons by neutrettos or neutrons probable.

38. A Study of the Production and Absorption of Mesotrons in the Substratosphere. GERHART GROETZINGER, E. O. WOLLAN AND MARCEL SCHEIN, *University of Chicago*.—In a coincidence-counter experiment carried out in an airplane at altitudes up to 9.3 km (22.9 cm Hg) an attempt was made to observe the production of mesotrons in an 8-cm lead block by some non-ionizing radiation other than photons. From our experiments it would seem that the number of mesotrons arising from such a creation is not greater than about 5 percent of the total number of mesotrons at this altitude. It appears further that photons are the main agent of the non-ionizing radiations which produce mesotrons at altitudes of 7 km. The experiment was also designed to give the absorption of mesotrons in lead of 19 cm and 27 cm thickness as a function of the altitude. Using these data and those obtained previously by Schein, Jesse and Wollan for 10 cm of lead, we have constructed an energy spectrum of the mesotrons at an altitude of 6.7 km. At this altitude about 35 percent of all the mesotrons have energies below 5.2×10^8 ev, while at sea level a very small fraction of the mesotrons have energies in this range. The experiment indicates also that neutrons with energies above 5×10^8 ev are not present in altitudes up to 9.3 km to an extent of more than about 4 percent of the number of mesotrons.

39. Wilson Cloud Chamber Study of Scattering and Stopping of Mesotrons in Lead. R. P. SHUTT AND T. H. JOHNSON, *Bartol Research Foundation of the Franklin Institute*.—Seven thousand nine hundred stereoscopic photographs taken in a 24″ cloud chamber have been used to study the stopping and scattering of mesotrons in lead. Above the chamber separated by fifteen cm of lead were two coincidence counters for controlling the expansions. Inside the chamber at 13-cm intervals were three lead plates one cm, five cm and one cm thick, respectively. Only those rays which had already passed through the counters were included in the count. Out of 4368 rays incident upon the upper surface and near the center of the five-cm lead plate all but 78 or 1.8 percent passed through it and were seen below. Similarly in the one-cm lead plate at the bottom of the chamber 31 rays or one percent of the 3069 incident rays were stopped. These values are in close agreement with those found under similar circumstances with coincidence counters. Analysis of the scattering of mesotrons showed that 4.6 percent of those traversing one cm of lead and 15.2 percent of those traversing five cm of lead are scattered more than 3°. There is apparently more large angle scattering than was expected from the simple theory of multiple Coulomb scattering and we may have an indication of a nuclear interaction.

40. Cloud Chamber Pictures of Cosmic-Rays at 29,000-Ft. Altitude. G. HERZOG* AND W. H. BOSTICK, *University of Chicago*.—On December 20, 1939, a 6″ diameter cloud chamber in a magnetic field of 708 oersteds was carried to a height of 29,300 feet in a Douglas DC-3 transport airplane. The maximum measurable $H\rho$ was 5.6×10^5 which for an electron corresponds to an energy of 1.7×10^8 ev. Out of 155 photographs taken at altitudes greater than 15,000 feet 51 slow mesotron tracks and 30 proton tracks were identified. The number of slow mesotrons is 9 percent of the number of electrons and fast mesotrons. Some very dense tracks may be due to fragments of heavy nuclei. On April 30, 1940, another flight was made to an altitude of 29,300 feet. This time, in order to stop slow mesotrons a copper plate was put in the middle of the chamber. By their specific ionization, their radii of curvature, and the stopping power of the copper plate 7 particles stopping in the plate are identified as slow mesotrons. A total of 28 slow mesotrons was observed in the flight, giving an occurrence rate over 15,000 feet of 9 percent as compared with electrons and fast mesotrons. In only two cases is there evidence for the disintegration of a mesotron and this evidence is not conclusive.

* Now with the Texas Company, Houston, Texas.

41. The Relative Abundance of the Stable Isotopes of Terrestrial and Meteoritic Iron. G. E. VALLEY AND H. H. ANDERSON, *Harvard University*.—Seven specimens of terrestrial iron obtained from various ores and widely different localities, and twelve meteoritic specimens from different types of meteorites have been examined. The type of mass spectrometer used produces a mono-energetic beam

of ions by means of a precisely constructed source. This is then passed through a semicircular magnetic momentum analyzer. The emergent ion current intensity, as measured by a vacuum tube electrometer, is assumed to be proportional to the abundance of the isotope in question. The iron, after purification to remove Cr, Co and Ni, as well as Pd, Cd, and Sn, was electro-deposited upon platinum wire. Ions were produced by electron collision with iron vapor liberated by hot filaments of this combination. No new stable isotopes of iron were discovered. The average values for all the terrestrial specimens and for all the meteoritic specimens follow. They may be compared with the previously published values of de Gier and Zeeman[1] and of Nier.[2]

THE STABLE ISOTOPES OF IRON

Mass number	54	56	57	58
Terrestrial	6.37	100	2.37	0.34
Meteoritic	6.32	100	2.32	0.33
de Gier and Zeeman	7.2	100	3.1	0.55
Nier	6.6	100	2.3	0.31

The differences between our various specimens are on the order of a few percent and can be accounted for by instrumental effects. We conclude that the abundance of the stable isotopes of iron does not depend upon the place of origin of the specimen within the solar system.

[1] de Gier and Zeeman, Proc. K. Akad. Amst. **38**, 959 (1935).
[2] A. O. Nier, Phys. Rev. **55**, 1143 (1939).

42. The Relative Abundance of the Calcium Isotopes. C. W. SHERWIN AND A. J. DEMPSTER, *University of Chicago.*—The ratio of the abundance of the calcium isotopes at 40 and 48 has been measured under different conditions with a variety of sources. The total charges carried by the singly charged ions in a given time were compared electrically. With a spark between two calcium rods a ratio of 460 to 1 was found. Using an iron furnace to evaporate the calcium, and electrons from a hot cathode to produce the ions, 440 to 1 was observed. This is in approximate agreement with Nier's result (525 to 1)[1] obtained with this type of source. The same result was obtained by evaporating the calcium from an alloy of calcium and copper in a furnace. Just before the last had been evaporated a higher intensity at 48 was observed. Calcium reacts violently with gold, silver and copper to form an alloy. With a spark source where one electrode was one of these alloys, very abnormal intensities of Ca^{48} could be obtained. With a very narrow spark between a copper electrode and a silver calcium alloy, the relative abundance of Ca^{48} was 1 to 52, approximately ten times the normal intensity. We may explain the observation by supposing that the rate of combination of the calcium vapor with copper is greater for the isotope of mass 40 than for the one of mass 48.

[1] A. O. Nier, Phys. Rev. **53**, 282 (1938).

43. Explanation of the Periodic Deviations from the Schottky Line. CHARLES J. MULLIN AND EUGENE GUTH, *University of Notre Dame.*—The periodic deviations from the Schottky line observed by Phipps and his collaborators[1,2] and by Nottingham[3] in measuring the thermionic emission of electrons from tungsten and tantalum can be interpreted as being due to two partial reflections of the electron waves on the potential hill at the surface of the metal. These partial reflections give rise to interference and thus to a periodic term in the transmission coefficient for the escaping electrons. The transmission coefficient is obtained by using the functions of the parabolic cylinder to establish the connection between the asymptotic expansions of the wave function to the left and right of the top of the potential hill. The calculated positions of the maxima and minima of the deviations agree very well with the observed positions. In agreement with experiment, it is found that the positions of the maxima and minima are sensibly independent of the temperature; and that the dependence of the amplitude on temperature increases as the applied field is increased. The calculated amplitude of the deviations increases with the field as does the observed amplitude. Both the amplitude and phase depend upon the work function of the emitting metal. No experimental data on this dependence are available, tungsten and tantalum having work functions which are very nearly equal.

[1] R. L. E. Seifert and T. E. Phipps, Phys. Rev. **56**, 652 (1939).
[2] D. Turnbull and T. E. Phipps, Phys. Rev. **56**, 663 (1939).
[3] W. B. Nottingham, Phys. Rev. **57**, 935 (1940).

44. The Exact Comparison of Small Currents. R. M. VANDERBERG, *University of Chicago* (*Introduced by A. J. Dempster*).—The two currents to be compared, approximately 10^{-12} amperes, are collected on electrodes connected to the intermediate cylinders of two triple condensers. The electrode systems are kept as near zero potential as possible by varying the potentials of the outer cylinders while the accuracy of these adjustments is tested by connecting an electrometer to one or the other of the inner cylinders at intervals. The ratio of the currents is given directly by the ratio of the compensating potentials set up on the outer cylinders, after correction for the difference of capacity between the outer and intermediate cylinders of the two condensers. The accuracy attainable was tested by inducing charges of a known ratio on the electrodes. A source of potential was connected to two condensers and by increasing the potential slowly, the induced charges provide two currents of constant ratio for testing purposes. It was found that ratios could be measured by the compensating method to an accuracy approaching one part in ten thousand. Charges set up when switch contacts are separated are the chief source of error.

45. Conduction of Electricity by Dielectric Liquids at High Field Strengths. HAROLD J. PLUMLEY, *University of Chicago* (*Introduced by A. J. Dempster*).—Certain liquid dielectrics, such as the pure paraffin hydrocarbons, which possess extremely low conductivities at moderate field strengths acquire some of the characteristics of semiconductors at field strengths in excess of 100,000 volts per cm. Thermionic emission, cold emission, collision ionization, and presence of ionizing impurities are the more important of the theories previously invoked to explain this effect. The results of our investigation of the dielectric properties of heptane at high field strengths tend to invalidate all four of these assumptions, although the last may not be definitely excluded at present. In the light of our experiments, which were conducted with very small electrode spacings in order to minimize the complicating

effects of space charge and ionic recombination, it seems reasonable to suppose that the highly nonconducting dielectric liquids should be included as extreme cases in the general class of weak electrolytes. The presence of appreciable conductivity under high electric fields is ascribed to the lowering of the energy of the ionic bond by the applied field. This mechanism is supported by the results of experiments designed to show the effects on the conductivity of heptane of the following: work function of electrode, use of unsymmetrical electrode configurations, progressive purification and long time stress application, magnitude of applied field, and, finally, variation of electrode spacing.

46. The Recovery of Dielectric Strength in High Pressure A.C. Arcs. W. M. BAUER AND J. D. COBINE, *Harvard Graduate School of Engineering.*—A direct oscillographic method has been employed in an investigation to determine the manner in which dielectric strength is recovered in short a.c. arcs after extinction. The results of this investigation extend the recovery curves to values of time so great that nearly complete recovery of dielectric strength is obtained. Observations cover a range of extinction time from 50 microseconds to 10 milliseconds; a pressure range from 1 to 32 atmospheres of nitrogen gas; and a current range from 0.25 ampere to 7.85 amperes. The current was supplied by a high potential transformer and was limited by reactance. An arc was obtained between graphite electrodes separated by a distance of 1 mm for the work at constant gap length. For comparison, a reignition characteristic is shown for an arc between copper electrodes. The results of these experiments show that for graphite electrodes the arc space recovers dielectric strength at a rate which decreases steadily with time, and that the sparking potential is approached asymptotically. For the copper arc, recovery is more rapid and reaches a knee in the curve after approximately 2 milliseconds, beyond which time there is practically no further increase in dielectric strength up to a time of 10 milliseconds.

47. Phase of Arc-Back in Rectifiers. ALBERT W. HULL AND FRANK R. ELDER, *General Electric Company.*—Thyratrons of FG-41 type were tested at over-voltage for arc-back in a circuit which simulates operating conditions very closely. Memory oscillograms showed the time in the cycle at which the arc-backs occurred. At a mercury-control temperature of 40°C, the distribution was nearly random, with a maximum at the time of highest negative anode voltage, and depending in the same manner that the average arc-back rate was found to depend on voltage. When the mercury-control temperature was raised to 64°C, all the arc-backs occurred at the beginning of negative voltage application. The negative voltage was applied 10 degrees after commutation, and its shape was similar to that of an average rectifier circuit. These results are interpreted on the theory recently advanced by Kingdon and Lawton,[1] which attributes arc-back to charging up of small non-conducting particles on the surface of the anode. At low vapor pressure, where the ions remaining from the discharge have time to diffuse to the electrodes before negative voltage is applied, the charging is produced by field emission and hence depends on voltage. At higher pressure, diffusion is interfered with, so that ions are present when negative voltage is applied.

[1] K. H. Kingdon and E. J. Lawton, Gen. Elec. Rev. **42**, 474 (1939).

48. The Stability of a Low Pressure Mercury Arc. PAUL L. COPELAND, *Illinois Institute of Technology,* AND W. H. SPARING, *Westinghouse Electric and Manufacturing Company.*—The stability of a low pressure arc increases rapidly as the arc current is increased, and there is no critical current which separates stable from unstable operation. In these experiments the mean life of a mercury arc operating under a carefully controlled set of conditions was determined by a statistical analysis of a hundred or more observed lives. The dependence of mean life upon both arc current and vapor pressure was investigated. The stability of the arc increased as the vapor pressure was raised from 0.001 to 0.004 mm Hg. In the first observations the cathode spot was free; later observations were made with the spot anchored. The marked increase of stability when the spot is anchored, observed by Tonks,[1] was studied. The results suggest that in either case the mean life rises exponentially with the arc current in the ranges used. For the arc operating at 0.0012 mm Hg pressure with a free cathode spot, the mean life T_m (seconds) may be computed from $T_m = 0.00343 \exp(2.427\, I)$ where I is the arc current in amperes. At the same pressure with the spot anchored, the mean life may be represented by $T_m = 0.000935 \exp(19.92\, I)$.

[1] L. Tonks, Physics **6**, 294 (1935).

49. Photoelectric Sensitization of Metal Surfaces in Group II by Optical Dissociation of Water Vapor. J. T. TYKOCINER AND L. R. BLOOM, *University of Illinois.*—Photo-cells made by evaporation on glass of Ca, Sr, Ba, Be, Mg, Zn and Cd and supplied with quartz windows were subjected to the irradiation from a quartz mercury arc ultraviolet source, the cathode being kept at a voltage below ionization potential while water vapor at very low pressures was introduced into the cell. In each case it was found that the sensitivity in vacuum of the surfaces increased with the time of exposure until maximum was reached. No increase was observed with the cell either in darkness or with the applied voltage reduced to zero. Precautions were taken to keep out all traces of mercury, to make certain that the effect was due to a direct photochemical dissociation of H_2O vapor. The time necessary to reach the maximum of sensitivity was found to depend on the H_2O vapor pressure and on the intensity of the ultraviolet source. The effect of higher pressures was to reduce gradually the sensitivity after maximum was reached. The maximum sensitivities obtained by this method varied for each metal. The greatest increase, about fifty times that of the pure untreated surface, was obtained with a Be surface. The smallest effect was noted with a Cd surface. A bulletin with details will be published by the University of Illinois Experiment Station.

Author Index to Abstracts of the Chicago Meeting

Allen, James S.—No. 25
Allison, Samuel K., Leonard C. Miller, Lester S. Skaggs and Nicholas M. Smith, Jr.—No. 14
Anderson, E. E. and J. E. Mack—No. 1
Anderson, H. H.—see Valley, G. E.

Bauer, W. M. and J. D. Cobine—No. 46
Bloom, L. R.—see Tykociner, J. T.
Bostick, W. H.—see Herzog, G.
Bowman, D. W.—see Green, J. B.
——— see Hurlburt, E. H.

Cleveland, Forrest F. and M. J. Murray—No. 7
Cobine, J. D.—see Bauer, W. M.
Collins, G. B. and B. Waldman—No. 20
Compton, A. H. and A. T. Monk—No. 33
Copeland, Paul L. and W. H. Sparing—No. 48
Crane, N. D.—see Herb, R. G.

Danielson, G. C. and K. Lark-Horovitz—No. 22
Dempster, A. J.—see Sherwin, C. W.
Dresden, M., W. T. Scott and G. E. Uhlenbeck—No. 35

Elder, Frank R.—see Hull, Albert W.
Elliott, D. R.—see King, L. D. P.

Gautier, T. N.—No. 32
Goldhaber, M. and R. D. O'Neal—No. 17
Green, J. B.—see Hurlburt, E. H.
———, **D. W. Bowman and E. H. Hurlburt**—No. 4
Griffith, R. L. and P. M. Harris—No. 23
Groetzinger, Gerhart, E. O. Wollan and Marcel Schein—No. 38
Guth, Eugene—No. 21
——— see James, Hubert M.
——— see Mullin, Charles J.

Haas, Arthur E.—No. 9
Hanson, A. O.—see Herb, R. G.
Harris, P. M.—see Griffith, R. L.
Haworth, L. J.—see Manley, J. H.
———, **J. H. Manley and E. A. Luebke**—No. 11
Herb, R. G., C. M. Turner, A. O. Hanson and N. D. Crane—No. 31
Herzog, G. and W. H. Bostick—No. 40
Hilberry, Norman—No. 36
Hull, Albert W. and Frank R. Elder—No. 47
Hurlburt, E. H.—see Green, J. B.
———, **D. W. Bowman and J. B. Green**—No. 3

Jacobs, James A. and William L. Whitson—No. 12
James, Hubert M. and Eugene Guth—No. 30
Johnson, Thomas H.—No. 34
——— see Shutt, R. P.

Kerst, Donald W.—No. 26
King, L. D. P. and D. R. Elliott—No. 16
Kirkham, Don—No. 27

Lark-Horovitz, K.—see Danielson, G. C.
Liebermann, Leonard N.—No. 5
Ludloff, H. F.—No. 29
Luebke, E. A.—see Haworth, L. J.
——— see Manley, J. H.

Mack, J. E.—see Anderson, E. E.
Manley, J. H.—see Haworth, L. J.
———, **L. J. Haworth and E. A. Luebke**—No. 18
Marshall, Fitz-Hugh—No. 24
Maxfield, F. A. and O. A. Mortensen—No. 8
Metropolis, N.—No. 6
Miller, Leonard C.—see Allison, Samuel K.
Monk, A. T.—see Compton, A. H.
Mortensen, O. A.—see Maxfield, F. A.
Mrozowski, S.—No. 2
Mullin, Charles J. and Eugene Guth—No. 43
Murray, M. J.—see Cleveland, Forrest F.

O'Neal, R. D.—No. 19
——— see Goldhaber, M.

Plumley, Harold J.—No. 45

Regener, Victor H. and Bruno Rossi—No. 37
Ringo, Roy—No. 10
Rossi, Bruno—see Regener, Victor H.

Schein, Marcel—see Groetzinger, Gerhart
Schilling, Harold K.—No. 28
Scott, W. T.—see Dresden, M.
Sherwin, C. W. and A. J. Dempster—No. 42
Shutt, R. P. and T. H. Johnson—No. 39
Skaggs, Lester S.—see Allison, Samuel K.
Smith, Nicholas M., Jr.—see Allison, Samuel K.
——— see Van Allen, J. A.
Sparing, W. H.—see Copeland, Paul L.

Turner, C. M.—see Herb, R. G.
Tykociner, J. T. and L. R. Bloom—No. 49

Uhlenbeck, G. E.—see Dresden, M.

Valley, G. E. and H. H. Anderson—No. 41
Van Allen, J. A. and Nicholas M. Smith, Jr.—No. 15
Vanderberg, R. M.—No. 44

Waldman, B.—see Collins, G. B.
Wheeler, John A.—No. 13
Whitson, William L.—see Jacobs, James A.
Wollan, E. O.—see Groetzinger, Gerhart